ANALYTICA CHIMICA ACTA

International monthly devoted to all branches of analytical chemistry
Revue mensuelle internationale consacrée à tous les domaines de la chimie analytique
Internationale Monatsschrift fur alle Gebiete der analytischen Chemie

ELSEVIER SCIENTIFIC PUBLISHING COMPANY
AMSTERDAM

Anal. Chim. Acta, Vol. 75, No. 1, 1–252, March 1975
Published monthly

Publication Schedule for 1975

Vol. **74,** No. **1**	January 1975	
Vol. **74,** No. **2**	February 1975	**(completing Vol. 74)**
Vol. **75,** No. **1**	March 1975	
Vol. **75,** No. **2**	April 1975	**(completing Vol. 75)**
Vol. **76,** No. **1**	May 1975	
Vol. **76,** No. **2**	June 1975	**(completing Vol. 76)**
Vol. **77,** No. **1**	July 1975	
Vol. **77,** No. **2**	August 1975	**(completing Vol. 77)**
Vol. **78,** No. **1**	September 1975	
Vol. **78,** No. **2**	October 1975	**(completing Vol. 78)**
Vol. **79,** No. **1**	November 1975	
Vol. **79,** No. **2**	December 1975	**(completing Vol. 79)**

Subscription price: Dfl. 570.00 plus Dfl. 54.00 postage, US$ 249.60 inclusive of postage. Subscribers in the U.S.A. and Canada receive their copies by airmail. Additional charges for airmail to other countries are available on request. For advertising rates apply to the publishers.

Subscriptions should be sent to:
Elsevier Scientific Publishing Company, P.O. Box 211, Amsterdam, The Netherlands.

GENERAL INFORMATION

Languages

Papers will be published in English, French or German.

Submission of papers

Papers should be sent to:

PROF. PHILIP W. WEST,
Coates Chemical Laboratories,
College of Chemistry and Physics,
Louisiana State University,
Baton Rouge 3,
La. 70803 (U.S.A.)

or to:

DR. A. M. G. MACDONALD,
Department of Chemistry,
The University,
P.O. Box 363
Birmingham B15 2TT (Great Britain)

Reprints

Fifty reprints will be supplied free of charge. Additional reprints (minimum 100) can be ordered at quoted prices. They must be ordered on order forms which are sent together with the proofs.

PRINTED IN THE NETHERLANDS

Reagents

MERCK

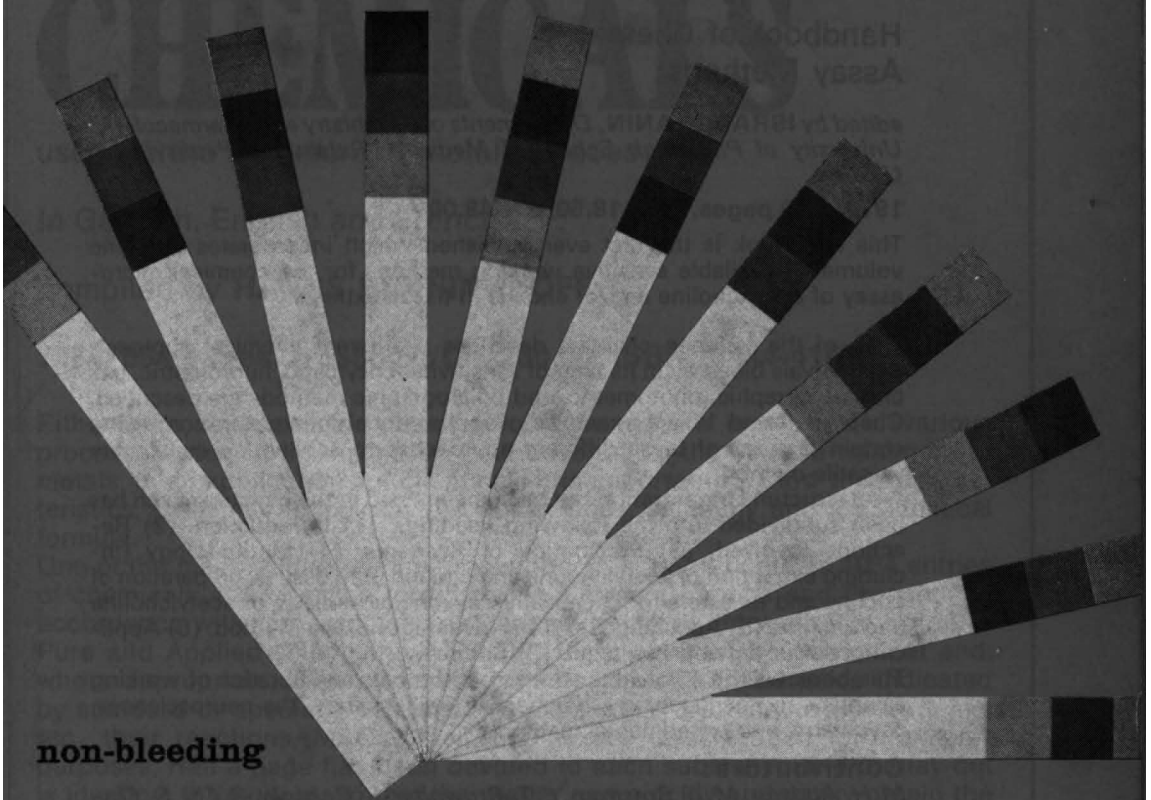

non-bleeding

Universal Indicator Strips: pH 0–14
Special Indicator Strips: pH 0–2.5
pH 2.5–4.5 pH 4.0–7.0 pH 6.5–10.0 pH 11.0–13.0
Neutralit® pH 5–10 Acilit® pH 0–6
Alkalit® pH 7.5–14

Special advantages:

Reactive zones sealed onto plastic strips

Non-bleeding

Prolonged immersion possible

Weakly buffered and even coloured solutions may be measured

Distinctive colour differences

Highly stable to light

Please request our special brochure

E. Merck, Darmstadt

317-EU

Chemistry, Electrochemistry, Surface Properties and Catalysis

INDEX OF CHEMICALS

used for the treatment of metal surfaces

In German, English and French.

compiled by **HANNS BENNINGHOFF**

1974. 654 pages. US$88.50/Dfl. 230.00. ISBN 0-444-41075-9

Either pure chemicals or chemical compounds are employed in various processes used in the extensive field covered by the surface treatment of metals. In all applications of chemicals it is important to know their characteristics, their interaction, mixture possibilities, solubility and the chemical formula.

One of the main features of the present book is that it contains 1034 entries of chemicals and chemical products, in German, English and French – in accordance with the recommendations made by the International Union of Pure and Applied Chemistry (IUPAC) – together with their empirical and, where appropriate, their structural formula, their characteristics indicated by standard or specially designed symbols, their solubility in water, acids, etc., their reactions, MAC values and hazard classification for transport purposes. Half a page has been devoted to each substance and the lay-out is identical throughout, so that the reader can quickly and easily obtain the information he requires. All the figures and other data given have been checked for accuracy and where there was any doubt the information was omitted.

The index is given in German, English and French, and also contains incorrect, popular and misleading names for chemicals so that it can also be regarded as a technical dictionary for chemicals. The work is completed by an alphabetical index of formulae of the chemicals listed.

The book fills a gap, and chemists as well as technologists concerned with the chemical and electrochemical treatment of metal surfaces either from the practical or theoretical point of view will derive considerable benefit from this new reference work.

Elsevier
P.O. BOX 211
AMSTERDAM - THE NETHERLANDS
1506 E

ANALYTICA CHIMICA ACTA
Vol. 75 (1975)

ANALYTICA CHIMICA ACTA

International monthly devoted to all branches of analytical chemistry
Revue mensuelle internationale consacrée à tous les domaines de la chimie analytique
Internationale Monatsschrift für alle Gebiete der analytischen Chemie

ELSEVIER SCIENTIFIC PUBLISHING COMPANY
AMSTERDAM

PRINTED IN THE NETHERLANDS

Analytica Chimica Acta, 75 (1975) 1–19

THE ELECTRODEPOSITION AND DETERMINATION OF RADIUM BY ISOTOPIC DILUTION IN SEA WATER AND IN SEDIMENTS SIMULTANEOUSLY WITH OTHER NATURAL RADIONUCLIDES

MINORU KOIDE and K. W. BRULAND*

Geological Research Division, Scripps Institution of Oceanography, La Jolla, California 92037 (U.S.A.)

(Received 18th April 1974)

The disequilibria existing between parent and daughter isotopes of the uranium and thorium series are valuable in explaining their geochemical behavior in sea water and sediments.

$$^{238}U \xrightarrow[4.5\cdot10^{9}\ yr]{\alpha} {}^{234}Th \xrightarrow[24.1\ day]{\beta} {}^{234}Pa \xrightarrow[1.18\ min]{\beta} {}^{234}U \xrightarrow[2.48\cdot10^{5}\ yr]{\alpha}$$

$$^{230}Th \xrightarrow[8.0\cdot10^{4}\ yr]{\alpha} {}^{226}Ra \xrightarrow[1620\ yr]{\alpha} {}^{222}Rn \xrightarrow[3.825\ day]{\alpha} \ldots {}^{210}Pb \xrightarrow[22.3\ yr]{\beta}$$

$$^{210}Bi \xrightarrow[5.0\ day]{\beta} {}^{210}Po \xrightarrow[138\ day]{\alpha} {}^{206}Pb$$

$$^{232}Th \xrightarrow[1.4\cdot10^{10}\ yr]{\alpha} {}^{228}Ra \xrightarrow[6.7\ yr]{\beta} {}^{228}Ac \xrightarrow[6.13\ h]{\beta} {}^{228}Th \xrightarrow[1.91\ yr]{\alpha} {}^{224}Ra \xrightarrow[3.64\ day]{\alpha}$$

$$^{220}Rn \xrightarrow[54.5\ s]{\alpha} \ldots \longrightarrow {}^{208}Pb$$

In order to understand further the geochemical processes involved in the recent development of ^{210}Pb and $^{228}Th/^{232}Th$ geochronologies in lacustrine and near shore marine sediments[1], a rapid and reliable method was desirable for ascertaining the radium isotopes (^{226}Ra and ^{228}Ra) as well as the other interrelated nuclides (^{210}Pb, ^{210}Po, ^{228}Th, ^{232}Th and ^{230}Th from the same sample) in sediments and sea water. For example, ^{210}Pb and ^{228}Th have been found to be deficient with respect to their radium parents in sea water[2,3] and to exist in excess in particulate matter and recent sediments[1]. In order to obtain a more precise sedimentation rate by ^{210}Pb geochronology, the activity of ^{226}Ra is desirable to account for the supported ^{210}Pb. As a result of this correction, the unsupported ^{210}Pb dating range may be increased from about 100 to 150 years. In sea water the relationship of ^{210}Pb to its parent ^{226}Ra can be used to calculate the residence time of ^{210}Pb. The 1620-year half-life of ^{226}Ra also makes it an ideal oceanographic tracer in applications to global deep water movements (resident times of the deep water are of the same order as the half-life of ^{226}Ra).

* Present address: Marine Studies, Division of Natural Sciences, University of California, Santa Cruz, Ca. 95060.

In near shore waters, the activity of ^{228}Ra is found[4–6] in excess relative to its long-lived parent, ^{232}Th. ^{228}Th, the daughter of ^{228}Ra, is rapidly removed to the deposits with solid phases and provides a basis for the $^{228}Th/^{232}Th$ geochronology. ^{228}Ra ($t_{\frac{1}{2}}=6.7$ years) also has potential as a tracer for water mass movements for periods of the order of 3–30 years[6,7].

Nearly all investigators measure ^{226}Ra indirectly by the ^{222}Rn emanation technique[8–10]. The ^{228}Ra, a more difficult determination was made by separating and measuring either the decay of its ^{228}Ac β-emitting daughter ($t_{\frac{1}{2}}=6.13$ h[11–13]), which is applicable when adequate sensitivity is available, or when higher detection sensitivity is required, from the growth of its ^{228}Th daughter[6,12,13]. However, Smith and Mercer[13] determined ^{228}Ra in large quantities of soil samples by incorporating the tracer ^{225}Ra ($t_{\frac{1}{2}}=15$ days), and measuring the growth of ^{228}Th.

Therefore, an effort was made to formulate a procedure that would simultaneously remove these uranium-thorium series nuclides from sea water and subsequently isolate and prepare them for either α- or β-counting. An aluminum phosphate coprecipitation technique was found to concentrate quantitatively all these isotopes from sea water. Radium is assayed in sea water and sediment by isotope dilution with ^{223}Ra and isolation and electrodeposition onto platinum discs. In sediments, naturally occurring ^{224}Ra can also be used as the yield monitor when related to ^{228}Th. ^{226}Ra is determined immediately by α-counting, whereas ^{228}Ra is assayed directly by β-counting the ^{228}Ra–^{228}Ac pair, or after a suitable time period by α-counting the ^{228}Th growth onto the plated sample. ^{210}Pb, ^{210}Po, thorium and uranium isotopes are plated and counted by pre-existing techniques[14–17].

EXPERIMENTAL

Apparatus

A 512-channel (Nuclear Data model-30A) and a 1024-channel (Packard Model-901) pulse-height analyzer coupled to surface barrier silicon detectors (Nuclear Diode and Ortec 20–60 Kev resolution) were used for α-counting. A NaI (Tl) detector enclosed in a shielded well was coupled to the above analyzer for γ-counting. Low-background β-counting systems in anti-coincidence (Sharp-series LB 100) were used coupled with specially fabricated thin "Q" gas flow, small volume detectors operated in the geiger region (background approximately 6 and 12 c.p.h.). The electrodeposition apparatus is shown in Fig. 1 and explained in the plating section.

Reagents

Aluminum nitrate solution. Prepare a solution of $Al(NO_3)_3 \cdot 9H_2O$ containing 150 mg of Al_2O_3 per ml.

Ammonium monohydrogenphosphate. Prepare a 120 mg ml^{-1} solution.

Lead carrier (12.0 mg ml^{-1}). Use a low β-emitting lead solution as a carrier for ^{210}Pb.

Anion exchange resin, AG-1-100-200 mesh.

Cation exchange resin, DOWEX-12X-200-400 mesh, and 8X-200-400 mesh.

The following radioactive materials were used: radium-223 tracer separated from actinium-227 (Amersham/Searles Corporation); thorium dioxide (1906 vintage;

U. S. Geological Survey, Denver, Colorado); radium-226 standard (U.S. Bureau of Standards; SRM 4955); thorium-234 tracer obtained by milking a uranium-238 solution; lead-210 standard (Bundesanstalt for Bodenforschung, Hannover, Germany); polonium-208 tracer (USAEC Health and Safety Lab. New York).

Procedure for sea water

Sea water (20 l) stored in collapsible polyethylene cubitainers (previously acidified at the time of collection with 100 ml of concentrated nitric acid and with 120 mg of stable lead carrier added) are transferred to an acid-cleaned pyrex carboy. Add the appropriate amount of ^{223}Ra tracer (5–10 c.p.m.)* along with 20 ml of aluminum nitrate and 25 ml of ammonium hydrogen-phosphate solutions. Stir the sea water until well mixed and let stand at least overnight. Bubble nitrogen to remove carbon dioxide (necessary if uranium is determined). Add approximately 100 ml of concentrated ammonia liquor while stirring. Adjust the pH with concentrated ammonia liquor to 5.8. The $AlPO_4$ will start to form as a white gelatinous precipitate. Continuously stir for a period of 8 h and then let stand overnight. Siphon off the sea water supernate (*ca.* 2 l of precipitate remains) and transfer the $AlPO_4$ precipitate to a 2-l beaker. Let stand overnight, then siphon off the supernate (the volume of $AlPO_4$ is *ca.* 400 ml). The volume of the precipitate is finally reduced by high speed centrifugation in two 50-ml polypropylene centrifuge tubes.

Dissolve the $AlPO_4$ with 5–6 ml of 4 *M* nitric acid, stir and heat in a hot water bath until complete dissolution of the precipitate**. Reduce the volume to 5 ml and add 35 ml of 90% fuming nitric acid to form lead nitrate. Stir, place in an ice bath, and ultrasonically agitate the precipitate for 15 min. Let stand in an ice bath for 1 h. Centrifuge and decant the supernate (save the supernate and note the date of thorium separation from radium). Add 40–45 ml of chilled 75% nitric acid (previously prepared by mixing 500 ml of 90% nitric acid and 1500 ml of concentrated nitric acid and stored chilled). Stir and ultrasonically agitate for 15 min in an ice bath. Centrifuge, combine the supernate with the previous supernate, and take to dryness for thorium and uranium analysis***. Volatilize the excess of nitric acid in the lead nitrate fraction on a hot water bath. Add 15 ml of 1.5 *M* hydrochloric acid to each test tube and heat in a water bath to dissolve the maximum amount of lead. Repeat the previous step with an additional 10–15 ml of acid for complete dissolution of the lead. Separate the lead by adsorption on a previously prepared anion-exchange column (Bio-Rad AG1-X8, 100–200 mesh,

* If Th, U, or ^{210}Po are to be determined, add the appropriate ^{234}Th, ^{232}U, or ^{208}Po tracer. ^{223}Ra is discussed further in the tracer section.

** For polonium nuclides, dissolve the $AlPO_4$ in 20–30 ml of 0.5 *M* HCl by warming in a hot water bath. Plate by previously described techniques[15]. Better yields were obtained by plating for longer time periods (6–8 h). After plating, take the solution to dryness and redissolve in 5 ml of 4 *M* HNO_3 and proceed with the separation.

*** For thorium and uranium nuclides in sea-water samples, dissolve the residue in *ca.* 20 ml of 10 *M* HCl, and separate uranium from the thorium by adsorbing the uranium onto an AG1 anion-exchange column previously washed with 10 *M* HCl. Wash further with 10 *M* HCl. Evaporate the eluant to dryness for thorium separation. Elute the uranium with distilled water, evaporate to dryness, and electroplate the uranium[16]. The thorium fraction is dissolved by heating in 30 ml of saturated aluminum nitrate solution. The thorium is then separated by previously described techniques[17].

ca. 12 ml resin volume with 1.4 cm i.d., previously washed with 1.5 *M* HCl). Collect a total of *ca.* 100 ml of 1.5 *M* hydrochloric acid for the radium fraction and subsequently take to dryness. Elute the lead with 75 ml of double-distilled water (note time of separation) and subsequently precipitate as lead sulphate, filter on a membrane filter (0.45 μm), dry to constant weight, mount, and β-count.

Dissolve the residue (mainly of calcium, barium, strontium, and residual aluminum phosphates) contained in the radium fraction with 2 ml of 1.7 *M* hydrochloric acid. Transfer the 2 ml of radium solution onto a previously prepared cation-exchange column (BioRad AG50W-X12, 200–400 mesh, hydrogen form, previously washed with 50 ml of 8 *M* hydrochloric acid, followed by 120 ml of 1.7 *M* hydrochloric acid). Allow the 2 ml to flow by gravity. Wash the beaker with 1.7 *M* hydrochloric acid in increments of several ml. Pass a total volume of 10 ml at about 1 ml min^{-1}. Add an additional 110 ml of 1.7 *M* hydrochloric acid and pass at the same rate. Elute the radium with 25 ml of 8 *M* hydrochloric acid into a 30-ml beaker. Evaporate to dryness and oxidize with a few drops of nitric acid. The final radium fraction should give a very clean separation essentially free from visual residue.

The above radium procedure for sea water can be done routinely to process two or more samples a day.

Experimental procedure for sediments

Dry several grams of sediment at 110°C and pulverize the sample. Weigh an appropriate amount of sediment (1–5 g) and ignite at 400°C to destroy most of the organic matter. Transfer to a 250-ml erlenmeyer flask, and add 120 mg of lead carrier, an appropriate amount of ^{223}Ra spike* (10–20 c.p.m. as explained in the preparation of ^{223}Ra tracer), 100 ml of concentrated hydrochloric acid diluted with water and small amounts of concentrated nitric acid. Digest at moderate heat for 2 h. Cool and centrifuge the sample. Wash residue thoroughly in 6 *M* hydrochloric acid, transfer the hydrochloric acid phases to a 250-ml beaker and slowly evaporate to dryness.

Add 100 ml of concentrated nitric acid and heat slowly (note time of thorium separation). Digest the insoluble nitrates to 75 ml and then cool and chill in an ice bath. Add 25 ml of 90% nitric acid (final HNO_3 concentration is 75%). Ultrasonically agitate the sample for 15 min. Let stand for 1 h and transfer the lead nitrate to a 50-ml polypropylene test tube. Centrifuge and save the supernate for thorium or uranium analysis. Transfer the remaining lead nitrate in the beaker to the test tube by rinsing with 75% nitric acid and centrifuge. Wash the lead nitrate with 40–45 ml of chilled 75% nitric acid and ultrasonically agitate for 15 min in an ice bath. Centrifuge, decant and combine with the first supernate. Evaporate the excess of nitric acid and heat the lead nitrate to dryness.

Separate the lead from the radium as in the sea-water procedure. The radium separation and plating are identical to the sea-water procedure. For the

* If other nuclides are to be determined, add the appropriate tracers (^{232}U, ^{234}Th, ^{208}Po). Omit ^{223}Ra tracer and add ^{234}Th tracer if radium is to be determined without addition of a spike. Follow the identical separation procedure, but allow the hydrochloric acid-leached solutions to stand for several days before Th–Ra separation.

thorium or uranium determination, volatilize most of the excess of nitric acid and dilute to 50 ml with double-distilled water. Add 5–10 mg of lanthanum carrier and separate the thorium by previously described techniques[17]. For the uranium separaton, take the supernate (HF) from the LaF_3 precipitation to dryness, redissolve in 8 *M* hydrochloric acid, and extract the iron with isopropyl ether. Take the 8 *M* hydrochloric acid fraction containing the uranium to dryness, oxidize with a few drops of concentrated nitric acid, redissolve in 8 *M* hydrochloric acid, and pass through an anion-exchange column (AG1-X8, 100–200 mesh). Elute uranium with distilled water and take to dryness. In order to insure an extremely clean plating, recycle the uranium residue through the isopropyl ether extraction and anion-exchange column using much smaller volumes. The final uranium is electroplated onto a platinum disc[16] and α-counted.

Procedure for the electrodeposition of radium

The described procedure for the electrodeposition of radium onto a 2.5-cm platinum planchet (actual plated area is 2.1 cm^2) resulted from various trials and errors. Although an extensive study for the various parameters for plating radium was not made, radium can be plated successfully by cathodic deposition with some latitude from the plating procedure adopted, *i.e.*, the hydrochloric acid concentration of the plating solution can be varied either way by a factor of two. Most of the radium is plated during the first 5–10 min. Radium will also plate onto a polished stainless steel planchet but owing to the repeated flaming of the planchet (for the volatilization of Rn and daughters) this approach is not recommended. Also, radium can be plated with ethanol which suggests that other polar solvents can be utilized.

Dissolve the final radium isolate (30-ml beaker free from visual residue) in 0.5 ml of 0.05 *M* hydrochloric acid in order to solubilize the radium salts. Quantitatively transfer the radium solution into the plating cell after pre-testing the cell planchet interface for possible leaks. Rinse the beaker several times with 2-propanol and transfer to the cell, resulting in a final volume of 5 ml. Flame the anode and insert into the cell with the anode face parallel and about 2 mm from the face of the cathode. Adjust the current to 100–150 mA at 40 V and plate for 20 min (the current can vary from 75 mA to 150 mA). At the end of plating, withdraw the anode from the solution and add 4–5 drops of ammonia solution before turning off the current (the apparent pH during plating is about 2). Rinse the cell with 2-propanol and dismantle the cell, Flame the planchet, note the time (for ^{222}Rn correction) and α-count the ^{226}Ra and ^{223}Ra or ^{224}Ra. A very faint or invisible coating will result on the planchet after flaming.

A uniform area plating cell was constructed for all the various nuclides (area of 2.1 cm^2) from a 2.5-cm diameter Millipore filter funnel and stem. Figure 1 illustrates a modified version of the filter funnel. The top of the funnel was cut in order to accommodate a teflon plug with notches as shown. This serves as an alignment guide for the anode wire as well as a means of relief for the gas bubbles generated during plating. The hole through the teflon plug should be slightly smaller than the anode wire in order to result in a tight fit. This allows the distance from the anode to cathode to be varied. The stem section was made from stainless steel with an added small O-ring groove (see Fig. 1). The depth of

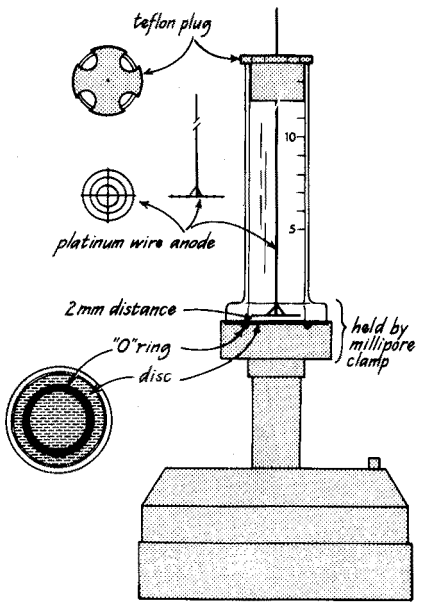

Fig. 1. Electrodeposition cell for radium.

the O-ring groove was cut just enough to allow a slight protrusion of the O-ring when placed into the groove. This insures a tight seal for the plating solution when the flamed platinum planchet along with the funnel is properly clamped into place with the clamp supplied in the Millipore funnel kit.

The stirring of the anode is not necessary if the anode is designed properly. It is important that the gas bubbles generated during plating should not be trapped between the cathode and anode. The anode design is illustrated in Fig. 1 and can be made by spot-welding 0.5-mm diameter platinum wire into several concentric rings. A gauze-type platinum or too closely spaced concentric rings will trap gas bubbles and result in a low radium yield. The plating yield for radium reaches 90% within 5 min and approaches 100% after 20 min.

Efficiencies

The radium as well as thorium, uranium and polonium nuclides were α-counted. The ^{228}Ra–^{228}Ac and ^{210}Pb–^{210}Bi were measured by low β-counting anticoincidence systems. The efficiencies of the detectors were checked by several methods in the following manner.

(1) A U.S. Bureau of Standards ^{226}Ra was aliquoted (28.6 d.p.m. $\pm$ 1.0) and combined with an aliquot of ^{223}Ra. The radium was evaporated to dryness, solubilized and electrodeposited. The ^{226}Ra and ^{223}Ra were α-counted and the ^{223}Ra yield was determined relative to an evaporated ^{223}Ra comparator (Table I). Efficiencies obtained by relating the yield of corrected ^{226}Ra to that of absolute ^{226}Ra are in good agreement. Multiple standards obtained by this method are in good agreement compared to the ^{232}Th method as shown in Table I.

(2) Aliquots of ^{226}Ra (U.S. Bureau of Standards) were evaporated and compared to the absolute ^{226}Ra value.

(3) The thorium efficiency was determined by a ^{232}Th standard prepared from a thorium dioxide (1906 vintage) in which the ^{228}Ra ($t_{\frac{1}{2}}=6.7$ year) had sufficient time to attain equilibrium (necessary for obtaining the ^{228}Ra efficiency). An aliquot of ^{232}Th standard was spiked with ^{234}Th and separated from ^{228}Ra and ^{224}Ra. The thorium was plated and α-counted, which resulted in a $^{228}Th/^{232}Th$ activity ratio equal to 1.0. This ratio was based on repeated standards. The chemical yield for thorium was obtained by relating the yield corrected activity to the absolute thorium value. The thorium efficiencies obtained by multiple standards are tabulated in Table I.

TABLE I

EFFICIENCIES OF DETECTORS

		Plated yield (%)	*Efficiency (%)*
USBS ^{226}Ra plated, with	I	94.4	34.4 ± 0.8
^{223}Ra as a yield tracer	II	100	35.3 ± 0.9
	III	96.5	35.2 ± 0.9
	IV	98.7	34.9 ± 0.9
Average			$35.0\ \sigma=\pm0.4$
USBS ^{226}Ra			34.5 ± 1.1
evaporated standards			34.2 ± 0.9
^{232}Th standard plated, with	I	60.5	34.7 ± 1.0
^{234}Th as a yield tracer	II	62.8	34.2 ± 0.6
	III	42.6	33.6 ± 1.0
	IV	52.3	33.6 ± 1.0
Average			$34.0\ \sigma=\pm0.5$
^{228}Ra standard from 1906 ^{232}Th	I	73.4	46.3 ± 0.6
std. plated and β-counted	II	52.3	46.4 ± 1.5
	III	52.4	44.9 ± 1.1
	IV	56.9	45.7 ± 1.4
Average			$45.8\ \sigma=\pm0.6$

(4) The ^{228}Ra efficiency was obtained by β-counting the immediate daughter ^{228}Ac ($t_{\frac{1}{2}}=6.13$ h; $E=2.11$ MeV max) which grows into equilibrium in a matter of days. ^{228}Ra ($E=0.05$ MeV) decays by soft β-emission and experimentally it will be considered as the ^{228}Ra–^{228}Ac couple. The radium plated fraction consisting of ^{228}Ra and unsupported ^{224}Ra separated from the 1906 ThO_2 standard by TTA/benzene extraction[11] was flamed to volatilize the ^{212}Pb and ^{212}Bi–^{208}Tl and immediately β-counted.

[In addition to the ^{228}Ra–^{228}Ac β-decay, there are three other nuclides in the ^{232}Th series that decay by β-emission, ^{212}Pb ($t_{\frac{1}{2}}=10.6$ h, $E=0.58$ MeV max), ^{212}Bi ($t_{\frac{1}{2}}=60.5$ min, $E=2.25$ MeV max) and ^{208}Tl ($t_{\frac{1}{2}}=3.10$ min, $E=1.80$ MeV max). By thorough repeated flaming of the planchet, it is possible to volatilize these β-emitting nuclides without loss of radium to a very low level and obtain

a *ca.* 60-min β-count for ^{228}Ra–^{228}Ac with minimal ingrowth of ^{212}Pb and ^{212}Bi–^{208}Tl. The growth of β-rays arising from ^{212}Pb and ^{212}Bi–^{208}Tl is calculated (by Bateman's equation) to be less than 5% of the ^{224}Ra within the first 60 min of counting. The activity level of these β-nuclides present at any time since the separation of radium from thorium is a function of the ^{224}Ra present which results from the combination of the decay of unsupported ^{224}Ra as well as the growth of ^{224}Ra from the ^{228}Th (growth of ^{228}Th from ^{228}Ra).]

The efficiency can be calculated by relating the yield-corrected ^{228}Ra β-activity to the absolute amount of ^{232}Th. The ^{228}Ra yield was obtained by α-counting the ^{224}Ra immediately after plating. The ^{224}Ra activity was corrected to the time of separation from the ^{228}Th, and the chemical yield of radium was obtained by relating the ^{224}Ra to the absolute value of ^{228}Th (this assumes a ^{224}Ra/^{228}Th activity ratio equal to unity at the time of separation). These yields were verified at a later date by α-counting the ^{228}Th growth from the ^{228}Ra. The ^{228}Ra standards were β-counted frequently after their separation from ^{232}Th. The plated planchets were covered with a thin mylar film (0.8 mg cm^{-2}) and an aluminum absorber (13 mg cm^{-2}). The efficiencies obtained by multiple standards are in good agreement (see Table I).

(5) The ^{210}Pb-^{210}Bi β-counting efficiency is a function of the quantity of lead carrier incorporated with the ^{210}Pb mainly as a result of self-absorption. The counting efficiencies were obtained by spiking ^{210}Pb standards with different amounts of lead carrier and subsequent separation from ^{210}Pb daughters. The separated lead, as lead sulfate, was uniformly deposited onto two copper planchets, each with an active area of 2.0 cm^2 and covered with thin mylar film (0.8 mg cm^{-2}). After the daughter ^{210}Bi ($t_{\frac{1}{2}} = 5.0$ days) had attained equilibrium, repeated counts were made by mounting the two planchets on each side of the β-detector and counted by an anticoincidence system. Figure 2 illustrates the relationship of the counting efficiency to the amount of lead sulfate. The ^{210}Pb standards were frequently used to monitor the sensitivity of the β-system.

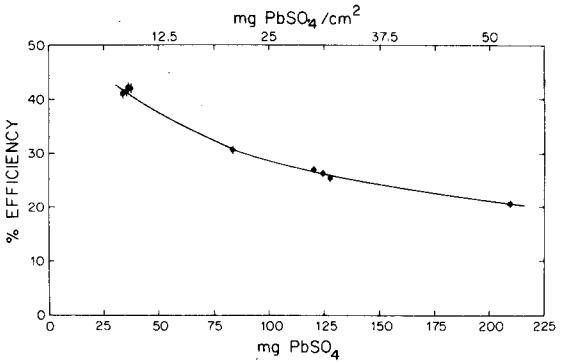

Fig. 2. The effect of lead carrier on the β-counting efficiency of ^{210}Pb–^{210}Bi.

(6) An aliquot of ^{208}Po tracer was evaporated and α-counted to determine the efficiency of the detector used to count the polonium samples. The efficiency found (35.7%) compared favorably with that determined by a ^{232}Th standard on the same detector.

RESULTS AND DISCUSSION

The criteria for the selection of a proper carrier were the simultaneous co-precipitation of radium and other related nuclides of interest from sea water as well as obtaining insignificant radium blanks. The technique of measuring ^{226}Ra in sea-water samples stored in 20-l glass bottles by radon emanation resulted in variable blanks from the ^{222}Rn contributed from the bottles. Typical bottle blanks can represent 50% of surface-water ^{226}Ra concentrations and 10% of Pacific deep water values[18]. Most previous workers concentrating radium isotopes from sea water used coprecipitation with barium sulfate which also has an inherent radium blank[12]. ^{226}Ra has been coprecipitated with calcium carbonate from 1-l sea-water samples[19]. However, coprecipitation from 20-l volumes investigated in this laboratory was incomplete. For other nuclides, previous investigators have used coprecipitation with iron(III) hydroxide[2,4,20] and calcium carbonate[19,21], but neither of these carriers quantitatively coprecipitates all of the radioisotopes of interest.

Aluminum phosphate as carrier

Aluminum phosphate was initially used as a carrier for coprecipitation of uranium from sea water[22]. However, this precipitate does not seem to have been used for the coprecipitation of radium (in addition to other alkaline earth elements), lead-210, polonium or thorium (although possibly for other actinides and lanthanide elements). The aluminum phosphate is easily solubilized with dilute acids.

The effectiveness of aluminum phosphate in the coprecipitation of radium was established by spiking sea water with ^{223}Ra, and following the adopted procedure on the initial precipitation step. The aluminum phosphate was subsequently γ-counted for recovery yields. The radium recovery on repeated aluminum phosphate fractions was in excess of 90%.

Lead carrier for ^{210}Pb determinations was added initially to the acidified sea water and precipitated simultaneously as lead phosphate with aluminum phosphate. The final lead recovery on 60 samples was 85–95%. In addition, ^{210}Pb was coprecipitated with aluminum phosphate without the addition of lead carrier (the lead was added after precipitation of aluminum phosphate). Close agreement for ^{210}Pb by both methods indicated the effectiveness of aluminum phosphate in scavenging lead (0.04_2 dpm l^{-1}, 0.04 dpm l^{-1}).

The ^{210}Po and ^{228}Th resulted in final yields of 60–70% and 70–80% respectively, indicating effective scavenging of both these nuclides.

Lead nitrate as carrier

The selection and utilization of lead nitrate in the procedure for the separation of radium (after the aluminum phosphate step, in the case of sea water) served two important functions. First, the radium along with lead, barium and some strontium and calcium were separated from thorium and uranium. Secondly, the same lead carrier previously added for ^{210}Pb was used. An early report by Willard and Goodspeed[23] suggested a nitric acid concentration of 80% (w/w) for the precipitation of radium, barium, strontium, and lead. However, Sunderman and Townley[24], using 80% nitric acid, found that calcium was also precipitated in significant quantities. With proper selection of the nitric acid

concentration (67–70% HNO_3), previous investigators[25,26] have reported a good separation between strontium and calcium. The separation of radium with a lead nitrate precipitation in 80% nitric acid has also been reported[27]. However, alkaline earth elements were not encountered as a contaminant in their samples, which obviated further purification procedures. In the present work on sea water and sediments, significant amounts of alkaline earth elements were encountered. With this step it is desirable to remove as much as possible of the strontium and calcium, although a radium purification step is incorporated later by cation exchange. Nitric acid solutions at 67–70% generally resulted in low radium yields; 75% nitric acid was found to be preferable and was adopted for the general procedure.

Cation exchange

Successful electrodeposition of radium is critically dependent on the purity of the radium isolated from other residues (mainly free of the other alkaline earth elements). Sea water and sediments contain sufficient barium, strontium, and calcium to necessitate a final radium isolation step.

Separation of radium from alkaline earth elements is generally accomplished by cation-exchange techniques. These elements are adsorbed onto the column in dilute acid solutions and subsequently removed by eluting with organic complexing agent. The radium, owing to its larger adsorption coefficient, is collected in the last fraction of the eluant. During initial experimentation, ammonium citrate[28,29], EDTA[30], and ammonium formate[31] were tried, but the electrodeposition was not satisfactory because slight residues remained even after oxidation and volatilization of the salts. Therefore, a cleaner method of separating radium from the alkaline earths with hydrochloric acid through a Dowex cation-exchange column[32,33] was further investigated to achieve the optimal separation of radium from barium, strontium, and calcium. ^{223}Ra tracer was utilized and aliquots at 5-ml intervals were counted by γ-spectrometry at the ^{223}Ra 0.270-KeV peak. Barium and strontium carriers were added without radio-tracers. The separation of the radium from barium and strontium was determined by visual means after each aliquot was taken to dryness. The final cation-exchange procedure adopted was based on the amount of the alkaline earths (Ba, Sr) contained in 20 l of sea water or several grams of sediment (Fig. 3) as well as on performing the radium separation in a reasonable time (2 h).

^{223}Ra tracer

The ^{223}Ra ($t_{\frac{1}{2}}=11.7$ days) tracer was prepared from an ^{227}Ac ($t_{\frac{1}{2}}=21.6$ years) source. Approximately 0.2 μCi of ^{223}Ra in equilibrium with ^{227}Ac, was separated from ^{227}Th ($t_{\frac{1}{2}}=18.2$ days) and ^{227}Ac. (The initial milking of ^{223}Ra was found to contain a small amount of ^{226}Ra, and was therefore discarded; subsequent milkings contained undetectable amounts of ^{226}Ra and ^{228}Ra.) The ^{227}Th was first separated by extraction at pH 2 into TTA/benzene[11]. The ^{227}Ac was subsequently separated by extraction into TTA/benzene at pH 5.5–6.0 (^{227}Ac was stripped with 2 *M* nitric acid from the TTA/benzene and saved for future milking of ^{223}Ra). The ^{223}Ra was further purified by placing the ^{223}Ra, contained in 1.5 *M* hydrochloric acid (2 ml volume) onto a previously prepared cation-exchange

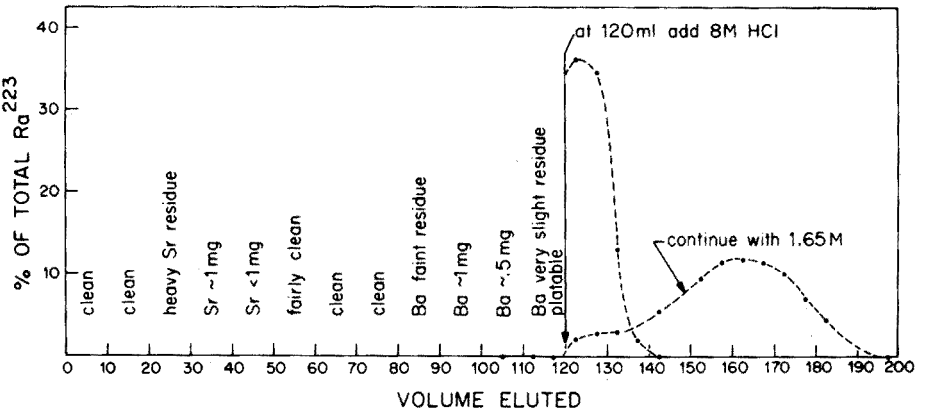

Fig. 3. A typical separation of radium from other alkaline earth elements. This spectrum was based on 5 mg of strontium and 2 mg of barium from ^{223}Ra.

column (BioRad AG50-X8, 200–400 mesh, 0.6-cm i.d. 10-cm column, flow rate at *ca.* 1 ml min^{-1}). The column was further washed with 80 ml of 1.5 *M* hydrochloric acid. The ^{223}Ra was then eluted with an additional 50 ml of the same acid. The purified ^{223}Ra was evaporated to dryness, any residual organic matter was oxidized with nitric acid, and the solution was diluted to 20 ml with dilute nitric acid.

In this way, a working tracer, sufficient to last three months, can be prepared by increasing the amounts of the stock tracer as the ^{223}Ra decays. Aliquots of ^{223}Ra were evaporated onto a platinum disc (same area as plated sample) and followed by α- and β-counting, and their purity was verified by decay over four half-lives. The final decay curves for each set of comparators based on frequent counts were utilized in obtaining the radium yield for samples initially containing the same amounts of ^{223}Ra.

In order to utilize properly the ^{223}Ra isotope dilution technique, three interrelated factors are involved in selecting the optimal ^{223}Ra activity level to be added to the samples before chemical separation. The following situations are encountered during the time of α-counting. First, the ^{226}Ra contained in the samples produces an α-daughter ^{222}Rn ($t_{\frac{1}{2}} = 3.825$ days), whose energy coincides with the lower energies of the yield tracer ^{223}Ra, thus enhancing the total ^{223}Ra counts. Secondly, the ^{226}Ra peak is affected by a small tailing of the ^{223}Ra α-counts, extending into the ^{226}Ra region and enhancing its total counts (Fig. 4). Both these corrections are small and can be minimized by proper selection of the ^{223}Ra activity. Thirdly, the proper level of ^{223}Ra should prevail after the time for processing of the samples as well as the time for decay of ^{224}Ra (present in sediments and near-shore sea water) are taken into consideration.

Radium samples are α-counted immediately after plating and flaming in order to minimize the contribution from the growth of ^{222}Rn. The growth of ^{222}Rn is calculated by using the mean growth time ($0.693 \times$ elapsed time) and is subtracted from the total ^{223}Ra counts. Sediment and sea-water samples are counted for approximately 500 min and 1250 min, contributing usually to a correction of 4.3% and 10% respectively relative to ^{226}Ra. Therefore, the ideal ^{223}Ra activity

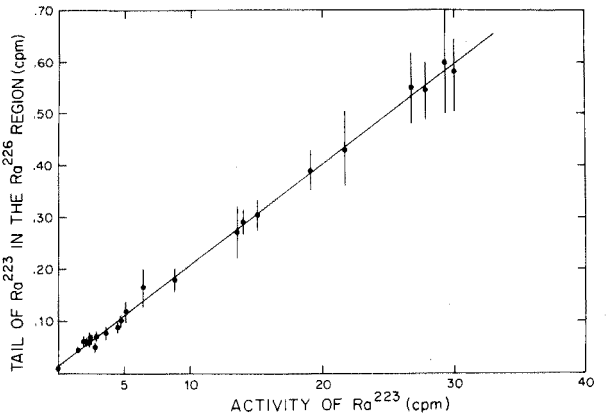

Fig. 4. The effect of ^{223}Ra activity into the ^{226}Ra energy region. These results are based on numerous ^{223}Ra-plated sample blanks.

at the time of α-counting should approximate the same peak height as the ^{226}Ra; or, owing to the broad energy spectrum of ^{223}Ra, the ^{223}Ra/^{226}Ra activity ratio should be about 2 (between 1.5 and 5, Fig. 5(a)). Thus, the ^{222}Rn contribution into the ^{223}Ra region will be reduced by at least a factor of 2 (or <2.2% and 5.0%, respectively). This spread in ^{223}Ra/^{226}Ra ratio is also compatible for minimal tailing of ^{223}Ra into the ^{226}Ra region. A linear correlation (Fig. 4) exists between the total activity of ^{223}Ra and the tailing of ^{223}Ra into the ^{226}Ra region. The corrected ^{226}Ra activity was obtained by subtracting 2.1% of the ^{223}Ra activity, which results in a ^{226}Ra correction of *ca.* 4%. If the activity level of ^{223}Ra relative to ^{226}Ra is too high (greater than 5 times), the samples are allowed to decay to the appropriate level before α-counting. The majority of the samples at the time of counting had less than 3 c.p.m. for ^{223}Ra. Since sediment and coastal sea-water samples contain ^{228}Th and hence its daughter ^{224}Ra ($t_{\frac{1}{2}}$=3.64 days), the ^{224}Ra α-energies (5.68 MeV, 94%, 5.45 MeV, 6%) concide with the region of ^{223}Ra activity. The chemically separated radium samples were allowed to stand for at least 15 days for ^{224}Ra decay before plating and counting. Radium results obtained by the ^{223}Ra isotope method for some representative sea-water, sediments, and plankton samples are shown in Tables II and III.

Internal ^{224}Ra method

Radium in sediments and any other samples containing comparable amounts of thorium can be determined by another technique which obviates the addition of ^{223}Ra tracer. Identical separation and plating procedures for radium are utilized, but additional separation and plating of the thorium nuclides are involved. Since the immediate daughter, ^{224}Ra ($t_{\frac{1}{2}}$=3.64 days), is in equilibrium with its parent, ^{228}Th, the natural ^{224}Ra is utilized as an internal spike and the recovery yield is determined by assaying for ^{228}Th as discussed in the efficiency section. The ^{224}Ra and ^{226}Ra are α-counted immediately after plating and flaming of the planchet in order to obtain the maximal counting rate for ^{224}Ra as well as minimizing the growth of the ^{226}Ra-daughter ^{222}Rn ($t_{\frac{1}{2}}$=3.825 days) (Fig. 5b). The yield for ^{224}Ra

TABLE II

RESULTS FOR SEA WATER

(All results are given as d.p.m./l)

No.	*Sample location*	*Depth (m)*	*^{226}Ra (α) by ^{223}Ra isotope dilution*[a]	*^{228}Ra (α) by growth of ^{228}Th*	*^{228}Ra (β) by $^{228}Ra/^{228}Ac$*	*^{210}Pb (β) by $^{210}Pb/^{210}Bi$*[a]	*^{228}Th(α) by ^{234}Th isotope dilution*	*^{210}Po(α) by ^{208}Po isotope dilution*
16–50	26°29.0′N 110°26.5′W	50	0.09[8]	0.17 ± 0.01	0.14 ± 0.01			
21–50	24°05.0′N 109°34.5′W	50	0.06			0.06[9]		0.07[6] ± 0.006
25	24°33.6′N 112°05.2′W	20	0.08[7]	0.02[8] ± 0.01	0.03[6] ± 0.01	0.03[2]		
14	27°22.5′N 110°41.3′W	20	0.09[2]	0.14 ± 0.01	0.12 ± 0.01	0.02[8]		
4	27°55.3′N 112°10.0′W	20	0.10[7]	0.09 ± 0.01	0.08 ± 0.01	0.02[0]		
12	27°50.4′N 111°04.0′W	20	0.10[9]	0.19 ± 0.01	0.18 ± 0.01	0.01[8]		
2B	28°16.0′N 112°22.5′W	727	0.19[4]	0.15 ± 0.01	0.13 ± 0.01	0.02[7]		
1B	28°16.0′N 112°23.5′W	727	0.19[1]			0.03[6]	0.006 ± 0.001	
10C	27°53.5′N 111°36.8′W	370	0.15[2]			0.02[8]	0.003 ± 0.001	
P.W. 3000 m	29°00′N 122°31.2′W	3000	0.37[5]		Not detectable	0.30		
Santa Monica basin		20	0.07[4]		0.01 ± 0.005	0.07[7]		0.04[7] ± 0.005

[a] Counting errors of ^{226}Ra and ^{210}Pb are less than 6%.

TABLE III

RESULTS FOR SEDIMENTS

(All results in d.p.m. g)

Location	*Depth (cm)*	*226 (α) by ^{223}Ra isotope dilution*	*^{226}Ra (α) by ^{224}Ra internal isotope dilution*	*^{228}Th (α) by ^{234}Th isotope dilution*	*^{232}Th (α) by ^{234}Th isotope dilution*	*^{228}Ra (α) by ^{228}Th growth*	*^{228}Ra (β) by $^{228}Ra/^{228}Ac$*	*^{210}Pb (β)*
San Pedro basin	0.5–1.0	5.70±0.19	5.64±0.21	3.83±0.07	1.77±0.05	1.7±0.2	1.4±0.1	89 ±2
33°30′N	1.5–2.0	5.03±0.22	5.04±0.22	1.59±0.06	1.80±0.05	1.5±0.1	2.0±0.1	70 ±2
118°19′W	6.0–7.0	4.63±0.18	4.55±0.20	1.69±0.04	1.93±0.04	1.8±0.1	2.0±0.1	16 ±0.5
	11.0–13.0	5.04±0.20	5.10±0.19	1.58±0.04	1.71±0.03	1.8±0.2	1.9±0.1	6.2±0.2
Santa Barbara Basin	10.4–11.2		3.5 ±0.3	1.38±0.04	1.58±0.05			46 ±1
33°45′W	40		3.8 ±0.3	1.76±0.06	1.83±0.06			5.6±0.2
118°52′W								
Particulate	100 m (July 72)		2.5 ±0.2	1.83±0.06	0.91±0.04			27 ±1
Santa Monica basin								
Composite plankton	0–100 m	0.48±0.04						3.2±0.1

is obtained by subtracting the contribution of ^{222}Rn, correcting the ^{224}Ra for decay to the time of separation from ^{228}Th, and relating it to the separately determined ^{228}Th values. However, the assumption is made that the ^{228}Th/^{224}Ra activity ratio at the time of thorium and radium separation is equal to unity. Experimentally, in order to compensate for possible disequilibrium that may arise as a result of preferential leaching, the hydrochloric acid-leached fractions are allowed to stand for at least several days before the separation of ^{224}Ra from ^{228}Th. The radium results obtained by this method on aliquots of identical sediment samples are in accord with the ^{226}Ra obtained by the ^{223}Ra isotope dilution technique (Table III), which substantiates the assumption that the ^{228}Th/^{224}Ra activity ratio is unity at the time of ^{228}Th and ^{224}Ra separation. There are two important considerations involved in selecting the ^{224}Ra method for the determination of radium in sediments as opposed to the isotope dilution technique. First, the ^{224}Ra and ^{226}Ra can be counted immediately after separation and plating, whereas by the ^{223}Ra technique, the natural ^{224}Ra is allowed to decay for a period of approximately 15 days before radium plating and counting (^{224}Ra, $E = 5.68$ MeV—94%, 5.45 MeV—6%; ^{223}Ra, $E = 5.75$ MeV—9%, 5.71 MeV—54%, 5.61 MeV—26%, 5.54 MeV—9%) as a result of the α-energies overlap. Secondly, the ^{224}Ra decays to an insignificant value in a much shorter time (*ca.* 30 days *vs.* 150 days, since greater ^{223}Ra activity is used compared to the natural ^{224}Ra, and ^{223}Ra also has a longer half-life). This enables the ^{228}Ra–^{228}Ac to be measured by β-counting earlier, with negligible contribution from the β-emitting daughters of the radium isotopes.

Radium-228 by β-counting

Of all the radium nuclides, ^{228}Ra is the only naturally occurring one to decay by β-emission (to actinium-228). Furthermore, ^{228}Ra in nature is usually found mixed with other radium nuclides whose daughters decay partially by β-emission; this results in mixtures of β-activities as well as different energies.

However, it would be highly desirable to determine ^{228}Ra by direct β-counting of ^{228}Ra–^{228}Ac as well as obtaining the results as soon as possible. A method is proposed which can accommodate the above conditions. This technique is based on the fact that all β-emitting nuclides other than ^{228}Ra–^{228}Ac are removed from the plated radium planchet to a very low level during the β-counting of ^{228}Ra–^{228}Ac. The sample count is related to a ^{228}Ra standard as explained in the ^{228}Ra efficiency section. Sediment samples also contain ^{226}Ra from the ^{238}U series, ^{224}Ra from the ^{232}Th series, and if a tracer is used, ^{223}Ra from the ^{235}U series; all produce their corresponding radon and its daughters. ^{222}Rn, an immediate daughter of ^{226}Ra, decays to two β-producing daughters ^{214}Pb and ^{214}Bi which can cause an interference for counting ^{228}Ra–^{228}Ac. When the planchet is properly flamed, all these nuclides are volatilized to a very low level. However, a correction can be obtained for this residual β-activity by the following procedure: plated ^{226}Ra standards (3–18 d.p.m.) are thoroughly flamed and β-counted, and the β-activity is related to the activity of ^{226}Ra. This correction (0.09 c.p.m. per d.p.m. of ^{226}Ra in the sample when a 13 mg cm^{-2} Al absorber is used) is subtracted from the ^{228}Ra–^{228}Ac β-activity. This correction is based on plated planchets with a faint sheen (without a barium residue). The sample is immediately counted for

a fraction of a day (*ca.* 400 min). When the $^{226}Ra/^{228}Ra$ activity ratio is very large. the β-counting can be interrupted by reflaming of the planchet. Repeated flaming experiments by α-counting samples and standards indicated that there is no detectable loss of ^{226}Ra. The ^{228}Ra results obtained by this method are presented in Tables II and III.

^{224}Ra is generally allowed to decay or can be present, as explained in the ^{228}Ra efficiency section. However, if ^{223}Ra is used, it is allowed to decay to a level where the contribution of its β-emitting daughters, ^{211}Bi ($t_{\frac{1}{2}}=36.1$ min) and ^{207}Tl ($t_{\frac{1}{2}}=4.79$ min) are insignificant.

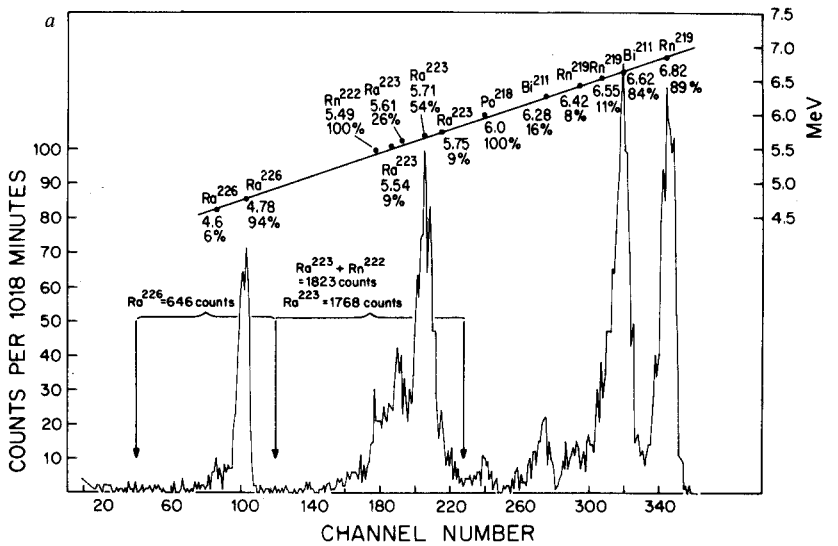

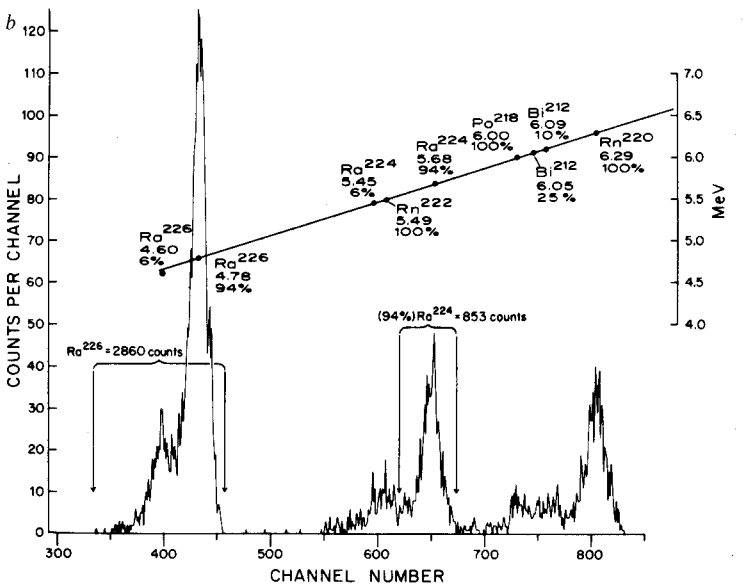

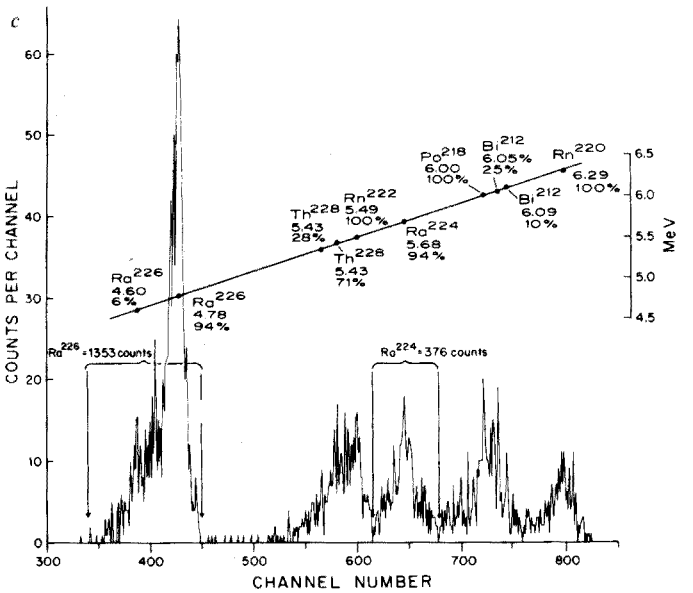

Fig. 5. (a) A typical sea-water sample with the ^{223}Ra isotopic dilution technique for the determination of ^{226}Ra. (b) A sediment sample with an internal ^{224}Ra technique for the determination of ^{226}Ra. (c) A typical sea-water sample with the ^{223}Ra isotopic dilution technique for the determination of ^{228}Ra; this spectrum was obtained after 6-months growth (16%) of ^{228}Th–^{224}Ra.

^{228}Ra by α-counting

After standing at least 3–12 months since the time of plating the radium isotopes, the planchet can be flamed once again to volatilize the ^{222}Rn and α-counted (Fig. 5c). The buildup of ^{228}Th and its short half-life daughter ^{224}Ra can be counted. The ^{224}Ra (5.68 MeV, 94%) is used to determine the amount of ^{228}Th buildup, since the ^{222}Rn α-energy falls in the region of the ^{228}Th. The initial ^{228}Ra can then be calculated (by Bateman's equations). The results obtained by α-counting are presented in Tables II and III.

This technique has obvious advantages over the previously published methods of chemically separating the ^{228}Th from a stored radium solution. The counting rate can be compared directly to the ^{226}Ra on the platinum disc for which the yield has already been determined by either the ^{223}Ra or ^{224}Ra spike techniques.

Contamination and blank

Little or no contamination of ^{226}Ra was found in reagents and multiple sample blanks (0.002 c.p.m. in ^{226}Ra region). The ^{228}Ra contamination determined at a later data was not detectable.

However, a small detector blank can be generated from recoil atoms[34] as a result of counting high activity relative to the activity of the sample such as ^{226}Ra and thorium nuclide standards. Different detectors were used to count only samples of the same level of activity. For example, the ^{226}Ra in sea water was about 0.5 c.p.m. while sediment samples contained approximately 2 c.p.m. When detectable buildup was evident (based on frequent monitoring of detector blanks) in the

region of interest, an alternative detector was used and the contaminated detector was allowed to stand for the decay of short half-life recoil atoms to take place (several weeks).

The authors are indebted to the following individuals: Dr. E. D. Goldberg of S.I.O. and Dr. K. K. Bertine of California State University at San Diego for advice and critical review of the manuscript, Dr. Y. Chung of S.I.O. for the ^{226}Ra USB standard, Dr. H. V. Weiss of N.U.C. for the ^{226}Ra USB standard and the ^{227}Ac tracer, Dr. J. Rosholt of U.S.G.S. for the thorium dioxide (1906 vintage), and Dr. V. Hodge and Dr. T. Folsom of S.I.O. for the polonium-208 tracer. The investigation was carried out under a grant from the U.S. Atomic energy commission, Division of Biology and Medicine, AT(04-3) 34, Project 84.

SUMMARY

An isotopic dilution method has been developed for the determination of ^{226}Ra and ^{228}Ra in sea water and sediments with ^{223}Ra as a yield tracer. An alternative procedure which obviates the need for ^{223}Ra is demonstrated for sediments by the assay of ^{224}Ra and ^{228}Th which occur naturally in sediments. In addition, a direct method for β-counting ^{228}Ra–^{228}Ac is proposed. Radium, polonium, thorium and uranium isotopes and ^{210}Pb are coprecipitated from sea water with aluminum phosphate carrier. The radium and lead-210 are coprecipitated with lead nitrate in sediment leachings. All radium procedures utilize identical chemical isolation and the cathodic electrodeposition of radium. Subsequently, the α-radiation emitted by ^{226}Ra, ^{223}Ra and ^{224}Ra is determined by pulse-height analysis; the ^{228}Ra–^{228}Ac and ^{210}Pb–^{210}Bi are measured by low background anticoincidence β-counting techniques. This method was used for samples containing 10^{-11}–$0.5 \cdot 10^{-12}$ g of ^{226}Ra and 10^{-13}–10^{-15} g of ^{228}Ra and gave a precision of 3–6% and 5–10% respectively, even though radium levels an order of magnitude less can be measured. The ^{226}Ra method is applicable to all environmental samples, whereas ^{228}Ra determinations are limited to applications where the $^{228}Ra/^{226}Ra$ activity ratio is greater than 0.1. This method is especially attractive for studies of parent–daughter disequilibria.

REFERENCES

1 M. Koide, K. W. Bruland and E. D. Goldberg, *Geochim. Cosmochim. Acta*, 37 (1973) 1171.
2 H. Craig, S. Krishnaswami and B. L. K. Somayajula, *Earth Planet Sci. Lett.*, 17 (1973) 295.
3 W. S. Broecker, A. Kaufman and R. M. Trier, *Earth Planet. Sci. Lett.*, 20 (1973) 35.
4 W. S. Moore and W. M. Sackett, *J. Geophys. Res.*, 69 (1964) 5401.
5 B. L. K. Somayajulu and E. D. Goldberg, *Earth Planet. Sci. Lett.*, 1 (1966) 102.
6 W. S. Moore, *Earth Planet. Sci. Lett.*, 6 (1969) 437.
7 A. Kaufman, R. N. Trier, W. S. Broecker and H. W. Feely, *J. Geophys. Res.*, 78 (1973) 8827.
8 E. Føyn, B. Karlik, H. Pettersson and E. Rona, *Nature (London)*, 143 (1939) 275.
9 W. D. Urry and C. S. Piggot, *Amer. J. Sci.*, 239 (1941) 633.
10 W. S. Broecker in T. Ichiye (Ed.), *Symposium on diffusion in oceans and fresh waters*, Lamont–Doherty Geological Observatory, Palisades, New York, 1965, p. 116.
11 F. Hagemann, *J. Amer. Chem. Soc.*, 72 (1950) 768.
12 W. S. Moore, *J. Geophys. Res.*, 74 (1969) 694.

13 K. A. Smith and E. R. Mercer, *J. Radioanal. Chem.*, 5 (1970) 303.
14 M. Koide, A. Soutar and E. D. Goldberg, *Earth Planet. Sci. Lett.*, 14 (1972) 442.
15 W. W. Flynn, *Anal. Chim. Acta*, 43 (1968) 221.
16 M. Koide and E. D. Goldberg in M. Sears (Ed.), *Progress in Oceanography, Vol. 3*, Pergamon, 1965, p. 172.
17 E. D. Goldberg and M. Koide, *Geochim. Cosmochim. Acta*, 26 (1962) 417.
18 Y. Chung and H. Craig, *Earth Planet. Sci. Lett.*, 17 (1972) 306.
19 Y. Sugimura and H. Tsubota, *J. Marine Res.*, 21 (1963) 74.
20 W. S. Broecker, A. Kaufman and R. M. Trier, *Earth Planet. Sci. Lett.*, 20 (1973) 35.
21 Y. Nozaki and S. Tsunogai, *Anal. Chim. Acta*, 64 (1973) 209.
22 J. A. Tschernichow and E. Guldina, *Z. Anal. Chem.*, 96 (1934) 260.
23 H. H. Willard and E. W. Goodspeed, *Ind. Eng. Chem., Anal. Ed.*, 8 (1936) 44.
24 D. N. Sunderman and C. W. Townley, *NAS-NA 3010*, (1970) 4.
25 E. J. Baratta and F. E. Knowles, *Anal. Chem.*, 43 (1971) 1138.
26 L. P. Gregory, *Anal. Chem.*, 44 (1972) 2113.
27 H. G. Petrow, O. A. Nietzel and M. A. De Sea, *Anal. Chem.*, 32 (1960) 926.
28 E. R. Tompkins, *J. Amer. Chem. Soc.*, 70 (1948) 3520.
29 W. H. Powers, H. W. Kirby, W. C. McCluggage, G. D. Nelson and J. H. Payne, Jr., *Anal. Chem.*, 31 (1959) 1077.
30 G. Duyckaerts and R. Lejeune, *J. Chromatogr.*, 3 (1960) 58.
31 H. Tsubota and Y. Kitano, *Bull. Chem. Soc. Jap.*, 33 (1960) 770.
32 R. M. Diamond, *J. Amer. Chem. Soc.*, 77 (1955) 2978.
33 G. M. Milton and W. E. Grumitt, *Can. J. Chem.*, 35 (1957) 541.
34 C. W. Sill and D. G. Olson, *Anal. Chem.*, 42 (1970) 1596.

Analytica Chimica Acta, 75 (1975) 21–30

DETERMINATION OF SILVER IN ROCKS BY A STOICHIOMETRIC RADIOREAGENT RADIOISOTOPE DILUTION TECHNIQUE

E. G. LILLIE
U.S. Geological Survey, Reston, Virginia 22092 (U.S.A.)
(Received 8th August 1974)

Few methods exist for the determination of silver in rock samples, largely because any useful technique must be applicable to silver concentrations of 0.1 p.p.m. or less. Most conventional spectrophotometric, atomic absorption, and spectrographic methods for silver are not capable of achieving the requisite sensitivity and hence are of no practical value in rock analysis. A colorimetric field method[1] for the determination of silver in soils and rocks that is usable down to 0.01 p.p.m. silver exists, but the precision of the method is only suitable for semiquantitative analysis. Furthermore, the variation in silver-content values[2] obtained by spectrographic analyses for the U.S. Geological Survey standard rocks indicates the unreliability of these methods. An atomic absorption technique[3] for the determination of silver in soils, sediments, and rocks involving an organic chelate extraction appears to be quite reliable but has a lower limit of 0.05 p.p.m. silver and so is unsuitable for many rocks. Although substoichiometric isotope dilution methods[4] that might accommodate the necessary low silver concentrations have been reported for silver, these have not been applied to rock analysis. Only neutron activation techniques[5,6] have provided reliable silver determinations in rocks.

The technique presented in this paper is a new but simple one. It is based entirely on the stoichiometric principle that one mole of silver iodide contains one mole of silver and one mole of iodide. An unknown amount of silver in the rock sample is diluted with an aliquot of ^{110}Ag tracer of known activity. After acid decomposition and isolation of the silver by solvent extraction, the silver is reacted with a known amount of radioactively labelled reagent iodide. The silver iodide formed is isolated by solvent extraction from any excess of silver or reagent, and the amount of silver present in the sample is determined from the ratio of the counting rate of the iodide to that of the silver in the isolated compound.

The method is capable of determining as little as 0.005 p.p.m. silver in rocks, is selective for silver, and is of more practical use on a routine basis than is neutron activation analysis. As is the case with substoichiometric isotope dilution analysis, losses of silver in the chemical operations do not affect the results. The present method, however, has the following additional advantages over substoichiometric isotope dilution techniques. (1) As long as some silver iodide is formed, neither the extent nor the reproducibility of the reaction is of any concern. (2) Because it is of no importance whether excess of silver or excess of reagent is present, the workable range is increased, and the necessity for guesswork

to estimate the concentration of complexing reagent to use is eliminated. (3) The isolation of the silver iodide need be neither complete nor reproducible as long as some silver iodide is separated and it is free of any uncomplexed silver or reagent.

EXPERIMENTAL

Reagents

All reagents were reagent grade and were used without further purification. The water used was distilled, passed through an ion-exchange column, and redistilled in a Vycor still.

Standard silver solution (1 mg Ag ml^{-1}). Dissolve 157.5 mg of silver nitrate in 100 ml of 0.5 *M* nitric acid. Prepare more dilute standards as necessary by dilution with 0.5 *M* nitric acid. Store in the dark.

Silver tracer solution. Dilute commercially available ^{110}Ag solution with 0.5 *M* nitric acid so that 0.01 ml yields about 8000 c.p.m. The silver tracer used in this work contained about 0.9 μg Ag ml^{-1}. Adjustments in dilution may be necessary to ensure that 0.01 ml of the tracer solution contains no more than 5–10 ng of silver. Store in the dark.

Perchloric acid–sodium tartrate solution. Dissolve 50 g of sodium tartrate in 1000 ml of 1 *M* perchloric acid.

Dithizone solution (0.01% w/v). Dissolve 20 mg of dithizone in 200 ml of xylene. Prepare fresh daily.

Acetic acid–sodium tartrate buffer solution. Dissolve 12.5 g of sodium tartrate in 500 ml of 4 *M* acetic acid.

Iodide tracer solution. Dilute commercially available carrier-free ^{131}I with 0.1 *M* potassium hydroxide so that 0.01 ml yields about 200,000 c.p.m. The half-life of ^{131}I is about 8 days; therefore, with this initial counting rate, the tracer will be usable for several weeks. Store in the dark.

Iodide solution (2 mg I ml^{-1}). Dissolve 236.2 mg of sodium iodide in 100 ml of 0.1 *M* potassium hydroxide. Dilute to 2 μg I ml^{-1} with 0.1 *M* potassium hydroxide. Store in the dark.

Apparatus

Glassware. Because both silver and silver iodide readily plate onto the surface of glassware, all glassware used must be thoroughly cleaned with sulfuric acid–dichromate cleaning solution and rinsed several times to ensure the complete removal of all traces of dichromate which might oxidize iodide to iodine.

Solvent extraction apparatus. All extractions in this method are performed by airstream mixing of the phases, as described by Greenland and Campbell[7]. Separatory funnels are placed in a rack under a fume hood. A glass capillary tube (1-mm i.d.) connected to a compressed air source with Tygon tubing is inserted into the open funnel top to the bottom of each funnel, and the phases are mixed by the airstream. To allow the phases to separate, the glass tube is merely raised above the liquid level. In this work, 18 samples were operated concurrently in this fashion and could be completely analyzed in a day.

Counting apparatus. A 3 × 3-in. NaI (Tl) detector coupled to two single-channel analyzers was used to count ^{110}Ag and ^{131}I simultaneously. The window

of one analyzer was adjusted to pass only the 0.88-MeV γ-ray of the ^{110}Ag. The other analyzer window was set to encompass the 0.36-MeV γ-ray of the ^{131}I. With small adjustments to these window settings, conditions can be found whereby the ^{110}Ag and the ^{131}I can be counted simultaneously with minimal mutual interference.

Procedure

Weigh enough rock sample (usually 500 mg) to yield about 5–75 ng of silver into a Teflon beaker. At the same time weigh into separate Teflon beakers about 500 mg of U.S. Geological Survey standard rock BCR-1 and about 1 g of DTS-1 or any other amount of a convenient standard rock of known silver content to yield 10–20 ng of silver. (The only function of these standards is to establish the magnitude of the silver blank.) Add 0.01 ml of silver tracer to each beaker and to a counting vial. Dilute the tracer in the counting vial to 5 ml with water for a silver counting standard. Add 10 ml of concentrated nitric acid, 15 ml of 40% hydrofluoric acid, and 1 ml of 72% perchloric acid to each beaker and evaporate overnight on a hot plate at a surface temperature of about 120°C.

Dissolve the residues by heating with 20 ml of perchloric acid–sodium tartrate solution. Cool and transfer the solutions to separatory funnels. Add 10 ml of dithizone solution and extract for 2 min. Discard the aqueous layers and wash the organic phases twice with 10 ml of water. Add 5 ml of 1 *M* hydrochloric acid and extract for 1 min. While continuing to mix the phases, add 10 ml of chloroform. Allow the phases to separate and discard the organic layers. Wash the aqueous phases 3 times with 5 ml of chloroform. Transfer the aqueous phases to clean Teflon beakers. Add 1 ml of concentrated nitric acid and evaporate to dryness on a hot plate at a surface temperature of about 220°C. Add 0.5 ml of concentrated nitric acid to the residues and again evaporate to dryness.

Remove the beakers from the hot plate and, while they are still hot, add 0.5 ml of 2 *M* nitric acid and swirl to dissolve the residues. Cool and add 5 ml of the acetic acid–sodium tartrate buffer solution. Transfer the solutions to *clean well-rinsed* funnels and add 5 ml of amyl alcohol. Prepare an iodide counting standard by adding 0.01 ml of iodide tracer to a counting vial and diluting it to 5 ml with water. Sample by sample, begin mixing the phases in each funnel and immediately add 0.01 ml of iodide tracer. After all the samples are mixing, and iodide tracer has been added to each funnel, add 0.05 ml of 2 μg ml^{-1} iodide solution. (Isotopic exchange between the iodide tracer and the added iodide occurs rapidly, and the order of addition here is merely to prevent the precipitation or extraction of silver iodide before the tracer is added. The iodide solution and the iodide tracer may be mixed and added in one step as long as the half-life of the tracer is taken into account.) Continue to mix the phases for 15 min; any amount of time over 5 min is sufficient for the reaction to take place. Allow the phases to separate, and discard the aqueous layers. Wash the organic phases sequentially with 10 ml of water and 5 ml of 0.005 *M* potassium hydroxide. Drain the organic phases into counting vials and count silver and iodide simultaneously in the samples, the silver and iodide counting standards, and the background.

Calculations

The silver and iodide counting rates obtained must be corrected for mutual

interference. To do this it is assumed, and experiment substantiates this, that the counting rate in any one peak is directly proportional to the counting rate at any other point in the same spectrum. The proportionality constant for any given isotope is given by:

$$k = \frac{a''}{a'} \tag{1}$$

where a' is the counting rate observed in the peak for the given isotope and a'' is the corresponding counting rate observed in any other given channel.

The true counting rate in the peak, a, of one of the isotopes in a mixture of two isotopes is, therefore, determined by subtracting the contribution of the other isotope from the observed total counting rate in the particular peak channel. In the case of a mixture of silver and iodide isotopes:

$$a_{\mathrm{I}} = a'_{\mathrm{I}} - q a_{\mathrm{Ag}} \tag{2}$$

where q is the proportionality constant (from eqn. 1) for silver, and

$$a_{\mathrm{Ag}} = a'_{\mathrm{Ag}} - p a_{\mathrm{I}} \tag{3}$$

where p is the proportionality constant (from eqn. 1) for iodide. Solving the simultaneous eqns. (2) and (3):

$$a_{\mathrm{I}} = \frac{a'_{\mathrm{I}} - q a'_{\mathrm{Ag}}}{1 - pq} \tag{4}$$

and

$$a_{\mathrm{Ag}} = \frac{a'_{\mathrm{Ag}} - p a'_{\mathrm{I}}}{1 - pq} \tag{5}$$

After subtracting the background counting rates from all the observed counting rates in both the iodide-peak and silver-peak channels, the proportionality constants, p and q, are determined, by means of eqn. (1), from the observed counting rates of the iodide and silver counting standards. The true iodide and silver counting rates for each sample can then be determined by eqns. (4) and (5), respectively.

The mass, m_{Ag}, in nanograms of silver present in each sample is determined by the following equation (the derivation of which will be presented later in this paper):

$$m_{\mathrm{Ag}} = 0.850\, m_{\mathrm{I}} \left[\frac{a_{\mathrm{I}} A_{\mathrm{Ag}}}{a_{\mathrm{Ag}} A_{\mathrm{I}}} \right] - m''_{\mathrm{Ag}} \tag{6}$$

where a_{I} and a_{Ag} have been defined previously, A_{Ag} and A_{I} are the observed counting rates of the silver and iodide counting standards in their respective peak channels, m_{I} is the mass in nanograms of iodide added, and m''_{Ag} is the silver blank.

The chief source of the silver blank is in the silver tracer. Therefore, the blank can be approximated from the specific activity of the tracer. The magnitude of the blank can be established further by the use of the standard rocks analyzed with the samples. Rearranging eqn. (6):

$$m''_{\mathrm{Ag}} = 0.850\, m_{\mathrm{I}} \left[\frac{a_{\mathrm{I}} A_{\mathrm{Ag}}}{a_{\mathrm{Ag}} A_{\mathrm{I}}} \right] - m_{\mathrm{Ag}} \tag{7}$$

where the known mass of silver, m_{Ag}, and the corresponding ratio of iodide to silver counting rates for each standard rock is used and an average for m''_{Ag} is taken.

RESULTS AND DISCUSSION

Theory

The principle behind the method described in this paper is a simple one of stoichiometry. By reacting a known mass of iodide of known specific activity with an unknown variable mass of silver of known total activity and separating the silver iodide thus formed from any excess of silver or iodide ions, the amount of silver originally present in the sample can be determined by the ratio of the counting rates of the iodide and silver in the isolated compound. The relationship between the mass of silver present in the sample and the counting rates of the silver and iodide in the separated silver iodide can be determined as follows:

$$m'_{Ag} = a_{Ag} \frac{(m_{Ag} + m''_{Ag})}{A_{Ag}} \tag{8}$$

where m'_{Ag} is the mass of silver separated as silver iodide, a_{Ag} is the counting rate of the separated silver, m_{Ag} is the original mass of silver present in the sample, m''_{Ag} is the mass of silver present in the reagents and silver tracer (the blank), and A_{Ag} is the counting rate of the silver counting standard. Similarly:

$$m'_I = a_I \frac{m_I}{A_I} \tag{9}$$

where m'_I is the mass of iodide separated as silver iodide, a_I is the counting rate of the separated iodide, m_I is the mass of iodide added, and A_I is the counting rate of the iodide counting standard.

By the laws of stoichiometry:

$$\frac{m'_I}{m'_{Ag}} = \frac{\text{mol. wt. I}}{\text{mol. wt. Ag}} = \frac{1}{0.850} = \frac{a_I m_I}{A_I} \times \frac{A_{Ag}}{a_{Ag}(m_{Ag} + m''_{Ag})} \tag{10}$$

Simplifying eqn. (10) and solving for m_{Ag}:

$$m_{Ag} = 0.850\, m_I \left[\frac{A_{Ag}}{A_I}\right]\left[\frac{a_I}{a_{Ag}}\right] - m''_{Ag} \tag{11}$$

For each set of experiments, the mass of added iodide and the counting rates of both the silver and iodide counting standards are constant; therefore, the mass of silver in the sample is directly proportional to the ratio of the counting rate of the iodide to that of the silver in the separated silver iodide. A plot of these ratios *versus* the mass of silver in the sample gives a straight line with a slope directly proportional to the product of the mass of the iodide added and the ratio of the standard counting rates and an intercept equal to the silver blank. Although the slope will change from day to day according to the half-lives of the isotopes involved, all quantities on the right-hand side of eqn. (11) can be measured easily. Therefore, this technique provides an absolute, rather than a relative, determination of silver.

Standard curve

It was established by means of standard silver solutions that the relationship between silver concentration and the ratio of the counting rate of the iodide to that of the silver in the isolated silver iodide, under the conditions described in this paper, does indeed conform to theory. However, attempts to carry pure silver solutions through the entire procedure led to erratic results, especially at low silver concentrations where the ratios were often higher than they should have been. Although the exact cause of this phenomenon is unknown, it was observed that silver tracer run through the procedure by itself as a blank often had a higher iodide-to-silver count ratio than did the same amount of silver tracer run with a standard rock of low silver concentration. Possibly this effect reflects the absence of salts during the evaporation process. The silver values for the U.S. Geological Survey standard rocks given in this paper were all calculated directly from eqn. (6), without reference to a standard curve, after separately determining the silver blank.

Separations

Several potential sources of interference with the final reaction of silver and iodide are present in the analysis of rock samples. It is essential, therefore, that several conditions be met in order for the silver iodide complexation to be performed properly. There must be (1) no metal present that will complex preferentially with iodide; (2) no ligand that silver will select over iodide; (3) no iodide from the sample; (4) no reducing agent, as silver is readily reduced to the metal; and (5) no oxidizing agent that would convert iodide to iodine.

Most of these conditions are easily met. The acid decomposition volatilizes mercury, the most likely metal to compete with silver for iodide. It also ensures the oxidation of sulfide and other sulfur products which are the most likely ligands to compete with iodide for silver, and it precludes the possibility of iodide from the sample.

The greatest problem involved in preparing the sample solution for the reaction between silver and iodide concerns the elimination of all oxidizing agents that might oxidize the added iodide to iodine. The acid concentration necessary to dissolve the sample residue and the large amount of iron(III) present in most rocks makes it imperative to isolate the silver in the sample.

Dithizone has long been used to separate silver from other elements. The extraction of silver dithizonate from acid media[8,9] into nonpolar solvents and its back-extraction into chloride solutions[9] is well known, the separation being highly selective for silver. Xylene was chosen as the solvent solely for practical reasons; being less dense than water, it facilitates the discarding of the aqueous phase from the separatory funnel.

It was found that under the conditions specified in this paper, more than 95% of the silver could be stripped from the xylene with 1 *M* hydrochloric acid. Most of the species formed on back-extraction is probably $AgCl_2^-$ and, theoretically, the low concentration of chloride needed to strip the silver should have no effect on the formation of silver iodide as the stability constant of the latter is much greater than for silver chloride species. In addition, any excess of $AgCl_2^-$ should not extract into amyl alcohol along with silver iodide as it is a charged species. In practice, the latter was found to be true. However, once the silver chloride

species had formed, the chloride could not be displaced by iodide, possibly because of structural differences between the silver chloride species and silver iodide. Therefore, it was necessary to remove the chloride by evaporation with nitric acid and thus convert the silver to the nitrate. This also facilitated the obtainment of optimal conditions for the complexation and separation of the silver iodide.

A method was sought to isolate silver iodide effectively from any excess of silver or iodide. Plating out or precipitation of silver iodide onto glassware was attempted without much success, as excess of silver inevitably accompanied the silver iodide. Therefore, a solvent was sought that would extract silver iodide. Hydrocarbons and substituted hydrocarbons were not effective, and many oxygenated solvents spontaneously oxidized the added iodide to iodine, which was then extracted. It was found, however, that amyl alcohol readily extracts silver iodide with negligible oxidation of iodide as long as the pH of the solution is maintained at 2 or above. Excess of silver is not extracted into amyl alcohol; however, the extraction of silver iodide seems to improve with increasing hydrogen ion concentration. Because the method requires neither the complete complexation nor the complete extraction of the silver iodide as long as no excess silver or iodide reagent accompanies it, it is more advantageous to avoid the oxidation of iodide to iodine than to improve the extent of complexation and extraction. Therefore, a buffer solution is used to keep the pH of the solution around 2.

Because the buffer solution is partially soluble in the amyl alcohol, the organic phase is washed after the extraction with water. The final wash with dilute potassium hydroxide removes any iodine that may have been extracted along with the silver iodide.

The method presented is independent of silver yield if no reagent blank is added after losses occur. The reagents used in this work had no appreciable amount of silver in them, and the main source of the blank, the silver tracer, is added before any separations. Hence, no correction for silver yield is necessary. The actual yields after the dithizone extraction, washes, and stripping are greater than 95%.

Analysis of rocks

The precision of this method was tested by analyzing replicates from each of three bottles of eight and from single bottles of five other U.S. Geological Survey standard rocks. To get the best estimate of precision and to minimize systematic errors, the various aliquots were randomized and analyzed over a period of several days. The results of these analyses are given in Table I. A one-way analysis-of-variance calculated from these analytical data is shown in Table II. The analytical relative deviation calculated from the within-bottles variance is less than 10% for all but two of the rocks, GSP-1 and G-2. Sampling error or inhomogeneous distribution of silver may account for the slightly larger relative deviations for these two rocks.

The F ratios in Table II show that, except for QL-1, no significant difference exists among the bottles of each standard taken. A difference that is significant at greater than the 99% confidence level was found between one of the bottles of QL-1 taken and the other two. Thus, the reliability of QL-1 as a standard, at

TABLE I

ANALYSES OF U.S. GEOLOGICAL SURVEY STANDARD ROCKS

Rock	*Silver ($\mu g\ g^{-1}$)*[a]
STM-1, Nepheline syenite	(0.078, 0.073, 0.084) (0.082, 0.078, 0.076) (0.084, 0.074, 0.076)
BCR-1, Basalt	(0.036, 0.035, 0.038) (0.033, 0.034, 0.033) (0.032, 0.036, 0.040)
RGM-1, Rhyolite	(0.094, 0.11, 0.093) (0.10, 0.11, 0.090) (0.092, 0.096, 0.11)
AGV-1, Andesite	(0.083, 0.081, 0.078) (0.083, 0.083, 0.077) (0.082, 0.079, 0.077)
QL-1, Quartz latite	(0.082, 0.075, 0.077) (0.062, 0.066, 0.062) (0.069, 0.061, 0.066)
BHVO-1, Basalt	(0.054, 0.054, 0.052) (0.056, 0.064, 0.056) (0.053, 0.058, 0.059)
GSP-1, Granodiorite	(0.077, 0.067, 0.064) (0.085, 0.079, 0.069) (0.092, 0.074, 0.069)
G-2, Granite	(0.048, 0.042, 0.042) (0.051, 0.035, 0.042) (0.044, 0.039, 0.047)
W-1, Diabase	(0.056, 0.064, 0.060, 0.059)
G-1, Granite	(0.043, 0.037, 0.037)
DTS-1, Dunite	(0.010, 0.009, 0.011, 0.010, 0.010)
PCC-1, Peridotite	(0.008, 0.008, 0.009, 0.008)
SDC-1, Mica schist	(0.046, 0.048, 0.048)

[a] Splits of given bottle in parentheses.

TABLE II

STATISTICAL STUDY OF SILVER ANALYTICAL DATA FOR U.S. GEOLOGICAL SURVEY STANDARD ROCKS

Rock	*Mean silver content ($\mu g\ g^{-1}$)*	*Analytical error*[a]	*Analytical relative deviation (%)*	*F ratio*
STM-1, Nepheline syenite	0.078	0.00475	6.1	<1, N.S.
BCR-1, Basalt	0.035	0.00249	7.1	1.3, N.S.
RGM-1, Rhyolite	0.099	0.00967	9.8	<1, N.S.
AGV-1, Andesite	0.080	0.00287	3.6	<1, N.S.
QL-1, Quartz latite[b]	—	0.00340	—	16.4, Sig.
BHVO-1, Basalt	0.056	0.00332	5.9	2.0, N.S.
GSP-1, Granodiorite	0.075	0.00927	12.4	<1, N.S.
G-2, Granite	0.043	0.00556	12.9	<1, N.S.
W-1, Diabase	0.060	0.00330	5.5	—
G-1, Granite	0.039	0.00346	8.9	—
DTS-1, Dunite	0.010	0.000707	7.1	—
PCC-1, Peridotite	0.008	0.000500	6.1	—
SDC-1, Mica schist	0.047	0.00115	2.4	—

[a] Standard deviation, calculated from within-bottles variance.

[b] As the F ratio shows significance at the 99% confidence level, an overall mean and analytical relative deviation could not be determined. Bottle by bottle, these figures are, respectively: A—0.078, 4.4%; B—0.063, 5.4%; C—0.065, 5.2%.

TABLE III

COMPARISON OF SILVER-CONTENT VALUES ($\mu g\ g^{-1}$) OF U.S. GEOLOGICAL SURVEY STANDARD ROCKS WITH VALUES OBTAINED BY NEUTRON ACTIVATION ANALYSIS

Rock	*This work*	*Brunfelt and Steinnes (Ref. 5)*	*Greenland and Fones (Ref. 6)*
W-1, Diabase	0.060	0.068	0.081
AGV-1, Andesite	0.080	0.094	0.11
BCR-1, Basalt	0.035	0.036	0.036
DTS-1, Dunite	0.010	0.010	0.008
G-2, Granite	0.043	0.040	0.049
GSP-1, Granodiorite	0.075	0.084	0.10
PCC-1, Peridotite	0.008	0.009	0.005
G-1, Granite	0.039	—	0.052

least for silver, is questionable.

To determine the accuracy of the method, the mean silver values for the U.S. Geological Survey standard rocks obtained by this method are compared with those obtained by neutron activation analysis in Table III. The results of Brunfelt and Steinnes[5] are in reasonable agreement with the present work. Except for BCR-1, DTS-1, and PCC-1, the results obtained by Greenland and Fones[6] are slightly higher than those obtained by both Brunfelt and Steinnes and by this method.

I am indebted to L. P. Greenland, P. Baedecker, and I. May for their helpful comments on this manuscript. I am especially grateful to L. P. Greenland for much encouragement throughout this work.

SUMMARY

A rapid procedure for the routine determination of nanogram amounts of silver in rocks is described. After dissolution of the sample with a hydrofluoric–nitric–perchloric acid mixture in the presence of ^{110}Ag tracer, the silver is separated by extraction as the dithizonate into xylene and back-extracted into dilute hydrochloric acid. After evaporation and removal of the hydrochloric acid, the silver is taken up in an acetic acid–sodium tartrate buffer solution and reacted with a constant amount of radioactively labelled iodide. The silver iodide formed is isolated by extraction into amyl alcohol, and silver is determined by the ratio of the counting rate of the iodide to that of the silver in the silver iodide complex. Results of the analyses of several U.S. Geological Survey standard rocks are given.

REFERENCES

1 H. M. Nakagawa and H. W. Lakin, *U.S., Geol. Surv., Prof. Paper*, 525-C (1965) C172.
2 F. J. Flanagan, *Geochim. Cosmochim. Acta*, 33 (1969) 81.
3 T. T. Chao, J. W. Ball and H. M. Nakagawa, *Anal. Chim. Acta*, 54 (1971) 77.

4 J. Ruzicka and J. Stary, *Substoichiometry in Radiochemical Analysis*, Pergamon, Oxford, 1968, pp. 111, 112.
5 A. O. Brunfelt and E. Steinnes, *Radiochem. Radioanal. Lett.*, 1 (1969) 219.
6 L. P. Greenland and R. Fones, *N. Jb. Miner. Mh.*, 9 (1971) 393.
7 L. P. Greenland and E. Y. Campbell, *Anal. Chim. Acta*, 67 (1973) 29.
8 E. B. Sandell, *Colorimetric Determination of Traces of Metals*, Interscience, New York, 3rd edn., 1959, pp. 812–814.
9 G. H. Morrison and H. Freiser, *Solvent Extraction in Analytical Chemistry*, Wiley, New York, 1965, pp. 173–177.

Analytica Chimica Acta, 75 (1975) 31–39

DETERMINATION OF 17 TRACE ELEMENTS IN GALLIUM ARSENIDE BY REACTOR NEUTRON ACTIVATION ANALYSIS

W. MAENHAUT*

Institute for Nuclear Sciences, Rijksuniversiteit Gent, Proeftuinstraat 86, B 9000 Gent (Belgium)

(Received 3rd September 1974)

In spite of the very high matrix activity induced, reactor neutron activation has frequently been applied for the determination of trace constituents in gallium arsenide[1–22]. However, only a few methods have been described which allow the determination of more than ten elements. These methods, which have been developed by Artyukhin *et al.*[1], Gilbert and Artyukhin[4], and Neeb *et al.*[16], involve rather complex chemical separations and NaI(Tl) γ-ray spectrometry of the different fractions obtained.

In this work, a method is presented for the determination of 17 trace elements by means of their long-lived radioisotopes. After decay of ^{72}Ga and ^{76}As, the ^{74}As activity, which is due to a (n,2n) reaction with the fast neutron component of the reactor, is separated from the non-volatile elements by distillation as arsenic trichloride. The radioactivities formed from scandium, chromium, iron, cobalt, nickel, zinc, silver, indium, tin, antimony, tellurium and six rare earth metals are determined by a single measurement of the distillation residue with a Ge(Li) detector. With the aid of a comparator method[23–25], the concentration of each element is calculated.

Nuclear data

The nuclear data of the radioisotopes formed by reactor irradiation of gallium arsenide are given in Table I[26–28]. It appears that only two radioisotopes are formed with a half-life longer than 1 day, *i.e.* ^{76}As and ^{74}As. After a decay period of about 30 days, however, the ^{76}As activity is reduced by a factor of 10^8, so that the Ge(Li) γ-ray spectrum of an irradiated gallium arsenide sample is nearly a pure ^{74}As spectrum. Because of this high ^{74}As activity, non-destructive analysis of trace elements at the p.p.b. level is not feasible.

The nuclear data of the elements determined in gallium arsenide, together with those of the flux monitors used, are summarized in Table II[26,27,29]. Only these reactions and γ-ray energies are given which have been used in this work. Most I_0/σ_{th} ratios have been determined by Van der Linden[30]. For the reaction ^{112}Sn(n,γ)^{113}Sn, however, the I_0/σ_{th} ratio has been determined previously[31], whereas for the reaction ^{122}Te(n,γ)^{123m}Te, it was calculated from the cross-section data given by Holden and Walker[26]. The reliability of this last value was checked by cadmium ratio experiments. These yielded a I_0/σ_{th} ratio of 22.9.

* Research associate of the "Nationaal Fonds voor Wetenschappelijk Onderzoek".

TABLE I

NUCLEAR DATA OF THE ISOTOPES FORMED BY REACTOR IRRADIATION OF GALLIUM ARSENIDE

Reaction	*Isotopic abundance, (%)*	*Cross-section[a] (barn)*	*Half-life*	*Decay mode and γ-energies (keV)*
$^{69}Ga(n, \gamma)^{70}Ga$	60	1.7	21.1 min	β^-; γ 173.0, 1042.0
$(n, p)^{69m}Zn$		$2.3 \cdot 10^{-3}$	13.9 h	I.T.438.7; β^-; γ
$(n, p)^{69}Zn$			57 min	β^-; γ
$(n, \alpha)^{66}Cu$		$1.5 \cdot 10^{-3}$	5.10 min	β^-; γ 1039.0
$(n, 2n)^{68}Ga$		$0.21 \cdot 10^{-3}$	68.2 min	β^+; E.C.; γ
$^{71}Ga(n, \gamma)^{72m}Ga$	40	0.1	37 ms	I.T.; γ
$(n, \gamma)^{72}Ga$		4.6	14.10 h	β^-; γ 630.1, 834.1
$(n, p)^{71m}Zn$		$0.16 \cdot 10^{-3}$	3.97 h	β^-; γ
$(n, p)^{71}Zn$			2.4 min	β^-; γ 511.6
$(n, \alpha)^{68m}Cu$		$0.038 \cdot 10^{-3}$	3.8 min	I.T.; γ; β^-
$(n, \alpha)^{68}Cu$			31 s	β^-; γ
$(n, 2n)^{70}Ga$		$0.76 \cdot 10^{-3}$	21.1 min	β^-; γ 173.0, 1042.0
$^{75}As(n, \gamma)^{76m}As$	100	4.4	1.9 μs	I.T.
$(n, \gamma)^{76}As$			26.3 h	β^-; γ 559.1
$(n, p)^{75m}Ge$		$1.3 \cdot 10^{-3}$	28.9 s	I.T. 139.8
$(n, p)^{75}Ge$			82.8 min	β^-; γ 264.6
$(n, \alpha)^{72m}Ga$		$0.13 \cdot 10^{-3}$	37 ms	I.T.; γ
$(n, \alpha)^{72}Ga$			14.10 h	β^-; γ 630.1, 834.1
$(n, 2n)^{74}As$		$0.24 \cdot 10^{-3}$	17.76 day	E.C., β^+, β^-, γ 595.9

[a] For (n, γ) reactions: thermal neutron cross-section[26]. For threshold reactions: estimated average cross-section in a fission neutron spectrum[28].

EXPERIMENTAL

Counting equipment and data processing

The radioactivities were measured with a Ge(Li) detector (Philips) of 14.2% detection efficiency. The energy resolution (FWHM) was 2.1 keV for the 1332.5-keV transition of ^{60}Co. The detector was connected to a Philips 56056/01 DC pre-amplifier, a Canberra 1413 amplifier, a 100-MHz Intertechnique C 44B ADC and an Intertechnique DIDAC 4000-channel memory. The DIDAC was interfaced to a PDP-11/20 computer, used for data transfer on magnetic tape. Processing of the spectra was performed with the aid of a PDP-9 computer. The FORTRAN program ANGEL was used for peak area integration[33].

Comparator method

For most of the elements analysed, a k-value, defined by eqn. (1)[25], was determined.

$$k = \frac{A_{sp}(T, t)\, S_c D_c}{A_{sp,c}(T, t)\, SD} \tag{1}$$

where $A_{sp}(T, t)$ is the specific photopeak count rate for a radioisotope formed by a

TABLE II

NUCLEAR DATA OF THE FLUX MONITORS AND OF THE ELEMENTS DETERMINED IN GALLIUM ARSENIDE

Reaction	*Isotopic abundance (%)*	*Thermal neutron cross-section (barn)*	I_o^a σ_{th}	*Half-life*	*γ-Energy (keV)*
$^{59}Co(n,\gamma)^{60}Co$	100	37	2.03	5.272 year	1173.2, 1332.5
$^{197}Au(n,\gamma)^{198}Au$	100	98.8	15.7	2.695 day	411.8
$^{96}Ru(n,\gamma)^{97}Ru$	5.5	0.25	23.1	2.89 day	215.8
$^{102}Ru(n,\gamma)^{103}Ru$	31.6	1.3	3.3	39.6 day	497.9
$^{45}Sc(n,\gamma)^{46}Sc$	100	26	0.50	83.8 day	889.3
$^{50}Cr(n,\gamma)^{51}Cr$	4.35	15.9	0.49	27.71 day	320.1
$^{58}Fe(n,\gamma)^{59}Fe$	0.31	1.14	1.4	44.6 day	1099.3
$^{58}Ni(n,p)^{58}Co$	68.3	0.104[b]		71.3 day	810.8
$^{64}Zn(n,\gamma)^{65}Zn$	48.9	0.78	2.2	243.7 day	1115.5
$^{109}Ag(n,\gamma)^{110m}Ag$	48.17	4	12.2	252 day	884.5
$^{113}In(n,\gamma)^{11m1}In$	4.3	7.8	27.3	49.51 day	190.2
$^{112}Sn(n,\gamma)^{113}Sn$	1.0	0.7	49	115 day	391.7
$^{116}Sn(n,\gamma)^{117m}Sn$	14.4	0.006	81	14 day	158.4
$^{123}Sb(n,\gamma)^{124}Sb$	42.7	4.06	28.4	60.20 day	602.7
$^{122}Te(n,\gamma)^{123m}Te$	2.4	3	23.3	119.7 day	158.8
$^{140}Ce(n,\gamma)^{141}Ce$	88.5	0.56	0.76	32.53 day	145.4
$^{146}Nd(n,\gamma)^{147}Nd$	17.2	1.3	2.03	10.99 day	531.0
$^{151}Eu(n,\gamma)^{152}Eu$	47.8	5800	0.67	13 year	344.2
$^{159}Tb(n,\gamma)^{160}Tb$	100	25	16.1	72.3 day	298.6
$^{168}Yb(n,\gamma)^{169}Yb$	0.14	3500	7.2	31 day	197.8
$^{176}Lu(n,\gamma)^{177}Lu$	2.6	2100	0.52	6.71 day	208.4

[a] I_0: Resonance integral; σ_{th}: thermal neutron cross-section.
[b] Average cross-section in a fission neutron spectrum[32].

(n,γ) reaction after an irradiation time T and decay time t; S, saturation factor $= 1-e^{-\lambda T}$; λ, decay constant; D, decay factor $= e^{-\lambda t}$; c, index referring to the comparator. The reaction $^{59}Co(n,\gamma)^{60}Co$ was used as comparator reaction. The specific photopeak count rate $A_{sp,c}(T,t)$ was derived from the sum of the 1173.2-keV and 1332.5-keV full-energy peak areas. The k-values were determined for a standard irradiation site in the Thetis reactor (University of Ghent), for which the thermal-to-epithermal flux ratio (ϕ_{th}/ϕ_{epi}) was equal to 23.8. In order to avoid errors from self-shielding and flux gradients, different nitric acid solutions containing an element of interest, the cobalt comparator and a high concentration of an element of low neutron cross-section, were prepared. From these solutions 100-μl volumes were pipetted into polythene vials, evaporated and irradiated. Tin, however, was irradiated in the metallic state; for indium 10 mg of an In–Al (1% In) alloy was used. Here, flux gradients were minimized by placing 10 mg of a Co–Al (2% Co) alloy as close as possible to the samples. After irradiation, the radioisotopes were dissolved in 20 ml of 12 M hydrochloric acid, which were transferred to a 20-ml glass vial for counting. The k-values obtained are listed in Table III.

Separation technique

For the separation of the arsenic matrix activity, a highly selective distillation

TABLE III

DETERMINATION OF k-VALUES FOR THE STANDARD IRRADIATION SITE IN THE THETIS REACTOR

Reaction	*γ-Energy used (keV)*	*k-Value*
$^{45}Sc(n,\gamma)^{46}Sc$	889.3	0.604
$^{50}Cr(n,\gamma)^{51}Cr$	320.1	$3.60 \cdot 10^{-3}$
$^{58}Fe(n,\gamma)^{59}Fe$	1099.3	$32.4 \cdot 10^{-6}$
$^{64}Zn(n,\gamma)^{65}Zn$	1115.5	$2.50 \cdot 10^{-3}$
$^{109}Ag(n,\gamma)^{110m}Ag$	884.5	$19.7 \cdot 10^{-3}$
$^{113}In(n,\gamma)^{114m}In$	190.2	$4.85 \cdot 10^{-3}$
$^{112}Sn(n,\gamma)^{113}Sn$	391.7	$0.188 \cdot 10^{-3}$
$^{116}Sn(n,\gamma)^{117m}Sn$	158.4	$0.174 \cdot 10^{-3}$
$^{123}Sb(n,\gamma)^{124}Sb$	602.7	$42.5 \cdot 10^{-3}$
$^{122}Te(n,\gamma)^{123m}Te$	158.8	$0.702 \cdot 10^{-3}$
$^{140}Ce(n,\gamma)^{141}Ce$	145.4	$8.95 \cdot 10^{-3}$
$^{146}Nd(n,\gamma)^{147}Nd$	531.0	$0.330 \cdot 10^{-3}$
$^{151}Eu(n,\gamma)^{152}Eu$	344.2	11.31
$^{159}Tb(n,\gamma)^{160}Tb$	298.6	0.177
$^{168}Yb(n,\gamma)^{169}Yb$	197.8	$38.1 \cdot 10^{-3}$
$^{176}Lu(n,\gamma)^{177}Lu$	208.4	0.256

method was developed, based on the volatility of arsenic trichloride. Special care was taken to retain tin and antimony in the distillation residue.

Procedure. Transfer the gallium arsenide sample (0.1 g), together with 100 μl of a carrier solution containing 1 mg of tin, 1 mg of antimony and 10 μg of the other elements analysed, to a 100-ml flask provided with a reflux condenser. Add 10 ml of 12 *M* hydrochloric acid and 2 ml of bromine. Heat the mixture gently until complete dissolution of the gallium arsenide sample has been achieved. Transfer the solution to a distillation apparatus described by Scherrer[34–36]. Rinse the 100-ml flask with two 5-ml portions of 12 *M* hydrochloric acid. For the collection of the distillate, place two traps in series. Fill the first with 10 ml of 6 *M* hydrochloric acid and the second with 10 ml of a 10% hydroxylammonium chloride solution. Pass a stream of CO_2 through the distillation apparatus and heat the gallium arsenide solution to 60°C. Keep the temperature constant for 15 min, during which time practically all bromine is distilled. Add 10 ml of a 10% hydroxylammonium chloride solution, in order to reduce the last traces of bromine to bromide and to reduce As(V) to As(III). Raise the temperature to the boiling point of the solution, which is approximately 109°C. After about 15 min, when a temperature of 111°C has been reached, stop the distillation. Introduce 10 mg of arsenic carrier together with 20 ml of 12 *M* hydrochloric acid into the distillation apparatus, and carry out a second distillation of arsenic trichloride. After the temperature again reaches 111°C, allow the distillation residue to cool and transfer it to a 20-ml glass vial. Rinse the distillation apparatus with two 5-ml portions of 12 *M* hydrochloric acid.

The results obtained for the tracer experiments when the distillation procedure described was applied, are given in Table IV. It appears that tin and antimony are almost quantitatively retained in the distillation residue, whereas for the arsenic

TABLE IV

DISTILLATION OF ARSENIC TRICHLORIDE

Element	*Tracer used*	*% in bromine distillate*	*% in 1st $AsCl_3$ distillate*	*% in 2nd $AsCl_3$ distillate*	*% in 2nd trap*	*% in distn. residue*
As	^{76}As	0.5	99	0.3	0.6	$<1.3\cdot10^{-3}$
Sn	^{113}Sn	<0.18	2.0	1.6	<0.18	96
Sb	^{124}Sb	<0.15	2.0	1.8	<0.15	97
Te	^{123m}Te	<0.03	0.6	0.6	<0.03	100

tracer a distillation yield of more than 99.999% is obtained after two distillations of arsenic trichloride.

Irradiation

Gallium arsenide samples of $1.5 \times 1.5 \times 10$ mm (weight about 0.1 g) were wrapped in aluminium foil and placed in a graphite irradiation container. For this type of sample, thermal neutron self-shielding can be neglected. Indeed, for a cylindrical sample of the same cross-sectional area, the thermal absorption factor amounts to 0.982, as can be calculated from the equations given by Zweifel[37,38]. Together with the samples, nickel standards and cobalt, gold and ruthenium flux monitors were irradiated. The irradiation took place in the BR 2 reactor (Mol, Belgium). The irradiation time was 10 days, at a thermal neutron flux of about $2\cdot10^{13}$ n cm^{-2} s^{-1}.

Treatment of the gallium arsenide samples after irradiation

After a decay period of about 20 days, each gallium arsenide sample was washed with water and submitted to the following decontamination procedure. First, it was placed for 5 min in an oxidizing mixture and heated to 76°C; the mixture consisted of 50 ml of 18 *M* sulphuric acid, 15 ml of 30% hydrogen peroxide and 15 ml of water. The sample was then etched for 2 min in a 1% solution of bromine in methanol and finally, it was placed for 5 min in 50% hydrofluoric acid. The sample was then weighed and transferred to a 100-ml flask. Dissolution and distillation of arsenic trichloride were carried out as described above. The distillation residue was transferred to a 20-ml glass vial, made up to 20 ml with 12 *M* hydrochloric acid, and counted for about 1000 min. A typical spectrum is shown in Fig. 1. Peaks which are due to the background are marked with (Bkgd).

Treatment of the standards and flux monitors

The cobalt, gold and ruthenium flux monitors were counted in a standard geometry with the Ge(Li) detector. As cobalt also served as comparator, the ^{60}Co activity was remeasured in the same conditions as the distillation residues from the gallium arsenide samples. This last geometry was also used for the counting of the nickel standards.

Calculation of results

The impurity concentrations for the different elements were obtained from the

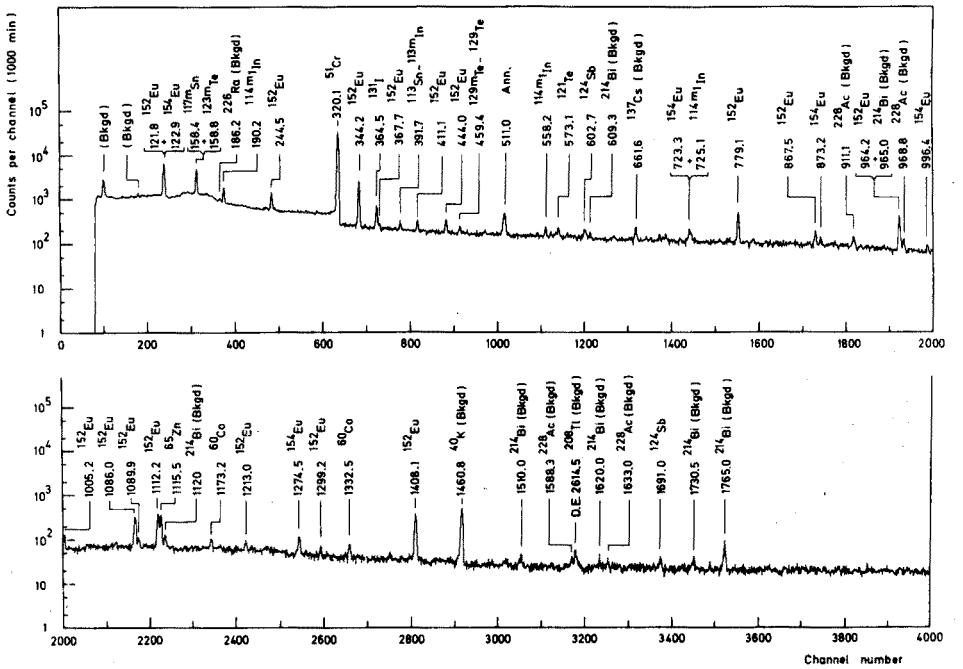

Fig. 1. Ge(Li) γ-ray spectrum of a distillation residue (decay time: 35 day).

net peak areas for distillation residues and standards. Nearly all standard net peak areas were computed with the aid of the comparator method[23–25]. For this purpose, the thermal-to-epithermal flux ratio in the BR 2 irradiation had to be known. This was derived from the measurement of the cobalt, gold and ruthenium flux monitors[25,39]. An average flux ratio of 113 was found.

Since all distillation residues contained only a very low ^{60}Co activity, correction for the background ^{60}Co activity was necessary. This correction was carried out with the aid of a pure background spectrum. For the 158.8-keV peak of ^{123m}Te and for the 1115.5-keV peak of ^{65}Zn, spectral interferences had to be taken into account. In the 158.8-keV peak area there was a contribution from the 158.4-keV peak of ^{117m}Sn. This contribution was derived from the 391.7-keV peak area of ^{113}Sn and from the ratio of the 158.4-keV to 391.7-keV peak intensities computed for the tin standard. The 1115.5-keV peak of ^{65}Zn was not fully resolved from the 1112.2-keV peak of ^{152}Eu. Here, the sum of both peak areas was determined, after which the contribution from the 1112.2-keV peak was calculated from the 1408.1-keV peak area and from the ratio of the 1112.2-keV to 1408.1-keV peak intensities in a pure ^{152}Eu spectrum. Because both ^{152}Eu and ^{154}Eu contributed to the 122-keV peak area, application of the comparator method was impossible for this peak. Therefore, the europium determination was based on the smaller 344.2-keV peak of ^{152}Eu. For distillation residues containing a low europium activity, the 344.2-keV peak area was calculated by multiplying the 122-keV peak area by the 344.2-keV to 122-keV peak intensity ratio, which was obtained for samples containing much higher europium activities. Finally, when a radioactivity sought was

TABLE V

ANALYSIS OF FOUR GALLIUM ARSENIDE SAMPLES

Sample / Analysis / Element	*1, dope elements: Cr, Sn*		*2, dope element: Si*		*3, dope element: Cr*		*4, dope element: Si*	
	1 p.p.b. (% error)	*2* p.p.b. (% error)	*1* p.p.b. (% error)	*2* p.p.b. (% error)	*1* p.p.b. (% error)	*2* p.p.b. (% error)	*1* p.p.b. (% error)	*2* p.p.b. (% error)
Sc	$< 6.6 \cdot 10^{-3}$	$< 8.2 \cdot 10^{-3}$	$< 7.2 \cdot 10^{-3}$	$< 10.1 \cdot 10^{-3}$	$< 6.2 \cdot 10^{-3}$	$< 4.5 \cdot 10^{-3}$	$< 5.6 \cdot 10^{-3}$	$< 5.6 \cdot 10^{-3}$
Cr	880(0.24)	875(0.30)	< 1.38	< 1.41	614(0.29)	602(0.26)	< 0.89	< 1.08
Fe	< 81	< 114	< 94	< 91	< 64	< 54	< 60	< 68
Co	0.128(17)	0.084(30)	0.090(27)	0.080(30)	0.057(30)	0.056(26)	0.218(10)	0.204(10)
Ni	< 39	< 63	< 45	< 61	< 38	< 28	< 36	< 33
Zn	50.9(2.8)	47.6(5.7)	7.64(27)	7.86(13)	12.3(8.0)	10.3(7.2)	3.44(22)	4.74(17)
Ag	< 0.67	< 0.80	< 0.74	< 0.99	< 0.63	< 0.44	< 0.58	< 0.55
In	32.7(3.4)	30.8(4.4)	10.1(6.7)	11.2(7.1)	24.8(4.1)	26.6(3.0)	10.1(5.7)	13.2(4.7)
Sn	176(13)	163(20)	< 96	< 98	< 79	< 65	< 89	< 69
Sb	0.49(9)	0.54(12)	0.254(12)	0.263(19)	0.46(9.6)	0.52(6.9)	0.47(9)	0.37(11)
Te	1520(1.2)	1330(1.5)	< 32	< 31	< 36	< 33	< 22	< 20
Ce	< 1.3	< 1.7	< 0.73	< 0.78	< 0.84	< 0.85	< 0.49	< 0.50
Nd	< 16	< 34	< 18	< 23	< 15	< 17	< 11	< 16
Eu	0.155(4.5)	1.09(1.0)	1.18(0.90)	0.028(15)	0.103(5.7)	0.216(2.2)	0.028(13)	0.016(20)
Tb	< 0.078	< 0.095	< 0.053	< 0.057	< 0.064	< 0.058	< 0.042	< 0.044
Yb	< 0.26	< 0.34	< 0.18	< 0.22	< 0.21	< 0.20	< 0.14	< 0.14
Lu	< 0.12	< 0.26	< 0.072	< 0.16	< 0.094	< 0.14	< 0.046	< 0.092

not detected, a detection limit was calculated, according to the convention of Currie[40].

RESULTS AND DISCUSSION

The results for four different gallium arsenide samples are given in Table V. The quoted errors are relative standard deviations on the peak areas of the samples, calculated from the counting statistics. Nine of the seventeen elements sought were not detected in any sample. The detection limits for these elements are, however, low. From the Table, duplicate analyses of one sample yield about the same results for most elements.

I am grateful to Prof. J. Hoste for his interest in this work and to Mr. J. Dewaele for his technical assistance. The financial support of the "Nationaal Fonds voor Wetenschappelijk Onderzoek" and the "Interuniversitair Instituut voor Kernwetenschappen" is gratefully acknowledged. Thanks are also due to Dr. L. De Laet from "Metallurgie Hoboken" for providing the samples.

SUMMARY

A method has been developed for the simultaneous determination of 17 trace elements in gallium arsenide. The method involves reactor neutron irradiation of the samples, distillation of the arsenic matrix activity and Ge(Li) γ-ray spectrometry. For a sample size of 0.1 g and a 10-day irradiation at $2 \cdot 10^{13}$ n cm^{-2} s^{-1}, the detection limits vary from 70 p.p.b. (tin) down to $5 \cdot 10^{-3}$ p.p.b. (scandium).

REFERENCES

1 P. I. Artyukhin, E. N. Gilbert and V. A. Pronin, *Radiokhimiya*, 9 (1967) 341.
2 E. Bujdoso, M. Miskei and G. Ormos, *Kohasz. Lapok*, 5 (1967) 236.
3 N. N. Dogadkin and Y. V. Yakovlev, *Yadernofiz. Metody Anal. Veshchestva*, (1971) 29.
4 E. N. Gilbert and P. I. Artyukhin, *Izv. Sib. Otd. Akad. Nauk SSSR, Ser. Khim. Nauk*, 2 (1967) 90.
5 D. E. Green, J. A. B. Heslop and J. E. Witley, *Analyst (London)*, 88 (1963) 522.
6 K. Kudo, H. Araki, M. Fujimoto and Y. Sato, *Radioisotopes*, 16 (1967) 16.
7 K. Kudo and N. Hishinuma, *J. Radioanal. Chem.*, 3 (1969) 369.
8 K. Kudo and N. Hishinuma, *J. Radioanal. Chem.*, 5 (1970) 331.
9 K. Kudo, H. Iso and T. Shigematsu, *J. Radioanal. Chem.*, 12 (1972) 451.
10 K. Kudo, T. Shigematsu and H. Iso, *Int. Conf. Modern Trends in Activation Analysis, 2–6 October 1972, Saclay, France.*
11 K. Kudo and N. Suzuki, *J. Radioanal. Chem.*, 19 (1974) 55.
12 G. V. Leushkina, E. M. Lobanov, A. G. Dutov and N. P. Matveeva, *Aktiv. Anal.*, Mater. Vses. Soveshch., 2nd edn., 1968, p. 23.
13 K. W. Lloyd, *Proc. Soc. Anal. Chem. Conf., Nottingham, England*, 1965, p. 108.
14 E. M. Lobanov, A. G. Dutov and G. V. Leushkina, *Dokl. Akad. Nauk Belorusskoi SSR*, 16 (1972) 985.
15 E. M. Lobanov, A. G. Ganiev, Y. A. Silvanovich and U. Khudaibergenov in B. P. Zverev (Ed.), *Aktivatsionnyii Analiz Chistykh Materialoe*, Izdatelstvo Fan Uzbekskoii SSR, Tashkent, 1968, p. 33.
16 K. H. Neeb, H. Stoeckert, R. Braun and H. P. Bleich. *Z. Anal. Chem.*, 245 (1969) 233.
17 S. Niese, *Kernenergie*, 7 (1964) 263.
18 S. Niese, *Int. Symp. Reinstoffe Wiss. Techn., Tagungsber.*, 2 (1965) 447.

19 H. Rausch and A. Salomon, *Talanta*, 15 (1968) 975.
20 H. Rausch and A. Salomon, *J. Radioanal. Chem.*, 3 (1969) 265.
21 M. N. Shulepnikov, G. I. Shmanenhova, Y. V. Yakovlev and N. N. Dogadkin, *Zh. Anal. Khim.*, 26 (1971) 1167.
22 K. B. Wolfstirn, *J. Phys. Chem. Solids*, 31 (1970) 601.
23 F. De Corte, A. Speecke and J. Hoste, *J. Radioanal. Chem.*, 3 (1969) 205.
24 F. De Corte, A. Speecke and J. Hoste, *J. Radioanal. Chem.*, 9 (1971) 9.
25 W. Maenhaut, F. Adams and J. Hoste, *J. Radioanal. Chem.*, 14 (1973) 295.
26 N. E. Holden and F. W. Walker, *Chart of the Nuclides*. Gen. Electric Co., Schenectady, N.Y., 1972.
27 I. M. H. Pagden, G. J. Pearson and J. M. Bewers, *J. Radioanal. Chem.*, 8 (1971) 127.
28 J. C. Roy and J. J. Hawton, *Report AECL-1181*, Chalk River, Canada, December 1960.
29 I. M. H. Pagden, G. J. Pearson and J. M. Bewers, *J. Radioanal. Chem.*, 8 (1971) 373.
30 R. Van der Linden, Ph. D. Thesis, University of Ghent, 1974.
31 W. Maenhaut, F. Adams and J. Hoste, *J. Radioanal. Chem.*, 16 (1973) 39.
32 *Standard Method for Measuring Neutron Flux by Radioactivation Techniques*, ASTM E 261-70, 1970.
33 J. Op de Beeck, to be published.
34 J. A. Scherrer, *J. Res. Nat. Bur. Stand.* Sect. A, 16 (1935) 253.
35 J. A. Scherrer, *J. Res. Nat. Bur. Stand.* Sect. A, 21 (1938) 95.
36 W. Maenhaut, F. Adams and J. Hoste, *J. Radioanal. Chem.*, 6 (1970) 83.
37 D. De Soete, R. Gijbels and J. Hoste, *Neutron Activation Analysis*, Wiley-Interscience, London, 1972.
38 P. F. Zweifel, *Nucleonics*, 18 (11) (1960) 174.
39 R. Van der Linden, F. De Corte and J. Hoste, *J. Radioanal. Chem.*, 13 (1973) 169.
40 L. Currie, *Anal. Chem.*, 40 (1968) 587.

Analytica Chimica Acta, 75 (1975) 41–46

DETERMINATION OF MERCURY IN BISMUTH BY NEUTRON ACTIVATION ANALYSIS

A. HIROSE, I. HORIUCHI and D. ISHII

Department of Applied Chemistry, Faculty of Engineering, Nagoya University, Furo-cho, Chikusa-ku, Nagoya 464 (Japan)

(Received 25th April 1974)

In previous papers[1,2], a new method for the separation and concentration of traces of mercury, gold, platinum and palladium in silver, copper and lead metals by the use of sulfur as a collector was reported. In the present work, the technique was applied to the determination of traces of mercury in bismuth by neutron activation analysis.

The neutron activation determination of mercury in various samples has been studied by many authors[3]. However, only Kim and Hoste[4] seem to have studied the determination of mercury in bismuth; mercury was separated from bismuth by deposition on a coarse metallic copper powder, followed by distillation of metallic mercury and amalgamation on a silver foil. The method should be satisfactory for obtaining a high radiochemical purity of mercury; but the separation steps are somewhat more complex and tedious than the technique to be described here.

The present method is rapid and simple in operation, and requires no special apparatus. In addition, high radiochemical purity and chemical yield of mercury could be obtained with good reproducibility, so that the determination of chemical yield was unnecessary.

EXPERIMENTAL

Apparatus

The Japan Atomic Energy Research Institute research reactor JRR-2 and the pneumatic tube system were used for irradiation.

The radiation detectors were a 41.5-cm^3 Ge(Li) semiconductor detector connected to a 1024-channel pulse-height analyzer, or a 3 × 3-in. NaI(Tl) scintillation counter connected to a 256-channel pulse-height analyzer.

A 600-W electric heater was needed. The filter assembly consisted of a Toyo filter holder KG-25, assembled with two pyrex tubes (25-mm i.d.) and a sintered glass disk. Toyo 0.45-μm pore-sized membrane filters were used.

Reagents

Ammonium sulfide. Commercial (colorless) ammonium sulfide solution (approximately 0.5 *M*) was standardized by iodimetry.

Standard mercury solution. Mercury(II) sulfate dried over sulfuric acid in a desiccator was dissolved in dilute nitric acid; the solutions were diluted with water

to various concentrations (0.05–100 μg Hg per 20 μl).

Standard radioactive mercury solution. Mercury(II) sulfate irradiated at a flux of $7 \cdot 10^{13}$ n cm^{-2} s^{-1} for 20 min was dissolved in dilute nitric acid; the solutions were diluted to 0.4–400 μg Hg ml^{-1} with water.

All the reagents used were of analytical grade, and deionized water was used throughout this work.

Procedure

Wrap the bismuth samples in aluminum foils. To prepare standards, drop 20 μl of standard mercury solutions on 2-cm diameter filter papers, dry at room temperature, and heat-seal in polyethylene bags.

Pack the samples and standards into a polyethylene capsule, and irradiate in a reactor at a thermal neutron flux of $7 \cdot 10^{13}$ n cm^{-2} s^{-1} for 20 min.

After cooling for several hours, open the capsule, take off the aluminum wrap, and transfer the bismuth to a 50-ml beaker. Add 40 μg of mercury carrier, dissolve in 10 ml of concentrated nitric acid, and dilute to 30 ml with water. To the solution, add 0.5 ml of ammonium sulfide solution with stirring, and stand at room temperature for about 10 min to redissolve the bismuth sulfide; then warm on a heater for a few minutes for ageing. Filter the mercury precipitate together with the sulfur precipitate on a membrane filter. Fold the membrane filter (and filter papers as standard samples) in the shape of a fan, and pack into a polyethylene bag. Measure the γ-ray spectrum by means of a Ge(Li) or NaI(Tl) detector, and determine the amount of mercury by comparing the net photo-peak activities of the 68–77-keV region in the sample and the corresponding standards.

Counting

Since activated bismuth emits 79-keV Po Kx-rays which interfere with the 77-keV γ-ray arising from ^{197}Hg, the photo-peak in the 68-keV region was selected for quantitative measurement when the counting was done with a Ge(Li) detector, to avoid any possibility of interference. When only the NaI(Tl) detector was available, the 68–77-keV region had to be used, because of the low resolution of the detector. When the intensity of the photo-peak activity was weak, the contribution of natural background was subtracted automatically.

RESULTS AND DISCUSSION

Volatilization losses of mercury

There is some possibility of losses of mercury by volatilization during the irradiation of sample and standard, during the dissolution of the bismuth sample, and during the warming of the sample solution to age the precipitates. These problems were checked in preliminary steps.

Losses of mercury during irradiation were concluded to be negligible for the following reasons: loss of mercury from the bismuth sample would be very small, because any loss by volatilization would occur only from the surface of the sample, and the surface was etched with nitric acid after irradiation. The possibility of loss of mercury from the filter paper in the standard sample would be somewhat larger than that of bismuth; however, detailed investigation by Takano and Ito[5] have shown

that losses are less than 5% and are similar to other experimental errors under the same irradiation conditions as in this work.

The loss of mercury during the dissolution of bismuth was checked as follows: 1 g of bismuth was transferred to a 50-ml beaker together with 1 ml of standard radioactive mercury solution (40 μg Hg), dissolved in 10 ml of concentrated nitric acid, and diluted to 30 ml with water. In this way, three samples were prepared; the radioactivities in the solutions were measured with the Ge(Li) detector and compared with the standards, prepared by dissolving the same weight of bismuth and diluting to 29 ml with water and then adding 1 ml of standard radioactive mercury solution. The net photo-peak count rates for these samples and standards showed no significant difference (1.6% as average). Therefore, losses of mercury during the dissolution of bismuth with nitric acid were concluded to be negligible.

TABLE I

LOSSES OF MERCURY DURING THE AGEING OF THE PRECIPITATES

Heating time (min)	*Hg found (%)*		*Hg loss (%)*
	Precipitate	*Filtrate*	
2–3	98.6	0.2	1.2
15–18[a]	87.9	0.2	11.9
15–18[a,b]	90.1	0.08	9.8

[a] Sample solution was boiled for about 15 min.
[b] Beaker containing the sample solution was covered with a watch glass.

However, as shown in Table I, considerable losses of mercury were observed in the ageing procedure of the sulfur precipitate when it was heated for a long time or boiled. Such losses could be reduced to negligible proportions by warming for a short time, and by covering the beaker with a watch glass.

Addition of mercury carrier

As shown in Table II, the recovery of mercury tended to decrease with decreasing amounts of mercury, but was almost quantitative for weights above 4 μg.

TABLE II

EFFECT OF THE AMOUNT OF MERCURY CARRIER

Hg carrier added (μg)	400	40	4	0.4
Hg recovered (%)	99	99	97	77

For sensitivity, 68–77-keV photons were chosen for quantitative measurements. The energies are, however, so low that self-shielding can occur. Therefore, a large amount of mercury carrier is undesirable, and 40 μg was chosen in this work. Sulfur can scarcely cause self-shielding, because of its low atomic number; accordingly, up to 8 mg was used, as described below.

Addition of ammonium sulfide

The effect of the amount of ammonium sulfide added was examined under the following conditions: the volume of sample solution was fixed at 30 ml and the weight of bismuth dissolved at 1 g. Table III shows that 0.01–2 ml of ammonium sulfide gave satisfactory results. For routine work 0.5 ml (8 mg S) was chosen to ensure the quantitative collection of the precipitate of mercury together with sulfur on a membrane filter.

TABLE III

EFFECT OF THE AMOUNT OF AMMONIUM SULFIDE

Ammonium sulfide added (ml)	0.01	0.05	0.5	1.0	2.0
Hg recovered (%)	99	99	99	98	97

Miscellaneous factors

The use of a filter paper instead of a membrane filter, to collect the precipitates, is not recommended because the paper did not provide complete recovery of mercury or sulfur.

The nitric acid concentration did not affect the quantitative separation of mercury from bismuth, in the range 1.5–9.5 *M*. However, 4–5 *M* is recommended in general, because of the short time required to re-dissolve the bismuth sulfide, and because of the useful amount of sulfur precipitate produced.

The procedure described above made it possible to treat 0.1–5 g of bismuth without trouble.

Reproducibility and results of analysis

The reproducibility of the procedure was checked as follows: 1 g of irradiated crude bismuth was dissolved in nitric acid, and the solution was diluted to 100 ml. The normal procedure was applied to a 20-ml portion of this solution. The results of four analyses by comparison with mercury standards are given in Table IV, which shows that the reproducibility of this method is satisfactory.

TABLE IV

REPRODUCIBILITY OF THE PROPOSED METHOD

(Each aliquot analysed contained 0.232 g of sample.)

Aliquot no.	*1*	*2*	*3*	*4*	*Mean*
Hg by Ge(Li) (μg)	28.4	28.5	28.9	27.3[a]	28.3
Hg by NaI(Tl) (μg)	27.1	28.3	28.2	27.4[a]	27.8

[a] Less reliable values.

The analytical results of mercury in crude and 99.999% bismuth are given in Table V, and a typical γ-ray spectrum used for the analysis of 99.999% bismuth is shown in Fig. 1.

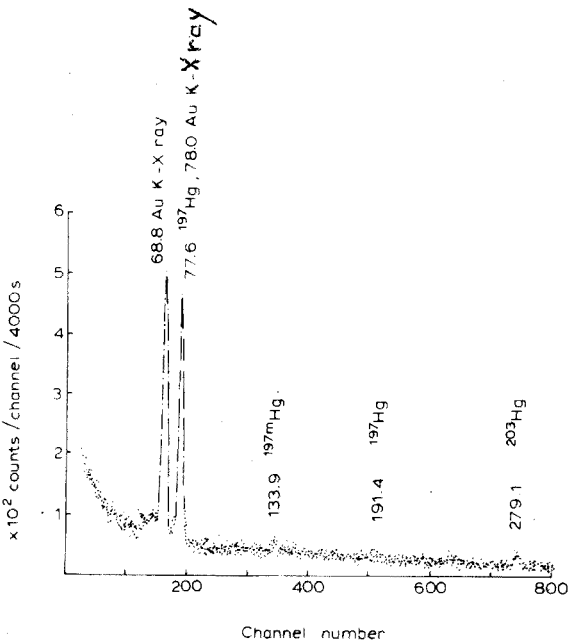

Fig. 1. γ-Ray spectrum of activated mercury separated from 99.999% bismuth sample, recorded with a Ge(Li) detector after cooling for about 6 h.

TABLE V

ANALYTICAL RESULTS FOR MERCURY IN BISMUTH

Sample no.	*Certified purity (%)*	*Sample taken (g)*	*Hg found (p.p.m.)*	
			Ge(Li)	*NaI(Tl)*
1-1	99.999	0.943	0.107	—
1-2		0.841	0.127	0.121
1-3		0.773	0.100	0.107
2-1	crude	0.665	120	—
2-2		0.449	105	—
2-3		0.232	121	119

Concentration factor

As can be seen in Fig. 1, the separation of bismuth was satisfactory and the photo-peak of the 89.8-keV Po Kx ray arising from activated bismuth was not observed, so that the concentration factor of mercury was not calculated accurately; it was estimated with the minimum detectable activity, namely with the value of $S/3\sigma_N$. Here, S is the net photo-peak count rate at the 89.8-keV region arising from irradiated bismuth, and σ_N is the statistical standard deviation of the background count rate at the 89.8-keV region in the γ-ray spectrum of mercury separated. The estimated value was more than $1.5 \cdot 10^3$.

Limits of detection and determination

In the present work, the limit of determination was defined by the level of 10% of the standard deviation (σ_s/S) of the net count rate (S) of the 68-keV full energy peak activity, and the limit of detection by $3\sigma_{N_b}$ (where N_b is the natural background count rate). If the weight of bismuth taken is 1 g, the counting interval is 10^4 s, the cooling time is 1 day, and the irradiation is done as described under Experimental, the values estimated for the limits of determination and detection were 0.006 and 0.0014 p.p.m., respectively.

The authors thank Dr. Y. Ito, Mr. T. Takano and other members of The National Universities' Laboratory for the common use of JAERI Facilities for their helpful advice in the irradiation of samples.

SUMMARY

A method has been developed for the determination of traces of mercury in bismuth by neutron activation analysis. After sample irradiation at a flux of $7 \cdot 10^{13}$ n cm^{-2} s^{-1} for 20 min, mercury was separated from bismuth by addition of ammonium sulfide and re-dissolution of bismuth (matrix) sulfide with nitric acid, and filtration of sulfur containing mercury on a membrane filter. The activity of the 68- or 68–77-keV region, counted with a Ge(Li) or NaI(Tl) detector, was used for quantitative measurements. The method was applied to bismuth samples containing 0.1–100 p.p.m. of mercury.

REFERENCES

1 A. Hirose and D. Ishii, *J. Chem. Soc. Japan, Ind. Chem. Sect.*, (1972) 1996.
2 A. Hirose and D. Ishii, *J. Radioanal. Chem.*, 20 (1974) 17.
3 G. J. Lutz, R. J. Boreni, R. S. Maddock and W. W. Meinke, *Activation Analysis: A Bibliography* NBS technical note 467, 1971.
4 J. I. Kim and J. Hoste, *Anal. Chim. Acta*, 35 (1966) 61.
5 T. Takano and Y. Ito, private communication.

Analytica Chimica Acta, 75 (1975) 47–60

TUBE-EXCITED ENERGY-DISPERSIVE X-RAY FLUORESCENCE ANALYSIS

PART I. COMPARISON WITH WAVELENGTH DISPERSION

R. DEWOLFS, R. DE NEVE* and F. ADAMS

Department of Chemistry, University of Antwerp, 2610 Wilrijk (Belgium)

(Received 15th July 1974)

X-Ray fluorescence analysis has been diversified into the classical wavelength dispersive method, and a newer non-dispersive or energy-dispersive method[1,2]. The latter is based on the use of a high-resolution semiconductor detector, mostly of the silicon–lithium drifted type for the spectrometry of the electromagnetic radiation. The detection efficiency of the spectrometer compared to that obtainable with a Bragg dispersive system allows a considerable reduction of the intensity of the primary radiation. This led to the use of radioactive sources in a highly compact, efficient and portable instrument for analysis of major and minor constituents. Recent advances in the performance characteristics of the Si(Li) detector and the pulse-handling electronics have made possible the use of x-energy dispersive systems (XES) at counting rates up to 20,000 c.p.s., thus allowing the exploitation of the method for multi-element determination of minor and trace constituents down to 1 p.p.m. These high fluorescence counting rates cannot any longer be safely and economically obtained with radioactive sources. This fact stimulated the development and use of x-ray tube-excited fluorescence systems consisting of a low-power, air-cooled, transmission x-ray tube or a higher-power, water-cooled tube with secondary target setup. The equipment is completed with a collimator system to shield the detector efficiently from scattered radiation from the tube, a high-quality Si(Li) detector and its associated pulse-amplification and pulse-analysis equipment. Most often the primary radiation is filtered so as to obtain a virtually monochromatic radiation of either the anode or the secondary target K–x radiation. Such systems are commercially available and are being advocated as a cheaper—and for some applications more powerful—alternative to the conventional sequential crystal-dispersive equipment for x-ray fluorescence.

The growing literature on the subject is mostly of an exploratory character. Little precise information is as yet available on the analytically important characteristics, merits or drawbacks of the XES technique compared to the wavelength-dispersive method and other analytical methods. It appeared therefore interesting as an introduction to a series of papers on applications of x-energy fluorescence, to examine the method closely, to compare its characteristics with the wavelength-dispersive method and to show the particular domain where the method is a valuable

* Present address: Metallurgie Hoboken-Overpelt, A. Greinerstraat 14, B-2710 Hoboken, Belgium.

alternative to other analytical methods. Cooper[3] compared energy-dispersive particle and photon-excited fluorescence analysis with protons, α-particles at different energies, a molybdenum transmission tube, and a radioactive source of either ^{55}Fe or ^{109}Cd. The comparison was applied to environmental samples. Perry and Brady[4] and Goulding and Jaklevic[2] compared α-ray- and x-ray-induced emission. A quantitative comparison of x-ray techniques consisting of wavelength-dispersive (multichannel and sequential) and XES methods with tube, isotope and charged-particle excitation intended for air particulate samples has been published by Birks *et al.*[5]. Walinga[6] comments briefly on the advantages and limitations of energy-dispersive analysis. Advantages are the multi-element character of the analysis; disadvantages are the limited resolving power and the rather stringent count-rate limitations. A comparison between energy-dispersive and wavelength-dispersive electron beam microanalysis has been made by Malissa *et al.*[7].

EXPERIMENTAL

Equipment

The wavelength-dispersive apparatus was a Philips PW 1450 modular x-ray spectrometer, provided with a Philips PW 1140 3-kW generator and a chromium target x-ray tube (Philips PW 218). Primary collimation of fluorescent radiation was obtained with a fine-entrance Soller slit collimator with spacing of 150 μm. A pentaerythritol dispersive crystal and a gas flow proportional detector (90% Ar, 10% CH_4), with a polypropylene window of 6 μm, were used for the measurement of low atomic number elements. For fluorescent x-rays with energy higher than 4 keV, a LiF (200) dispersive crystal and a combination of gas flow and sodium iodide scintillation detectors were used. Automatic pulse-height selection was based on the sine θ potentiometer principle. A fixed window with a width of 120% of the baseline was used. Characteristic radiation from the chromium anode could, when necessary (*e.g.* measurement of MnK_α), be filtered out by insertion of an aluminium filter between the x-ray tube window and the sample.

For the energy-dispersive measurements, a Kevex subsystem 0810 and a Siemens Kristalloflex 2 generator (4 kW) were used. The tube was a water-cooled x-ray tube with tungsten anode (Siemens A G W 61). Excitation of the samples was done with fluorescent K-radiation obtained by exciting a secondary target consisting of molybdenum or titanium with the tube spectrum. The MoK_α radiation obtained with the molybdenum target was filtered from the scattered tube-Bremsstrahlung and characteristic radiation from the tungsten anode with a molybdenum filter. No filtering was used with the titanium target. Suitable collimation was provided between secondary target and sample and between sample and detector to insure that the only mass which could scatter the radiation directly into the detector was the sample and possibly its substrate.

The collimator at the detector side consisted of pure aluminium with a 2-mm diameter aperture. This limited the radiation to the central portion of the detector thus diminishing the inefficiently collected interactions in the edge regions. Only a 4.5-mm^2 oval area of the sample was therefore measured. The entire system was optimized to obtain an effective monochromatic exciting radiation with no detectable spectral interferences when a pure sample was fluoresced. The secondary target

system used is more amply described by Porter[8].

The Si(Li) detector was a Kevex Mark AA 30 $mm^2 \times 3$ mm mounted in a cryostath with a 0.0025-mm beryllium window. A cooled FET preamplifier with pulsed optical feedback (Kevex 2002) was used with an x-ray amplifier (Kevex 4510P) at a time constant of 6 μs. The amplifier incorporated a base-line restorer and pulse pile-up rejector. A Northern Econ II 4096-channel analyser with 200-MHz ADC is used. The entire energy-dispersive system is shown schematically in Fig. 1.

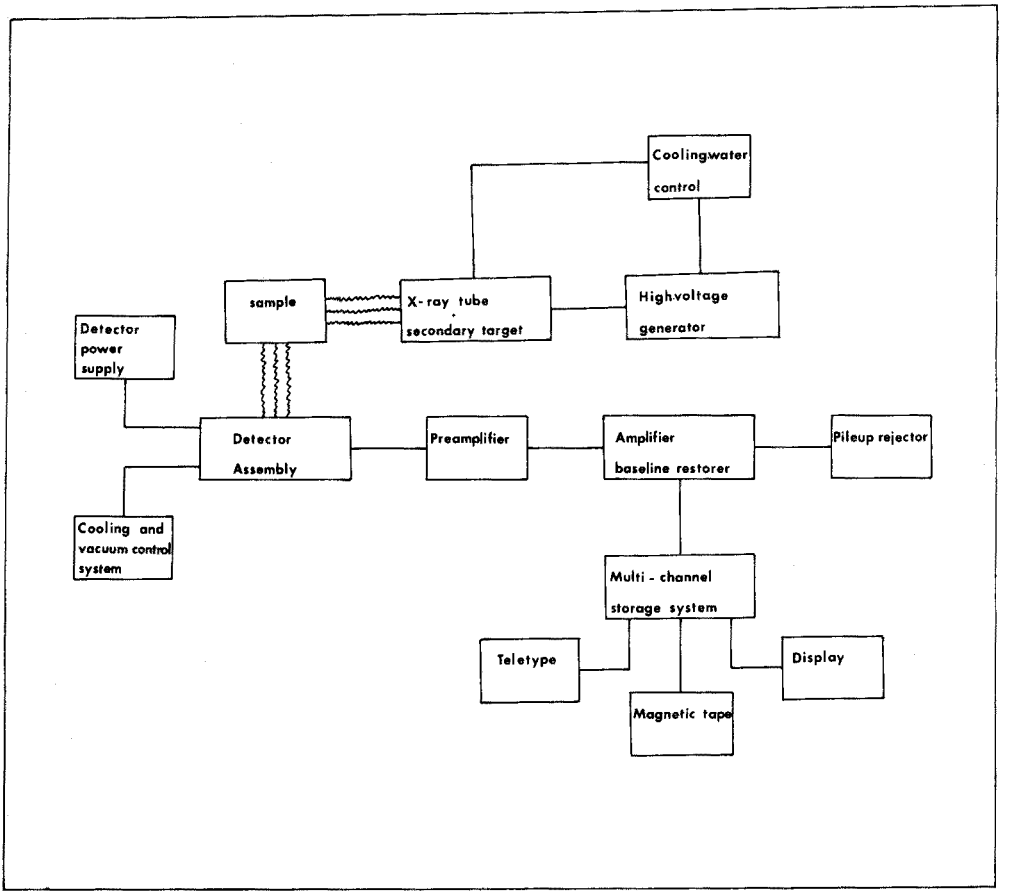

Fig. 1. Schematic representation of the energy-dispersive system.

The wavelength-dispersive instrument can be considered as a representative example of the sequential crystal spectrometer used under routine analytical conditions. The energy-dispersive system is representative of the secondary target excitation conditions. It should be noted that other possible instrumentation for XES is based on: (1) the use of a low-power transmission tube yielding a more or less comparable degree of monochromatic radiation, albeit at a much lower primary tube-power consumption level; (2) the direct excitation of the sample with the x-ray

Bremsstrahlung continuum at high efficiency but very poor detection limits since the continuum reaches the detector via scattering in the sample.

Samples

Two representative samples from the metallurgical industry were used: (i) an agglomerate for lead production with a relatively heavy matrix containing about 40% of lead; (ii) a slag from lead production with a matrix containing about 26% of silicon dioxide and 15% of calcium oxide. Both samples were measured in pellet form and can be considered as infinitely thick.

As a typical example of a thin specimen, an air particulate sample collected on Whatman 41 cellulose filter was used. The filter backing material weighed 8.5 mg cm^{-2} and contained 0.7 mg cm^{-2} of air particulate material.

In order to investigate spectral interferences, samples containing neighbouring atomic number elements were prepared. Four samples were prepared by the fusion of 100 mg of Fe_2O_3, Co_3O_4, As_2O_3 or GeO_2 with 20 g of potassium pyrosulfate. After cooling, the material was ground and pressed into pellets. Two additional samples were made in the same way but contained, respectively, 100 mg of Fe_2O_3 plus 100 mg of Co_3O_4, and 100 mg of GeO_2 plus 100 mg of As_2O_3.

RESULTS

Energy resolution

The resolution of a number of spectral lines expressed as full width at half maximum (FWHM) in electron volt, was determined for both systems. The results are summarized in Table I. They can be considered as representative for a high-quality photon spectrometer used under conditions which are a compromise between counting rate and resolving power. Resolution which was higher by 10–40 eV at low energy could be obtained by sacrificing the detection efficiency and (or) imposing limitations on the counting rate.

For the crystal instrument, the resolving power depends on a number of experimental conditions, so that the results mentioned should only be considered typical for the type of instrument used. A full width at half maximum value of only 5 eV should be possible for the FeK_α-line, with dispersive crystals.

The results of Table I illustrate the well-known fact that the resolving power of the crystal instrumentation is tremendously higher than that of the photon spectrometers especially at low energies. The resolution of the XES system is just barely sufficient to resolve the K_α lines and several spectral interferences need to be taken into account. In the energy region up to 10 keV, K_α lines of an element will partially interfere with the K_β radiation of the preceding atomic number element. Other possible interferences are those due to L- or M-radiation of high Z-elements with K-lines of low Z elements, and to the occurrence of a silicon escape peak of low intensity at an energy of 1.73 keV (SiK_α) less than the fluorescent radiation. However, corrections for these interferences should be easy to perform, since the entire energy spectrum is measured simultaneously and the results are directly available for digital calculation. Most manufacturers of the energy-dispersive instrumentation have recognized this fact by offering a minicomputer-coupled system with suitable software.

TABLE I

FWHM OF X-RAY SPECTRAL LINES AS A FUNCTION OF ENERGY

Spectral line	*Energy (keV)*	*Wavelength dispersion*		*Energy dispersion*
		Counter-dispersive crystal	*FWHM (eV)*	*FWHM (eV)*
SiK_α	1.740	F[a]–PE[b]	4.5	142
SK_α	2.308	F–PE	8.5	149
ClK_α	2.622	F–PE	10.3	148
KK_α	3.313	F–PE	15.8	151
CaK_α	3.690	F–PE	20.2	154
TiK_α	4.508	F–LiF[c] (200)	17.0	155
VK_α	4.949	—	—	160
CrK_α	5.411	—	—	164
MnK_α	5.895	—	—	170
FeK_α	6.400	F–LiF (200)	35.5	173
CoK_α	6.925	F–LiF(200)	39.3	175
NiK_α	7.472	F–LiF(200)	43.0	180
CuK_α	8.041	F–LiF(200)	51.9	183
		S[d]–LiF(200)	38.2	—
ZnK_α	8.631	F–LiF(200)	61.0	188
		S–LiF(200)	45.3	—
GeK_α	9.876	F–LiF(200)	80.0	200
		S–LiF(200)	60.0	—
PbL_α	10.549	—	—	212
PbL_β	12.611	F–LiF(200)	126.6	232
		S–LiF(200)	83.0	—

[a] F, flow counter.
[b] PE, pentaerythritol dispersive crystal.
[c] LiF(200), lithium fluoride dispersive crystal, cut parallel to the (200) plane.
[d] S, NaI (Tl) scintillation counter.

Spectral interference

Spectral interference was investigated by measuring the K_α intensities of two elements with neighbouring atomic number, present at known concentration (iron, cobalt and germanium, arsenic). For the wavelength-dispersive measurement, the chromium target x-ray tube was operated at 60 kV and 40 mA, the counting time was 10 s, and a LiF (200) dispersive crystal and a combination of gas flow and sodium iodide scintillation detectors were used. For energy-dispersive measurement, the tungsten target x-ray tube was operated at 40 kV and 30 mA, with a molybdenum secondary target. The measuring time was 3000-s live-time, and dead time amounted to 30% at the input count rate of 2500 c.p.s.

The results are summarized in Table II. Net intensities were obtained by subtracting the background in the immediate neighbourhood of the peaks. No appreciable interference occurs with the wavelength dispersion. The Fe K_α-intensity in sample 2 is due to a contamination of the excitation system, and corresponds to an apparent iron content of 1.7 mg in the sample. With energy dispersion the Fe and CoK_α radiations are sufficiently resolved. Indeed, the counting rate of cobalt in the energy channels of iron is of the order of 0.1% only. The reverse situation of

TABLE II

INFLUENCE OF IRON ON CoK_α-INTENSITY AND OF GERMANIUM ON AsK_α-INTENSITY IN SYNTHETIC SAMPLES

Sample no.	*Fe (% weight)*	*Co (% weight)*	*Wavelength dispersion*		*Energy dispersion*		
			FeK_α[a] (counts)	*CoK_α[a] (counts)*	*FeK_α[b] (counts)*	*CoK_α[b] (counts)*	*CoK_α[c] (corrected)*
1	0.35	—	28260	0	67127	9845	—
2	—	0.37	702	34917	129	105671	—
3	0.35	0.37	27967	34734	66899	113202	103393
	Ge (% weight)	*As (% weight)*	*GeK_α[a] (counts)*	*AsK_α[a] (counts)*	*GeK_α[b] (counts)*	*AsK_α[b] (counts)*	*AsK_α[c] (corrected)*
4	0.35	—	37568	96	469612	5687	—
5	—	0.38	42	49179	167	680496	—
6	0.35	0.38	37588	48728	471440	689815	684107

[a] Net peak intensity, counting time 10 s.
[b] Net integrated peak over full width at tenth maximum, counting time 3000 s live.
[c] Corrected value using the intensity ratios FeK_α/FeK_β resp. GeK_α/GeK_β.

iron activity measured in the energy channels of cobalt K_α is thus almost exclusively due to the spectral interference of FeK_β. Both the interference of cobalt on iron, and vice versa, can be corrected mathematically *e.g.* by using an experimentally determined interference factor. It is clear that in the latter case this considerably lowers the precision of cobalt determination. The interferences are less severe for the higher energy radiation of germanium and arsenic.

It should be remembered that the crystal-dispersive method, despite its high resolving power at low energy, is not always free from spectral interference. Indeed, often there is interference from tube anode impurities (*e.g.* iron and copper) plus higher order reflections. For instance, with a chromium target tube the determination of chromium is impossible, unless a filter is used, and also there may be interference of the second-order SnK_α radiation with PbL_β, and of second-order PbL_β radiation with FeK_α.

Intensity and peak-to-background ratio

The intensity expressed as a counting rate in c.p.s., and the peak-to-background ratio obtained with both methods, are summarized in Tables III and IV. For wavelength-dispersive measurement, the chromium tube was operated at 60 kV and 40 mA. A pentaerythritol dispersive crystal and a gas flow detector were used for measurement of low Z radiation (from SiK_α up to CaK_α); a LiF (200) dispersive crystal and a combination of a gas flow and a sodium iodide scintillation detector were used for measurement of x-rays of higher energy.

For energy-dispersive measurement of low Z elements (from SiK_α up to CaK_α), the tungsten anode x-ray tube was operated at 20 kV and 35 mA, with a titanium

TABLE III

INTENSITIES AND PEAK-TO-BACKGROUND RATIOS FOR INFINITELY THICK SAMPLES

Spectral line	*Concentration*[a] *(% by weight of the element)*	*Wavelength dispersion*		*Energy dispersion*	
		Net intensity[b] *(c.p.s.)*	*Peak-to-background*	*Net intensity*[c] *(c.p.s. live)*	*Peak-to-background*
(i) Agglomerate for lead production					
CaK_α	4.82	137445	694	671	16.2
FeK_α	9.62	43655	255	57.5	50.2
CuK_α	4.51	24926	98	63.2	44.5
ZnK_α	5.59	33250	120	106	64.4
PbL_β	39.86	63705	231	621	72.0
(ii) Slag from lead production					
CaK_α	10.51	259212	751	1151	25.5
FeK_α	20.30	153420	650	583	121
CuK_α	0.39	3334	16	17.3	9.0
ZnK_α	12.13	90980	263	719	118
PbL_β	1.26	3577	21	68.4	16.3

[a] Determined by wet chemical analysis.
[b] Net peak intensity.
[c] Net integrated peak-intensity over full width at tenth maximum, dead time 30%.

ABLE IV

ITENSITY, PEAK-TO-BACKGROUND RATIO AND DETECTION LIMIT FOR AN AIR PARTICULATE AMPLE ON WHATMAN 41

ectral e	*Concentration*[a] *($\mu g\ cm^{-2}$)*	*Wavelength dispersion*			*Energy dispersion*		
		Net intensity[b] *(c.p.s.)*	*Peak-to-background ratio*	*Detection limit ($\mu g\ cm^{-2}$)*	*Net intensity (c.p.s. live)*	*Peak-to-background ratio*	*Detection limit ($\mu g\ cm^{-2}$)*
K_α	—	965	193	—	16.3	2.50	—
K_α	—	107	21.4	—	—	—	—
K_α	—	6480	324	—	81.3	4.51	—
K_α	16.99	3060	153	0.024	40.1	2.65	0.156
K_α	27.95	41582	831	0.005	250	16.6	0.041
K_α	30.66	58820	327	0.007	608	47.8	0.017
L_α	<0.20	213	2.80	—	—	—	—
K_α	<2.17	1172	15.0	—	0.64	0.98	—
K_α	41.82	1487	49.6	0.146	85.7	78.6	0.048
K_α	14.20	2928	41.8	0.038	50.1	58.8	0.025
K_α	<0.25	47	0.45	—	0.68	1.16	—
K_α	0.805	58	0.48	0.145	0.84	1.43	0.070
K_α	6.15	1341	10.6	0.049	35.4	28.1	0.019
K_α	0.694	77	0.35	0.127	8.04	2.29	0.015
L_β	—	95	0.42	—	10.21	1.80	—

Determined by neutron activation analysis.
Net peak intensity.
Net peak intensity integrated over full width at tenth maximum, dead time 15%.

secondary target. Excitation of medium and high Z elements was obtained with a tungsten tube operated at 40 kV and 10 mA for the infinitely thick samples, and 40 kV and 40 mA for the thin air-particulate sample, with a molybdenum secondary target. Dead time amounted to 30% at an input count rate of about 2500 c.p.s. for infinitely thick samples, and to 15% at an input count rate of about 1000 c.p.s. for the thin sample.

The background counting rate was measured in the immediate vicinity of the peaks for the wavelength dispersion. For the energy-dispersive method, the background intensity was obtained by interpolation from regions of the spectrum which were free from fluorescence radiation. With the thin air-particulate sample, backgrounds were calculated with empirically determined factors, relating the background to coherent and incoherent backscatter of secondary target radiation on the sample and its substrate.[9]

Tables III and IV show that the intensities obtained by crystal dispersion are up to 200 times higher than those obtained by energy dispersion. The peak-to-background ratio is up to 50 times higher for low Z-elements. For higher Z-elements, the peak-to-background ratio becomes similar for both systems. The figure even becomes higher for the air-particulate material. The peak-to-background ratio is related to the sensitivity of the method. The detection limit is often defined as $kB^{\frac{1}{2}}/m$, where the proportionality factor k can be taken equal to 3 if the 3σ convention is adopted with a 99.7% probability that the background deviates by not more than 3σ; B is the background and m the sensitivity of the measurement, expressed in counts per mass or concentration unit and per unit of time. Several comments are in order here.

(a) When directly applied, the definition of the detection limit gives superior sensitivity for the wavelength-dispersive method. This is not a fair comparison, however, because so much more information is gathered with the energy-dispersive instrument than with a crystal spectrometer. In conventional sequential spectrometers, two measurements are performed: one on the peak, and the other on the background for every element. In a typical multi-element determination with an energy-dispersive arrangement, 10–15 elements can be measured simultaneously with pertinent background information.

This allows the experimenter to count the sample correspondingly longer: whereas 10–30-s measurements are typical for single element determinations with wavelength-dispersive systems, a 10–30-min analysis time is acceptable in the other case. This corresponds to the time necessary for the use of scanning crystal spectrometers. Table IV shows the lower detection limit that can be derived for a number of elements in a thin sample. The detection limit is based on the use of a 10-s measurement for the wavelength-dispersive method and 1000 s for the energy-dispersive method.

(b) The low values of the sensitivity factor m in the energy-dispersive method are caused indirectly by the count-rate limitations imposed on the x-ray spectrometer. In some applications, emphasis can be placed on the processing of high counting rates with a less than optimal resolution, *e.g.* for the analysis of a single higher-Z element.

(c) It is worth noting that the increased sensitivity for the analysis of the thin air-particulate sample compared to the infinitely thick samples is due to

reduction of the scattering of the monoenergetic primary radiation. The origin of the background for both methods is basically different. In the energy-dispersive method it is mainly due first to inefficient collection of the charge carriers produced in the detector for part of the interactions, and secondly to Bremsstrahlung production in sample and detector. The second of these contributions only is fundamental; the first can be and is periodically ameliorated by technological advances in detector design[8]. In the wavelength-dispersive setup, the background is due to scattering in the sample, the collimators and other material, of the primary polychromatic radiation. In most commercial instrumentation, the detection of primary radiation scattered in sample holder and sample vicinity is not efficiently prevented for thin samples. That the signal-to-noise ratio is actually higher in the wave-length dispersive instruments is mainly due to the superior resolving power which allows the integration of signal and background over a much narrower interval.

Typical x-ray spectra of the air-particulate sample, obtained by wavelength dispersion and energy dispersion, are given in Figs. 2–4.

Reproducibility and precision of the measurements

The maximal obtainable precision depends on counting statistics of the net fluorescent counting rate. The sensitivity is low, for the energy-dispersive method and thus excessive measurements may be necessary to obtain a high precision. It is sometimes customary, mainly in industrial applications, to obtain a statistical precision of 0.1% relative. This is possible in sequential wavelength-dispersive systems but is not feasible with XES as can be judged, for example, from the data in Table III.

With the net counting rates obtainable, a statistical precision of 1–4% is a more logical figure. Moreover, when mathematical corrections are necessary to take into account spectral interferences and background continuum, precision better than a few percent relative is out of reach for a second reason.

Despite the low net counting rates obtained, the XES method is seriously influenced by the problem of dead-time losses. Indeed, the long duration pulses give rise to random coincident detection of two or more events. Therefore, modern systems incorporate pulse pile-up rejectors and accurate dead-time correction systems. These systems and especially the latter circuit do not always function accurately. They should be critically examined because failure leads to counting losses and errors which are directly proportional to the integral input counting rate. Table V gives the results of a test of the XES equipment used here. A radioactive source of ^{57}Co was placed in a fixed position facing the detector and was measured repeatedly as a function of increasing input counting rates due to fluorescence and scatter of the MoK_α primary radiation on the source backing. The system functions accurately to within 1–2% up to 12,000 c.p.s. Higher counting rates become impossible at the shaping time constants used with the instrument, but with time constant decreased to 2 μs, a three times higher counting rate limit should be possible. This lowering of the time constant would however have the detrimental effect of decreasing the resolving power by 20 eV at low energies.

Similar pulse overlap effects do not occur in the crystal equipment because the pulses measured are limited by the crystal goniometer system to those of interest and higher-order reflections only. Moreover, the pulse duration can be

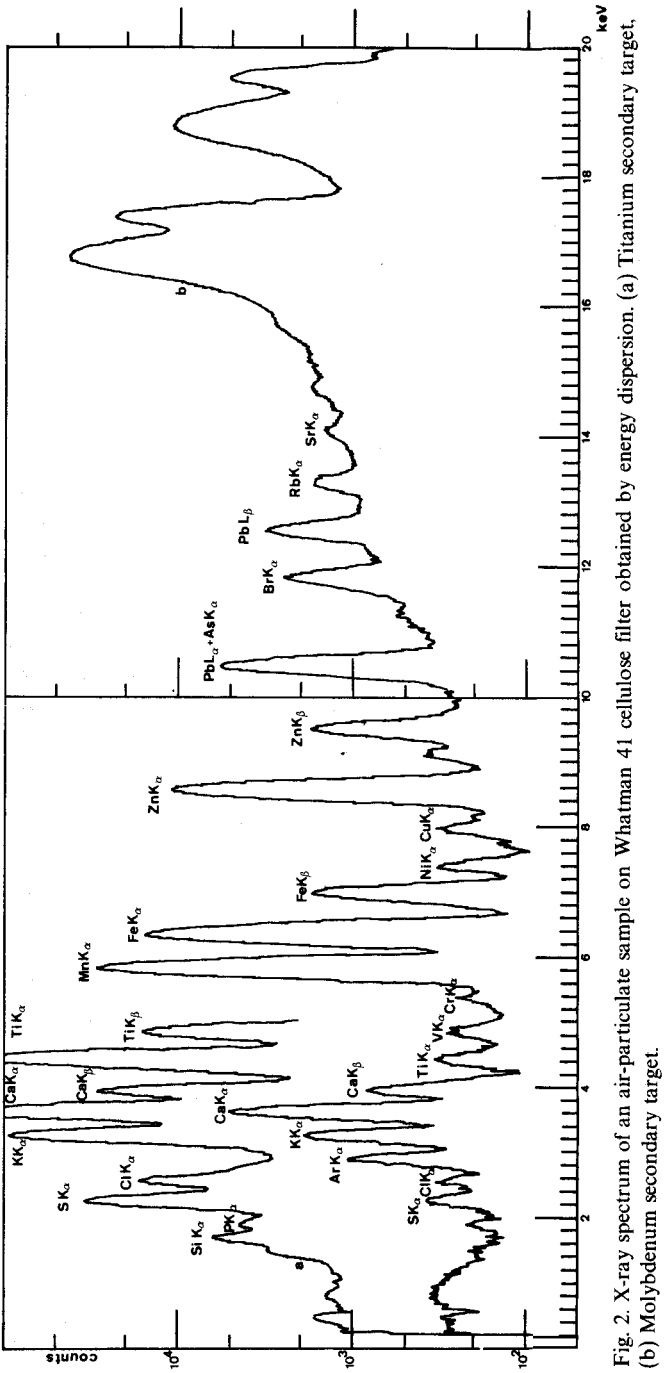

Fig. 2. X-ray spectrum of an air-particulate sample on Whatman 41 cellulose filter obtained by energy dispersion. (a) Titanium secondary target, (b) Molybdenum secondary target.

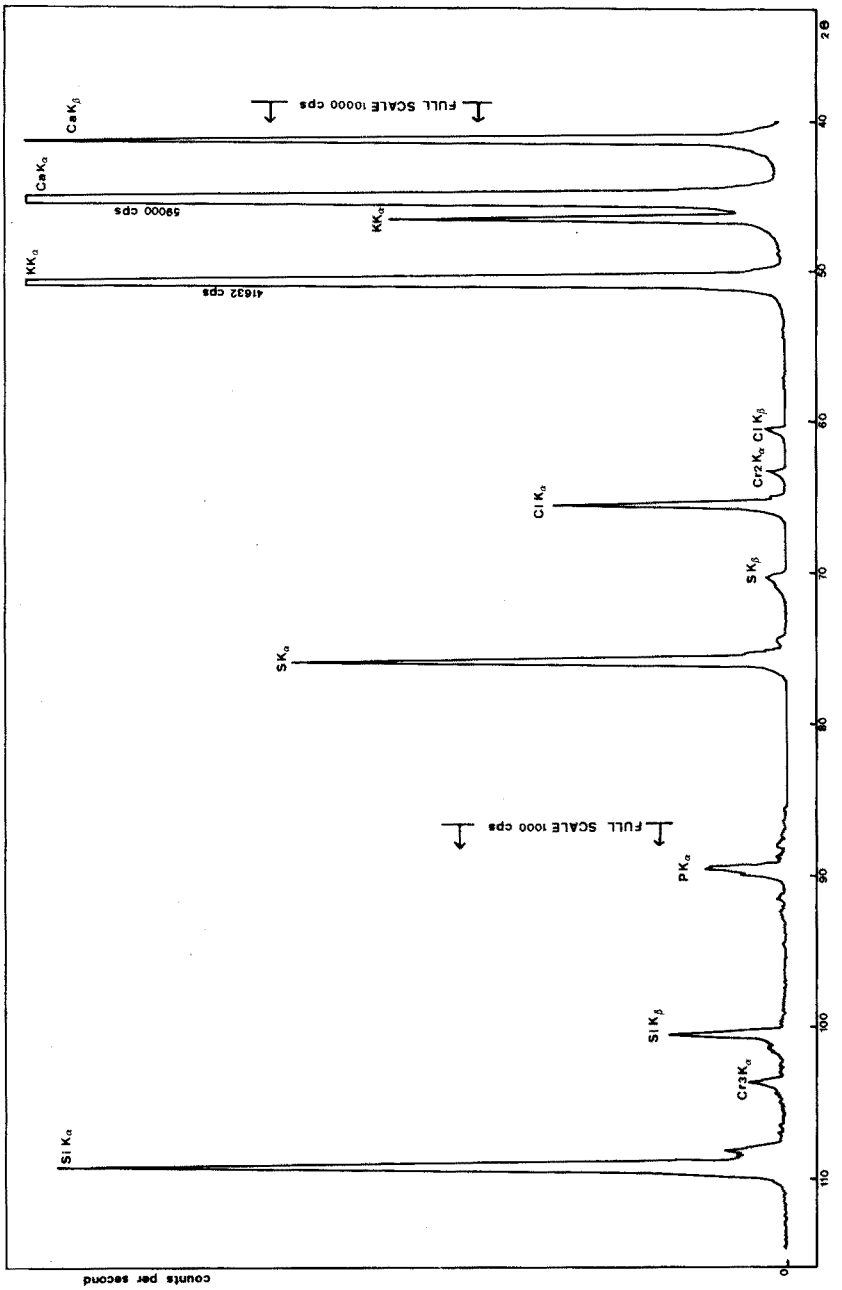

Fig. 3. X-ray spectrum of low Z elements in an air-particulate sample obtained by wavelength dispersion.

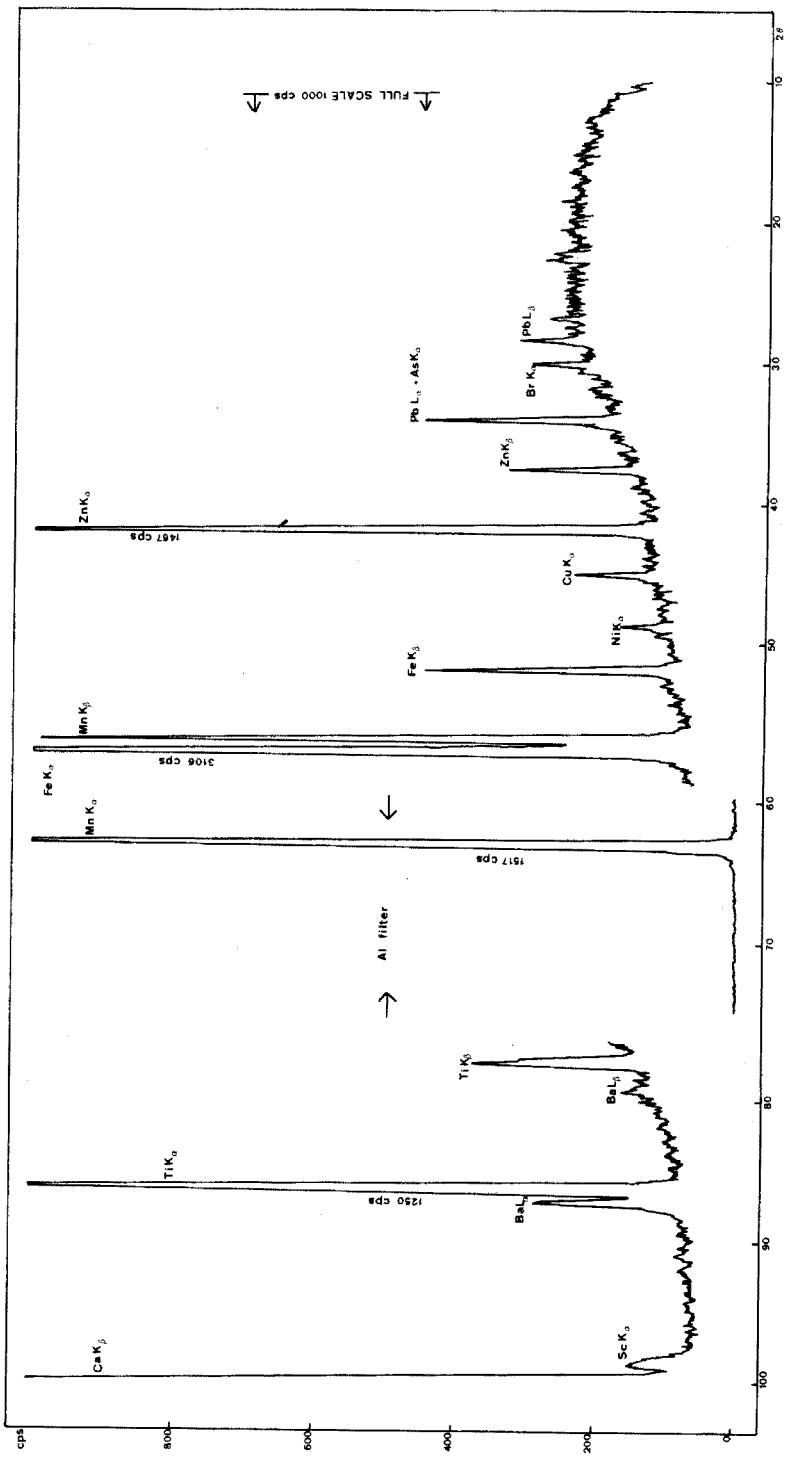

Fig. 4. X-ray spectrum of medium Z elements in an air-particulate sample obtained by wavelength dispersion.

TABLE V

INTENSITY OF FeK_α RADIATION AND 14.36-keV γ-RADIATION FROM A ^{57}Co-SOURCE, AS A FUNCTION OF INTEGRAL INPUT COUNTING-RATE

Input counting rate (c.p.s.)	*FeK_α net intensity (counts/1000 s)*	*14.36-keV net γ-intensity (counts/1000 s)*
1765	168922	40072
2264	169018	40317
2725	169855	40273
3132	169494	40477
3615	169741	41296
4150	169829	41277
4590	171009	41118
5003	169617	41784
5785	170047	42370
6000	169970	41695
10885	170229	41380
11000	168128	41057
11650	170002	41468

reduced to a fraction of a microsecond in this case, without affecting the resolving power. With comparable sample geometry and exciting radiation, matrix effects should be comparable for both systems.

DISCUSSION

The crystal-dispersive method allows a much higher resolution of the spectral lines. It is only for energies higher than about 15 keV that the resolving power of the x-energy spectrometer becomes comparable. The spectral interferences unavoidable in the Si(Li) x-ray spectra can be taken into account by calculation. This can most easily be done by using precisely determined correction factors obtained by measuring pure spectra. More refined techniques can be adopted which could yield a somewhat higher precision: *e.g.* mathematical least-squares deconvolution of the Gaussian components of the composite spectrum, or spectrum stripping methods.

These techniques have been adapted from a quite similar situation of less than required energy resolution in γ-ray spectrometry[10,11]. It is clear that no method can get rid of the statistical nature of the spectral results. Moreover, it should be recognised that additional statistical errors may be introduced. For instance, in the spectrum-stripping methods which involve consecutive subtraction of the pure components of the spectrum, propagation of the counting errors is unavoidable. It should be recognised that a reduction in precision and sensitivity is introduced by the correction for spectral interferences.

Medium Z elements such as cadmium, barium, tin, silver ($40 < Z < 60$) which are determined through the measurement of their L-radiation in classical x-ray fluorescence, can only be determined through their K-radiation in XES. Moreover, their presence at high concentration may result in such a crowded x-ray spectrum at lower energies that correction procedures for spectral interference become dubious at best.

A major factor differentiating the XES method from the crystal diffractive method is the use of monochromatic primary radiation. A drawback of this is the reduced sensitivity compared to direct x-ray tube excitation. A major advantage is the fact that correction for absorption and possibly enhancement effects is basically less complicated. An exact mathematical correction for matrix effects becomes possible. Also quantitative analysis becomes less difficult in XES.

Comparing the drawbacks and merits for both types of instruments, it becomes apparent that the XES method is of advantage in a type of analysis which can be defined as follows: the multi-element analysis, with a low precision of 2–10%, of thin samples (< 10 mg cm^{-2}) of environmental or related composition. Routine analysis of industrial samples with high precision remains the domain of sequential and multichannel crystal instruments. In further publications in this series a number of pertinent determinations will be described.

SUMMARY

A secondary target tube excited x-ray fluorescence apparatus was compared with a conventional sequential wavelength dispersive spectrometer. Representative samples from the lead industry, an agglomerate for the lead production and a typical air particulate sample collected on cellulose filter were used in the comparison.

The following factors were considered: resolving power, spectral interferences, intensity and peak-to-background ratio, sensitivity, reproducibility and precision. The energy dispersive method is advantageous for the multi-element analysis with limited precision of thin samples of environmental composition.

REFERENCES

1 R. Woldseth, *X-Ray Energy Spectrometry*, Kevex Corporation, Burlingame, California, 1973.
2 F. S. Goulding and J. M. Jaklevic, *Ann. Rev. Nucl. Sci.*, 23 (1973).
3 J. A. Cooper, *Nucl. Instrum. Methods*, 106 (1973) 525.
4 S. K. Perry and F. P. Brady, *Nucl. Instrum. Methods*, 108 (1973) 389.
5 J. V. Gilfrich, P. G. Burkhalter and L. S. Birks, *Anal. Chem.*, 45 (1973) 2002.
6 J. Walinga, *Chem. Weekbl.*, 69 (1973) L-47.
7 H. Malissa, M. Grasserbauer and E. Hoke, *Microchim. Acta*, 5 (1974) 465.
8 D. E. Porter, *X-Ray Spectrom.*, 2 (1973) 85.
9 P. Van Espen and F. Adams, *Anal. Chim. Acta*, 75 (1975) 61.
10 P. Quittner, *Gamma-Ray Spectroscopy, with particular Reference to Detector and Computer Evaluation Techniques*, Hilger, London, 1972.
11 F. Adams and R. Dams, *Applied Gamma-ray Spectrometry*, Pergamon, Oxford, 2nd edn., 1970.

Analytica Chimica Acta, 75 (1974) 61–85

TUBE-EXCITED ENERGY-DISPERSIVE X-RAY FLUORESCENCE ANALYSIS

PART II. ENERGY-DISPERSIVE X-RAY FLUORESCENCE ANALYSIS OF AIR PARTICULATE MATERIAL

P. VAN ESPEN and F. ADAMS

Department of Chemistry, Universitaire Instelling Antwerpen, Universiteitsplein 1, 2610 Wilrijk (Belgium)

(Received 29th August 1974)

Gaseous pollutants (NO_x, SO_2, CO, hydrocarbons) have been monitored for some time. The study of these compounds dates from the 1940's in some problem areas. Interest in particulate pollution is much more recent, but nevertheless there is considerable interest in a complete inventory of the elements present in the air. The particulate material is recognised as a relatively small but important portion of polluted air. A variety of methods has been utilized for the multi-element analysis of air-borne particulate material: emission spectrometry[1,2], x-ray fluorescence spectrometry[3,4], neutron activation analysis[5,6], and atomic absorption spectrometry[7,8]. Hwang critically compared the different methods[9]. The emission spectrometric and x-ray fluorescence methods suffer from the high capital outlay and from poor precision and accuracy. Nuclear methods have the advantage of being very sensitive and free from interferences but need very expensive reactor facilities. Atomic absorption spectrometry becomes difficult when a large number of elements must be determined, because, in contrast to the other methods, only one element can be determined at a time.

The rapidly expanding scientific literature on energy-dispersive x-ray emission analysis[10,11] illustrates that this technique has become an increasingly important tool for elemental analysis. Although the method cannot measure every element in the concentration range of environmental samples, it has the potential of providing the rapid, non-destructive, low-cost, multi-element analyses required for monitoring the behaviour of many elements in air. The method has been applied for air particulate analysis or other thin samples with a radioisotopic source, x-ray tube, or charged particle excitation. Several authors have compared these three excitation mechanisms[12–15]. For very small samples, protons of a few MeV provide the highest sensitivity but require an expensive accelerator facility. Isotopic sources do not provide the sensitivity needed for the determination of more than 5–7 elements. A suitable x-ray tube arrangment provides a compromise between the two excitation mechanisms and offers distinct advantages except for the smallest sizes of sample.

The present paper describes a method for the analysis of air particulate material for some 15 elements and discusses the methodology of the analytical procedure. Numerous factors have to be taken into account such as: absorption effects of the low-energy fluorescent radiation, background subtraction and spectral influence, and quantification of the intensity.

EXPERIMENTAL

Instrumentation

The instrumentation used consists of a molybdenum secondary target water-cooled tube system used here at 40 mA, 40 kV, a 30 mm² Si(Li) detector and amplifier (all from Kevex, Burlingame, Calif.) and a conventional multichannel analyser (Northern Scientific NS 701). The instrumentation has been more fully described in an earlier publication[16], where it was compared with conventional crystal diffraction fluorescence equipment for the analysis of air particulate material.

A precise analysis requires a well stabilized high voltage supply to ensure a constant and easily reproducible fluorescing beam intensity. The equipment used, and in fact most instrumentation used for energy dispersive fluorescence analysis, is less well stabilized in output than the crystal fluorescence spectrometers. A number of 20 repetitive measurements of copper $K\alpha$ radiation (12 min per measurement) were performed by excitation of an aluminium matrix containing 1% of copper. The results were critically examined by the mean square successive difference method described by Hooton and Parsons[17] to reveal drift (slow changes) and oscillations (instantaneous changes). A number of statistical tests can be applied to the data

TABLE I

CONDITIONS FOR THE STABILITY OF THE SPECTROMETER

Statistical[a] *criterion*	*Value measured*[a]	*Significance*[b]	*Corrected measured value*	*Significance*
$\bar{x}=\sigma^2$	35.847	—	36.976	—
n	20		20	
$s^2=\frac{\Sigma(x_i-\bar{x})^2}{n-1}$	691.302	—	50.003	—
$\delta^2=\frac{\Sigma((x_i+1)-x_i)^2}{n-1}$	387.741	—	81.073	—
$\chi^2=\frac{(n-1)S^2}{\sigma^2}$	366	H.S.[c]	18.18	N.S[d]
$\eta_s=\frac{\delta^2}{s^2}$	0.56	Low H.S.	1.62	N.S.
$\eta_x=\frac{\delta^2}{\sigma^2}$	10.82	H.S.	2.19	N.S
$t_s=\frac{(1-\eta_s/2)(n+1)(n-1)}{n-2}$	3.40	H.S.	0.90	N.S
$t_x=\frac{(1-\eta_x/2)(n+1)(n-1)}{n-2}$	−20.80	H.S.	−0.45	N.S.

[a] The symbols have their customary meaning: $\bar{x}$, mean; n, number of measurements (20; 12 min per measurement); χ^2, chi-squared; the other symbols are defined.
[b] See Tables II and III.
[c] Highly significant.
[d] Not significant.

TABLE II

INFLUENCE OF INSTRUMENTAL CONDITIONS ON STATISTICAL PARAMETERS

Apparatus conditions	χ^2	η_s	η_x	t_s	t_x
Stable	N.S.[a]	N.S.	N.S.	N.S.	N.S.
Drift	H.S.[b]	Low H.S.	N.S. or low H.S.	Large positive H.S.	N.S. or large positive H.S.
Oscillations	N.S.	High H.S.	High H.S.	Large positive H.S.	Large negative H.S.
Drift + oscillations	H.S.	Low H.S.	High H.S.	Large positive H.S.	Large negative H.S.
Unstable, but no drift, no oscillations	H.S.	N.S. or H.S.	High H.S.	N.S.	Large negative H.S.

[a] N.S. = Not significant.
[b] H.S. = Highly significant.

TABLE III

CRITICAL VALUES FOR χ^2, t AND η FOR 20 MEASUREMENTS

Level of significance	0.995	0.975	0.025	0.005
χ^2	6.84	8.91	32.85	38.58
t	−2.86	−2.09	2.09	2.86
Level of significance	0.99	0.95	0.05	0.01
η	1.04	1.30	2.70	2.96

which when combined are more sensitive than the usual criterion for acceptable equipment stability in which the set of observed replicate counts is expected to lie within the range $\pm 3\sigma$ about the mean. The results are summarized in Tables I–III. For a thorough explanation of the meaning of the tests the original paper should be consulted[17]. It appears that all tests are highly significant when applied to the data and no test is significant when applied after normalization with scattered molybdenum radiation. The instrument is subject both to drift and oscillations which can thus entirely be traced back to insufficient stabilization of the tube and not to the measurement equipment.

The correction method is inapplicable for the analysis of air particulates material because the aerosol accounts for up to 35% of the total mass of the filter (up to 3 mg cm^{-2} compared to 8–9 mg cm^{-2} for the cellulose filter). Nevertheless, the normalization of the intensity is useful for different specific relative measurements on the same sample. The most stable measurements are possible after a warm-up period of the high-voltage supply of *ca.* 30 min at low power. A stability of $\pm 2\%$ is then possible for time periods of at least 4–6 h.

The precision of the energy calibration and of the routine determination of the peak area by addition of a number of channels around the peak maximum intensity, depends critically on the stability of the spectrometer. For repeated analysis of the Mn $K\alpha$ radiation over a period of 3 months the peak maximum is given by the 297.07 ± 0.01 channel. The conversion from channel number to energy

is given by the relation.

$$E(\text{keV}) = 20.02 \cdot 10^{-3} \text{ channel number} - 1.94 \cdot 10^{-3} \quad (1)$$

The $K\alpha$ energy used for calibration is weighted by the intensity through the relation

$$\lambda_{K\alpha} = \frac{\lambda\alpha_1 + \theta\lambda\alpha_2}{1 + \theta} \quad (2)$$

where $\theta = I_{K\alpha_2}/I_{K\alpha_1}$, and λ = wavelength (Å) (3)

The multichannel analyser allows the selection of a number of energy regions. The integrated activity of these regions can either be visualised on a digital counter or printed on teletype. A number of channels corresponding nearly to one tenth maximum was chosen for the integration of every analytically important radiation. Table IV shows the energy regions used for the elements of interest. The regions span some 90% of the total peak area and this fraction is constant if the resolving power does not depend on the integral counting rate.

TABLE IV

ENERGY REGIONS USED IN THE SPECTRUM

Element	*Energy (KeV)*[a]	*Channel maximum*	*Integration channel start–channel end*
Cl	2.622	131.8	125–139
K	3.312	166.5	157–174
Ca	3.690	185.5	178–192
Ti	4.508	226.0	219–233
V	4.949	248.1	240–256
Cr	5.411	271.1	263–279
Mn	5.895	295.9	288–304
Fe	6.400	320.0	312–328
Co	6.925	347.3	339–356
Ni	7.472	374.7	366–383
Cu	8.041	403.0	395–412
Zn	8.631	432.7	424–442
As	10.532	526.6	517–538
Br	11.907	595.0	585–605
Pb	$L\beta_1 = 12.611$		
Incoherent scatter	—	—	820–851
Coherent scatter	17.443	871.4	862–884

[a] $K\alpha$ except where noted.

Figure 1 shows the change of the resolution and the displacement of the peak maximum amplitude as a function of integral counting rate up to a counting rate of $15 \cdot 10^3$ c.p.s. When it is considered that the counting rate of the samples and of the standards for calibration is lower than 2000 c.p.s. it is clear that the integration procedure provides a constant fraction of the full energy peak. Counting losses caused by pile-up and spectrometer dead-time are efficiently corrected by the use

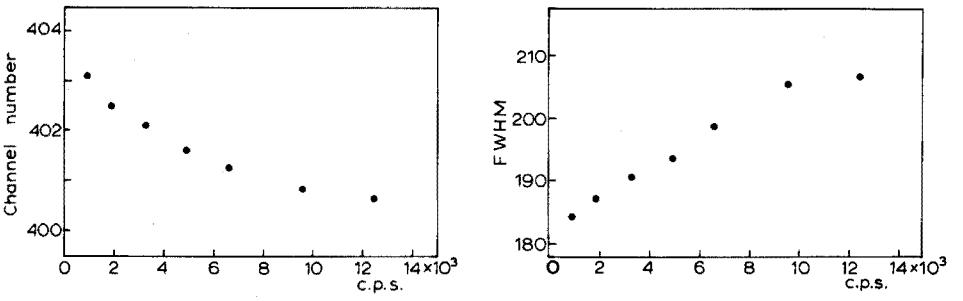

Fig. 1. Peak maximum shift and energy resolution deterioration as a function of integral counting rate.

of an adequate correction circuit[16]. Moreover, these losses are only significant at counting rates appreciably higher than the maximum value used here.

Sampling of atmospheric particulates

Aerosols are collected by a filter technique. The commonly used filters are the glass fibre, organic fibre or membrane type. The selection of an optimal filter depends on factors such as collection efficiency, flow rate, and decrease of the flow rate during sampling and, when the air particulate material is not removed from the filter before analysis, on its impurity level relative to that of the sample collected. Much attention has been devoted to the selection of a single filter material as a compromise between all these factors. In this work, the conclusions of the work of Dams *et al.*[18] were followed in their search for the optimal filter for neutron activation analysis of aerosols, and the Whatman 41 cellulose filter was selected. The procedure can, however, rapidly and easily be adapted to polystyrene membrane and other filter materials of sufficient purity. The samples measured were taken on a 63-cm^2 filter for 24 h at a flow rate of about 20 m^3 h^{-1}.

With the secondary target x-ray fluorescence set-up used, the analysed filter area is only a few mm^2 (4.5 mm^2, oval) so that it is necessary to ensure that the particulate material is sufficiently homogeneously distributed on the substrate. Table V gives the results of 6 measurements at different positions of a single filter. The count rate for every element was normalized to the incoherently scattered $K\alpha$ excitation radiation. The error from inhomogeneous distribution and inhomo-

TABLE V

HOMOGENEITY OF THE PARTICULATE MATERIAL

Element	*Mean counting rate (counts/2000 s)*	*Standard deviation (%)*	
		Experimental	*Counting statistics*
Ca	26.454	2.2	0.6
Mn	13.085	2.6	0.9
Fe	20.472	1.5	0.7
Br	4.380	4.3	1.5
Pb	5.491	3.9	1.4

geneities in composition on the very small analysed surface is thus maximally of the order of 3%.

The sample position during the analysis is another factor which could critically influence the results. Indeed, it proved difficult to control the vertical position of the analysed surface to better than 0.3 mm without a support for the filter. Influence of the sample position on the measured fluorescence counting rate was investigated by measuring a thin sheet of photographic paper at heights of respectively −1.65, +1.65, 3.30 and 4.95 mm relative to the standard measuring position. The results are shown in Table VI. The photographic paper was used because it is a matrix comparable to the filter paper, but contains a few elements at an easily detectable concentration with excellent homogeneity. The intensity varies by about 5% per mm around the standard measurement position, so that the maximum uncertainty on the flatness of the sample induces an error of 1–2%. The reduction of the intensity is due to the divergence of the beam of exciting radiation. It is necessary to place the samples as reproducibly as possible in the measuring position. The loaded filter papers were evenly pressed between two concentric plexiglass rings.

TABLE VI

EFFECT OF THE VERTICAL POSITION OF THE FILTER

Distance (mm)	*Intensity relative to normal position*		*Corrected*			
			With incoherently scattered radiation		*With coherently scattered radiation*	
	Ba Lα	*Br Kα*	*Ba Lα*	*Br Kα*	*Ba Lα*	*Br Kα*
−1.65	104.7	103.2	103.1	101.6	100.3	98.9
0.00	100.0	100.0	100.0	100.0	100.0	100.0
+1.65	93.5	93.3	97.8	97.5	100.9	100.6
+3.30	84.5	84.2	95.3	94.9	101.3	100.8
+4.95	73.7	73.5	93.5	93.2	100.4	100.1

As appears from Table VI, the coherently scattered primary radiation can be used to correct for fluctuations in the sample position. The use of the incoherently scattered radiation for correction is less effective, because of the geometrical dependence of the Compton interaction cross-section, and consequently should not be employed for the normalization.

The use of normalization to the coherently scattered primary radiation is only possible for repeated measurements of the same sample, since the intensity of the scattered radiation is proportional to the product of the beam intensity times the total number of atoms in the beam.

Correction for the background continuum

The net counting rate must be obtained from the integral counting rate in the selected channels, which consists of contributions from fluorescent characteristic radiation, from the background continuum and, in some cases, from interfering

radiation. Interfering radiation can arise from: single and multiple scattering of the exciting radiation in the sample, in the air, and in surrounding material; Compton scattering in the detector; and loss of charge carriers in poorly formed detector regions. Figure 2 shows a background spectrum of a mylar foil (0.68 mg cm^{-2}), a millipore filter HAWP (5.52 mg cm^{-2}) and a Whatman 41 filter (8.8 mg cm^{-2}). The background continuum increases as a function of the mass of the sample. The lowest detection limits for various elements are thus obtainable for small samples on thin backings. The background contribution from scattering in the air path is negligible for samples collected on Whatman or Millipore membrane filters. All measurements could be performed in air since elements lower than potassium, where absorption of the characteristic radiation becomes important, were excluded.

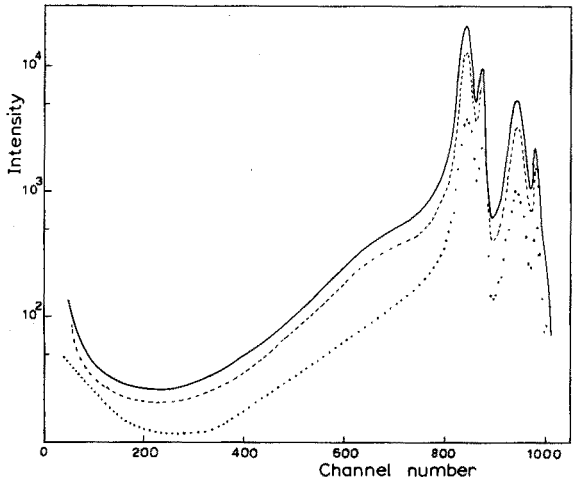

Fig. 2. Background spectrum of a mylar foil (.....); a millipore membrane filter (-----); and a Whatman 41 cellulose filter (——).

A commonly used method to estimate the background radiation consists of interpolation from measurements at the low- and high-energy sides. In a normal air particulate sample, all elements of the first transition series are present, hence the spectrum is too crowded with peaks to allow a measurement of the background anywhere below about 9 KeV. Another method is therefore required. A method was devised which utilizes the primary coherently and incoherently scattered radiation. The ratio of the background radiation at any energy interval of interest to the coherently or incoherently scattered radiation may be considered to be constant for samples of similar composition and dimensions. Any of these ratios can be determined with suitable samples.

To investigate the applicability of this method the backgrounds of a number of blank Whatman 41 filters were carefully measured. Possible variations in the ratio of the background at a particular energy to the coherently or incoherently scattered radiation could be due to fluctuations in mass or in composition of these filters. Three different blank samples were measured at different locations in the surface. The results are summarized in Table VII. There is no significant difference between

TABLE VII

MEAN BACKGROUND OF 3 CELLULOSE FILTERS

Integration zone of element	*Mean background (counts/2000 s)*	*Standard deviation*	
		Experimental (s)	*Counting statistics (σ)*
Cl	575	25	24
K	739	24	27
Ca	417	39	20
Ti	373	15	19
V	436	21	21
Cr	474	14	22
Mn	508	17	23
Fe	740	98	38
Co	760	34	27
Ni	790	21	28
Cu	1016	31	32
Zn	1228	51	35
As	2839	53	53
Br	4931	125	70
Pb $L\beta$	6621	135	81

the standard deviation, s, of these measurements and the variation to be expected from counting statistics, σ. Except for a small iron peak and the argon K radiation from the air, the background spectra obtained over up to 24 h were free from spectral interferences. A factor influencing the direct application of a background obtained from the primary scattered radiation is due to the material collected on the filter itself. In fact, this material has a profound influence on the background characteristics as is directly apparent from the change of the ratio of coherently to incoherently scattered radiation as a function of filter loading (Fig. 3). The accurate measurement of this ratio can in fact become the basis of a determination of total suspended particulate material collected on the filter. Direct weighing of the material collected is difficult owing to the hygroscopic character of the cellulose filter. The contribution of the background at any appropriate energy can therefore be imagined as being built up of a contribution proportional to the coherent scatter peak and one proportional to the incoherent peak. Giauque *et al.*[19] proposed the following formula when the effective Z of the material changes:

$$B_j = (I_{coh} + I_{incoh}) \left(\frac{I_{coh}}{I_{coh} + I_{incoh}} S_j + R_j \right) \tag{4}$$

where I_{coh} and I_{incoh} are the intensities of the coherent and the incoherent peak, respectively; B_j is the background at the energy used for the determination of element j; and S_j and R_j are two constants pertaining to element j. S_j and R_j can be determined by measurement of a background filter and filters loaded with material so as to change the effective atomic number, Z. To prevent spectral interferences, filters loaded with pure aluminium powder (0.3 mg cm^{-2}) and molybdenum powder (0.6 and 0.7 mg cm^{-2}) were used. The ratio of coherent to incoherent radiation

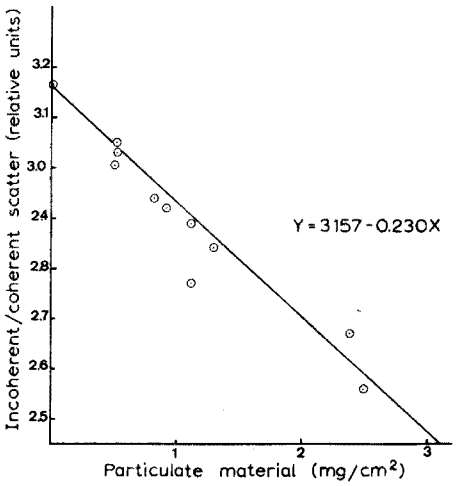

Fig. 3. Ratio of incoherently to coherently scattered primary radiation as a function of particulate material on the filter.

fluctuated between 0.3151 and 0.4352 for these samples. The values obtained for S_j and R_j ranged from $-0.179 \cdot 10^{-3}$ and $1.325 \cdot 10^{-3}$ for potassium to $-1.706 \cdot 10^{-3}$ and $12.952 \cdot 10^{-3}$ for lead and proved to be sufficiently constant over a period of 3 months. Nevertheless, their value was extremely dependent on the geometry of the secondary target setup and the sample positioning so that their value should be periodically checked. They proved to be nearly independent of the amount of material on the filter over the range 0–2 mg cm^{-2} of material.

The precision of the background calculation by this method is apparent from the data presented in Table VIII where the background measured for a cellulose filter was measured for 50000 s and calculated with the coefficients. The residual background was negligible for most elements except rubidium which was located close to the coherently scattered Mo-background peak. The coefficients were used for the determination of the background of other materials such as millipore filter (5.5 mg cm^{-2}) or an aluminium foil (50 mg cm^{-2}) with much less precise results, especially in the latter case, presumably because the widely differing thickness of the material gave rise to a considerable difference in the extent of multiple scattering in the sample itself.

Interferences

Figure 4 shows the spectrum of a blank filter and the spectrum of a filter loaded with mg amounts of copper. At high energies both spectra overlap. Because of the low energy of the Cu $K\alpha$ radiation there is a continuum background contribution from scattering and inefficient collection of the fluorescent radiation. This contribution to the background should be taken into account. Other interferences which should not be overlooked are the silicon escape peak and direct spectral interferences of $K\beta$ on $K\alpha$, L on K, and random sum peaks. The latter interference depends on the counting rate and is virtually absent at the low counting rates encountered with air particulate samples. The former interferences are constant except for the

TABLE VIII

ACCURACY OF BACKGROUND CORRECTION FOR WHATMAN 41 FILTER

Element	*Background (counts/5000 s)*	*Residual background (counts/50000 s)*	*Deviation (%)*	*Apparent concentration ($\mu g\ cm^{-2}$)*
Cl	14.516	1528±165	+10.5	0.75
K	17.748	194±187	N.S.	—
Ca	10.460	143±144	N.S.	—
Ti	8.941	376±134	4	0.01
V	10.049	406±141	4	0.01
Cr	10.461	−63±144	N.S.	—
Mn	10.620	−252±145	N.S.	—
Fe	27.186[a]	−58±233	N.S.	—
Co	15.592[a]	201±176	N.S.	—
Ni	16.146	64±149	N.S.	—
Cu	20.881	−1107±204	5.3	−0.007
Zn	23.434	−1676±216	7	−0.008
As	48.192	−769±310	N.S.	—
Se	65.287	1090±361	1.7	0.003
Br	88.946	1554±421	1.7	−0.004
Pb	132.674	−4879±518	3.7	−0.037
Rb	175.273	−14625±600	8.3	−0.006
Sr	241.710	−6145±695	2.5	−0.002

[a] Detector contamination with ^{57}Co: 0.306 c.p.s. at Fe$K\alpha$; 0.033 c.p.s. at Co$K\alpha$.

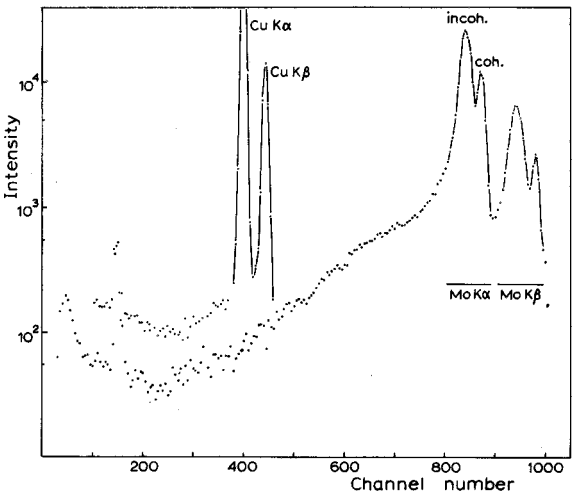

Fig. 4. Background spectrum of blank cellulose filter and one loaded with 1 mg of copper powder.

influence of absorption, which can be neglected for air particulate samples. The spectral interference and the detector interference were treated simultaneously by measuring a filter loaded with a single element. After correction for the background by eqn. (4), the fractional influence of the pertinent element at all integration regions was determined. The influence factors α_{ij} thus obtained provide a correction term at

TABLE IX

INFLUENCE COEFFICIENTS α_{ij}

Correction to be applied on counting rate of element i for 1000 counts of element j.

Element i	*Element j*											
	K	*Ca*	*Ti*	*V*	*Cr*	*Mn*	*Fe*	*Co*	*Ni*	*Cu*	*Zn*	*Pb Lβ*
Cl	—	16.6	6.91	1.23	1.10	1.20	1.01	0.70	0.64	0.67	0.58	12.26
K	—	20.2	5.54	6.41	1.83	2.03	1.17	0.86	0.73	0.79	0.68	1.58
Ca	108.4	—	5.76	4.44	6.57	2.25	0.79	0.96	0.72	0.68	0.61	1.03
Ti			—	6.78	3.47	2.72	3.45	0.86	0.75	0.61	0.66	0.67
V			146.9	—	5.85	5.04	1.99	2.39	0.94	0.66	0.69	0.98
Cr				149.3	—	5.41	3.08	2.10	1.34	0.69	0.70	0.82
Mn					139.4	—	4.18	3.69	2.22	0.73	0.70	0.84
Fe						138.1	—	4.03	4.30	2.82	1.00	1.07
Co							126.6	—	3.89	1.55	2.76	1.19
Ni								99.5	—	2.86	1.60	1.43
Cu									72.39	—	2.43	1.84
Zn									1.30	41.39	—	3.67
As												1151.1

the energy of element i for the presence of j. These are tabulated in Table IX but depend on the instrumentation used and especially on the detector characteristics. Such influence factors are often applied both in classical wavelength-dispersive analysis and in x-energy spectrometry[20,21].

Finally the measured peak intensities I_j can be corrected for background and spectral interferences.

$$I_j' = I_j - B_j - \Sigma_i \alpha_{ji} I_i' \tag{5}$$

In practice an iteration method is used, since the measured peak intensity $I_i - B_i$ is available instead of true interfering peak intensity I_i'. Two successive iterations, whereby first $I_i - B_i$ and then the calculated result I_i' are used, are sufficient when manual calculations are performed.

Calibration

To obtain the concentration of the element from the net peak intensities requires the measurement of at least one standard per element or the knowledge of a set of physical constants which take into account source intensity, the geometrical factor, the cross-section of the fluorescent x-ray production, the detection efficiency, *etc.* It has been argued that owing to the monochromatic nature of the exciting radiation, a relatively small number of elementary standards could be used for the determination of all elements of interest when pertinent literature data are used for a number of physical constants. The following is based on the argument and notation of Giauque *et al.*[19] but a similar treatment can be found in almost any source book on x-ray fluorescence[21].

If the measured sample is homogeneous and of uniform thickness, then the measured fluorescent intensity of an element j in a layer dx is the product of three

probability terms P_1, P_2 and P_3. These terms describe, respectively, that the primary radiation reaches a thickness x below the sample surface, that the element j absorbs the primary radiation in a layer dx and emits K (or L) radiation with an energy E_j, and finally that this radiation reaches the detector and gives rise to a count in the full energy peak. On substituting appropriate expressions and neglecting any enhancement effects in the sample one obtains:

$$dI = G_1 \exp(-\mu_1 \rho \operatorname{cosec} \phi_1 x)\tau_j(1-1/J_{KL}) \times \omega_K f \rho_j \operatorname{cosec} \phi_1 G_2 \exp(-\mu_2 \rho \operatorname{cosec} \phi_2 x) Ab_j \varepsilon_j I_0 dx \quad (6)$$

where G_1, G_2, are geometrical coefficients;

μ_1, μ_2, mass absorption coefficients for the primary (1) and fluorescent radiation (2) expressed in $cm^2\ g^{-1}$;

ρ, ρ_j, density of the sample and of element j in the sample;

τ_j, photo-electric mass absorption coefficient of element j at the excitation energy;

J_{KL}, absorption jump ratio;

ω_K, Auger yield for the K-radiation;

f, fraction of the radiation emitted as $K\alpha$ radiation;

Ab_j, absorption factor for the air path;

ε_j, full energy peak detector efficiency including any absorption in beryllium window, dead layers of the detector and material obstructing the radiation.

Integration over the total thickness of the sample and arranging constant terms yields the expression

$$I_j = GI_0 K_j \varepsilon_j Ab_j \rho_j 1/k(1-\exp(-kd)) \quad (7)$$

where $k = \mu_i \rho \operatorname{cosec} \phi_1 + \mu_2 \rho \operatorname{cosec} \phi_2$

$$K_j = \tau_j(1-1/J_{KL})\omega_K f$$

$$G = G_1 G_2 \operatorname{cosec} \phi_2$$

and for very thin samples

$$I_j = GI_0 K_j \varepsilon_j Ab_j \rho_j d = GI_0 K_j \varepsilon_j Ab_j C_j \quad (8)$$

since $\rho_j d = C_j$ = mass of element j in g cm^{-2}.

To use eqn. (8), an accurate knowledge of K_j, Ab_j and ε_j is necessary. K_j can be obtained from literature data. τ_j and J_{KL} are given by McMaster *et al.*[22]. The exciting radiation has to be considered as consisting of two mono-energetic lines with energies of 17.443 KeV and 19.633 KeV (Mo $K\alpha$ and $K\beta$) and with relative intensities obtained by direct measurement through coherent scattering on a thin silver foil of 79.3% Mo $K\alpha$ and 20.7% $K\beta$. The total photoelectric absorption coefficient is then calculated as the weighted sum of the contributions at the two energies. Accurate fluorescence yields are tabulated by Fink *et al.*[23]. The transition probability factor, f, can be calculated from the ratios $I_{K\alpha}/I_{K\beta}$ as given by Hansen *et al.*[24]. The data used in this work for τ_j, ω_K and f are summarized in Table X.

Absorption in air was taken into account; the values used were a composition of 21.0% O_2, 78.0% N_2 and 1.0% A, a density of $1.20 \cdot 10^{-3}$ g cm^{-3} at room temperature, and a measured air path from the sample to the beryllium window

TABLE X

PHYSICAL CONSTANTS USED FOR THE CALIBRATION

Element	τ_{tot}	ω_K	f	$1-1/J_{KL}$	K_j	Ab_j	ε_j
17 Cl	10.47	0.0942	0.9804	0.8946	0.865	0.315	0.863
19 K	14.71	0.138	0.9489	0.8869	1.708	0.554	0.932
20 Ca	17.31	0.163	0.9355	0.8903	2.349	0.648	0.951
21 Sc	19.25	0.190	0.9235	0.8834	2.983	0.724	0.964
22 Ti	21.32	0.219	0.9137	0.8828	3.766	0.783	0.974
23 V	23.16	0.250	0.9047	0.8860	4.641	0.830	0.980
24 Cr	26.90	0.282	0.8983	0.8861	6.038	0.865	0.985
25 Mn	29.36	0.314	0.8913	0.8839	7.262	0.893	0.989
26 Fe	34.91	0.347	0.8863	0.8784	9.430	0.914	0.991
27 Co	37.96	0.381	0.8836	0.8806	11.252	0.931	0.993
28 Ni	43.83	0.414	0.8828	0.8727	13.980	0.944	0.994
29 Cu	45.80	0.445	0.8819	0.8743	15.716	0.954	0.995
30 Zn	51.56	0.479	0.8809	0.8685	18.894	0.963	1.000
31 Ga	54.28	0.510	0.8794	0.8649	21.054	0.969	1.000
32 Ge	56.41	0.540	0.8776	0.8618	23.037	0.974	1.000
33 As	61.66	0.567	0.8741	0.8610	26.313	0.979	1.000
34 Se	64.50	0.596	0.8687	0.8547	28.540	0.982	1.000
35 Br	70.02	0.622	0.8641	0.8566	32.236	0.985	1.000

of 4.15 cm. This term was amenable to experimental verification, of course, by measurements *in vacuo*.

The detection efficiency term ε_j is the most complicated and is impossible to determine theoretically, owing to the largely unknown detector shape and dimensions. Except for the absorption in the beryllium window, the detection efficiency can safely be considered constant throughout the energy range of interest (2–15 KeV). Absorption in the beryllium window was estimated for the specified thickness of 1 mil ($2.54 \cdot 10^{-3}$ cm) and for a density of 1.848 g cm^{-3}. Values for Ab_j and ε_j are also summarized in Table X.

Determination of the calibration curve

In eqn. (8), I_j is experimentally determined and K_j, ε_j and Ab_j can be obtained as explained in the previous paragraph. With a limited number of calibration standards, it is then possible to calculate I_0G. Pure elements or compounds vacuum-evaporated on mylar foil were used as standards. These were obtained from Micromatter Co. (Seattle, Washington, U.S.A.). The specified mass C_j and the measured specific fluorescent intensity $I_j/\mu g$ obtained for a 40 KV, 40 mA tube operation during a 2000-s measurement are shown in Table XI. The calibration standards can safely be considered as being homogeneous and accurate to better than 5%. Moreover, they may be considered as nearly infinitely thin sources. Absorption is less than 1% in every case.

By dividing the measured intensities by $K_j\varepsilon_jAb_j$, from Table X one should obtain a constant value for I_0G, since this product does not depend on j in any respect. As is apparent from the results in column 5, Table XI, this is clearly not the case. There is a systematic increase of the constant towards high Z. An attempt was

made to explain this discrepancy by an erroneous assumption of the composition of the excitation spectrum. The use of 100% $K\alpha$ Mo-radiation in the calculation instead of the $K\alpha$, $K\beta$ mixture has a very small influence on the values of K_j ($< 0.5\%$) over the energy range of interest. A second possible cause of the discrepancy is an erroneous absorption correction for the air path. This factor had some effect as is apparent from the measurement of the standards *in vacuo* (Table XI, column 6). The reason for the discrepancy between theoretical and experimentally determined values of Ab_j is unknown, but could hardly be attributed to an erroneous estimate of the air path length by as much as a factor 2.

TABLE XI

CALIBRATION DATA

Element	*Chemical form*	*Concn.* C_j ($\mu g\ cm^{-2}$)	*Counting rate* I_0.2000 s μg^{-1}	*Calibration term*		
				I_0G	I_0G *vacuum*	I_0G_{emp}
Cl	KCl	23.3	86	364.3	391.8	—
K	KCl	25.7	299	339.5	388.2	—
Ca	CaF	23.1	479	318.1	374.1	494.9
Ti	Metal	54	1062	378.9	368.1	463.9
Cr	Metal	58	2197	415.7	411.4	488.5
Fe	Metal	55	3464	437.6	400.0	440.7
Cu	CuS	46	6881	455.5	429.6	481.3
Br	CsBr	24	15187	469.0	462.3	485.1

The remaining deviation of I_0G is probably due to insufficiently accurate knowledge of one or more of the physical constants used. Especially the transition probability term, f, could be inaccurate; for its value differs greatly throughout the literature. Another systematic error may be caused by a deviation of the detection efficiency from unity at higher energies (*e.g.* > 5 KeV), possibly owing to the detection of radiation at peripheral poorly compensated detector regions.

An empirical correction term was used in the air absorption term to obtain the values of I_0G_{emp} tabulated in Table XI, column 7, for the elements calcium, titanium, chromium, iron, copper and bromine:

$$Ab_{j_{emp}} = \exp(-(\mu)_{air}\rho_{air}x\alpha) \tag{9}$$

I_0G_{emp} is nearly constant at 475.5 ± 20.1 when a value for $\alpha = 2.0$ is used. The deviations from the mean are less than 4.0% except for iron as is apparent from Table XI. Renewed measurements were made of the iron standard but were consistently too low. A loss of evaporated material from the mylar film might explain this discrepancy. Rejecting the result of iron, a slightly higher value for the mean I_0G and a somewhat lower standard deviation are obtained. In both cases, however, the scatter on the results is lower than the certified precision of the standards.

The above arguments clearly illustrate that large systematic errors may occur when physical constants are used indiscriminately in energy-dispersive x-ray fluorescence analysis. Table XII shows the final calibration terms used in the analysis for the specified conditions. They were obtained by interpolation. For K, Cl and for

TABLE XII

CALIBRATION COEFFICIENTS USED FOR ANALYSIS

Element	$I_g \cdot 2000$ ($s\ \mu g^{-1}$)	*Element*	$I_g \cdot 2000$ ($s\ \mu g^{-1}$)	*Element*	$I_g \cdot 2000$ ($s\ \mu g^{-1}$)
Cl	85.6[a]	Mn	2744	Ga	9429
K	299.3[a]	Fe	3739	Ge	10411
Ca	460.6	Co	4630	As	12007
Sc	733.8	Ni	5917	Se	13113
Ti	1088	Cu	6801	Br	14893
V	1508	Zn	8351	Pb ($L\beta$)	5230[a]
Cr	2139				

[a] Experimentally determined with calibration standard.

Pb, analysis of which had to be based on the *L*-radiation, the experimentally determined coefficients were used as obtained directly with a thin film standard.

Absorption of the fluorescent radiation

Absorption effects are frequently considered as being negligible for samples consisting of cellulose or membrane filters loaded with particulate material. To ascertain whether this assumption is applicable for the lowest Z elements from which data became available in the conditions used (Mo excitation air path), real samples were measured normally and upside down so that the fluorescent radiation had to pass through the bulk of the filter material. Also, measurements were performed with sample filters in the path of the fluorescent radiation between sample and detector. The first experiment gives some indication of the influence of the cellulose substrate on material which is not present at the filter surface but located deeper. The second experiment provides an extreme situation of absorption by the particulate material and by the cellulose filter substrate. The results of these measurements and also direct calculation gave a clear indication that care should be taken for the lowest elements determined in this work, *viz.* Cl to Ti.

That no systematic errors from absorption or other phenomena are induced for higher atomic number elements is apparent from the data shown in Fig. 5, where the measured intensity for a few elements normalized to the lead $L\beta$ radiation is plotted as a function of particulate loading of the filter. The three filters were obtained simultaneously. Normalization to lead was necessary because the amount of aerosols on each filter was not known with a sufficient precision.

More quantitative information on the absorption and also a correction for it, is dependent on how the particulate material is distributed on or in the filter. Absorption of the primary radiation can safely be neglected owing to its high energy compared to the fluorescent radiation of the above-mentioned elements; then when homogeneous distribution of particulate material throughout the filter medium is assumed, the correction is part of eqn. (7).

$$t = 1/kd(1 - \exp(-kd)) \tag{10}$$

with $k = \mu_2 \rho \operatorname{cosec} \phi_2$.

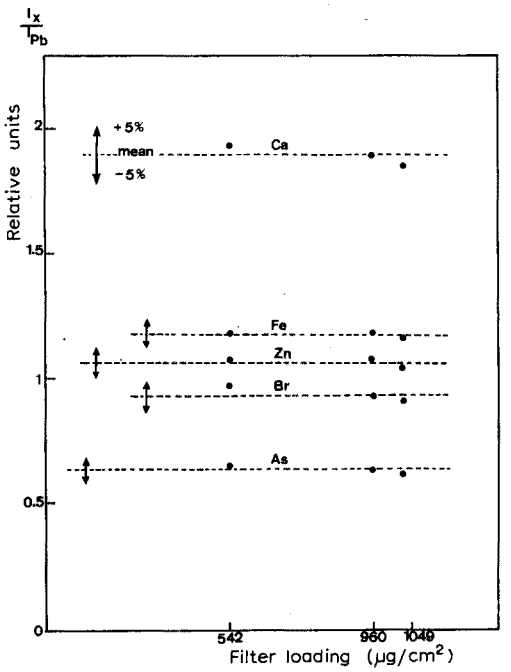

Fig. 5. Counting rate normalized to Pb $L\beta$ radiation as a function of particulate material on the filter.

This relation can give only a very crude correction because the material is clearly not homogeneously distributed. In reality, much particulate material is present on the outer cellulose fibers and the material is distributed as a function of depth, in a manner which is very difficult or impossible to measure. Moreover, since the elements are distributed on particles of different size, this function would depend on the element in question and on the origin of the aerosol (industrial, rural, background). The real distribution of the material can be visualized by a model in which the entire particulate loading of the filter is considered as present in a pure "aerosol" layer but at a specific depth below the filter surface. A simple correction can then be applied for the absorption of the radiation by the filter material on the way to the detector, and another correction term for self-absorption of the particulate material; a, the mean fractional "equivalent" depth of the material below the surface it is then only necessary to obtain the following constants: μ_f, the mass absorption coefficient of the filter material; μ_A, the mass absorption coefficient of the aerosol material; a, the mass fractional "equivalent" depth of the material below the surface of the filter; and d, the thickness of the particulate material (g cm^{-2}. ρ_A). These present no real problems.

For the previously considered exact distribution, the correction takes the form

$$t = \int_0^D \exp(-\mu(x)\rho(x)\, x \operatorname{cosec} \phi_2) F(x) dx \qquad (11)$$

where $\mu(x)$, $\rho(x)$ and $F(x)$ are unknown functions of the depth below the surface.

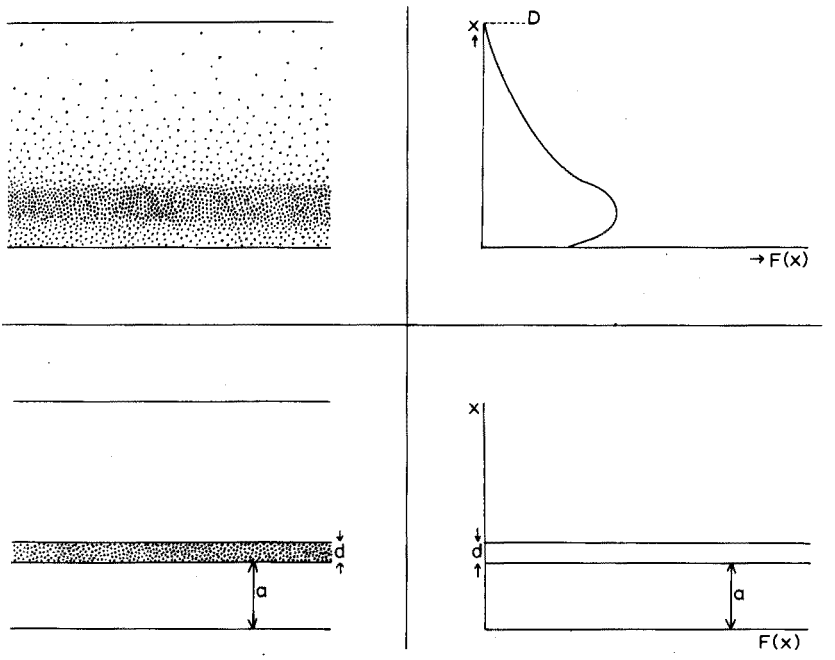

Fig. 6. Schematic representation of a likely distribution of aerosols through the filter and the distribution idealized for absorption correction.

For the idealized condition, the total correction term is the product of a correction for the filter t_F and a correction for the material t_A:

$$t = t_F t_A = \exp(-\mu_f \rho_f \operatorname{cosec} \phi_2 a) \times \frac{1}{\mu_A \rho_A d \operatorname{cosec} \phi_2} (1 - \exp(\mu_A \rho_A d \operatorname{cosec} \phi_2)) \tag{12}$$

The mass absorption coefficients μ_f and μ_A can be obtained from tabulations or can be derived experimentally. The latter depends on fluctuations in the composition of the aerosol material. For the relatively small corrections necessary for the determinations in this work, a "mean" aerosol composition was used. The results of some experimental determinations are given in Table XIII together with the mass absorption coefficients for the cellulose matrix (glucose) and a typical rural and city dust sample. At low Z, below chlorine, a sound correction will probably become increasingly difficult to apply, when the bulk composition is not known precisely except through measurement of μ_A of the actual sample itself.

The one remaining term in eqn. (12) is the equivalent penetration depth, a, which may be determined by measuring a typical sample in duplicate, once with the particulate material facing the primary radiation side, and once with the filter reversed. The intensity ratio between the two measurements is given by

$$R = \exp(\mu_f \operatorname{cosec} \phi_2 \rho_f (D - 2a)) \tag{13}$$

TABLE XIII

MASS ABSORPTION COEFFICIENTS FOR Cl, K, Ca AND Ti RADIATION WITH A CELLULOSE FILTER MATRIX AND AIR DUST

Element	μ_f ($cm^2\ g^{-1}$)		μ_A ($cm^2\ g^{-1}$)		
	Exp.	*Calc.*	*Exp.*[a]	*Calc.*[b]	*Calc.*[c]
Cl	196	209	317	401	219
K	102	110	111	230	113
Ca	74.4	73.5	145	167	78
Ti	41.5	44	166	132	85

[a] Industrial sample.
[b] Milan city dust composition[27].
[c] Rural composition: 76% C, 9% O, 2% Al, 4.2% Si, 2.9% Ca, 0.09% Fe.

Thus R allows a, or alternatively the fraction a/D to be calculated; a should be determined for every element and may depend on the type of particulate material and on the filter loading.

The value of a was estimated rather imprecisely for a typical sample as 0.20 and 0.16 for calcium and potassium, respectively. More reliable values are currently obtained through the use of more sensitive excitation with lower-energy primary radiation.

All constants needed for an experimental determination of the absorption can be obtained from 3 relative measurements of the same sample in different geometrical conditions (up and down, without, and up, with, a particulate-loaded filter in the radiation path). The scattered radiation can be used to correct for any instrumental factors and a high precision, practically dictated by counting statistics, is obtainable. In principle, these three measurements of an unknown filter allow the absorption correction and of course all analytical results to be measured.

RESULTS

The method presented here has been carefully tested in preparation for routine analytical work. Various samples were analysed several times over a period of several months. The results of a set of 6 measurements on the same sample provided a mean deviation per measurement of 5–6%, including all steps of the analytical procedure. A check of the calibration procedure was possible by the measurement of two very thin standards of the same type as those used for the calibration procedure itself, namely for zinc and nickel evaporated on mylar, which were not available initially. Both agreed within 5% with the calibration data.

The x-ray fluorescence method was checked by the analysis of 15 samples by instrumental neutron activation.The instrumental neutron activation procedure applied has been in use for several years and has been thoroughly tested on various standardized samples; one of the chief virtues of the method is its near independence from phenomena related to the composition, the sample size, etc. Compared to the x-ray fluorescence method with its inherent dependence on matrix absorption and enhancement, it can be considered as a primary standardization method when

applied by an experienced analyst. The results of the comparative analyses are shown in Table XIV. For those elements which were precisely determined by both methods, *e.g.* Fe, Zn, the agreement is in general very satisfactory. For lead, no results were available by instrumental neutron activation analysis, because no significant radioactivity was produced on neutron irradiation. Other elements were determined with poor precision by neutron activation analysis owing to their inherently low sensitivity. For the results obtained by x-ray fluorescence, the precision stated was obtained from the counting statistics (one standard deviation) and excludes any other factor responsible for imprecision. For the results of the instrumental neutron activation analysis, a realistic standard deviation for the entire analysis is given. The results for potassium and calcium obtained by x-ray fluorescence were systematically too low. Indeed, no correction was applied for the already considerable absorption. All samples were obtained in a heavily industrialized zone to the North of Ghent, Belgium and were analysed by i.n.a.a. at the Institute of Nuclear Sciences, Ghent, Belgium. Table XV shows the corrected results for potassium and calcium which compare much better with the values obtained by i.n.a.a., but some unexplained discrepancies persist.

Another test on the accuracy of the present method was offered in two interlaboratory comparison studies. One was an intercomparison organised by the Commission of Health of the E.E.C. at the Joint Center of Ispra. More than 30 laboratories participated in the determination of selected constituents or in multielement determinations. Various techniques were applied for inorganic constituents, such as instrumental neutron activation analysis, atomic absorption spectrometry, wavelength-dispersive x-ray fluorescence, emission spectrometry, wet chemical analysis, and electrochemical and spectrophotometric methods. Our determinations were the only ones which were done by energy-dispersive x-ray analysis. The samples sent to the participants were gram amounts of homogenized and sieved ($297 + 12$ μm) dust collected in the centre of the city of Milan. The homogeneity was stated to be better than 10% for samples of 20 mg or more. For analysis by the proposed method, it was necessary to place homogeneously milligram amounts on a cellulose filter substrate to simulate a normally obtained loaded filter; this was achieved by the puff-technique[19]. A detailed procedure for the microanalysis of powdery material by this method will be described separately. The mean concentrations of all elements of interest obtained in the intercomparison study and in this work, are compared in Table XVI. Except for lead, the results agree favourably with the mean concentration. This not only proves the validity of the proposed method but also the homogeneity of the material at the submilligram level. The standard deviation shown was obtained from 10 independent determinations; this deviation relates to the analytical procedure, the sample inhomogeneity and the sample preparation and weighing.

An intercomparison study was also organised in the spring and summer of 1974, on the analysis of inorganic constituents in an actual sample of aerosols collected on a membrane filter. Also some rock standard material and a spotted solution of a few elements placed on the same type of support were circulated for analysis. On the actual particulate material, the results of the present determinations could be compared with the most likely concentration present as outlined at the Annual x-ray Conference (Denver, August 1974). A detailed survey of submitted

TABLE XIV

COMPARISON OF THE ANALYSIS OF 15 SAMPLES BY X-RAY FLUORESCENCE AND INSTRUMENTAL NEUTRON ACTIVATION

Sample	*Concentrations found (ng m^{-3} of air)*							
	Potassium		*Calcium*		*Titanium*		*Vanadium*	
	X.r.f.	*I.n.a.a.*	*X.r.f.*	*I.n.a.a.*	*X.r.f.*	*I.n.a.a.*	*X.r.f.*	*I.n.a.a.*
1	1569±32	2102±105	4920±36	5482±550	134±5	129±58	103±5	93±5
2	1013±29	1428±70	7476±43	8735±660	145±6	97±54	133±5	148±7
3	1124±37	1603±80	22.446±76	25.513±2550	252±7	383±101	353±7	421±20
4	2100±30	3130±105	6737±34	10.426±967	191±5	154±102	160±4	157±8
5	1281±20	2080±100	6416±28	7646±700	155±4	208±71	144±3	132±6
6	1145±20	2152±110	10.814±36	13.280±965	187±5	247±90	212±4	233±12
7	940±27	1004±50	2470±27	2543±349	175±6	140±23	51±4	31±3
8	920±30	1127±56	2624±28	2290±362	188±7	153±25	50±4	38±4
9	1004±30	1201±60	2699±30	2441±362	211±7	161±25	45±4	27±3
10	1744±36	2449±120	8600±48	8035±804	170±6	140±39	117±5	77±5
11	1279±32	1726±173	6323±41	7982±1188	180±7	209±68	113±5	91±9
12	1588±38	2442±125	15.761±65	17.296±2024	262±7	197±109	133±5	123±6
13	2194±30	2700±135	10.272±44	13.577±1465	237±6	268±72	62±4	44±4
14	501±20	698±70	889±15	1157±272	60±5	43±23	37±3	30±3
15	1393±25	2230±110	7309±30	10.301±1250	498±8	591±120	61±5	49±5

Sample	*Chromium*		*Manganese*		*Iron*		*Nickel*	
	X.r.f.	*I.n.a.a.*	*X.r.f.*	*I.n.a.a.*	*X.r.f.*	*I.n.a.a.*	*X.r.f.*	*I.n.a.a.*
1	17.5±3	12±1	376±5	364±18	1914±8	1900±95	30.5±1	25±21
2	23±3	21±1	307±4	333±16	2813±10	3197±160	26±1	31±21
3	58±4	47±2	1050±7	1082±54	6788±15	7215±360	32±1	35±26
4	40±3	37±4	507±4	519±26	6126±11	5624±280	48±1	30±30
5	33±2	31±3	361±3	357±36	5351±9	5294±265	33±1	42±16
6	45±3	46±2	590±4	684±34	6741±10	7495±375	37.5±1	37±17

7	22±3	13±1	107±3	119±6	2650±10	2195±110	14±1	<200
8	21±3	15±2	93±3	92±6	2733±10	2612±130	15±1	<200
9	23±3	20±2	103±3	92±5	3006±10	2927±145	15±1	<300
10	24±3	22±1	336±5	309±15	2244±9	1993±100	37±1	20±20
11	28±3	19±1	222±4	208±10	2636±10	2120±106	36±1	<20
12	25±4	28±3	454±5	496±25	3845±11	4146±207	37±2	<40
13	18±3	11±1	122±3	139±7	2655±8	2494±125	18±1	30±20
14	4.7±2	4.3±0.4	224±3	221±11	704±7	768±38	11±1	54±10
15	9±3	7±1	1308±7	1379±84	1275±7	1325±65	16±1	15±15

Sample	*Copper*		*Zinc*		*Arsenic*		*Bromine*	
	X.r.f.	*I.n.a.a.*	*X.r.f.*	*I.n.a.a.*	*X.r.f.*	*I.n.a.a.*	*X.r.f.*	*I.n.a.a.*
1	32±1	—	926±4	933±50	11.4±3	18±2	137±1	143±14
2	30±1	50±20	778±3	845±42	11±3	17±1	96±1	104±10
3	44±2	—	910±4	940±50	12±3	16±1	101±1	93±9
4	50±1	88±14	858±3	851±85	14±3	26±1	254±1	327±33
5	35±1	43±8	623±2	651±65	18±2	28±3	177±1	242±24
6	41±1	—	636±2	704±35	15±2	26±2	172±1	242±24
7	76±2	68±14	696±3	644±64	29±3	28±1.5	53±1	56±12
8	74±2	83±16	640±3	637±32	30±3	30±2	43±1	46±9
9	114±2	116±23	736±4	720±36	35±3	36±2	65±1	69±14
10	40±1	59±24	1067±4	1010±100	15±3	20±1	141±2	144±14
11	54±2	53±20	1014±4	890±89	15±3	16±2	136±2	132±7
12	45±2	94±18	1016±4	1148±115	12±4	23±2	123±2	139±14
13	16±1	32±16	244±2	256±50	11±2	10±1	76±1	76±8
14	10±1	18±9	157±2	215±43	9±2	8±1	57±1	57±1
15	15±1	56±23	308±3	347±68	22±2	25±1	63±1	64±9

TABLE XV

CORRECTED RESULTS FOR CALCIUM AND POTASSIUM

Sample loading (mg cm^{-2})	*Concentration found (ng cm^{-3})*					
	Calcium			*Potassium*		
	Measured	*Corrected*	*I.n.a.a.*	*Measured*	*Corrected*	*I.n.a.a.*
0.91	4920	6237	5482±550	1569	2183	2102±105
0.82	7476	9384	8735±660	1013	1399	1428±70
1.09	22446	29190	25513±2550	1124	1590	1603±80
2.38	6737	9870	10426±967	2100	3273	3130±105
2.38	6414	9397	7646±700	1281	1997	2080±100
2.49	10814	16005	13280±965	1145	1798	2152±110
0.53	2470	3073	2543±350	940	1271	1004±50
0.49	2624	3197	2290±362	920	1242	1127±56
0.53	2699	3298	2441±362	1004	1358	1201±60
1.12	8600	11121	8035±804	1744	2475	2449±120
0.93	6323	8069	7982±1188	1279	1789	1726±173
1.30	15761	20729	17296±2024	1588	2291	2442±125

TABLE XVI

INTERLABORATORY COMPARISON UNDER E.E.G. AUSPICES

Element	*No. of labs.*	*Mean value[c] (p.p.m.)*	*Error range[a]*	*Our result ± one standard deviation[b] (p.p.m.)*
Ca	15	43150	12193	45600±2700
Ti	7	2740	700	2900±200
V	10	1995	1100	2000±100
Cr	10	200	87	130±60
Mn	18	1265	350	1480±100
Fe	21	35093	6170	36700±1700
Co	10	18.5	7	<80
Ni	13	1470	600	1200±100
Cu	9	650	87	800±200
Zn	16	7450	2000	8980±500
As	7	93	28	120±70
Br	9	624	150	820±40
Pb	14	5800	1700	7770±460

[a] Difference between lowest and highest reported value.
[b] Standard deviation obtained from 10 independent determinations.
[c] Neutron activation analysis.

results is not available at the time of writing. Anomalous results were again obtained for lead; this was traced to an erroneous background subtraction and is now remedied.

DISCUSSION

The method described here for the analysis of some 15 elements in air

particulate material possesses sufficient accuracy (about 5–10%). The analysis is rapid and non-destructive and can be used routinely. The instrument is equipped with a 15-position sample changer. If each sample is counted for a "live" measurement time of 2000 s, which is amply sufficient as can be judged from the counting statistics in Table XVII, the maximum throughput of samples is about 50 per day. Data reduction is done with a computer, although it could easily be performed manually. The peak intensities are extracted from the spectrum by searching for the energy intervals given in Table IV when an output on magnetic tape is applied. Alternatively, the integration intensity of the peaks as printed on the teletype output of the multichannel analyser, can be fed directly to the computer. The first possibility is to be preferred because a permanent record of each spectrum remains available for later reference, and operator rechecks. The procedure is free from time-consuming human intervention. A large computer facility is not essential for the analysis of the x-ray spectra; a small digital computer (12–16 K) or even a larger programmable calculatng machine is sufficient.

Work is now in progress on the analysis of low Z elements from Al to Cl. Vacuum operation and a lower excitation radiation (Ti $K\alpha$) are then necessary. Moreover, considerably more attention must then be devoted to the matrix absorption effects. It is not entirely clear whether the method for correction for absorption is applicable for the lowest Z elements, from Al to S. If the molybdenum secondary radiator were replaced by a higher Z one, barium or one of lower rare earths, a few elements might become apparent in the mass region of atomic number 40–56.

TABLE XVII

DETECTION LIMIT AND LIMIT FOR DETERMINATION WITH 10% PRECISION

(Whatman 41 cellulose filter, Mo-excitation, 2000-s measurement)

Element	*Detection[a] limit (ng cm^{-2})*	*Limit determination[a]*	*Typical concentration[b]*
Cl	1300	4600	$3 \cdot 10^3$
K	430	1500	$1.5 \cdot 10^4$
Ca	210	750	$3 \cdot 10^4$
Sc	130	470	7
Ti	85	300	$2 \cdot 10^3$
V	65	230	$3 \cdot 10^3$
Cr	50	170	$2 \cdot 10^3$
Mn	40	130	$7 \cdot 10^2$
Fe	30	100	$3 \cdot 10^4$
Co	25	90	$3 \cdot 10^1$
Ni	23	75	$3 \cdot 10^2$
Cu	22	75	$2 \cdot 10^3$
Zn	20	65	$4 \cdot 10^3$
As	21	65	$7 \cdot 10^1$
Se	21	65	10
Br	22	70	$1 \cdot 10^3$
Pb	75	230	$1 \cdot 10^4$

[a] Detection limit and determination with 10% precision based on the convention proposed by Currie[26].
[b] 24-h sampling in polluted environment over 63-cm^2 cellulose filter at 300 l min^{-1}.

In Table XVII, the detection limit and the limit for determination with 10% precision[26] is shown for a number of elements. The lowest amount detectable on a cellulose filter of 9 mg cm^{-2} is 20 ng cm^{-2} for zinc. When one realises that only a 4.5-mm^2 portion of the sample surface is measured, this means that absolute amounts of 1 ng of zinc can be detected in a 0.5-mg sample consisting of filter and down to 50 μg of particulate material. The sensitivity remains acceptable for lower Z elements such as titanium. The lowest elements can, of course, be fluoresced much more effectively with primary radiation of lower energy.

More sensitive determinations should be possible if a thinner filter medium were employed. A high sensitivity is also of importance for the analysis of particulate material which has been separated into fractions of different size with a cascade impactor. The method could easily be adapted for such samples, but the measuring time should then be increased to compensate for the reduction in sample size.

It may be concluded that the use of the monoenergetic exciting radiation of molybdenum obtained with a secondary target set-up, a conventional water-cooled x-ray tube and a semiconductor detector, permits many trace elements from chlorine to strontium to be determined in particulate material collected on cellulose filters. The method can be applied easily and is more rapid and economical than other multielement analytical techniques such as neutron activation analysis and emission spectrometry. The use of a single element thin film standard or a few of these to calibrate for the determination of many elements appears to be possible, although great care should be taken to prevent systematic errors. Absorption of the fluorescent radiation can be remedied by a simple correction method.

Thanks are due to Prof. Dr. J. Hoste and Dr. R. Dams, from the Institute of Nuclear Sciences, Ghent for providing the samples analysed by neutron activation analysis. The help of R. Nullens in some of the experiments is gratefully acknowledged. Dr. R. Dewolfs participated in the analysis of the intercomparison samples.

SUMMARY

The use of monoenergetic exciting radiation of molybdenum obtained with a secondary target set-up, a conventional water-cooled tungsten anode x-ray tube and a Si(Li) semiconductor detector permits many trace and minor constituents from chlorine to strontium to be determined in particulate material collected on cellulose filters. The method is rapid and economical compared to other multielement techniques. The use of one or more single-element thin-film standards to calibrate for the analysis of many elements appears to be possible, but some systematic errors must be prevented. Absorption of the fluorescent radiation is remedied by a simple correction method. The precision and the accuracy of the method were critically examined by independent analysis of a number of samples with instrumental neutron activation analysis and by interlaboratory comparisons on the same samples.

REFERENCES

1 A. Sugimae, *Anal. Chem.*, 46 (1974) 1123.
2 S. S. Hochheiser, F. J. Burman and G. B. Morgan, *Environ. Sci. Technol.*, 5 (1971) 679.

3 P. Grennfelt, A. Akerstrom and C. Brosset, *Atmos. Environ.*, 5 (1971) 433.
4 H. R. Bowman, J. G. Conway and J. G. Asaro, *Environ. Sci. Technol.*, 6 (1972) 558.
5 W. H. Zoller and G. E. Gordon, *Anal. Chem.*, 42 (1970) 257.
6 R. Dams, J. A. Robbins, K. A. Rahn and J. W. Winchester, *Anal. Chem.*, 42 (1970) 861.
7 H. W. Edwards, *Anal. Chem.*, 41 (1969) 1172.
8 C. D. Burnham, C. E. Moore, E. Kanabrocki and D. M. Hattori, *Environ. Sci. Technol.*, 3 (1969) 472.
9 J. Y. Hwang, *Anal. Chem.*, 44 (1972) 21A.
10 R. Woldseth, *X-ray Spectrometry*, Kevex Corp., Burlingame, Calif., 1973.
11 F. S. Goulding and J. M. Jaklevic, *Ann. Rev. Nucl. Science, Vol. 23*, Annual Reviews Inc., Calif., 1973.
12 J. A. Cooper, *Nucl. Instrum. Methods*, 106 (1973) 525.
13 S. K. Perry and F. P. Brady, *Nucl. Instrum. Methods*, 108 (1973) 389.
14 J. V. Gilfrich, P. G. Burkhalter and L. S. Birks, *Anal. Chem.*, 45 (1973) 2002.
15 J. Walinga, *Chem. Weekbl.*, 69 (1973) L-47.
16 R. Dewolfs, R. De Neve and F. Adams, *Anal. Chim. Acta*, in press.
17 K. A. Hooton and M. L. Parsons, *Anal. Chem.*, 45 (1973) 2218.
18 R. Dams, K. A. Rahn and J. W. Winchester, *Environ. Sci. Technol.*, 5 (1972) 441.
19 R. Giauque, F. Goulding, J. M. Jaklevic and R. H. Pehl, *Report of the Lawrence Radiation Laboratory*, University of California, 1972 LBL 647.
20 A. S. M. de Jesus, *X-ray Spectrom.*, 2 (1973) 179.
21 R. Jenkins and J. L. de Vries, *Practical X-ray Spectrometry*, McMillan, London, 1970.
22 W. McMaster, N. Del Grand, J. Mallett and J. Hubbell, *Compilation of X-ray Cross-sections*, Report of the Lawrence Livermore Laboratory, University of California, UCRL-50174, 1969, section 2, rev. 1.
23 R. Fink, R. Jopson, H. Mark and C. Swift, *Rev. Mod. Phys.*, 38 (1966) 513.
24 J. Hansen, H. Freund and R. Fink, *Nucl. Phys. A*, 142 (1970) 604.
25 D. C. Camp, J. A. Cooper and J. R. Rhodes, *X-ray Spectrom.*, 3 (1974) 47.
26 L. Currie, *Anal. Chem.*, 40 (1968) 586.
27 R. Dams, *Studie van de Anorganische Samenstelling van Atmosferische aerosolen*, University of Ghent, Belgium, 1974.

Analytica Chimica Acta, 75 (1975) 87–94

THE DETERMINATION OF GALLIUM BY ATOMIC ABSORPTION SPECTROMETRY

A. CHOW and W. LIPINSKY

Department of Chemistry, University of Manitoba, Winnipeg, Manitoba, R3T 2N2 (Canada)

(Received 3rd June 1974)

Gallium in ores has been determined by only a few techniques, most of which require some form of preliminary separation to concentrate the metal or to remove analytical interferences. Onishi[1,2] has used a benzene extraction before complexation with rhodamine B to detect fluorimetrically as little as 0.01 μg of gallium. Isopropyl ether has also been used as an extractant in conjunction with a rhodamine B determination[3]. Methyl isobutyl ketone has been used[4] as extractant before the determination of gallium by flame spectrometry, and has been used[5] with titanium(III) chloride before analysis by atomic absorption spectrometry.

Atomic absorption spectrometry should provide a very convenient and accurate method for the determination of gallium in solutions obtained from ores. Gallium has been determined in aqueous solution[6] by extraction, with methyl isobutyl ketone and 1-pentanol, of the 8-hydroxyquinolinate for direct aspiration. For the determination in ores, Pollock[5] used titanium(III) chloride and methyl isobutyl ketone to extract gallium from a hydrochloric acid solution of limonite. This procedure provided similar values to an unstated spectrometric method. It has been noted[3], however, that the direct determination of gallium in 7 *M* hydrochloric acid solutions of ores gave values 50% or more higher than those obtained by solvent extraction and spectrometric determination with rhodamine B. In addition, it was observed that the analysis could not be completely corrected, directly, by the method of standard additions, and that the absorbances obtained were very dependent on hydrochloric acid strength. Similar interference problems have been discussed by Elliott and Stever[7] and by Fletcher[8] in their analyses of ores. In these cases, the combination of molecular absorbance and scattering caused by some constituents in the ore matrix caused the difficulty, which was labelled collectively as background.

The analysis of ores for gallium most commonly requires the use of a solvent extraction procedure. In many circumstances, this step serves to concentrate the gallium for analysis, and, simultaneously, to isolate the gallium from interferences. When the sample solutions are already sufficiently concentrated, however, or if multiple samples have to be analyzed, it can be a time-consuming procedure to treat and extract each one.

The present paper describes the use of a nitrous oxide–acetylene flame for the determination of gallium by atomic absorption spectrometry and the application to ore solutions. It was considered that this method might eliminate many of the difficulties encountered with the use of air–acetylene flames, permitting direct gallium analysis and thus avoiding extended sample manipulation.

EXPERIMENTAL

Apparatus

A Perkin-Elmer Model 306 atomic absorption spectrophotometer was used with appropriate Varian hollow-cathode lamps. A Centaur 5-μl micropipetter was used for standard additions.

Chemicals

Gallium standards were prepared by dissolving electronic grade gallium (Alusuisse, 99.9999% purity) in a minimal amount of aqua regia, and diluting to an appropriate volume with 1% hydrochloric acid. All gallium standards were stored in glass containers, as it was observed that several types of plastic (both polyethylene and polypropylene) adsorbed appreciable amounts of dilute gallium solutions. For example, a 125-ml polyethylene bottle adsorbed 50% of a 10 p.p.m. gallium solution in 0.1% hydrochloric acid in one day.

Reagent-grade chemicals and solvents were used throughout. Solutions for the diverse ion study were prepared by dissolving the salt in water or an appropriate acid, and diluting to volume. All water used was double-distilled and deionized.

Gallium-containing ores and mill products were provided through the courtesy of the Tantalum Mining Corporation of Canada Ltd., Bernic Lake, Manitoba, Canada.

Instrumental settings

Optimal conditions for fuel and oxidant pressure and flow rate were found to be acetylene 9 p.s.i., 5 l min^{-1}, and air 30 p.s.i., 27 l min^{-1} for an air–acetylene flame, and acetylene 8 p.s.i., 7 l min^{-1} and nitrous oxide 30 p.s.i., 13 l min^{-1} for a nitrous oxide–acetylene flame. The solution aspiration rate was 5 ml min^{-1} with air–acetylene and 3 ml min^{-1} with nitrous oxide–acetylene flames.

The gallium hollow-cathode lamp was run at 15 mA and the line at 287.4 nm used for analysis. A hydrogen continuum source operated at 22 mA, and a platinum hollow-cathode lamp operated at 20 mA with the platinum line at 299.8 nm, were both used for background absorption studies. In all cases the slit width was 0.7 nm and the values were obtained from the average of five consecutive 2-s integration periods.

Calibration

Calibration curves were prepared for gallium with air–acetylene and nitrous oxide–acetylene flames. A linear response over the range 0–150 p.p.m. gallium and a sensitivity of 2.1 p.p.m., were obtained with air. With nitrous oxide, a linear response from 0–100 p.p.m. and a sensitivity of 0.8 p.p.m. were found. Sensitivity is defined as the concentration required to give 1% absorption.

Effect of various acids and bases

The effects of several acids and sodium hydroxide on the determination of gallium were investigated with both the air–acetylene and nitrous oxide–acetylene flame. Samples were prepared containing the same amount (10 p.p.m.) of gallium

and the appropriate concentration of either hydrochloric acid, nitric acid, sulphuric acid or sodium hydroxide. Similarly, blanks were prepared with no gallium but with the same acid or base concentration. The apparent gallium concentration of the samples was determined by using the auto-concentration mode of the atomic spectrometer with a scale expansion of 20–50 times. Each value obtained for a sample was corrected by subtracting the appropriate blank value. One sample of each set was taken to be exactly 10 p.p.m. gallium (after correction for the blank) and the other samples in that set were measured relative to it. Five or more 2-s integration values were obtained for each sample and the averages are reported in Table I. The blanks reported were calculated in apparent p.p.m. gallium, the

TABLE I

EFFECT OF VARIOUS ACIDS AND BASES ON THE APPARENT CONCENTRATION OF GALLIUM[a]

Acid or base concentration (M)		*Air/acetylene*		*Nitrous oxide/acetylene*	
		Blank	*Ga*[b]	*Blank*	*Ga*[b]
HCl	0.01	0.6	12.1	0.7	11.2
	0.05	0.1	10.0[c]	—	10.0[c]
	0.1	0.5	10.1	—	9.8
	0.5	0.1	9.4	—	9.9
	1.2	0.1	8.9	0.7	9.4
	2.4	0.6	8.8	1.3	10.0
	4.8	0.5	7.6	—	9.5
	7.2	0.6	6.4	0.9	9.1
HNO_3	0.016	−0.1	10.0[c]	0.7	10.0[c]
	0.08	−0.2	9.9	—	10.1
	0.16	0.1	9.8	—	10.0
	0.8	0	9.7	—	10.3
	1.6	−0.2	9.6	0.7	10.5
	3.2	−0.5	9.8	—	10.1
	6.4	−1.3	10.2	—	9.8
	9.6	−1.4	10.2	0.8	9.5
H_2SO_4	0.01	−0.1	10.0[c]	0.7	10.0[c]
	0.06	0.1	10.0	—	10.0
	0.12	0.3	9.5	—	9.8
	0.6	0.9	8.5	0.5	9.6
	1.8	2.8	7.3	—	8.4
	3.6	5.9	5.5	—	7.1
	7.2	7.5	4.7	0.8	5.4
NaOH	0.01	0.4	10.0[c]	1.0	10.0[c]
	0.05	0.7	9.8	—	9.9
	0.1	0.3	10.1	0.7	9.5
	0.5	2.4	10.2	—	9.3
	1.0	4.2	9.5	1.1	8.5

[a] 10.0 p.p.m. gallium taken.
[b] Apparent gallium concentration in p.p.m. after correction for blank.
[c] Solution used to set calibration equal to 10.0 p.p.m.

blank value of pure water being taken as zero. The average deviation in the values reported for the blanks and the samples was 0.3 units or less, with an overall average of 0.15 units.

The effect of hydrochloric acid was significant when an air–acetylene flame was used; there was a 24% reduction in apparent gallium concentration over the range 0.05–4.8 *M*, compared with only a 5% variation when nitrous oxide was used. The hydrochloric acid blanks showed no significant variation with either flame.

Nitric acid samples showed no real difference in the determination of gallium with either flame over a wide range of acid concentrations, but the blanks varied by 1.5 p.p.m. apparent gallium when the air–acetylene flame was used. Significant variations in apparent gallium concentration were caused by increasing sulphuric acid concentration when either flame was used, although the effect was less with the nitrous oxide flame. In addition, the sulphuric acid blanks were constant for the nitrous oxide flame, while with air–acetylene, the blanks varied greatly. Sodium hydroxide solutions did not show significant variations in the apparent gallium analysis, except at high concentration, but again the blanks showed a considerable variation when an air–acetylene flame was used.

Overall, it can be seen that the use of a nitrous oxide–acetylene flame provides a method much less subject to interference by variation in acid and base strength. Blanks are also much more consistent and can be ignored as a source of error. The air–acetylene flame can be used for gallium determinations provided that solutions of samples and standards can be carefully matched, but blanks are significant and must be corrected for; however, these would be less significant for more concentrated gallium solutions.

Effect of various salts

The effect of various salts on the determination of gallium was investigated for both flames. Samples were prepared containing 10 p.p.m. gallium in 2.0 *M* hydrochloric acid and 100, 1000 or 5000 p.p.m. of the particular salt. The apparent gallium concentration of these solutions was determined by comparison with a solution containing only 10 p.p.m. gallium in 2.0 *M* acid; scale expansion was used with the auto-concentration mode of the instrument. The results of this study are recorded in Table II.

Only minor effects were observed with either flame for any of the salts at the 100 and 1000 p.p.m. level except in the case of aluminium with the air–acetylene flame. Since aluminium often occurs with gallium, the removal of this interference by use of the hotter nitrous oxide flame is significant. At the 5000 p.p.m. level, several salts affected the determination, particularly iron, lead, tin, chromium and aluminium with the air–acetylene flame. The use of the nitrous oxide–acetylene flame reduced these interferences significantly, although chromium and lead still had a substantial effect. High concentrations of sodium also influenced the analysis for gallium with the nitrous oxide flame, but these concentrations would rarely be found in routine samples.

Analysis of gallium ore

A finely-ground and roasted ore was carefully mixed and subdivided to provide a series of samples weighing 4–5 g. Sample A was placed into a 125-ml

TABLE II

EFFECT OF VARIOUS SALTS ON APPARENT GALLIUM CONCENTRATION

(10.0 p.p.m. gallium taken in 2 *M* HCl)

	Apparent gallium concentration					
	Air/acetylene			*Nitrous oxide/acetylene*		
Salt concentration (p.p.m.)	*100*	*1000*	*5000*	*100*	*1000*	*5000*
Salt added						
NaCl	10.5	10.7	10.0	10.5	10.5	11.0
NaBr	9.9	10.3	10.5	9.8	10.6	11.0
NaOAc	10.2	10.0	10.8	9.9	10.3	11.3
$NiCl_2$	9.8	10.0	10.1	10.1	9.7	9.7
$CuCl_2$	9.8	9.8	9.7	10.5	10.1	9.3
$FeCl_3$	9.8	10.5	13.4	9.6	9.9	9.8
K_2CrO_4	10.3	10.1	14.6	10.1	10.0	12.1
$SnCl_2$	10.2	10.4	8.8	9.7	9.8	9.9
$Bi(NO_3)_3$	10.4	10.1	9.4	10.5	9.5	9.1
$PbNO_3$[a]	10.5	10.3	12.2	9.8	9.3	11.8
$CdCl_2$	10.0	9.3	9.6	9.3	9.6	9.5
$CoCl_2$	10.0	10.4	10.0	10.2	10.3	10.4
$AlCl_3$	10.6	11.3	12.5	9.8	9.6	10.7
$ZnSO_4$	10.3	10.2	9.4	9.8	10.3	10.0

[a] In dilute nitric acid.

round-bottomed flask equipped with a condenser with 50 ml of 6 *M* hydrochloric acid. Sample B was similarly treated with 7.5 *M* hydrochloric acid. Samples A and B were heated on a hot plate so that the acid refluxed for about 6 h. Sample C was treated similarly with 50 ml of a solution 2 *M* in hydrochloric acid and 6 *M* in sulphuric acid. The ore solutions were cooled and then passed through a Gelman glass fiber (type A) filter. Each residue was washed with water, the washings were added to the filtrate, and the filtrate was diluted to 100 ml in a volumetric flask.

A fourth sample, D, weighing 100 g, was treated with 700 ml of 7.5 *M* hydrochloric acid in a 1-l round-bottomed flask. The sample was heated on a hot plate for 6 h with the acid under reflux conditions. After cooling, the sample was filtered and the analysis carried out on the undiluted filtrate.

The direct determination of gallium in the ore solutions without correction was carried out with the spectrometer in the auto-concentration mode. The instrument was calibrated by a gallium standard solution with approximately the same metal concentration as the unknown ore solution. A linear calibration curve had been previously obtained.

A second method of determination involved the method of standard addition, in this instance with 5-μl additions of a 1000 p.p.m. gallium standard with a push-button micropipetter to minimize dilution. The procedure[9] used was to calibrate the concentration mode of the atomic absorption spectrometer so that it indicated the final concentration of the added standard only, while the sample

plus added standard was being aspirated. The sample alone was set to read zero on the auto zero control. The concentration of gallium in the sample was then displayed as a negative number when water was aspirated. A series of additions were done to confirm the linearity of response.

The third method of gallium analysis involved the use of background correction by both the continuum and two-line methods[10]. In the first case, the absorbance for the ore solution was measured at the gallium wavelength of 287.4 nm with first the gallium hollow-cathode lamp and then the hydrogen continuum lamp; the difference gave the corrected value of absorbance for gallium in the solution. The two-line method involved measuring the absorbance of the ore solution, with the gallium lamp, at 287.4 nm and then measuring the absorbance of the sample at the 299.8-nm line of the platinum hollow-cathode lamp; again the difference in absorbance gave a corrected value for the true concentration of gallium in the solution.

The analyses of the ore samples for gallium are summarized in Table III for the various methods. It is evident that neither the method of standard additions nor the method of background correction would be sufficient singly to provide satisfactory gallium values with an air–acetylene flame. For all of the samples, the standard addition method provided only a minor correction of 10–15% while the background correction amounted to 25–60% of the uncorrected value. The nitrous oxide–acetylene flame eliminated the need for most of these corrections with the standard addition, providing about a 2% change and the background correction providing about the same. Evidently, the hotter nitrous oxide–acetylene flame minimizes the causes of the background effect[12] and in addition increases the sensitivity for gallium.

The presence of extremely high concentrations of interfering substances may produce a more significant error even with a nitrous oxide–acetylene flame, especially if the gallium concentration is very low. In this case, either the two-line or hydrogen continuum method can be used to correct successfully for this, though this would be a more tedious procedure. The use of a deuterium background corrector would also provide a means of correction with little extra effort, but this equipment is still not common.

CONCLUSIONS

The use of a nitrous oxide–acetylene flame for the atomic-absorption spectrometric determination of gallium was shown to be much less affected by variation in acid and base strength and by various diverse ions than the method with the air–acetylene flame. Accordingly, gallium solutions can be analyzed directly without a preliminary extraction even in the presence of complex or varying matrices. In addition, the sensitivity of the method was found to be 2.5 times that with the air–acetylene flame, which allows utilization of more dilute samples without preconcentration. The advantage of the application of the nitrous oxide–acetylene flame to solutions of gallium-containing ore was demonstrated. In this case the need for precise matrix matching of solvent and dissolved salts is minimized. The need for background correction and for some form of matrix compensation, such as standard addition which were shown to be essential for

TABLE III

EFFECT OF ANALYTICAL METHOD ON GALLIUM DETERMINATION OF ORE

(Methods A–D are outlined in the text. All results are given as p.p.m. of gallium)

Sample	*A*		*B*		*C**		*D*	
	i[a]	*ii*[b]	*i*[a]	*ii*[b]	*i*[a]	*ii*[b]	*i*[a]	*ii*[b]
Method								
Direct determination	6.51±0.08	3.54±0.03	5.23±0.05	3.47±0.06	4.20±0.08	1.81±0.09	6.83±0.06	2.21±0.09
Standard addition	5.60±0.04	3.61±0.09	4.56±0.07	3.52±0.04	3.93±0.04	1.92±0.07	6.22±0.07	2.24±0.07
Background correction	2.06±0.08	0.02±0.04	1.01±0.07	0 ±0.09	2.06±0.07	0.01±0.04	4.02±0.04	0 ±0.01
Corrected gallium concentration	3.54±0.04	3.59±0.04	3.55±0.04	3.52±0.06	1.87±0.07	1.91±0.03	2.20±0.08	2.24±0.05

[a] Air–acetylene flame used.

[b] Nitrous oxide–acetylene flame used.

* Two-line method used for background correction.

air–acetylene flames, were minimized or eliminated when the nitrous oxide–acetylene flame was used.

The atomic absorption technique with the nitrous oxide–acetylene flame provides a convenient, fast method for the determination of gallium in solution even in the presence of such complex matrices as ores, and requires no specialized equipment or close matching of matrix.

The authors wish to express their thanks to the National Research Council of Canada, the Research Board of the University of Manitoba, and to the Manitoba Research Council for their financial support.

SUMMARY

The use of a nitrous oxide–acetylene flame for the determination of gallium by atomic absorption spectrometry was compared with the use of air–acetylene flames. The nitrous oxide method provided higher sensitivity and was much less sensitive to acid and base composition and to diverse added salts. Significant matrix and background effects, which occurred when gallium was determined in ore solutions with the air–acetylene flame, were eliminated with the nitrous oxide–acetylene flame.

REFERENCES

1 H. Onishi, *Anal. Chem.*, 27 (1955) 832.
2 H. Onishi and E. B. Sandell, *Anal. Chim. Acta*, 13 (1955) 159.
3 G. N. Lypka and A. Chow, *Anal. Chim. Acta*, 60 (1972) 65.
4 M. S. Cresser and J. Torrent-Castellet, *Talanta*, 19 (1972) 1478.
5 E. W. Pollock, *At. Absorption Newslett.*, 10 (1971) 77.
6 H. K. L. Gupta, F. J. Amore and D. F. Boltz, *At. Absorption Newslett.*, 7 (1968) 107.
7 E. V. Elliott and K. R. Stever, *At. Absorption Newslett.*, 12 (1973) 60.
8 K. Fletcher, *Econ. Geol.*, 65 (1970) 588.
9 H. Kahn, J. Kerber and D. Manning, *Amer. Lab.*, June 1973, p. 55.
10 H. Kahn and D. Manning, *Amer. Lab.*, August 1972, p. 51.
11 G. R. Kornblum and L. De Galan, *Spectrochim. Acta*, 28B (1973) 139.
12 D. C. Manning, *At. Absorption Newslett.*, 5 (1966) 127.

Analytica Chimica Acta, 75 (1975) 95–100

SPECTROPHOTOMETRIC DETERMINATION OF BORON IN SILICEOUS MATERIALS WITH AZOMETHINE H

G. D. SCHUCKER, T. S. MAGLIOCCA and YAO-SIN SU

Research and Development Laboratories, Corning Glass Works, Corning, New York 14830 (U.S.A.)

(Received 9th August 1974)

A rapid method for determining boron as a minor constituent in a wide variety of siliceous materials was needed in this laboratory. The acid–base titration method with manitol–sodium hydroxide[1–3], and direct flame emission spectrometry[4] are not generally applicable for low levels of boron ($< 1\%$) or to samples of limited quantity. Other more sensitive flame spectrometric methods[5–7] involve separation procedures which detracts from their usefulness in routine work.

The application of colorimetric methods to the direct determination of boron in glasses, glass-ceramics, refractories, and other types of siliceous materials presents some special problems owing to the complexity of the matrices involved and the difficulty attending sample decomposition. The anthraquinone reagents such as carminic acid[8], quinalizarin[9], and others[10] require a concentrated sulfuric acid medium which forms precipitates with common glass constituents such as barium, strontium, and lead. Curcumin[11] in an ethanolic medium has been used for determining macro quantities of boron in glass; however, the procedure is sensitive to many variables. Other colorimetric methods are based on the reaction of boron with fluoride and basic dyes[12–16]. While these procedures are quite useful for certain applications such as boron determinations in hydrofluoric acid etches of glass surfaces, solvent extraction steps are required and the absorbance of the colored complex is not directly proportional to the quantity of boron present.

A desirable feature for a rapid colorimetric boron method would be a reagent directly applicable in aqueous medium. Most of the methods of this type have severe drawbacks for glass analysis. Chromotropic acid[17] is affected by the presence of silica, victoria violet[18] requires a basic medium and is critically pH-dependent, and phthalic violet[19] is influenced by high levels of sodium and potassium chloride which would be introduced if the usual alkali carbonate fusion were used to decompose the glass followed by hydrochloric acid dissolution of the melt.

Another reagent of this type, azomethine H, has been used for the determination of boron in soils and plant materials[20, 21], steels[22], and organic boron compounds[23]. It appeared this reagent might meet the requirements for a rapid and reliable analytical method for directly determining minor levels of boron in a wide range of siliceous materials. This paper describes investigations undertaken to develop a suitable method.

EXPERIMENTAL

Equipment

Absorption spectra were taken on a Hitachi–Perkin Elmer Model 139

spectrophotometer in 1-cm glass cells. Measurements of pH were made with a Corning Model 12 research pH meter.

Polyethylene labware, platinum dishes, and low-boron ware made of glass such as Corning Code 7913 were used whenever possible. Use of borosilicate glassware should be restricted to short duration; it is suitable for pipetting, and diluting to known volumes.

Reagents

All chemicals were analytical grade. Aqueous reagents were prepared in distilled deionized water.

Azomethine H (10 g l^{-1}). Dissolve 0.5 g of azomethine H (Pierce Chemical Company) and 1 g of ascorbic acid in about 30 ml of water with gentle heating and dilute to 50 ml. This solution was prepared fresh before each use.

Buffer solution. In a beaker containing 80 ml of acetic acid and 20 ml of water, dissolve 50 g of ammonium acetate. Adjust the pH to 4.5 with acetic acid and ammonia.

Masking solution. Weight 25 g of the tetra-sodium salt of EDTA (ethylenedinitrilotetraacetic acid) and 10 g of the di-sodium salt of NTA (nitrilotriacetic acid) into a beaker. Dissolve the salts in about 300 ml of water. Adjust the pH of the solution to 4.5 with acetic acid. Dilute to 500 ml.

Standard boron solution (1000 μg B_2O_3 ml^{-1}). Dissolve 1.776 g of boric acid in 1 l of water. From the stock solution prepare fresh before each use a dilute standard solution containing 20 μg B_2O_3 ml^{-1}.

Calibration curve

Transfer aliquots of the dilute standard boron solution covering the range 0–100 μg B_2O_3 to 25-ml volumetric flasks. Add 5.0 ml each of buffer, masking, and azomethine H solutions, swirling the flask after each addition to mix the reagents. Dilute to volume with water. Allow the solutions to stand for at least 4 h. Longer times of standing can be used if more convenient. No net change in absorbance between standards and blank was noted for up to 18 h. Measure the absorbance of the standard solutions at 415 nm in 1-cm cells against the reagent blank as reference. Prepare a calibration curve by plotting concentration of B_2O_3 *versus* the net absorbance of the standard solutions.

Samples

Accurately weigh a suitable size sample (containing 0.2–20 mg B_2O_3) into a small platinum dish. Add 5–10 times the sample weight of anhydrous sodium carbonate, mix by gentle stirring with a platinum rod, cover, and fuse over a blast burner until the sample has completely decomposed. Cool the dish, add about 5 ml of water, and then neutralize the melt with 6 *M* hydrochloric acid (about 5 ml of acid per g of flux). Keep the dish almost completely covered during neutralization to avoid loss from spattering. Other acids such as nitric, perchloric, or acetic can be used. It may be necessary to digest on a steam bath to aid dissolution of the melt. Transfer the sample quantitatively to a 250-ml Vycor beaker and add sufficient masking solution to react with all interfering elements such as iron, aluminum, titanium, etc., plus a few ml in excess. Carefully heat to boiling for about 30 s

to expel carbon dioxide. Cool, and adjust the pH to 4.5 with sodium hydroxide solution (50%). Again heat to boiling and allow to remain hot but below boiling for 5–10 min to promote the complexation reactions. While still hot, filter, if necessary, to remove any precipitate. Collect the filtrate directly in a 200-ml volumetric flask and wash the paper and residues well with hot water. Cool and dilute to volume.

Transfer a suitable aliquot, 1–10 ml, to a 25-ml volumetric flask. Add 5.0 ml each of the buffer and masking solutions. Prepare a reagent blank. Mix the solutions and heat gently on a steam bath for 5–10 min. Cool, add 5.0 ml of azomethine H solution and dilute to volume. Mix well and allow to stand for at least 4 h. Measure the absorbance of each sample at 415 nm in 1-cm cells against the reagent blank as reference. Calculate the amount of B_2O_3 in the samples from the calibration curve.

RESULTS AND DISCUSSION

Listed in Table I are results for boron in a variety of siliceous materials obtained by the proposed method and compared with results obtained by other accepted procedures. It can be seen that excellent results can be obtained in quite diverse matrices with the azomethine H method. Replicate (10) determinations on National Bureau of Standards No. 92 low-boron glass (0.70% certified) gave a mean result of 0.68%, with a standard deviation of 0.03% and a relative standard deviation of about 3%.

The absorption spectrum of the aqueous solution from the reaction of azomethine H with boron shows maximum absorbance at 415 nm in agreement with studies by Basson *et al.*[20] and others[22,23]. Work by Wolf[21] was carried out at

TABLE I

COMPARISON BETWEEN THE AZOMETHINE H AND OTHER METHODS FOR DETERMINING BORON IN SILICEOUS MATERIALS

Type of Sample[a]		B_2O_3 (%)	
		Azomethine H	*Other methods*
Glass-ceramic	Si–Al–Zn–Mg–Ti–Li	0.25, 0.23, 0.25	0.27[b], 0.25[c]
Glass-ceramic	Si–Al–Zn–Mg–Ti–Li	0.17, 0.15, 0.16	0.15[b], 0.16[c]
Ophthalmic glass	Si–Al–Zn–K–Mg	0.93, 0.94	0.79[b], 1.1[d]
Lime glass	Si–Al–Ca–Na	0.81, 0.79	0.81[b], 0.92[d]
Casting powder	Si–Na–Li–Ca–Sr–F	1.95, 1.89	1.94[d], 1.96[d]
Opal glass	Si–Al–Zn–Na–Ca,F–K	1.45, 1.41	1.38[d], 1.42[d], 1.47[d]
Soda lime glass	Si–Al–Na–Mg–Ca	0.98, 0.96	—
NBS 92	Si–Na–Al–Ca–Zn–K–Ba	0.68	0.70[e]

[a] Constituents given in decreasing order of weight percentages.
[b] Thionine extraction method.
[c] Emission spectrographic method.
[d] Titrimetric method (mannitol–NaOH).
[e] NBS certified value.

430 nm with no reasons given for this wavelength selection. The present work confirms 415 nm to be more sensitive and less subject to measurement errors. The calibration curve was rectilinear from 0–100 μg B_2O_3 in 25 ml of solution. The molar absorptivity of the boron–azomethine complex is $9 \cdot 10^3$. This is an advantage over the thionine–tetrafluoroborate methods[13,15] which exhibit non-linear analytical curves at higher boron concentrations.

The published methods[20–23] on the determination of boron with azomethine H do not recommend the same conditions for optimal color development. Therefore, studies were carried out to determine the change in absorbance of the colored azomethine H–boron complex as a function of the following variables: pH of the aqueous solution, time of standing for color development, concentration of azomethine H reagent, and presence of other elements.

pH of the reaction medium

Two sets of solutions, one containing a constant amount of boron (40 μg B_2O_3) and another with no boron, were buffered to various pH levels. Azomethine H was added to each set and the absorbance of the boron-containing solutions at each pH interval was measured against the corresponding boron-free solution as blank. Figure 1 shows that the absorbance difference between the test solution and blank is maximal between pH 4 and 5. Therefore, pH 4.5 was selected as optimal for color development. Values of pH suggested by other workers varied from 4.8 (ref. 21) to 5.2 (ref. 22).

Reaction rate

The reaction between boron and azomethine H is not instantaneous. One previous study indicated that the color of the complex develops over a 2-h period and then is stable for 40–50 min[23]. Other workers[22] found it required 4 h to reach maximal absorbance, whereupon no further change was observed for 20 h.

Two solutions, one containing 40 μg B_2O_3, and one without boron, were buffered to pH 4.5 and reacted with azomethine H. The difference in absorbance between the two solutions was measured at various time intervals. Figure 2 shows

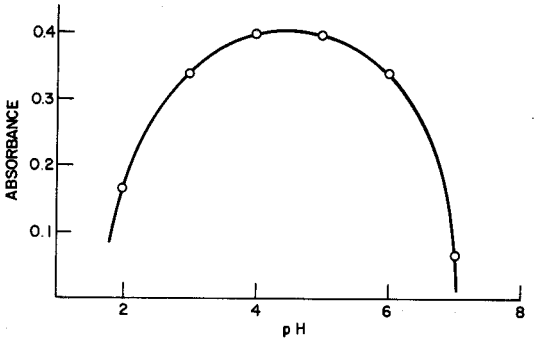

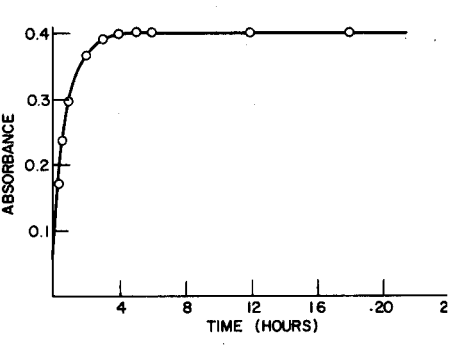

Fig. 1. Effect of pH on the absorbance of the azomethine H–boron complex. B_2O_3-40 μg; time-4 h; 1-cm cell, 415 nm.

Fig. 2. Approach to absorbance equilibrium. B_2O_3 −40 μg; pH-4.5; 1-cm cell, 415 nm.

that the absorbance increases rapidly during the first few hours. A maximum is reached after 4 h and no further change was noted after 18 h of standing. During this time, the absorbance of the test solution did increase; however, the blank darkened correspondingly, possibly owing to oxidation of the reagent.

Concentration of the azomethine H

The intensity of the color obtained when azomethine H is reacted with boron depends on the concentration of the reagent in solution. Concentrations suggested by previous workers vary from 6 g l^{-1} to 9 g l^{-1}. Figure 3 shows results obtained when a constant amount of boron was reacted with varying concentrations of reagent at pH 4.5. Since the formation of the complex is reversible, no maximum value was obtained. However, at concentrations greater than about 8 g l^{-1}, absorbance changes were relatively small. Since it is difficult to obtain clear solutions at very high reagent concentrations, 10 g l^{-1} was chosen as optimal.

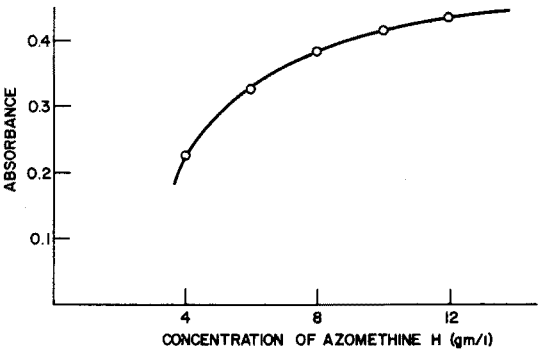

Fig. 3. Effect of azomethine H concentration on the absorbance of the colored complex with boron. B_2O_3 – 40 μg; pH-4.0; 1-cm cell, 415 nm.

Previous investigators suggest that the reagent solution is stable for several weeks[20]. During this study, it was found that fresh reagent should be prepared just before each use since precipitates were observed to form after 1–2 days of standing.

Presence of other elements

Previous studies[20, 22] have shown the azomethine H method to be relatively free of interference from other elements. Species said not to influence the method include: Sb, As, Ba, Bi, Cd, Ca, Cs, Co, K, Li, Mg, Mn, Nd, Ni, Nb, Pb, Re, Se, Na, Sr, Ta, Te, Tl, Th, W, U, Zn, NO_3^-, PO_4^{3-}, Cl^-, F^-, SO_3^{2-}, $C_2O_4^{2-}$. Of the elements commonly occurring in glasses, only Al, Ti, Zr, Fe, and Cu cause problems. The influence of these elements can be effectively overcome by addition of the EDTA–NTA masking solution proposed by Wolf[21]. This study showed that an additional masking agent was needed just before color development to prevent completely interference from large quantities of elements such as titanium and zirconium which frequently occur in some of the more complex glasses and ceramics.

SUMMARY

A rapid and simple colorimetric method is described for the determination of minor levels of boron in siliceous materials with azomethine H. The reaction is carried out in aqueous medium. Samples are decomposed by alkaline fusion and taken up in dilute acid, and interferences are masked with an EDTA–NTA solution. After pH adjustment, the boron is reacted with azomethine H and the absorbance of the colored product is measured at 415 nm. The precision and accuracy are about $\pm 3\%$ relative as indicated by analysis of National Bureau of Standards No. 92 low-boron glass. The procedure has been applied to a wide variety of glasses and glass-ceramics and compared with other accepted methods.

REFERENCES

1 M. Hollander and W. Rieman, *Ind. Eng. Chem., Anal. Ed.*, 17 (1945) 602; 18 (1946) 788.
2 J. P. Williams, D. E. Campbell and T. S. Magliocca, *Anal. Chem.*, 31 (1959) 1560.
3 *ASTM Book of Standards, Part 17*, American Society for Testing and Materials, Philadelphia, 1974, p. 134.
4 R. W. Morrow, *Anal. Lett.*, 5 (1972) 371.
5 E. J. Agazzi, *Anal. Chem.*, 39 (1967) 233.
6 W. J. Maeck, M. E. Kussey, B. E. Ginther, G. V. Wheeler and J. E. Rein, *Anal. Chem.*, 35 (1963) 62.
7 J. C. M. Pau, E. E. Picket and S. R. Koirthyohann, *Analyst (London)*, 97 (1972) 860.
8 D. L. Callicoat and J. D. Wolszon, *Anal. Chem.*, 31 (1959) 1434.
9 A. H. Jones, *Anal. Chem.*, 29 (1957) 1101.
10 E. C. Cogbill and J. H. Yoe, *Anal. Chim. Acta*, 12 (1955) 455.
11 J. J. McIntosh and J. E. Cox., *J. Amer. Ceram. Soc.*, 43 (1960) 123.
12 L. Pasztor, J. D. Bode and Q. Fernando, *Anal. Chem.*, 32 (1960) 277.
13 L. Pasztor and J. D. Bode, *Anal. Chem.*, 32 (1960) 1530.
14 L. Pasztor and J. D. Bode, *Anal. Chim. Acta*, 24 (1961) 467.
15 B. L. Goydish, *Microchem. J.*, 15 (1970) 572.
16 O. B. Skaar, *Anal. Chim. Acta.*, 28 (1963) 200.
17 D. F. Kuemmel and M. G. Mellon, *Anal. Chem.*, 29 (1957) 378.
18 C. A. Reynolds, *Anal. Chem.*, 31 (1959) 1102.
19 V. Patrovsky, *Talanta*, 10 (1963) 175.
20 W. D. Basson, R. G. Bohmer and D. A. Stanton, *Analyst (London)*, 94 (1969) 1135.
21 B. Wolf, *Soil Sci. Plant Anal.*, 2 (1971) 363.
22 R. Capelle, *Anal. Chim. Acta.*, 24 (1961) 555; 25 (1961) 59.
23 T. M. Shanina, N. E. Gelman and V. S. Mikhailovskaya, *J. Anal. Chem., USSR*, 22 (1967) 663.

Analytica Chimica Acta, 75 (1975) 101–109

CHARACTERIZATION OF COMPLEXES INVOLVED IN THE SPECTROPHOTOMETRIC DETERMINATION OF COBALT WITH 4-(2-PYRIDYLAZO)RESORCINOL

M. ŠIROKI, Lj. MARIĆ, Z. ŠTEFANAC and M. J. HERAK
Laboratory of Analytical Chemistry, Faculty of Science, The University of Zagreb (Yugoslavia)
(Received 15th July 1974)

4-(2-Pyridylazo)resorcinol (PAR) was first suggested as a sensitive reagent for the spectrophotometric determination of cobalt in 1959 by Pollard *et al.*[1]. The composition and stability constants of cobalt–PAR chelates have been reported, and the cobalt(II)–PAR species, with a metal-to-ligand ratio of 1:2, has been said to exist in aqueous solutions[2–6]. The data concerning the oxidation state of cobalt are discrepant; some investigations have provided evidence for the cobalt(III) state[7–10]. In the present work, experiments were undertaken to separate the cobalt–PAR complexes and characterize them in the solid state. Moreover, solution studies were carried out, and the extraction behavior of complexes in the presence of some organophilic cations was investigated. The results obtained gave additional information about the nature and properties of the complexes in question.

EXPERIMENTAL

Reagents and chemicals

All the chemicals used were Analar grade. Merck monosodium salt of 4-(2-pyridylazo)resorcinol, and Fluka tetraphenyl-phosphonium and -arsonium chloride, and chloroform containing 0.5–1% ethanol, were used.

Standard solution of cobalt(II). Cobalt(II) chloride hexahydrate was dissolved in water to give a $1 \cdot 10^{-2}$ *M* solution. The solution was standardized by gravimetric determination of cobalt with 1-nitroso-2-naphthol and by titration with EDTA with xylenol orange as indicator. Solutions of lower concentrations were obtained by dilution.

Cobalt(III) solution. The cobalt(III) solution was prepared by passing a stream of oxygen through an aqueous solution of cobalt(II) chloride, containing ammonium chloride.

Extraction procedure

Aqueous solutions (about 10 ml) containing cobalt, PAR, buffer and tetraphenyl-phosphonium or -arsonium chloride were extracted twice with 5 ml of chloroform. Solutions were shaken for 2 min in 50-ml separating funnels. Organic layers were collected in a volumetric flask (10 ml) and diluted to the mark with chloroform.

Determination of $(C_6H_5)_4X$–Co–PAR ratio in the organic phase

The molar ratio of metal to ligand, and of the extractant to the Co–PAR complex were determined by Job's continuous variations, mole-ratio and slope-ratio methods. Concentrations used are given in Figs. 3–5. The absorbance of the chloroform phase was measured at 520 nm. The ionic strength of the aqueous phase was kept constant at pH 8.

Preparation of solid complexes

To the cobalt(II) or (III) solutions (50 ml of $2 \cdot 10^{-2}$ *M*), an equal volume of buffer solution was added and the pH was adjusted to 8. An aqueous solution of the monosodium salt of 4-(2-pyridylazo)resorcinol (100 ml of $2 \cdot 10^{-2}$ *M*) was then added under stirring. After a few minutes, tetraphenyl-arsonium (0.84 g) or -phosphonium chloride (0.75 g) dissolved in a minimum of water was added. The reaction mixture was transferred to a separatory funnel and extracted twice with about 20 ml of chloroform. The chloroform phases were collected in a conical flask and about a threefold volume of petroleum ether was added. The mixture was left refrigerated for 2–3 h and the precipitate, obtained as a dark red film on the bottom of the flask, was dissolved in a minimum of ethanol at 50°C. To the cool solution (20 ml) a four-fold volume of ether (80 ml) was gradually added. The mixture was left refrigerated, and in a few days red "crystals" were obtained in 60–70% yield. They were washed with ether and dried *in vacuo* over calcium chloride. Analytical data are given in Table I.

TABLE I

ELEMENTAL ANALYSES DATA

Compound		*Element*				
		C	*H*	*N*	*As or P*	*Co*
$[(C_6H_5)_4As][CoR_2]$	*Calc. (%)*	63.59	3.95	9.68	8.62	6.78
	Found (%)	63.42	3.97	9.98	8.65	6.66
$[(C_6H_5)_4As][CoR_2]\cdot 2H_2O$	*Calc. (%)*	61.06	4.24	9.29	8.28	6.51
	Found (%)	60.72	4.66	9.36	7.92	6.38
$[(C_6H_5)_4P][CoR_2]$	*Calc. (%)*	66.98	4.16	10.19	3.76	7.15
	Found (%)	66.51	4.69	9.80	3.28	6.91
$[(C_6H_5)_4P][CoR_2]\cdot 2H_2O$	*Calc. (%)*	64.18	4.46	9.77	3.60	6.85
	Found (%)	64.42	4.84	9.52	3.22	6.65

Analytical procedures

Cobalt in the isolated complex compounds was determined as follows: the substance (about 30 mg) was destroyed in a Kjeldahl flask with concentrated sulfuric acid (1 ml), to which 4–5 drops of concentrated nitric acid were added. The mixture was heated until oxides of nitrogen were expelled. The procedure was repeated three times. The final solution was transferred to a volumetric flask, diluted to 50 ml and titrated with a standard EDTA solution and xylenol orange as indicator, at pH 6.

Arsenic was determined by a final EDTA titration after the substance had been destroyed by the flask combustion method. The arsenic was precipitated as silver arsenite and the precipitate was dissolved in tetracyanonickelate[11].

Phosphorus was determined by the precipitation of ammonium phosphomolybdate, after the substance had been destroyed by the Kjeldahl method[12].

Carbon, hydrogen and nitrogen were determined by the usual microanalytical methods.

Physical measurements

Visible spectra and absorbance measurements of solutions were made on a Perkin Elmer Coleman 124 and Beckman Model DU-2 spectrophotometer, respectively. Infrared spectra of the isolated compounds were recorded on a Perkin Elmer spectrophotometer Model 257 in the region 4000–650 cm^{-1}, in KBr pellets and in nujol mulls. Nuclear magnetic resonance spectra were recorded with a Varian A-60 spectrometer at room temperature. Electron spin resonance spectra of solid complexes were taken with a Varian E-3 ESR spectrometer with a modulation frequency of 100 KHz.

Magnetic susceptibility was determined by the Gouy method at room temperature. X-ray powder photographs were obtained in a 0.3-mm capillary with a 57.54-mm Phillips camera, Cu-α radiation and exposure time of 2 h. Conductivity measurements were performed in methanol ($1.5 \cdot 10^{-6}$ ohm^{-1} cm^2) for 10^{-3}–10^{-5} *M* solutions with a Tacussel Electronic CD 7A conductivity bridge and a cell with a cell constant of 1.318 cm^{-1}.

RESULTS AND DISCUSSION

The cobalt–PAR complex, formed in aqueous solutions under the experimental conditions generally used in spectrophotometric determinations, can be extracted by tetraphenylarsonium or tetraphenylphosphonium chloride in chloroform. The cobalt–PAR complex in aqueous solution has maximum absorption at 510 nm and its molar absorptivity is $5.7 \cdot 10^4$ at pH 8 in a borate-buffered medium. The presence of the tetraphenyl-onium salts under these conditions does not effect either the position or the intensity of the absorption maximum. The visible spectrum of the chloroform extracts has maximum absorbance in the range 515–520 nm (Fig. 1) and the molar absorptivity is $6.0 \cdot 10^4$–$6.4 \cdot 10^4$ depending on the excess of ligand present. The absorption maximum of the extracts does not change in wavelength on variation of the reactant concentration, buffer composition or oxidation state of cobalt, indicating the presence of one extracted complex species.

The dependence of the extraction on pH was studied; in the pH region where the cobalt–PAR complex is most stable (pH 6–9), the pH of the aqueous solution has no effect on the absorbance of the organic phase (Fig. 2).

The extraction behavior confirms the existence of an anionic complex species in aqueous solution. In order to determine the composition of the extracted complex with respect to the Co–PAR and $(C_6H_5)_4X$–(Co–PAR) ratios, Job's method, as well as the mole-ratio and slope-ratio methods, were used. All experiments were done in borate and in an ammonia–ammonium chloride buffered medium starting with solutions of cobalt(II) chloride, cobalt(II) chloride in a reducing medium, and with

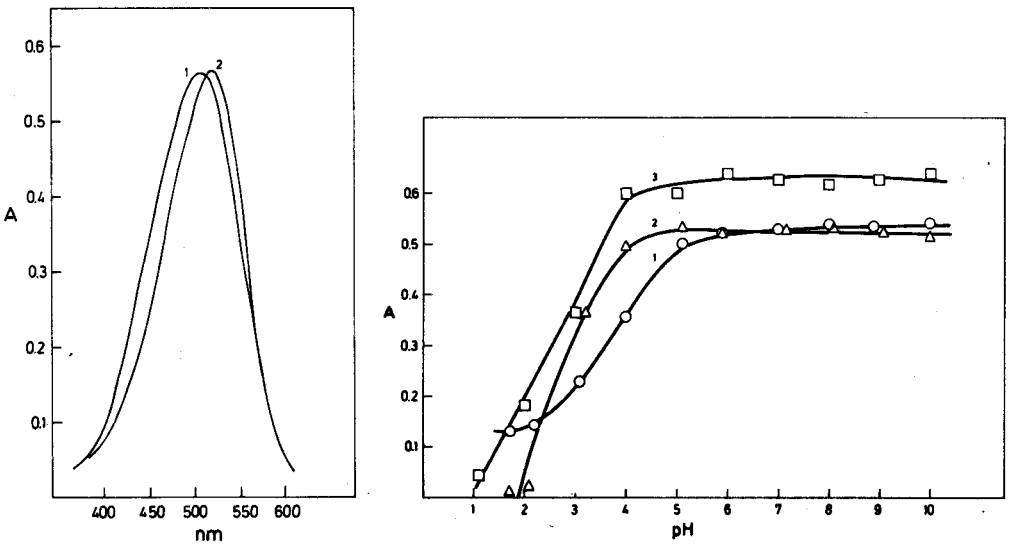

Fig. 1. Visible spectra of cobalt–PAR complex. (1) Aqueous solution; (2) chloroform phase, obtained by extraction with tetraphenylarsonium or phosphonium chloride.

Fig. 2. Dependence of absorbance on pH. (1) Aqueous system Co–PAR at $\lambda_{max} = 510$ nm; (2) organic phase, system $(C_6H_5)_4P$–Co–PAR at $\lambda_{max} = 520$ nm; (3) organic phase, system $(C_6H_5)_4P$–Co–PAR with excess of PAR and reagent blank as reference.

a cobalt solution previously oxidized to the cobalt(III) state, respectively. Some results are given in Figs. 3–5. They show that the molar ratio for the tetraphenyl-onium–cobalt–PAR species transferred into the organic phase was 1:1:2 for all systems studied. The molar ratio value indicated that the anionic cobalt–PAR complex bearing one negative charge must be present in aqueous solution.

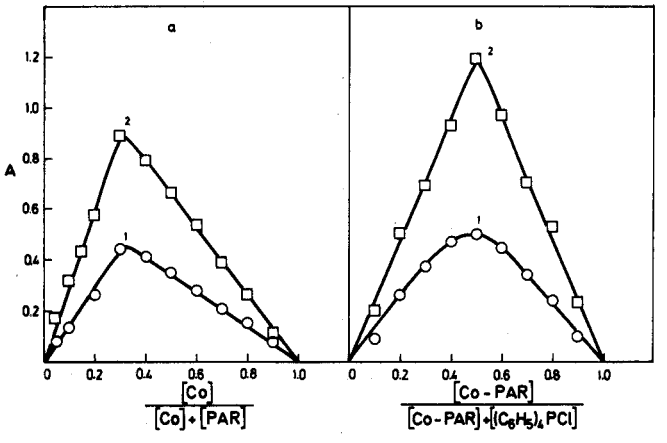

Fig. 3. Determination of composition of the extracted complex by Job's method. (a) Co:PAR ratio: (1) $[Co]+[PAR] = 2.5 \cdot 10^{-5}$ *M*; (2) $[Co]+[PAR] = 5.0 \cdot 10^{-5}$ *M*. (b) Extractant: (Co–PAR) ratio: (1) $[Co\text{–}PAR]+[(C_6H_5)_4PCl] = 2.5 \cdot 10^{-5}$ *M*; (2) $[Co\text{–}PAR]+[(C_6H_5)_4PCl] = 5.0 \cdot 10^{-5}$ *M*.

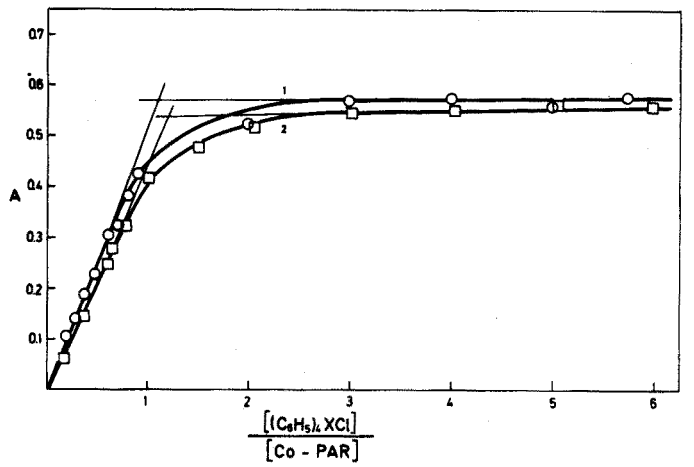

Fig. 4. Determination of composition of the extracted complex by mole ratio method. (1) Co(III) solution, $[Co\text{–}PAR]=1\cdot10^{-5}$ *M*, X=P; (2) Co(II) solution, $[Co\text{–}PAR]=1\cdot10^{-5}$ *M*, X=As.

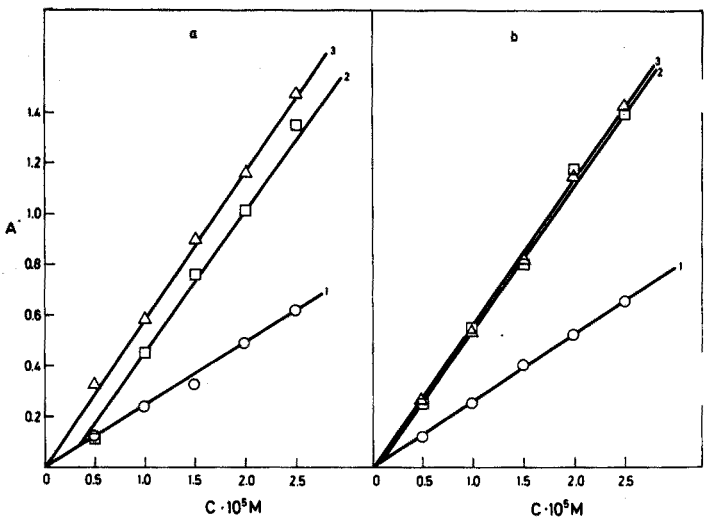

Fig. 5. Determination of composition of extracted complex by slope ratio method. (a) Co(II) solution; (b) Co(III) solution. (1) $[Co]=4\cdot10^{-4}$ *M*, $[(C_6H_5)_4XCl]=1\cdot10^{-2}$ *M*, [PAR] is varied; (2) [Co]= [PAR]$=4\cdot10^{-4}$ *M*, $[(C_6H_5)_4XCl]$ is varied; (3) $[PAR]=4\cdot10^{-4}$ *M*, $[(C_6H_5)_4XCl]=1\cdot10^{-2}$ *M*, [Co] is varied.

From these results, and also from the previous investigations on cobalt–PAR complexes formed in acidic solutions[7,8,10], it is possible to predict that also under the conditions used here (pH 8), an oxidation to cobalt(III) occurs during the formation of cobalt–PAR chelates and that the $[Co(III)R_2]^-$ complex ion would be expected in both the cobalt(II) and the cobalt(III) solution. The $[Co(III)R_2]^-$ complex ion is then extracted into chloroform by an ion-pair formation mechanism:

$$[(C_6H_5)_4X]^+ + [CoR_2]^-_{aq} = [(C_6H_5)_4X][CoR_2]_{org}$$

where X=As, P; and R refers to the divalent anion of 4-(2-pyridylazo)resorcinol (PAR, abbreviated as H_2R)[13,14].

The solid compounds separated correspond to the above composition. They were characterized by elemental analyses, i.r., visible, n.m.r. and e.p.r. spectra, x-ray powder photographs and magnetic susceptibility measurements. Compounds obtained by the procedure described in the experimental part are hydrates containing 2–4 molecules of water. The water present cannot be removed by calcium chloride or phosphorus pentachloride at room temperature. When the substances were heated in the pistol drier under water-pump vacuum, with ethanol as heating liquid, they lost some water and were converted to dihydrates. The compounds lost all their water when they were slowly heated to the melting points observed for the hydrates (about 120°C). A long heating time must be avoided, in order to avoid decomposition. Anhydrous complexes show rather sharp melting points, the arsonium derivative at 188–190°C, and the phosphonium derivative at 160–165°C. Analytical data for the compounds are given in Table I.

The compounds are soluble in alcohols, chloroform, acetone, dimethylsulfoxide, nitromethane and nitrobenzene, less soluble in water, and insoluble in apolar organic solvents. The molar conductivity values for methanolic solutions at concentrations between $1 \cdot 10^{-3}$ and $5 \cdot 10^{-5}$ M ($\lambda_M = 55$–65 ohm^{-1}cm^2), as well as conductivity extrapolated to infinite dilution, are lower then would be expected for 1:1 electrolytes. These results can be treated as evidence for association[15–18]. In the solid state, the compounds seemed to be polymeric, showing only diffuse lines in x-ray powder photographs despite an external crystalline form. In the visible

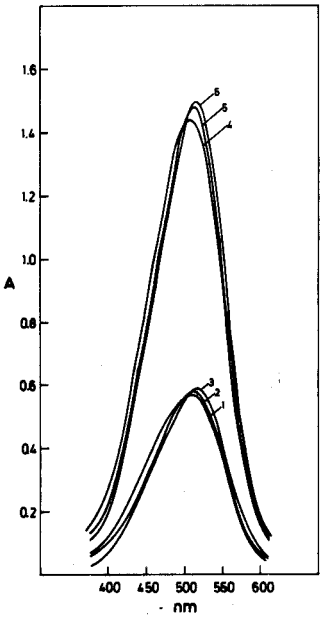

Fig. 6. Visible spectra of isolated complexes in solution. $1 \cdot 10^{-5}$ M Solutions of $[(C_6H_5)_4As][CoR_2]2H_2O$ in (1) water, (2) methanol and (3) chloroform. $2.5 \cdot 10^{-5}$ M Solutions of $[(C_6H_5)_4P][CoR_2]2H_2O$ in (4) water, (5) methanol and (6) chloroform.

spectra of all compounds (Fig. 6), only one broad maximum appears, at 510 nm ($\varepsilon = 5.7 \cdot 10^4$) in aqueous, 515 nm ($\varepsilon = 5.9 \cdot 10^4$) in methanolic, and 518 nm ($\varepsilon = 6.0 \cdot 10^4$) in chloroform solution. Visible spectra of the solutions made to correspond with analytical systems and spectra of dissolved complexes are identical.

In the i.r. spectra of the compounds, assignment of a few relevant bands was done, based on the comparison of the spectra of cobalt complexes with the spectra of some other metal–PAR complexes[19], and the spectra of uncoordinated PAR (monosodium salt of 4-(2-pyridylazo)resorcinol) and tetraphenylarsonium or phosphonium chloride. As expected, characteristic changes in intensity, position and the number of bands occur upon coordination.

In the spectrum of the free ligand two strong bands appear at 1630 and 1600 cm^{-1}, and two of low intensity at 1580 and 1560 cm^{-1}. The spectra of the complexes, however, show only one very strong band, at about 1590 cm^{-1}, that comprises C=C and C=N stretching modes. The broad multiple absorption band appearing in the spectra of the free ligand from 1500 to 1470 cm^{-1}, is shifted upon coordination and split into two strong bands, at 1490 and 1460 cm^{-1}. A new strong band appears in this region in the spectra of the complexes, at 1390 cm^{-1}, which is not present in the spectrum of the ligand. According to previous assignment[20–24], this band is most probably due to N=N stretching. The presence of this band with high intensity in the spectra of complexes may be related to the asymmetry of the azo-group introduced by coordination through the lone pair of a single nitrogen atom. The absorption in the region 1350–1100 cm^{-1}, originated mainly in various C–O, C–N and C–H stretching and deformation modes, is expected to be strongly affected by oxygen and nitrogen coordination, as observed in the spectra of the complexes. Strong bands found in the spectrum of monosodium salt of 4-(2-pyridylazo)resorcinol at 1330 and 1220 cm^{-1} are shifted to lower frequencies with changes in intensity and the number of bands as shown in Table II.

From the i.r. spectra it is evident that the characteristic absorption bands for

TABLE II

CHARACTERISTIC BANDS IN INFRARED SPECTRA (CM^{-1}) AND TENTATIVE ASSIGNMENTS OF SOME COORDINATED PAR VIBRATIONAL MODES

(1700–1000 cm^{-1} region)

NaHR·H₂O	*[(C₆H₅)₄As][CoR₂]·2H₂O*	*[(C₆H₅)₄P][CoR₂]·2H₂O*	*Assignment*
1630 m			
1600 s			
1580 w	1590 vs	1590 vs	ν(C=C,C=N)
1560 w			
1490 vs, broad	1485 } vs	1490 } vs	
1445 s, sharp	1460 }	1460 }	
	1390 vs	1390 vs	ν(N=N)
	1295 } vs	1295 } vs	
1320 s	1280 }	1280 }	
	1250 s	1250 s	ν(C–O, C–N)
1220 vs	1175 vs	1175 vs	δ(C–O, C–N, C–H)
	1145 vs	1145 vs	

the coordinated PAR ligand are located in the region of absorption which originates mainly in the N=N, C–N and C–OH vibrational modes, indicating a tridentate coordination of PAR molecules as expected. There is spectral evidence for a single nitrogen lone pair nature of the metal–azo bonding, rather than for the π-olefinic type. The tridentate coordination of PAR is in agreement with the stereochemistry of Co(II) and Co(III), which then would achieve a coordination number of six. The solid complexes were found to be diamagnetic. For the Co(II) d^7 state, paramagnetism is expected regardless of the stereochemical environment, while Co(III) complexes, with very few exceptions, have diamagnetic ground states[25]. It seems that the donor atoms of PAR make a strong contribution to the ligand field, and that the trivalent state of cobalt is stabilized in cobalt–PAR complexes so that in solutions of cobalt(II) the formation of chelates involves an oxidation to cobalt(III). Cobalt(II) was not detected in the molecules from the e.s.r. spectra of the solid complexes. Even in complexes isolated from solutions of cobalt(II) in the presence of a reducing agent, only traces of paramagnetic impurities (less then 10^{-4} M) were detected. Information provided by proton magnetic resonance spectra support the proposed structure of the complexes, including the 2 molecules of the ligand in the form of a divalent anion bonded to cobalt(III) in symmetric stereochemical arrangement. The corresponding protons of both ligand molecules are magnetically equivalent, judged by their identical chemical shift values. Chemical shifts and spin–spin interaction will be discussed in more detail later.

The authors wish to thank Dr. Z. Sliepčević for some C–H analyses, Dr. K. Adamić for taking the e.s.r. spectra and Dr. B. Prodić-Kojić for the x-ray powder photographs.

SUMMARY

Complex species involved in the spectrophotometric determination of cobalt with 4-(2-pyridylazo)resorcinol (PAR = H_2R) were studied in solution and in the solid state. An anionic $[Co(III)R_2]^-$ species was extracted from aqueous solution in chloroform by tetraphenylarsonium or tetraphenylphosphonium chloride. Stable tetraphenylarsonium and tetraphenylphosphonium salts of di-4-(2-pyridylazo)resorcinolo cobaltate(III) with the formula $[(C_6H_5)_4X][Co(III)R_2]$ where X = As,P; and $R = C_{11}H_7N_3O_2^{2-}$, were isolated from the chloroform phase. The complexes were characterized by elemental analyses, visible, i.r., p.m.r., e.s.r. spectra, x-ray powder photographs, magnetic susceptibility and conductivity measurements. The spectral evidence and magnetic properties indicate a tridentate coordination of two 4-(2-pyridylazo)resorcinol dibasic anions, bonded to cobalt(III) in a symmetric arrangement with both azo groups coordinated to the cobalt atom through a single nitrogen lone pair.

REFERENCES

1 F. H. Pollard, P. Hanson and W. J. Geary, *Anal. Chim. Acta*, 20 (1959) 26.
2 W. J. Geary, G. Nickless and F. H. Pollard, *Anal. Chim. Acta*, 26 (1962) 575; 27 (1962) 71.
3 A. I. Busev and V. M. Ivanov, *Zh. Anal. Khim.*, 18 (1963) 208.

4 A. I. Busev, V. M. Ivanov and Z. Nemceva, *Zh. Neorg. Khim.*, 13 (1968) 511.
5 A. Corsini, I. M. L. Yih, Q. Fernando and H. Freiser, *Anal. Chem.*, 34 (1962) 1090.
6 B. E. Eftimova and D. H. Nonova, *Dokl. Bolg. Akad. Nauk*, 23 (1970) 1111; 24 (1971) 1671; *Anal. Chim. Acta*, 62 (1972) 456.
7 A. Corsini, Q. Fernando and H. Freiser, *Inorg. Chem.*, 2 (1963) 224.
8 T. Iwamoto and M. Fujimoto, *Anal. Chim. Acta*, 29 (1963) 282.
9 T. Yotsuyanagi, R. Yamashita and K. Amoura, *Anal. Chem.*, 44 (1972) 1091.
10 Lj. Marić, Master of Science Thesis, Faculty of Science, University of Zagreb, Yugoslavia.
11 Z. Štefanac *Microchim. Acta*, (1962) 6.
12 F. Pregl and I. Grant, *Quantitative Organic Microanalysis*, I. A. Churehil, London, 1951, p. 141.
13 M. Hniličkova and L. Sommer, *Collect. Czech. Chem. Commun.*, 26 (1961) 2189.
14 A. I. Busev and V. M. Ivanov, *Zh. Anal. Khim.*, 22 (1967) 382.
15 R. D. Feltham and R. G. Hayter, *J. Chem. Soc., London*, (1964) 4587.
16 C. M. Harris, R. S. Nyholm and D. J. Phillips, *J. Chem. Soc., London*, (1960) 4379.
17 A. I. Popov and R. E. Humphrey, *J. Amer. Chem. Soc.*, 81 (1959) 2043.
18 D. F. Evans and R. L. Kay, *J. Phys. Chem.*, 70 (1966) 366.
19 M. Široki and C. Djordjević, *J. Less-Common Metals*, 23 (1971) 228; *Anal. Chem.*, 43 (1971) 1377.
20 R. J. W. Le Fevre, M. F. O'Dwyer and R. L. Werner, *Aust. J. Chem.*, 6 (1953) 341.
21 R. Kübler, W. Luttke and S. Weckherlin, *Z. Elektrochem.*, 64 (1960) 650.
22 K. Ueno, *J. Amer. Chem. Soc.*, 79 (1957) 3066.
23 A. L. Balch and D. Petridis, *Inorg. Chem.*, 8 (1969) 2247.
24 R. G. Denning and J. Thatcher, *J. Amer. Chem. Soc.*, 90 (1968) 5917.
25 F. A. Cotton and G. Wilkinson, *Advanced Inorganic Chemistry*, Interscience, New York, 3rd edn., 1972.

Analytica Chimica Acta, 75 (1975) 111–117

THE DETECTION OF AMMONIA AND NITROGEN DIOXIDE AT THE PARTS PER BILLION LEVEL WITH COATED PIEZOELECTRIC CRYSTAL DETECTORS

K. H. KARMARKAR and G. G. GUILBAULT

Department of Chemistry, University of New Orleans, New Orleans, La. 70122 (U.S.A.)

(Received 16th August 1974)

In recent years coated piezoelectric quartz crystals have been developed as selective and sensitive air pollution sensors. The pioneering work of Sauerbrey[1] on the theoretical aspects and of King[2–4] on the practical applications of piezoelectric quartz crystals opened a new line for the detection and measurement of gases and vapors. The principle of detection by a piezoelectric quartz crystal is that the frequency of vibration of an oscillating crystal can be decreased by the presence of a foreign material on its surface. A gaseous pollutant is selectively absorbed by the coating on the crystal surface, thereby increasing the weight on the crystal and decreasing the frequency of vibration. The decrease in frequency is a measure of the amount of gas absorbed. King[4] and Karasek and Tiernay[5] used coated quartz crystals as sensitive g.c. detectors. Frechette and Fasching[6] have used a coated crystal as a sensor for sulfur dioxide pollution in a static system. The ability of coated piezoelectric quartz crystals to detect pollutants at the parts per billion level was shown by Karmarkar and Guilbault[7] in which sulfur dioxide was detected as low as 1 p.p.b. by using a sensitive cell design and selective and sensitive amine coatings.

This paper describes new coatings for the piezoelectric crystals in the detection of ammonia and nitrogen dioxide in the parts per billion range. The i.r. spectra of the gas–solid reaction, and the results of a study of interference from other pollutants, are also presented.

EXPERIMENTAL

Apparatus

Figure 1 shows the experimental set-up with a piezoelectric crystal detector in a flow system. The cell design is based on a design described by the authors earlier[7], and is the most sensitive one for a flow system. The cell is made from a flattened pyrex tube (1.6 cm o.d.). A pyrex 14/20 ground joint is connected to the flattened tube which facilitates the change or removal of the crystal from the detector cell, if necessary. The crystal is situated in the flattened position of the cell, the parallel walls of which are separated by a distance of 0.6 cm. The parallel cell walls are 2 cm long and 1.2 cm wide making the effective cell volume about 1.5 cm^3 ($2 \times 1.2 \times 0.6$ cm^3). The column effluent is equally divided by two 0.5-cm (o.d.) pyrex tubes. These tubes are connected through the two parallel walls in such a way that their tapered ends (0.2 cm o.d.) reach as close to the center of the opposite faces of the crystal as possible. This arrangement ensures the maximum

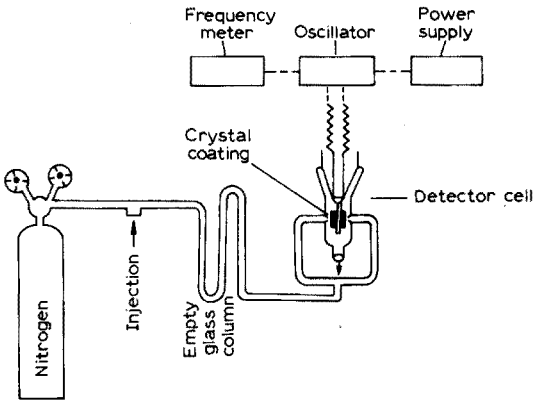

Fig. 1. Experimental set-up with a piezoelectric crystal detector.

amount of the sample gas reacting with the coating at any moment, and therefore the sensitivity is greatly increased. The gas escapes through an exit tube (0.7 cm o.d.) connected at the bottom of the cell. Dry nitrogen at a rate of 20 cm^3 min^{-1} is used as carrier gas which passes through an empty 30 cm long and 0.7 o.d. pyrex column. The crystals used in this study were 9 MHz AT cut quartz crystals with silver-plated metal electrodes on both sides and were obtained from Jan Crystals, Florida. A low-frequency OX transitor oscillator was built from an oscillator kit (International Crystal Co., Oklahoma). Two tungsten–nickel (W–Ni) leads connected the crystal to the oscillator. The oscillator was powered by a Heathkit 1–30 V d.c. variable power supply (Model 1P-28). Even though the applied voltage had no effect on the sensitivity of the crystal under these conditions, it was always kept constant at 9 V. A Systron-Donner frequency meter, Model 8050, with a range of 0–30 MHz and a resolution of 0.1 Hz, was used for a digital read-out of frequency.

Reagents

Ucon 75-H-90,000 and Ucon-LB-300X (Union Carbide Corp., from Analabs, Inc., Connecticut) were used as coatings. NH_3, NO_2, SO_2, H_2S, NO, CO, and CO_2 (Matheson Co., Inc.) were used from lecture bottles. Benzene, acetone, methanol and chloroform were of Technical grade.

Method of application of coatings

The Ucon compounds are dissolved in proper solvent (*e.g.*, chloroform) and the solutions are applied on the entire surface of the electrode on both sides with a tiny brush. The organic solvent evaporates quickly leaving the Ucon compounds on the crystal. The amount of Ucon-75-H-90,000 coating used was equivalent to a decrease of 7000 Hz and that of Ucon-LB-300X corresponded to a decrease of 9000 Hz in the basic frequency (9 MHz) of the crystal. These coated crystals are then exposed to a 1 : 3 mixture of nitrogen dioxide and nitrogen in a small pyrex chamber for about 5 min; nitrogen dioxide reacts with the coatings and this causes a further decrease of frequency of about 3000 Hz and 4000 Hz respectively for the two coatings.

Test gas dilution

The test gases are diluted with nitrogen by the syringe method earlier described by the authors[7] and also by Karasek and Tiernay[5]. Pure test gas (1 ml) is sucked in a 10-ml syringe. Then the syringe is filled to capacity with dry nitrogen. The desired dilution of the test gas is obtained by repeating the above procedure for the required number of times. A 5-ml test mixture is always injected to observe the response, except when 1 ml of ammonia mixture is injected as for the curve C of Fig. 6.

I.r. measurements

Pyrex glass cells with KBr windows were built in order to obtain i.r. spectra of pure Ucon substrate films and of the compounds formed on exposure to nitrogen dioxide of the Ucon substrates. Figure 2 shows the i.r. cell used. A small amount of Ucon solution is placed on the KBr windows; as the solvent evaporates a thin film of Ucon is formed on the KBr surface. The cell is evacuated by a rotary pump. A 1:3 nitrogen dioxide–nitrogen mixture is then injected into the cell, sufficient time is allowed for the reaction to occur, and the cell is again evacuated. This ensures removal of all unreacted nitrogen dioxide. I.r. specta are taken on the Perkin-Elmer 257 Grating IR spectrometer.

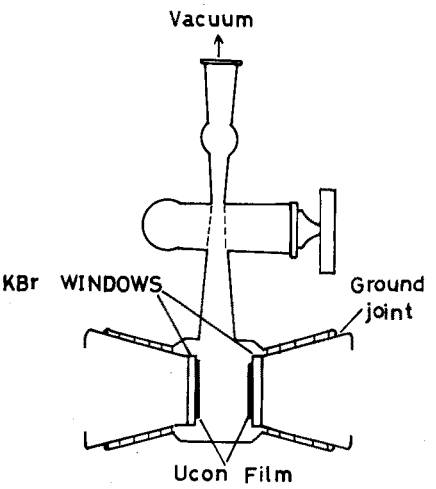

Fig. 2. Pyrex infrared cell with KBr windows.

RESULTS AND DISCUSSION

Both Ucon-75-H-90,000 and Ucon-LBL-300X coatings showed sensitivity to ammonia and nitrogen dioxide only after an exposure to nitrogen dioxide for about 5 min. This suggests that nitrogen dioxide reacts with Ucon coatings and new compounds are formed on the crystal. These new compounds act as sensitive coatings for ammonia and nitrogen dioxide. Ucon fluids and lubricants are polyalkylene glycols with less known structures. The fact that new compounds are formed on reacting with nitrogen dioxide is evident from the appearance of new bands and some band shifts observed in the i.r. spectra of these substances. Figures 3 and 4 show the i.r. spectra of Ucons before and after reaction with nitrogen dioxide.

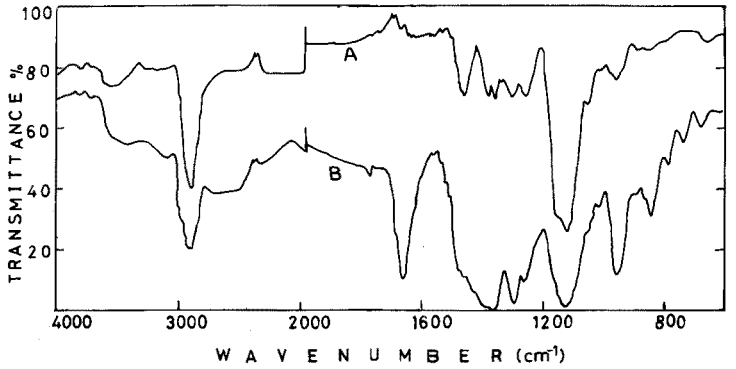

Fig. 3. (A) I.r. spectrum of pure Ucon-75-H-90,000; (B) I.r. spectrum of Ucon-75-H-90,000 exposed to NO_2.

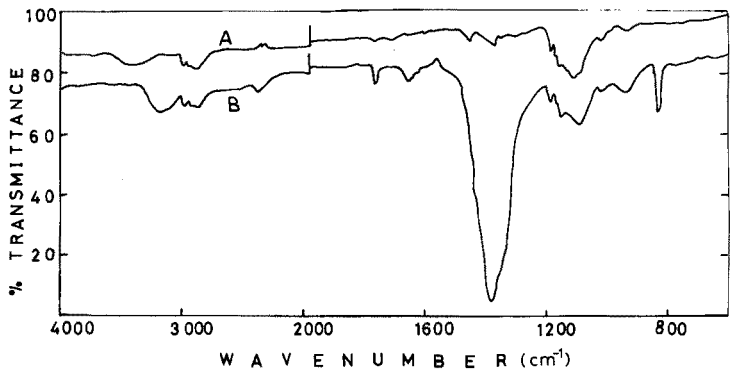

Fig. 4. (A) I.r. spectrum of pure Ucon-LB-300X; (B) I.r. spectrum of Ucon-LB-300X exposed to NO_2.

It is known that Ucon-75-H-90,000 is made by reacting ethylene oxide, propylene oxide and ethylene glycol, but its real structure is not known. Under these circumstances, it is reasonable to suggest that in Fig. 3 the new bands at 1650 cm^{-1} and between 800 cm^{-1} and 700 cm^{-1} show the presence of covalent nitrite[8], R–O–NO. The broad band between 1500 cm^{-1} and 1320 cm^{-1} may represent a nitroso (R–NO) compound. Similarly, in Fig. 4, the new band at 1380 cm^{-1} represents a nitroso (R–NO) compound. The band at 1380 cm^{-1} together with another new band at 830 cm^{-1} might even show the presence of ionic nitrate. But this seems rather less probable.

Figures 5 and 6 show calibration plots for ammonia and nitrogen dioxide on the two Ucon substrates exposed to pure nitrogen dioxide. The responses are fairly linear between 1 p.p.b. and 1 p.p.m. on both coatings. At about 1 p.p.m. the curves seem to bend but become linear again, and remain so for a quite large concentration range. The position of bending depends on the amount of mixture injected. For example, when 1 ml of ammonia mixture was injected instead of 5 ml, a curve linear between 1 p.p.m. and 50 p.p.m., and a sort of bending above 50 p.p.m. resulted (Fig. 6, Curve C). It seems possible that concentrations lower

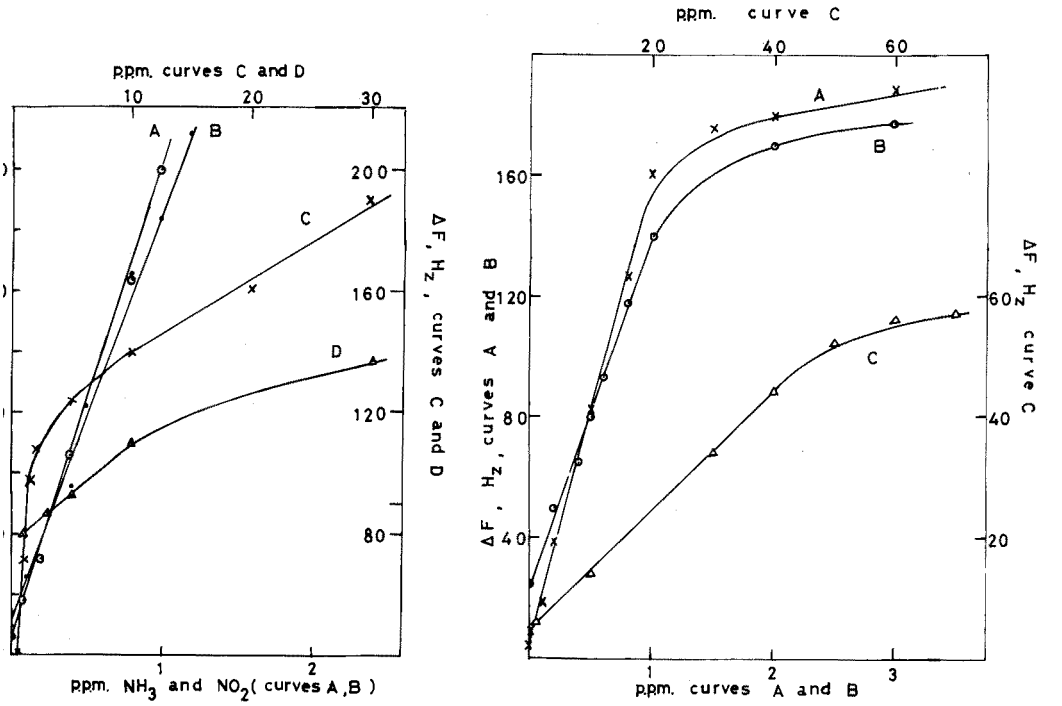

Fig. 5. Calibration plots for NH_3 and NO_2 on Ucon-75-H-90,000 substrate exposed to NO_2: Curves A and D for NH_3; B and C for NO_2.

Fig. 6. Calibration plots for NH_3 and NO_2 on Ucon-LB-300X substrate exposed to NO_2; Curve A for NO_2; curves B and C for NH_3.

than 1 p.p.b. could be detected if 10-ml or 15-ml mixtures were injected instead. The response is fast, and reversibility is observed at low concentrations of pollutants. At concentrations above 1 p.p.m., however, a long time (about 20–30 min) is required to observe reversibility.

Interferences and drawbacks

The most important drawback with the piezoelectric crystal detectors is that they give response for atmospheric moisture. The present detectors gave a response of about 300 Hz for 5 ml of laboratory air, but no response for dry laboratory air. Under varying conditions of humidity, it may be difficult to differentiate between moisture response and a pollutant response. This problem may be solved by using a drier to remove moisture or by using two crystals simultaneously; one measuring pollutant plus moisture, and the other measuring only moisture. The actual concentration of the pollutant can then be obtained from the difference between the two responses. The work on the latter procedure is in progress. Another shortcoming noted about Ucon coating is that the crystal loses all activity if kept exposed to air for long times (1 h). But this also is not serious since the activity can easily be restored by re-exposing the crystal to a nitrogen dioxide–nitrogen mixture for 5 min. The process of this reaction seems critical since in some cases irreversible

TABLE I

INTERFERENCE STUDY

Coating	*Gas and interfering concentrations*								
	CO (p.p.m.)	*CO_2 (p.p.m.)*	*NO (p.p.m.)*	*SO_2 (p.p.m.)*	*H_2S (p.p.m.)*	*Acetone (p.p.m.)*	*Methanol (p.p.m.)*	*Chloroform (p.p.m.)*	*Benzene (p.p.m.)*
Ucon-75-H-90,000 exposed to NO_2	No interf.	No interf.	1000	5000	10000	2000	1000	500	600
Ucon-LB-300X exposed to NO_2	No interf.	No interf.	1000	10000	20000	2000	1000	600	600

responses with Ucon-75-H-90,000 coatings were observed.

It was observed that oganic pollutants produce larger interferences than the inorganic ones. Table I contains the results of the interference study. The interfering concentrations are those which produce response roughly equivalent to a response for 1 p.p.b. of either nitrogen dioxide or ammonia. Since the concentrations of all the interfering substances are much higher than that ever found in air, no interference is expected. Thus, the systems described may prove valuable for the sensitive and specific detection of nitrogen dioxide and ammonia.

The authors wish to acknowledge gratefully the financial assistance of the Army Research Office (Grant No. ARO DAHC 74 G0119) in carrying out this research project.

SUMMARY

Ucon-75-H-90,000 and Ucon-LB-300X are the new substrates used on the piezoelectric crystal detectors. On exposure to nitrogen dioxide these substrates form new compounds on the crystal which are sensitive to nitrogen dioxide and ammonia. With these coatings it is possible to detect nitrogen dioxide and ammonia in the parts per billion range. Some problems are caused by atmospheric moisture and high concentrations of organic pollutants.

REFERENCES

1 G. Sauerbrey, *Z. Phys.*, 155 (1959) 206.
2 W. H. King, Jr., in A. W. Czanderna (Ed.), *Vacuum Microbalance Techniques, Vol. 8*, Plenum Press, New York, 1971, pp. 183–200.
3 W. H. King, Jr., *Environ Sci. Technol.*, 4 (1970) 1136.
4 W. H. King, Jr., *Anal. Chem.*, 36 (1964) 1735.
5 F. W. Karasek and J. M. Tiernay, *J. Chromatogr.*, 89 (1974) 31.
6 M. W. Frechette and J. L. Fasching, *Environ. Sci. Technol.*, 7 (1973) 1135.
7 K. H. Karmarkar and G. G. Guilbault, *Anal. Chim. Acta*, 71 (1974) 419.
8 J. R. Dyer, *Applications of Absorption Spectroscopy of Organic Compounds*, Prentice-Hall, New Jersey, 1965, p. 31.

Analytica Chimica Acta, 75 (1975) 119–126

CATALYTIC–KINETIC DETERMINATION OF IODIDE, MANGANESE AND MOLYBDENUM WITH THE USE OF AN ABSORPTIOSTAT

H. WEISZ and K. ROTHMAIER

Lehrstuhl für Analytische Chemie, Chemisches Laboratorium der Universität Freiburg i.Br. (G.E.R.)

(Received 8th July 1974)

In catalytic–kinetic analytical methods which are based on "open systems" such as flow methods[1–3], steady-state methods[4] or "stat" methods[5–13], some external influence is exerted on the catalyzed reaction during its course:

$$A + B \xrightarrow{K} X + Y$$

In the "stat" methods, this influence can be achieved by keeping constant a preset value of concentration of one of the reactants or reaction products. Here, a reactant A is added at the same rate as it is consumed by the reaction with the second reactant B present in a comparatively high concentration; or, a reaction product X is removed at the same rate as it is formed by the reaction. This is done by adding a substance R, which reacts very quickly with the reaction product X. The concentration of the catalyst K can be derived from the rate of addition which is just necessary to keep constant the particular concentration required. For keeping constant a certain preset state of the system, some suitable property can be used, for example, an electrochemical potential[5–10], the polarization of electrodes (biamperostat)[11], chemiluminescence[12], spectrophotometric absorption, etc. For the potentiostatic methods[5–8], which have been used with a platinum electrode, the ratio of the concentrations (activities) of the oxidized and reduced form of a reactant is kept constant. In the case when an ion-selective electrode is used, the concentration of one of the reactants is kept constant[8]. For the pH-stat methods, the protons consumed or produced by the reaction are replaced or neutralized by the addition of standard acid or base, respectively, in order to keep constant the pH value of the system, which is measured, for example, by a glass electrode[9,10]. A pH-stat method has been described, where the pH is checked spectrophotometrically by coupling a suitable colour indicator to the main reaction[13].

For the absorptiostat ("Extinktiostat") technique to be discussed in this paper, a preset absorbance is maintained constant by adding a coloured reactant. This may be illustrated by the well known example of the iodide-catalyzed reaction between cerium(IV) and arsenic(III).

$$\underset{\text{yellow}}{2\,Ce(IV)} + As(III) \xrightarrow{I^-} \underset{\text{colourless}}{2\,Ce(III)} + As(V)$$

To a solution containing the iodide and an excess of arsenic(III), a standard cerium(IV) solution ("indicator substance") is added until, after a certain phase of development, a preset absorbance value is reached. Each deflection from this preset

value, caused by the course of the catalyzed reaction, is compensated by adding the necessary volume of cerium(IV) solution.

The rate of the catalyzed reaction is described by the following equation[14]:

$$-\frac{d[Ce(IV)]}{dt} = k[As(III)][Ce(IV)][I^-] \quad (1)$$

Arsenic(III) is present in such an excess that its concentration can be regarded as being constant for the measuring time. Because now the cerium(IV) standard solution is added in exactly the same measure as it is consumed by the reaction with arsenic(III), the concentration of cerium(IV), [Ce(IV)], is also constant, and we can write:

$$-\frac{d[Ce(IV)]}{dt} = k^*[I^-] \quad (2)$$

The iodide concentration $[I^-]$ to be determined (catalyst) also remains constant, of course, and so the reaction can be regarded as pseudo zero order. The change of the reaction volume caused by the addition of cerium(IV) standard solution can be neglected, and so the rate of addition of the cerium(IV) is proportional to the iodide concentration (eqn. 2) and, consequently, a measure for its determination.

In the work described here, iodide has been determined by means of the above-mentioned reaction, and manganese by its catalytic action on the oxidation of malachite green with periodate. The accelerating action of molybdenum on the reaction between iodide and hydrogen peroxide has also been applied for its determination.

EXPERIMENTAL

Apparatus

The apparatus used (see Fig. 1) consisted of a colorimeter (Universal Kolorimeter Modell J, Lange, Berlin) and the Combititrator 3D (Metrohm, Herisau, Switzerland). The Combititrator itself consisted of a mV/pH meter, a controller (Impulsomat), and an automatic burette connected to a recorder. The

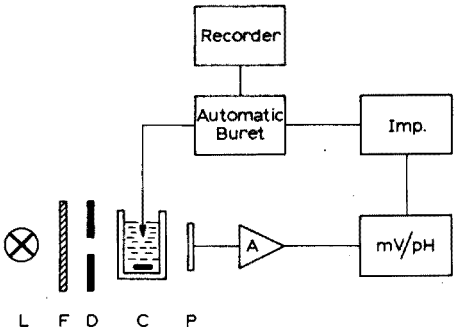

Fig. 1. Apparatus. L, Source of light; F, monochromatic filter; D, iris diaphragm; C, thermostated reaction cell with magnetic stirrer; A, amplifier [$Z_f/Z_i = 330$ kΩ/1000 Ω]).

optical cell used had a path length of 23 mm and a volume of about 75 ml and was jacketed for temperature control. The signal of the photocell (P) was amplified. The resulting potential was taken up by the mV meter; this actual potential was compared in the controller (Imp.) with the preset working potential, which in turn corresponded to a certain working absorbance, and consequently to a defined concentration of the reactant to be kept constant. Each difference between the actual and the preset working potential during the course of the reaction in the cell, caused a signal to the automatic burette. The deficit of the coloured reactant was compensated by adding the necessary volume of the standard solution of this reactant to the reaction mixture.

DETERMINATION OF IODIDE BY USE OF THE CERIUM(IV)–ARSENIC(III) REACTION

The reaction between cerium(IV) and arsenic(III) is catalyzed by iodide[15].

Solutions

Cerium(IV) sulphate solution: A 0.005 M solution in 0.5 M sulphuric acid was freshly prepared daily from 0.1 M cerium(IV) sulphate solution in 0.5 M sulphuric acid, and placed in the supply bottle of the burette.

Arsenic(III) solution: A 0.2 M solution was prepared from 9.892 g of As_2O_3 dissolved in 200 ml of 0.1 M sodium hydroxide, then mixed with 35 ml of 10 M sulphuric acid, the solution being diluted to 500 ml with twice-distilled water.

Potassium iodide stock solution: 1 mg I ml^{-1}.

Procedure

Before the determinations, the Combititrator was adjusted as follows (compare instruction manual): continuous pulse limit 5 mV, adaption $dE/dVol$ 6 units, automatic burette (total volume 10 ml) 5 units, recorder 15 mm min^{-1}. The temperature of the thermostat was 30°C. The starting potential was adjusted to 540 mV by aid of the iris diaphragm of the colorimeter (blue filter, max. about 415 nm). The preset working potential (set-point potential) was adjusted (about 440 mV) so that the continuous pulse was interrupted between 1.5 and 2.0 ml of the cerium(IV) solution.

Into the cell, x ml of iodide sample solution, $(40-x)$ ml of twice-distilled water, and 5 ml of arsenic(III) solution were transferred. After the solution had reached 30°C (about 10 min), the reaction was started by switching on the measuring unit and so adding the cerium(IV) solution to the reaction mixture.

Evaluation and results

For evaluation, the cotangent of the inclination angle α of the line plotted by the recorder was graphically determined for the measuring range between 4.00–8.00 ml (see Fig. 2). This value was identical with the rate of addition of the cerium(IV) solution ($\cot \alpha = 4(\text{ml})/t(\text{s})$).

In order to prepare the calibration graph, 4 measurements were performed with known iodide concentrations (0.5, 1.0, 3.0 and 5.0 μg I^-/45 ml). This linear calibration graph was prepared before each series of measurements.

Some results are listed in Table I.

TABLE I

DETERMINATION OF IODIDE

Iodide (μg/45 ml)		*Rel. error (%)*
Given	*Found*	
0.52	0.54	+3.8
0.82	0.83	+1.2
1.03	1.16	+12.6
1.33	1.33	±0.0
1.42	1.40	−1.4
2.27	2.16	−4.8
2.31	2.53	+9.5
3.20	3.16	−1.2
3.99	3.93	−1.5
4.88	5.17	+5.9

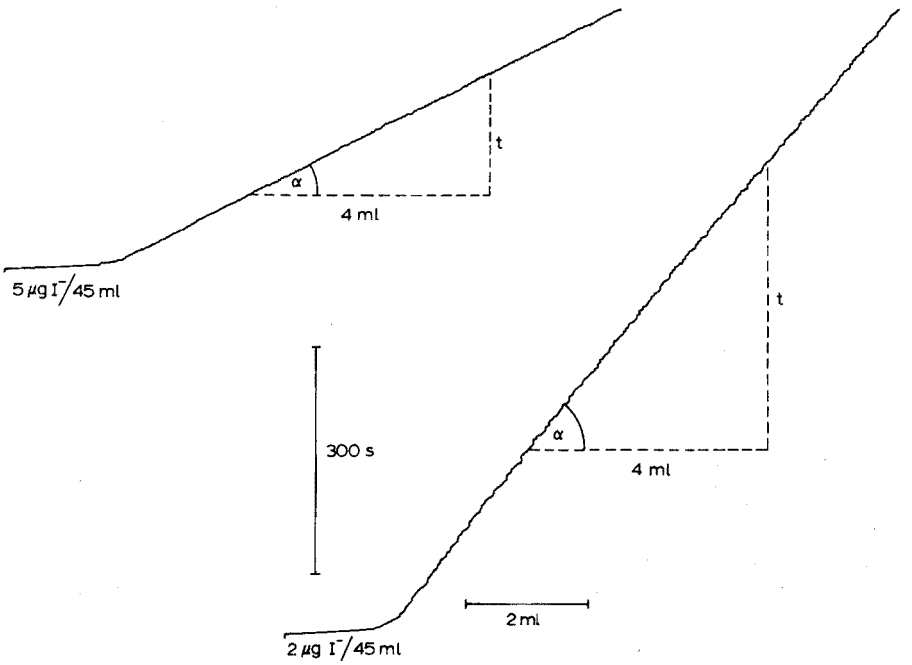

Fig. 2. Recorder graphs; 2.0 μg I^-/45 ml and 5.0 μg I^-/45 ml.

DETERMINATION OF MANGANESE BY USE OF THE MALACHITE GREEN–PERIODATE REACTION

The oxidation of malachite green by periodate is catalyzed by manganese[16].

$$IO_4^- + \text{malachite green} \xrightarrow{Mn^{2+}} IO_3^- + \text{colourless products}$$

Solutions

Buffer solution: 276 g of NaH_2PO_4 and 120 ml of glacial acetic acid were made up to 1 l with twice-distilled water, and 210 ml of 0.1 *M* sodium hydroxide were added.

Manganese chloride stock solution: 100 μg Mn ml^{-1}.

Procedure

The Combititrator was adjusted as follows: continuous pulse limit 7 mV, adaption d*E*/d*Vol* 10 units, automatic burette (total volume 10 ml) 5 units, recorder 15 mm min^{-1}. The temperature of the thermostat was 30°C. The starting potential was adjusted to 600 mV by means of the iris diaphragm (wavelength 617 nm; interference filter). The set point potential (about 20 mV) was adjusted so that the continuous pulse was interrupted after the addition of 1.5–2.0 ml of malachite green solution.

Into the cell, x ml of manganese sample solution, $(41-x)$ ml of twice-distilled water, 2 ml of 0.2 *M* sodium periodate solution, and 2 ml of buffer solution were transferred. After 10 min the reaction was started by adding the aqueous malachite green solution (0.1 mg ml^{-1}) to the thermostated reaction mixture from the burette.

Evaluation and results

The value of cot α was taken from the recorder graph for the measuring range 4.00–8.00 ml.

The linear calibration graph was prepared with the following manganese concentrations: 1.0, 2.0, 5.0, 7.5, and 10.0 μg Mn/45 ml.

Some results are given in Table II.

TABLE II

DETERMINATION OF MANGANESE

Manganese (μg/45 ml)		*Rel. error (%)*
Given	*Found*	
1.15	1.11	−3.5
2.06	2.10	+1.9
2.92	2.86	−2.1
3.30	3.27	−0.9
4.16	4.18	+0.5
4.96	4.98	+0.4
6.68	6.50	−2.7
7.85	7.95	+1.3
8.20	8.20	±0.0
9.80	9.90	+1.0

DETERMINATION OF MOLYBDENUM(VI) BY USE OF THE IODIDE–HYDROGEN PEROXIDE REACTION

The oxidation of iodide with hydrogen peroxide is accelerated by molybdenum-(VI)[17,18]

$$2I^- + 2H^+ + H_2O_2 \xrightarrow{Mo(VI)} I_2 + 2H_2O$$

The rate of the catalyzed reaction obeys the following equation[18]:

$$\frac{d[I_2]}{dt} = -\frac{1}{2}\frac{d[I^-]}{dt} = k[I^-][H_2O_2][Mo] \quad (3)$$

In this stat method, a defined preset absorbance caused by the iodine formed by the reaction is kept constant by removing the excess of iodine. This is achieved by controlled addition of ascorbic acid.

$$I_2 + \text{ascorbic acid} \rightarrow 2I^- + \text{dehydroascorbic acid} + 2H^+$$

In this procedure, the iodine as well as the iodide concentration always remains constant. The change of hydrogen peroxide in the system can be neglected (owing to its comparatively high concentration; see below), the proton concentration remains constant (see the above-mentioned equations) and, consequently, the rate of addition of ascorbic acid is directly proportional to the molybdenum concentration and so also a measure for its determination.

$$\frac{d[I_2]}{dt} = -\frac{1}{2}\frac{d[I^-]}{dt} = -\frac{d[\text{ascorbic acid}]}{dt} = k^*[Mo] \quad (4)$$

Equation (4) shows that a linear relationship is to be expected.

Solutions

Ascorbic acid solution (0.001 M). This solution was freshly prepared daily from 0.2 *M* ascorbic acid solution and poured in the supply bottle of the burette.

Hydrogen peroxide solution (1 M). This was prepared daily from 30% hydrogen peroxide solution.

Molybdenum stock solution: 1 mg Mo ml^{-1} ($Na_2MoO_4 \cdot 2H_2O$).

Procedure

The Combititrator was adjusted as follows: continuous pulse limit 7 mV, adaption dE/dV 9 units, automatic burette (total volume 10 ml) 3 units, recorder 15 mm min^{-1}. The temperature of the thermostat was 30°C. Here, it was not necessary to amplify the signal of the photocell. The starting potential was adjusted to 165 mV by means of the iris diaphragm of the colorimeter (blue filter, max. about 415 nm). The set point potential (about 145 mV) was adjusted so that the continuous pulse was interrupted after 1.5–2.0 ml of ascorbic acid solution had been added.

Into the cell, x ml of molybdenum sample solution, $(37-x)$ ml of twice-distilled water, 1 ml of hydrogen peroxide solution, and 1 ml of 1 *M* sulphuric acid were transferred. After the solution had reached 30°C, 1 ml of potassium iodide solution (10^{-2} *M*) was added. The absorbance of the iodine produced by the reaction increased and therefore a decrease of the potential was caused. When the potential actually measured in the solution reached 120 mV (4–15 min for 100–10 μg Mo), the ascorbic acid solution was added from the automatic burette by switching on the measuring unit. Thus, the potential increased until the set point potential (145 mV) was reached. This value was always kept constant by adding the ascorbic acid solution from the automatic burette.

Evaluation and results

For evaluation, the value of the cot α was taken from the recorder graph for the measuring range 5.00–10.00 ml.

In order to prepare a calibration graph, 5 measurements were performed with known molybdenum concentrations (10, 30, 50, 75, and 100 μg Mo/40 ml). This linear calibration graph was prepared before each series of measurements.

Some results are listed in Table III.

TABLE III

DETERMINATION OF MOLYBDENUM

Molybdenum (μg/40 ml)		*Rel. error (%)*
Given	*Found*	
13.0	12.0	−7.7
19.0	17.5	−7.9
29.7	31.0	+4.4
36.5	34.5	−5.5
42.0	44.5	+6.0
51.3	57.0	+11.1
64.0	66.5	+3.9
71.0	68.5	−3.5
82.6	83.5	+1.1
98.7	96.0	−2.7

SUMMARY

The kinetic–catalytic determination of several catalysts by use of an absorptiostatic method is described. The determination of iodide in the range 0.5–5.0 μg/45 ml is based on its catalytic action on the cerium(IV)–arsenic(III) reaction. The catalytic action of manganese(II) on the reaction of malachite green with periodate was used for its determination in the range 1–10 μg/45 ml. The determination of molybdenum(VI) in the range 10–100 μg/40 ml is based on its accelerating action on the oxidation of iodide with hydrogen peroxide.

REFERENCES

1 A. M. Wilson, *Anal. Chem.*, 38 (1966) 1784.
2 H. Weisz and H. Ludwig, *Anal. Chim. Acta*, 62 (1972) 125.
3 H. Ludwig, H. Weisz and T. Lenz, *Anal. Chim. Acta*, 70 (1974) 359.
4 H. Weisz and H. Ludwig, *Anal. Chim. Acta*, 60 (1972) 385.
5 H. Weisz, D. Klockow and H. Ludwig, *Talanta*, 16 (1969) 921.
6 D. Klockow, H. Ludwig and M. A. Giraudo, *Anal. Chem.*, 42 (1970) 1682.
7 H. Weisz, K. Rothmaier and H. Ludwig, *Anal. Chim. Acta*, 73 (1974) 220.
8 D. Klockow, H. Weisz and K. Rothmaier, *Z. Anal. Chem.*, 264 (1973) 385.
9 K. M. Møller, *Biochim. Biophys. Acta*, 16 (1955) 162.
10 H. V. Malmstadt and E. H. Piepmeier, *Anal. Chem.*, 37 (1965) 34.
11 S. Pantel and H. Weisz, *Anal. Chim. Acta*, 70 (1974) 391.
12 H. Weisz and S. Pantel, *Anal. Chim. Acta*, 74 (1975) 275.

13 R. E. Karcher and H. L. Pardue, *Clin. Chem.*, 17 (1971) 214.
14 P. A. Rodriguez and H. L. Pardue, *Anal. Chem.*, 41 (1969) 1369.
15 E. B. Sandell and J. M. Kolthoff, *J. Amer. Chem. Soc.*, 56 (1934) 1426.
16 A. A. Fernandez, C. Sobel and S. L. Jacobs, *Anal. Chem.*, 35 (1963) 1721.
17 K. B. Yatsimirskii and L. P. Afanaseva, *Zh. Neorg. Khim.*, 11 (1965) 319.
18 K. B. Yatsimirskii, *Kinetic Methods of Analysis*, Pergamon, Oxford, 1966.

Analytica Chimica Acta, 75 (1975) 127–138

ANALYTISCHE EIGENSCHAFTEN VON HYDROPHILEN GLYKOLMETHACRYLAT-POLYMEREN MIT CHEMISCH GEBUNDENEM 8-OXYCHINOLIN

Z. SLOVÁK, S. SLOVÁKOVÁ und M. SMRŽ

Forschungsinstitut für reine Chemikalien, Lachema, Brno (Tschechoslowakei)

(Eingegangen den 6 August 1974)

8-Oxychinolin eignet sich durch seine analytischen Eigenschaften und genügende Reaktivität, die seinen Einbau in die Polykondensate oder seine Anknüpfung an ein geeignetes Polymer ermöglicht, besonders gut zur Herstellung von Chelatations-Ionenaustauschern. Vernon und Eccles[1] stellten eine Reihe von früher beschriebenen 8-Oxychinolin enthaltenden polymeren Materialien dar, und setzten sich kritisch mit ihren Eigenschaften auseinander. Es zeigte sich, dass eine Mehrzahl der untersuchten Stoffe eine höchst zögernde Einstellung der Sorptionsgleichgewichte innerhalb von mehreren Stunden, bedingt wahrscheinlich durch eine ungenügende Porosität, aufwies. Die besten analytischen Eigenschaften besass ein makroporöses vernetztes Polystyrol mit 8-Oxychinolin, das chemisch über Azo-Gruppen gebunden war. Eine 50%-ige Sättigung dieses Geles durch zweiwertiges Kupfer erfolgte in weniger als 1 Stunde. Ein durch 8-Oxychinolin modifiziertes Silikagel[2] oder poröses Glas[3] verfügt offensichtlich über höhere Reaktionsgeschwindigkeiten, die einige analytische Trennungen ermöglichen. Der Substitutionsgrad und dadurch auch die Austauschkapazitäten sind aber im Vergleich zu den organischen Polymeren bedeutend niedriger.

Durch eine heterogene Suspensionskopolymerisation von Oxyalkylmethacrylaten und Alkylendimethacrylaten wurden neutrale hydrophile Gele hergestellt mit einer Innenstruktur, die zwischen einem Aerogel und einem Xerogel liegt[4]. Diese Polymere zeichnen sich durch eine grosse innere Oberfläche und eine definierte Porosität aus. Die gute mechanische und hydrolytische Beständigkeit zusammen mit der Reaktivität der Hydroxylgruppen machen aus diesen Stoffen eine geeignete Ausgangsbasis für weitere chemische Modifizierungen. Diese Arbeit beschäftigt sich mit analytischen Eigenschaften von einem selektiven Ionenaustauschmaterial mit 8-Oxychinolingruppen, die biegsam über Seitenketten an das makroporöse, hydrophile Grundpolymer chemisch gebunden waren. Über die Synthese dieser Materialien soll an anderer Stelle später berichtet werden.

EXPERIMENTELLER TEIL

Chemikalien und Geräte

Tabelle I gibt eine Übersicht der untersuchten Proben und der Eigenschaften der zugehörigen Oxyalkylmethacrylat-Ausgangspolymeren Spheron (La-

TABELLE I

ÜBERSICHT DER PROBEN UND ZUGEHÖRIGEN AUSGANGSMATERIALIEN

Probe	*Ausgangsgel Spheron*[a]			*Zwischenprodukt*	
	Polymer	*Ausschlussgrenze*	*Korngrösse (μm)*	*Typ*	*mÄquiv.-NH_2 g^{-1}*
I	a		*ca.* 100	B	0,92
II	a	$500 \cdot 10^3$	40–63	A	0,74
III	a		20–40	A	0,70
IV	a		63–100	A	0,90
V	b	$280 \cdot 10^3$	40–63	A	0,97
VI	b		40–63 (Staub)	A	0,18
VII	c	$150 \cdot 10^3$	40–63	A	0,61
VIII	d	$4000 \cdot 10^3$	< 63	A	0,57

[a] Angaben über die Ausgangsgele von dem Hersteller; Ausschlussgrenze als Molekulargewicht von Dextranen ausgedrückt, dynamisch getestet.

chema, Brno) und der Zwischenprodukte A und B. Diese Zwischenprodukte enthielten am Ende einer aliphatischen Kette entweder eine *p*-Phenylaminogruppe (A) oder eine Benzidingruppe (B). 8-Oxychinolin wurde an die aromatischen Aminogruppen durch Azokupplung gebunden.

Für die Untersuchungen wurden stets Einwaagen der trockenen Proben benutzt. Alle verwendeten Chemikalien waren analysenrein. Die Konzentrationen der Metall-Grundlösungen (1 mg ml^{-1}) wurden komplexime trisch überprüft.

Alle Bestimmungen der Metallkonzentrationen wurden mit Hilfe der Atom-Absorptions-Spektrometrie (A.A.S.) ausgeführt. Die Arbeitsbedingungen richteten sich nach Angaben des Herstellers des Gerätes.

Für die Kolonnenversuche wurde eine Apparatur zusammengestellt (Abb. 1) die aus einer 5 ml-Bürette B, einer peristaltischen Pumpe P, einer Glaskolonne K und dem AA-Spektrophotometer Modell 303 Perkin-Elmer mit einem angeschlossenen Linienschreiber bestand. Die Verbindungen zwischen der Bürette und

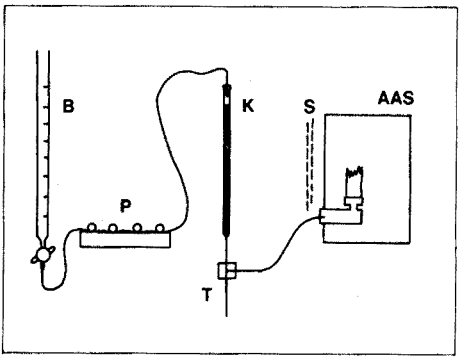

Abb. 1. Blockschema der chromatographischen Apparatur. B, 5-ml Bürette; P, Peristaltische Pumpe; K, Glaskolonne; T, Teflon-T-Stück; S, Asbestnetz als Wärmeschutz; AAS, Atom-Absorptions-Spektrophotometer.

der Kolonne wurden aus PVC-Schläuchen, die Leitung zwischen der Kolonne und AAS mit einer Teflonkapillare, Innendurchmesser 0,3 mm, durchgeführt. Der T-Stück T diente für das Zusaugen von destilliertem Wasser und wurde aus einem Teflonblock hergestellt, Bohrung ∅ 0,8 mm. Die benutzten Glaskolonnen hatten folgende Ausmasse: (a) ∅ 2,66 mm, Länge 200 mm, Säulenhöhe 175 mm (0,97 ml) gefüllt mit Probe II; (b) ∅ 4,0 mm, Länge 115 mm, Säulenhöhe 103 mm (1,3 ml) gefüllt mit Probe VIII, gesonderte Korngrösse 20–40 μm.

Bestimmung von Sorptionsvermögen

Eisen(III) bei pH 5 (Abb. 2): 100 mg der untersuchten Probe wurden mit 5 ml einer 0,1 *M* Azetatpufferlösung pH 5,0 überschichtet. Man gab 0,5 ml 0,33 *M* $FeCl_3$-Lösung dazu und schüttelte mechanisch 90 Minuten. Nach dem Filtrieren, Waschen mit verdünnter Pufferlösung und Wasser wurde das gebundene Eisen mit etwa 10 ml 3 *M* HCl in vier Portionen und mit 10 ml Wasser aus dem Filter eluiert und anschliessend quantitativ bestimmt.

Eisen(III) und Kupfer(II) in 0,05 M Säure (Abb. 2): Zu 50 mg der untersuchten Probe wurden 5 ml 0,05 *M* HNO_3 mit insgesamt 2,10 mg Eisen(III), bzw. 5 ml 0,05 *M* HCl mit 1,615 mg Kupfer(III) zugegeben. Nach 60 minutigem Schütteln wurde die restliche Konzentration von Metallen in der flüssigen Phase bestimmt.

Verschiedene Kationen bei pH 5: 200 mg Probe II wurde in eine kurze Glaskolonne, ∅ 8 mm, Säulenhöhe 12 mm, eingefüllt. Die Lösungen wurden direkt auf die Probe in folgender Reihe zugefügt: 5 ml Azetatpuffer pH 5 (0,04 *M*); 12 ml einer etwa 0,05 *M* Lösung des untersuchten Kations in derselben Pufferlösung; 10 ml Pufferlösung in einigen Portionen; 5 ml Wasser in 2–3 Portionen; 10 ml der Elutionssäurelösung und 10 ml Wasser in einigen Portionen. Die letzten 20 ml (Säure und Wasser) wurden in einem 25 ml Messkolben gefangen und das anwesende Metall anschliessend quantitativ bestimmt. Zum Vorbeugen der Hydrolyse bei Eisen(III) wurde dieses aus 25 ml einer 0,025 *M* Lösung in 1 *M* Azetatpuffer sorbiert. Die benutzten Metallsalze, Elutionslösungen sowie die erhaltenen Ergebnisse sind in Tabelle II zusammengestellt.

pH-Abhängigkeit des Sorptionsvermögens für Eisen(III) und Kupfer(II) (Abb. 3): Probe II wurde nach dem unter für 0,05 *M* Säure angegebenen Verfahren getestet. Für die Einstellung von pH 1,15–3,3 benutzte man 0,05 *M* Glycin–HCl–NaCl-Pufferlösungen, bei pH 3,6, 4,2 und 4,8 wurden 0,1 *M* Azetatpufferlösungen benutzt.

Einstellungsgeschwindigkeit der Gleichgewichte

Zu 50 mg einer Probe wurden 5 ml 0,1 *M* Azetatpufferlösung pH 5 gegeben. Nach 20 minutigem Stehen wurden 50 μl einer Fe^{3+}-Standardlösung (1 mg ml^{-1}) mit einer Mikropipette vorsichtig, um ein vorzeitiges Mischen zu verhindern, zur Oberfläche der Lösung gegeben. Nach der gewünschten Dauer von intensivem Mischen wurden etwa 2 ml Lösung durch ein aufgesetztes Mikrofilter in eine Pipette zur späteren Eisenbestimmung eingesaugt.

Auf die gleiche Weise wurde die Sorption von 50 μg Pb^{2+} bei pH 2,61 (0,1 *M* Glycin–HCl–NaCl) und 50 μg Co^{2+} bei pH 5,6 (0,1 *M* Azetatpuffer) untersucht.

Das Studium der Desorption erfolgte beim Ansäuren des Reaktionsgemisches mit gebundenem Metall: zu 3,5 ml einer 0,1 *M* Glycinlösung in 0,1 *M* NaCl wurden 50 μg Pb^{2+} gegeben. Nach 10 Minuten, als gesamtes Blei sorbiert wurde (in einem Parallelversuch bestätigt), wurden 1,5 ml 0,1 *M* HCl zugefügt, wobei 5 ml derselben Glycinpufferlösung entstand, die bei der Sorption verwendet wurde (pH 2,61). Nach dem Schütteln wurden die Blei-Konzentrationen in bestimmten Zeitabständen bestimmt.

Bestimmung der Verteilungskoeffizienten

Vergleich der Proben, Verteilungskoeffizienten für Cd^{2+} und Co^{2+} bei pH 1,42 (Abb. 5): 50 mg einer Probe wurden mit 5 ml einer 0,05 *M* Glycin–HCl–NaCl-Pufferlösung pH 1,42, die 25 μg Cd^{2+} oder 50 μg Co^{2+} enthielten, versetzt. Nach 60 minutigem Schütteln wurden die Metall-Gleichgewichtskonzentrationen bestimmt und daraus die Verteilungskoeffizienten K_1^s berechnet.

$$K_1^s = \frac{[\mathrm{Me}]_s}{[\mathrm{Me}]_1}\left(\frac{\mathrm{w/w}}{\mathrm{w/v}}\right)$$

pH-Abhängigkeit der K_1^s-Werte für Al^{3+}, Cd^{2+}, Co^{2+}, Cr^{3+}, Cu^{2+}, Fe^{3+}, Mn^{2+}, Ni^{2+}, Pb^{2+} und Zn^{2+} (Abb. 6): Zu 50 mg der Probe II wurden 5 ml einer Pufferlösung, bzw. einer 0,1 *M*; 0,2 *M* oder 1,0 *M* HCl-Lösung, gegeben, und 50 μl (= 50 μg Me) der entsprechenden Metallstandardlösung zugefügt. Nach 60 minutigem Schütteln wurden die Gleichgewichtskonzentrationen bestimmt und K_1^s berechnet. Es wurden Azetatpufferlösungen pH 3,6; 4,2; 4,8 und 5,6 mit einer Ionenstärke von 0,1 (KCl), und weiter Glycin–HCl–NaCl-Pufferlösungen 1,15; 1,42; 1,93; 2,28 und 2,92 mit einer Ionenstärke von 0,1 benutzt. Die Bestimmung von K_1^s für Mn^{2+} wurde ausserdem bei einer Ionenstärke von 0,4 (KCl) ausgeführt. K_1^s für Cu^{2+} bei pH 1 wurde auch bei der Ionenstärke 1,0 (NaCl) gemessen.

Kolonnenversuche

Die Kolonne wurde mit etwa 5 ml 1 *M* HCl bei maximal erreichbarer Geschwindigkeit durchgespült. Nach dem Öffnen der Kolonne wurde die über dem Gel befindliche Flüssigkeit mit Luft herausgedrückt. Man gab zweimal etwa 0,1 ml Wasser auf die Kolonne und drückte es mit Luft hinein. Danach folgten zweimal 0,1 ml einer zur totalen Sorption des untersuchten Metalls geeigneten Pufferlösung und schliesslich die Probelösung in dem gleichen Puffer. Während der Sorption wurde die Lösung nur sehr langsam in die Kolonne hineingedrückt um eine schmale Zone der sorbierten Metalle zu erzeugen. Nun wurde durch zwei 0,1 ml Portionen Wasser die Pufferlösung in dem oberen Teil der Säule ersetzt, damit die Elutionslösung nicht mit dem Puffer in Berührung kommen konnte. Die Bürette und die Zwischenverbindungen wurden mit Elutionsflüssigkeit durchgespült und gefüllt. Das leere Volumen in der Kolonne wurde vorsichtig gefüllt und der Verbindungsschlauch blasenfrei angesetzt. Der Ausfluss der Kolonne wurde über einem T-Stück mit A.A.S. verbunden. A.A.S. wurde eingeschaltet und gleichzeitig mit dem Einschalten der Pumpe wurde der Vorschub des Registriergerätes gestartet. Die Durchflussgeschwindigkeit konnte man durch die Einstellparameter der Pumpe beeinflussen; sie wurde aus der Volumenabnahme in der Bürette und aus dem Papiervorschub berechnet.

Bei raschem Wechsel der Elutionslösung während einer Trennung wurde nach dem Öffnen der Kolonne die Bürette durchgespült und mit neuer Lösung gefüllt. Nach dem Hineindrücken der restlichen Flüssigkeit über dem Gel in die Kolonne wurde die neue Lösung unmittelbar auf die Chromatographiesäule geleitet.

ERGEBNISSE UND DISKUSSION

Aus den publizierten Angaben über die mit 8-Oxychinolin modifizierten Materialien[1–3], die man auch als selektive Ionenaustauscher bezeichnen kann, folgt, dass die Eigenschaften des Grundpolymers und die Art der Bindung der Oxingruppe an das makromolekulare Gerüst für das zum Teil auch sehr unterschiedliche Verhalten der Materialien verantwortlich sind. Deshalb war es sinnvoll das neu synthetisierte Material mit Rücksicht auf die Eigenschaften des Ausgangspolymers, d.h. besonders die Porenweite und Korngrösse, die Art der Seitenkette mit gebundenem Oxin (A und B), und schliesslich den Substitutionsgrad, zu untersuchen. Das Porenvolumen bei allen untersuchten Gelen betrug 1,25–1,5 ml g^{-1}.

Die Synthese der oxinhaltigen Produkte wurde vor allem auf den Aufbau einer biegsamen und reichlich langen Seitenkette ("spacer") gezielt (Typ A). Ein Zwischenprodukt des Typus B wurde ähnlich wie ein Benzidinderivat von Karboxymethylzellulose synthetisiert[5]; seine Kette ist im Vergleich zu A weniger biegsam. Die Bindung von 8-Oxychinolin durch Azokupplung, bedingt durch seine Reaktivität, erfolgt überwiegend in der *p*-Stellung zu der Oxygruppe.

Die physikalischen Eigenschaften der modifizierten Gele unterscheiden sich von jenen der Ausgangsgele nur unwesentlich. Auffallend ist die gute mechanische Festigkeit und kleine Quellung (Volumenzuwachs von 30–40%), die in einem breiten pH-Gebiet von 0–9 und bei Ionenstärken 0–1 praktisch konstant bleibt. Die hydrolytische Beständigkeit ist in schwach basischen, neutralen und sauren Lösungen sehr gut; erst nach wiederholter längerer Einwirkung von starken Säuren in Konzentrationen mehr als 2 *M* kommt es zur langsamen Degradation.

Das Sorptionsvermögen (Austauschkapazität) gehört zusammen mit der Einstellungsgeschwindigkeit von Gleichgewichten und der Selektivität zu den wichtigsten untersuchten Eigenschaften. Bei einem Vergleich der Proben (Abb. 2) kann man feststellen, dass in genug sauren Lösungen eine zu erwartende Proportionalität zwischen der Häufigkeit der Funktionsgruppen und der Kapazität besteht (Kupfer(II) in 0,05 *M* HCl), und zwar ohne Rücksicht auf die weiteren Eigenschaften des Ausgangsgeles. Die gefundenen Kapazitäten waren zwar bedeutend niedriger, als es den Gehalten an Aminogruppen in den Zwischenprodukten entsprach; man muss jedoch bedenken, dass die Konzentration von Aminogruppen aus Elementaranalysen berechnet wurde, dass wahrscheinlich nicht jede Aminogruppe für das Anknüpfen eines Oxinmoleküls verwendet wurde, und das nicht jede gebundene Oxingruppe für die Chelatationsreaktion zugänglich war. Die hohen Werte der Kapazitäten für Eisen(III) bei pH 5 können durch teilweise Hydrolyse und unselektive Sorption erklärt werden; sie sind vor allem bei den Proben mit einem grösseren Staubanteil zu verzeichnen.

Die Sorptionsvermögen der Probe II für 9 Kationen bei pH 5 stehen mit kleinen Ausnahmen bei Kobalt(II) und Nickel(II) mit den publizierten Komplex-

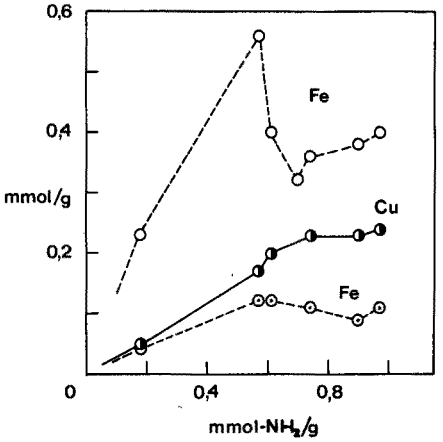

Abb. 2. Sorptionsvermögen für Cu^{2+} und Fe^{3+} in Abhängigkeit von dem Substitutionsgrad. (◑) Cu^{2+} in 0,05 *M* HCl; (⊙) Fe^{3+} in 0,05 *M* HNO_3; (○) Fe^{3+} bei pH 5.

TABELLE II

SORPTIONSVERMÖGEN DER PROBE II BEI pH 5

Metallion	*Metallsalz*	*Elutionssäure*	*Sorptionsvermögen*	
			mg Me g^{-1}	*mMol Me* g^{-1}
Mn^{2+}	$MnCl_2$	1 *M* HCl	4,82	0,09
Al^{3+}	$Al(NO_3)_3$	1 *M* HCl	3,35	0,12
Pb^{2+}	$Pb(NO_3)_2$	1 *M* HNO_3	46,5	0,22
Zn^{2+}	$Zn(NO_3)_2$	1 *M* HCl	13,9	0,21
Cd^{2+}	$Cd(NO_3)_2$	1 *M* HCl	20,5	0,18
Co^{2+}	$Co(NO_3)_2$	2 *M* HCl	10,1	0,17
Ni^{2+}	$Ni(NO_3)_2$	2 *M* HCl	10,7	0,18
Fe^{3+}	$Fe(NO_3)_3$	2 *M* HCl	19,7	0,35
Cu^{2+}	$Cu(NO_3)_2$	4 *M* HCl	16,0	0,25

bildungskonstanten[6] in Einklang (Tab. II). Bei einem Vergleich der Eigenschaften eines modifizierten Geles mit den Literaturangaben für Oxin muss man jedoch die Verschiedenartigkeit der chemisch gebundenen, also substituierten, und begrenzt beweglichen Funktionsgruppe beachten. Die Frage, ob bei den Bedingungen eines Metallüberschusses auch andere Komplexe als 1:1 entstehen können, ist für die praktischen Zwecke der Auswertung von kleiner Bedeutung; Vernon und Eccles[1] geben an, dass Kupfer(II) vorwiegend als ML_2 gebunden wird. Aus den publizierten Werten der Komplexbildungskonstanten K_2, die zehnmal niedriger als K_1 sind[6], sowie aus den bestimmten durchschnittlichen Ligandenzahlen für die untersuchten Metallionen bei ihren kleinen Konzentrationen (vgl. unten), kann man jedoch schliessen, dass bei einem Metallüberschuss vorwiegend 1:1-Komplexe gebildet werden. Für diese Annahme spricht auch der Umstand, dass die Resultate differentieller Bestimmungen der Sorptionsvermögen von dem Metallüberschuss unabhängig waren.

Die Acidität der Lösungen bewirkt die Ionisierung des Oxins und somit auch die "Konzentration" der reaktionsfähigen Form. Ihr Einfluss wird deshalb merklicher bei kleinen Metallkonzentrationen im Vergleich zu Sorbens (vgl. Abb. 6) als bei den Bestimmungen von Sorptionsvermögen (Abb. 3).

Die Geschwindigkeit der Sorption hängt merklich von der Zugänglichkeit der funktionellen Gruppen ab. Dank der weniger biegsamen Seitenkette des Zwischenproduktes B, trotz des gleichen Ausgangsgeles wie bei Proben II–IV und hoher Substitution, verfügte die Probe I über eine unvergleichbar kleinere Sorptionsgeschwindigkeit als die Gele mit der Struktur A: Bei sonst gleichen Bedingungen,

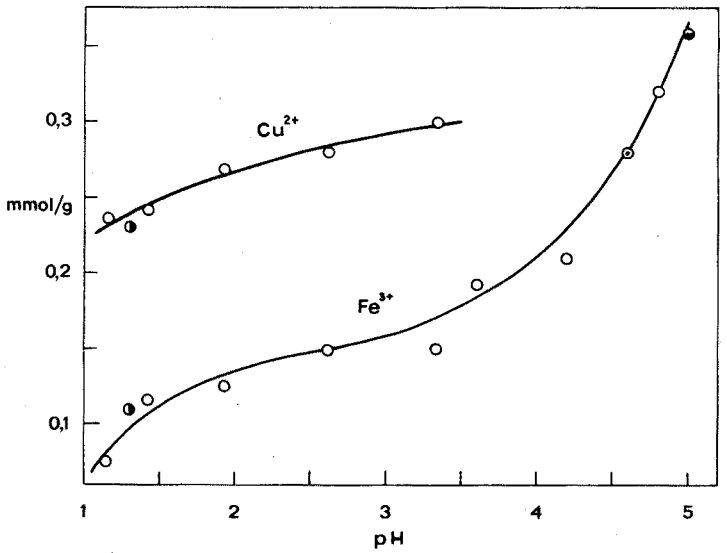

Abb. 3. Sorptionsvermögen der Probe II in Abhängigkeit von pH. (◑) Sorptionsvermögen in 0,05 *M* Säure; (⊙, ◒) Bestimmungen nach Elution.

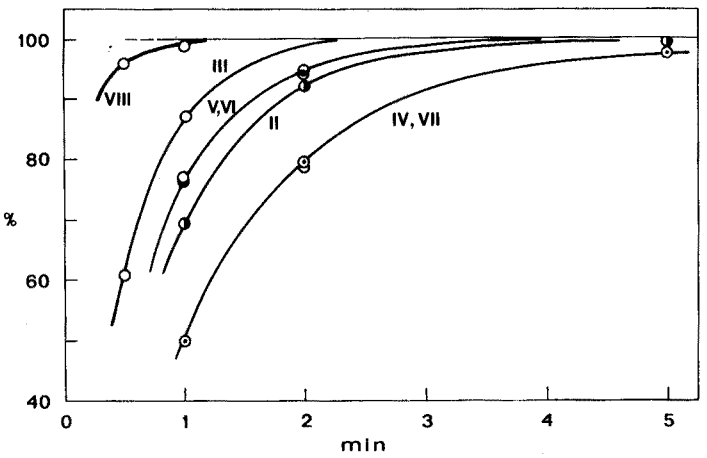

Abb. 4. Sorptionsgeschwindigkeit von 50 μg Fe^{3+} aus 5 ml bei pH 5. 50 mg der untersuchten Probe. I–VIII, siehe Tabelle I.

bei welchen alle anderen Proben II–VIII untersucht wurden (Abb. 4), sorbierte die Probe I nach 1; 2; 5; 10; 30 und 60 min nur 6; 11; 19; 24; 54 und 68% der anwesenden Eisen(III)-Menge. Die gemessenen Geschwindigkeiten (Abb. 4) zeigen den Einfluss von Korngrösse, d.h. der leichtzugänglichen Oberflächengrösse (Proben II und III), von der Häufigkeit von Oxingruppen (V und VI), und von der Porenweite (VII und VIII). Der Einfluss der Häufigkeit der Funktionsgruppen ist bei einem genügenden Sorbensüberschuss nicht sehr bedeutend—er kann durch den erhöhten Staubanteil in der Probe VI ausgeglichen werden. Die Porenweite spielt dagegen eine entscheidende Rolle auch wenn die Poren gegenüber der Grösse der hydratisierten Ionen unvergleichbar weiter sind. Die Ergebnisse der Geschwindigkeitsmessungen wurden bei der totalen Sorption von Kobalt(II) bei pH 5,6, ohne Möglichkeit etwaiger Hydrolyse, bestätigt. Bei der Untersuchung der Geschwindigkeit von Gleichgewichtseinstellung der Sorption von Blei(II) bei pH 2,61 (K_1^s 63) durch die Probe II wurden nur wenig kleinere Geschwindigkeiten gemessen: 71 und 94% der sorbierbaren Menge nach 2 bzw. 5 Minuten.

Der umgekehrte Vorgang, die Desorption, verläuft wesentlich schneller: nach 1 Minute wurde immer das volle Gleichgewicht eingestellt. Im Hinblick auf die unvergleichbar höhere Diffusionsgeschwindigkeit von H^+-Ionen im Vergleich zu den hydratisierten Metallkationen, und unter Berücksichtigung der Tatsache, dass die chemisch identischen Funktionsgruppen in den Proben I–VIII sehr grosse Reaktionsgeschwindigkeitsunterschiede aufweisen, kann man annehmen, dass der limitierende Vorgang ein Diffusionsprozess ist.

Für die Beurteilung der Selektivität eines Sorbens geht man oft aus den pH-Abhängigkeiten von Sorptionsvermögen aus[1]. Den praktischen Anwendungsbedingungen näher und somit richtiger ist jedoch die Bestimmung von Verteilungskoeffizienten K_1^s bei einem grossen Sorbensüberschuss. Aus der verwendeten Definition von K_1^s folgt, dass seine Grösse bei sonst gleichen Reaktionsbedingungen

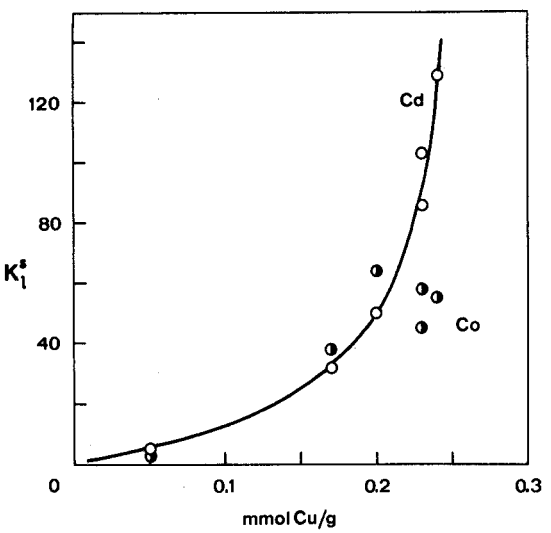

Abb. 5. Verteilungskoeffizienten für Co^{2+} und Cd^{2+} als Funktion der Häufigkeit von zugänglichen Funktionsgruppen (Sorptionsvermögen für Cu^{2+}) bei pH 1,42.

der Häufigkeit von zugänglichen Funktionsgruppen im Sorbens, also seinem Sorptionsvermögen proportional sein sollte, und zwar linear bei der Bildung von ML-Komplexen, nichtlinear bei der Bildung von höheren Komplexen. Dies folgt aus dem Massenwirkungsgesetz und aus der kleineren Wahrscheinlichkeit der gleichzeitigen Anwesenheit von mehreren für ein Metallion gleichzeitig zugänglichen Funktionsgruppen bei einem kleineren Sorptionsvermögen. In Abb. 5 werden die gemessenen K_1^s-Werte für Cadmium(II) Kobalt(II) mit den Sorptionsvermögen für Kupfer(II) der untersuchten Proben verglichen.

Das Sorptionsgleichgewicht

$$M + nHL \rightleftharpoons ML_n + nH^+$$

kann durch eine Konstante K charakterisiert werden:

$$K = \frac{[ML_n][H^+]^n}{[M][HL]^n}$$

Unter Berücksichtigung der Tatsache, dass in der festen Phase keine freien Metallionen, in der Lösung dagegen keine Komplexe bestehen, und dass die überschüssige Ligandkonzentration ML (nur in der festen Phase) als konstant angesehen werden kann, folgt für K_1^s:

$$K_1^s = \frac{[\text{total Me}]_s}{[\text{total Me}]_l} = \frac{[ML_n]}{[M]} = K\frac{[HL]^n}{[H^+]^n} = K'\frac{1}{[H^+]^n};$$

$$\log K_1^s = n\,\text{pH} + K''.$$

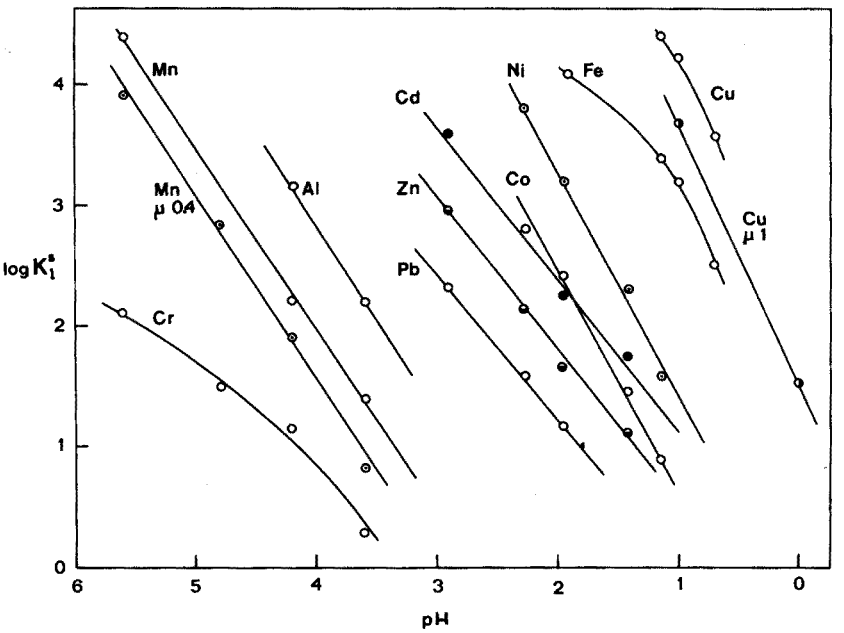

Abb. 6. Verteilungskoeffizienten für verschiedene Kationen in Abhängigkeit von pH und Ionenstärke. Probe II; falls nicht anders angegeben, Ionenstärke 0,1.

TABELLE III

DURCHSCHNITTLICHE LIGANDENZAHL BEI DER SORPTION VON KATIONEN

Kation	*Ligandenzahl*	*Kation*	*Ligandenzahl*
Cr^{3+}	1	Cd^{2+}	1,3
Mn^{2+}	1,5	Co^{2+}	1,9
Al^{3+}	1,6	Ni^{2+}	1,8
Pb^{2+}	1,15	Fe^{3+}	2
Zn^{2+}	1,25	Cu^{2+}	2,0

Die Steigungen der gemessenen linearen Abhängigkeiten der log K_1^s-Werte von pH für zehn verschiedene Kationen (Abb. 6, Tab. III) geben unmittelbar die durchschnittliche Anzahl von Liganden mit welchen das Kation bei den gegebenen Reaktionsbedingungen (Konzentrationsverhältnis Metall:Sorbens) gebunden wird. In den meisten Fällen werden gleichzeitig Komplexe 1:1 und 1:2 gebildet. Cu^{2+}, Fe^{3+}, Ni^{2+} und Co^{2+} werden bei kleinen Konzentrationen überwiegend als 1:2-Komplexe sorbiert. Die Bildung eines elektroneutralen Komplexes FeL_3 ist aus sterischen Gründen unwahrscheinlich. Das Mengenverhältnis der gebildeten Komplexe 1:1 und 1:2 wird bei dem gleichen pH, derselben Ionenstärke und bei einem konstanten Volumenverhältnis Lösung:Sorbens durch die Konzentration des sorbierten Kations in der Ausgangslösung bestimmt, und zwar so, dass der Anteil der 1:1-Komplexe sich mit wachsender Metallkonzentration vergrössert. Man kann dadurch die beobachtete Abhängigkeit der K_1^s-Werte von dem Mengenverhältnis Metall:Sorbens zu erklären versuchen. Die Nichtkonstanz der Verteilungskoeffizienten bei veränderlichen Metallkonzentrationen zusammen mit den verschiedenen Geschwindigkeiten der Sorptions- und Desorptions-Vorgänge kann man als Hauptgründe für die Verbreitung der Elutionspeaks der Metalle bei den chromatographischen Versuchen ansehen.

Die Kolonnenversuche zeigten, dass bei Bedingungen, bei welchen keine Sorption möglich ist, die eluierten Zonen der Metalle sehr schmal und scharf sind (z.B. Mn^{2+} in 0,1 *M* HCl, Zn^2 in 0.2 *M* HCl, Abb. 7), bei begrenzter Sorption beobachtet man asymmetrische Peaks mit einer scharfen Vorderkante (Mn^{2+} bei pH 2,92; Pb^{2+} bei pH 1,25) und schliesslich asymmetrische auseinandergezogene Zonen (Pb^{2+} bei pH 1,42, Zn^{2+} bei pH 1,42, Cd^{2+} in 0,2 *M* HCl, Abb. 7). Aus diesen Gründen ist es vorteilhaft für Metalltrennungen die genügenden Unterschiede unter den Verteilungskoeffizienten auszunutzen und die Kationen frontal bei genügender Säurekonzentration zu eluieren. Auf die Weise war es möglich ein kompliziertes Gemisch von je 10 μg Mn^{2+}, Co^{2+}, Fe^{3+} und Cu^{2+} zu trennen (Abb. 8). Bei einer quantitativen Überprüfung der Trennung wurden in den zugehörigen getrennt gefangenen Fraktionen 8,8 μg Mn, 6 μg Co, 9,8 μg Fe und 10,0 μg Cu bestimmt. Die chromatographischen Trennungen von verwandten Kationen werden an einem weitporigen Material (Kolonne b) möglich unter der Voraussetzung, dass das weniger haftende Metall frontal eluiert wird, und dass das sorbierte Kation die Kolonne höchstens bei einem Verhältnis des Elutionsvolumens zu freiem Volumen 2–3 verlässt (Abb. 7). In diesem Fall könnten die Ergebnisse durch eine Gradientelution verbessert werden.

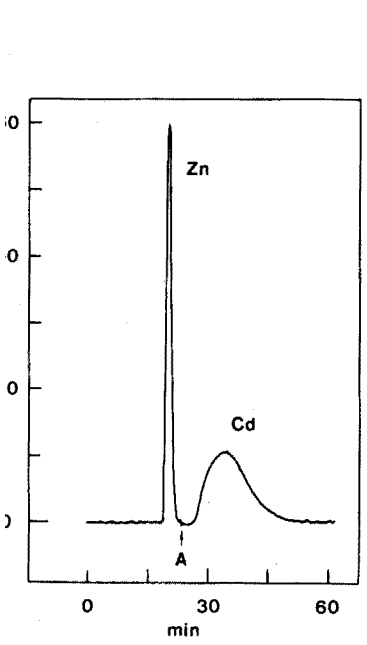

Abb. 7. Chromatographische Trennung von 5 μg Zn^{2+} und 10 μg Cd^{2+}. Kolonne b, 0,2 *M* HCl. A, Wechsel der Hohlkatodenlampe im A.A.S.

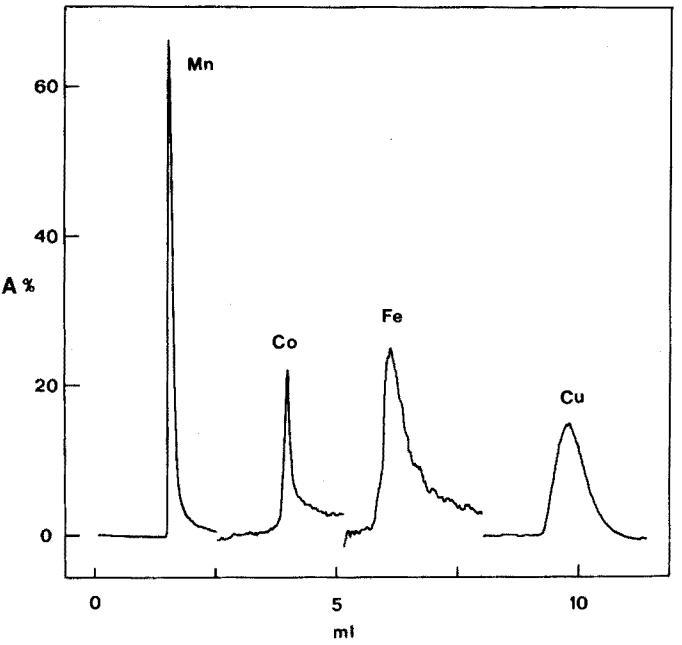

Abb. 8. Sukzessive Elution von je 10 μg Mn^{2+}, Co^{2+}, Fe^{3+} und Cu^{2+}. Kolonne a; *ca.* 0,3 ml Elutionslösung/min. Für Co^{2+} und Fe^{3+} dreifache Skalendehnung bei A.A.S.

Bei allen Kolonnenversuchen bewährte sich die Apparatur mit A.A.S. in der Rolle eines selektiven kontinuierlichen Detektors. Durch eine Reihe von Versuchen wurde eine sehr gute Reproduzierbarkeit der Bestimmung der Elutionsvolumina und auch eine lineare Abhängigkeit der maximalen Absorptionswerte von den auf die Kolonne gegebenen Mengen des Kations nachgewiesen.

Die Anwendungsmöglichkeiten der studierten Materialien für praktische Trennungen von Metallen sind in Wirklichkeit viel breiter, als es nur der Ausnützung der pH-Abhängigkeiten von Verteilungskoeffizienten entsprechen würde. Ganz offen bleiben die Möglichkeiten von selektiven Sorptionen und Desorptionen bei Anwesenheit von starken Komplexbildnern.

Die hohen Werte der Verteilungskoeffizienten sind nur wenig von der Ionenstärke abhängig (vgl. Abb. 6, Mn^{2+} und Cu^{2+}). Diese Tatsache, zusammen mit der hohen Selektivität für Schwermetalle, könnte sowohl bei den analytischen Problemen, z.B. bei Abwässeranalysen, als auch bei wirksamer Reinigung von konzentrierten Salzlösungen, z.B. von Pufferlösungen, ausgenutzt werden.

ZUSAMMENFASSUNG

8-Oxychinolin, über eine Azo-Gruppe und eine flexible Seitenkette an ein hydrophiles makroporöses Kopolymer von Glykolmethacrylat mit Glykolmonomethacrylat gebunden, weist hochselektives Verhalten gegenüber von Schwer-

metallionen auf. Die Austauschkapazität des Materials beträgt für Schwermetallionen etwa 0,2 mMol Me g^{-1}, die Sorptionsgleichgewichte werden innerhalb von 5–10 Minuten voll eingestellt. Die Verteilungskoeffizienten für zehn Metallionen wurden in Abhängigkeit von pH und der Ionenstärke gemessen; ihre Werte betragen in günstigen pH-Bereichen mehr als 10^4. Auf mögliche Anwendungen bei chromatographischen Trennungen von Metallen, bei der Spurenanalyse sowie bei selektiver Reinigung von konzentrierten Salzlösungen wird hingewiesen.

SUMMARY

8-Hydroxyquinoline, bound to the azo group and the flexible side chain of a hydrophilic macroporous copolymer of glycoldimethacrylate and glycolmonomethacrylate, possesses high selectivity for heavy metal ions. The exchange capacity of the resin is about 0.2 mmole Me g^{-1} for heavy metal ions. Sorption equilibrium is complete after 5–10 min. Partition coefficients for 10 metal ions were determined as a function of pH and ionic strength; in the optimal pH range, their magnitudes exceeded 10^4. The exploitation of this material in chromatographic separation of metals, trace analysis, and selective purification of concentrated salt solutions, is discussed.

LITERATUR

1 F. Vernon und H. Eccles, *Anal. Chim. Acta*, 63 (1973) 403.
2 J. M. Hill, *J. Chromatogr.*, 76 (1973) 455.
3 *Pierce Previews*, Pierce Chemical Co., U.S.A., December, 1973.
4 J. Čoupek, M. Křivánková und S. Pokorný, *Abstract IUPAC International Symposium on Macromolekules, Helsinki, 1972, Vol. I*, S. 415.
5 A. J. Bauman, H. H. Weetall und N. Weliky, *Anal. Chem.*, 39 (1967) 932.
6 J. Bjerrum, G. Schwarzenbach und L. G. Sillén, *Stability Constants, Part I. Organic Ligands*, The Chemical Society, London, 1957.

Analytica Chimica Acta, 75 (1975) 139–148

GAS–LIQUID CHROMATOGRAPHY ON PHENYL-SUBSTITUTED POLYSILOXANE STATIONARY PHASES. ALCOHOLS AND ALCOHOL BENZOYL DERIVATIVES

J. B. PÍAS* and L. GASCÓ

Departamento de Ingeniería y Servicios Básicos, División de Química Analítica, Junta de Energía Nuclear Madrid-3 (Spain)

(Received 25th June 1974)

The g.l.c. separations of derivatives of organic substances are of considerable importance, for such separations often offer considerable advantages compared with direct separations of the substances themselves. Correlations found between the retention data of such derivatives and their structures can, moreover, give information additional to the results found for the original compounds chromatographed in the same columns.

Since Kováts' introduction[1] of the retention index concept, this system of tabulation of retention data has received increasing support. Apart from its descriptive value, in many cases it allows the establishment of simple correlations between the retention data and the structure of the chromatographed compounds. Its applications to qualitative analysis and to the evaluation of stationary phases are considerable. It is clear that indices must be obtained with accuracy if all their advantages are to be obtained. Very accurate measurements of indices have been accomplished in capillary columns and in some fields, where resolution plays a vital role, this type of column becomes absolutely essential. For practical reasons, conventional packed columns continue to be used in many cases but the accuracy of the indices obtained from these columns is smaller. A review of the literature shows a lack of agreement between different sources. The observed discrepancies may be due to imperfect instrumentation and above all to the use of rather ill-defined stationary phases. Adsorption on the solid support is also an important source of error, especially if polar substances are run on a nonpolar column. If these factors were taken into account, retention indices in this type of column could be obtained with good reliability.

Separations of a number of alcohol benzoate derivatives have been achieved by some workers[2–4], although retention indices were not used.

The present work is concerned with the chromatographic elution, at various temperatures, of a large number of alcohols and alcohol benzoyl derivatives in columns containing Chromosorb G support (AW-DMCS(HP)) coated with stationary phases of stated composition and of great thermal stability, such as SE-30, OV-3, OV-7, OV-11, OV-17 and OV-25. These phases form an increasing scale of polarity based on the same type of substitution, from the nonpolar SE-30 to the moderately

* Present address: Department of Chemistry, The University of Birmingham, P.O. Box 363, Birmingham B15 2TT, England.

polar OV-25. This fact could be used advantageously in order to establish correlations between retention parameters and the molecular structure of the alcohols. Retention data, as retention indices, and values of the temperature dependence of the retention index ($\partial I/\partial T$) of alcohols and benzoates, are presented. The reported information could be also a significant help in the analysis of volatile alcohol constituents in foodstuffs.

EXPERIMENTAL

Standard compounds

Standard benzoates of quite high purity were prepared in the laboratory by the conventional method of benzoylation with alcohols and benzoyl chloride. Reference n-alkanes of the highest purity available were obtained commercially.

Stationary phases and support

Silicone gum rubber SE-30 (General Electric Co.); OV-1, OV-3, OV-7, OV-11, OV-17 and OV-25 (Ohio Valley Specialty Chemical Co.); tetrahydroxyethylethylenediamine (THEED; Hewlett Packard); and Chromosorb G (AW-DMCS (HP); 80–100 mesh; J. Manville) were used.

Retention index measurement

Relative retentions in Kovats' index units were obtained from chromatograms of suitable mixtures of alcohols containing n-alkanes as standards. Retention times were measured directly from the chromatograms as retention distances and corrected for dead volume by deduction of the air peak calculated by the method of Peterson and Hirsch[5]. The adjusted retentions were then used for index calculations by means of the expression:

$$I = 100\,N + 100\,n\,\frac{\log_{10}R_x - \log_{10}R_N}{\log_{10}R_{N+n} - \log_{10}R_N}$$

where R_x, R_N and R_{N+n} are the adjusted retentions of the solute and n-alkanes possessing N and $(N+n)$ carbon atoms respectively. Accurate calculation of indices based on this expression necessarily implies linearity between the logarithms of the adjusted retentions of the N and $(N+n)$ n-alkanes with their own number of carbon atoms. This has been taken into consideration in all the chromatographed sequences. A programme in a desk computer "Olivetti Programma 101" was used to calculate the indices[6].

Chromatographic separation

After an optimization study, the separations were carried out under the conditions listed in Table I. Alcohols were injected in different sequences with the appropiate reference n-alkanes by means of a 1-μl Hamilton microsyringe. The starting point was indicated on each chromatogram by means of a foot-switch attached to the recorder. Figure 1 shows a typical chromatogram. Retention distances were measured with an accuracy of ± 0.05 mm and, in most cases, two or three determinations were carried out. The column efficiency was approximately the

TABLE I

CHROMATOGRAPHIC CONDITIONS FOR THE SEPARATION OF ALCOHOLS AND BENZOATES

Equipment	Perkin Elmer F-11 gas chromatograph (with single column) fitted with a flame-ionization detector
Columns	Stainless steel, 1 m × 2 mm i.d.
Packing	5% (w/w) SE-30 on Chromosorb G (AW-DMCS (HP)), 80–100 mesh 5% (w/w) OV-3, OV-7, OV-11, OV-17 and OV-25 plus 0.05% (w/w) THEED on Chromosorb G (AW-DMCS (HP)) 80–100 mesh
Operation temperatures	(°C) oven, 100 (T_1), 120 (T_2) and 140 (T_3); injection port, 240
Argon flow rate	6–50 ml min^{-1}
Air flow rate	350 ml min^{-1}
Hydrogen flow rate	20 ml min^{-1}
Detector attenuation	× 50, × 100, × 200
Chart speed	30, 60 and 240 cm h^{-1}
Sample	*ca.* 0.1 μg

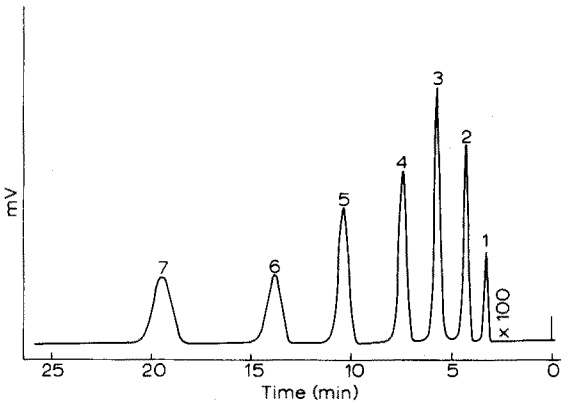

Fig. 1. Chromatogram of a mixture of n-alkanes and alcohols. Column of OV-3 at 100°C. Flow rate, 10 ml min^{-1} (Chromatographic conditions in Table I). (1) Octane; (2) 2-methyl-1-pentanol; (3) nonane; (4) 2-methyl-2-heptanol; (5) decane; (6) 2-ethyl-1-hexanol; (7) undecane.

TABLE II

ROHRSCHNEIDER CONSTANTS OF THE POLYSILOXANE PHASES

Stationary phase	*Methyl replacement* %	*x*	*y*	*z*	*u*	*s*
OV-1	0	0.16	0.20	0.50	0.85	0.48
SE-30	0	0.16	0.20	0.50	0.85	0.48
OV-3	10	0.42	0.81	0.85	1.52	0.89
OV-7	20	0.70	1.12	1.19	1.98	1.34
OV-11	35	1.13	1.57	1.69	2.66	1.95
OV-17	50	1.30	1.66	1.79	2.83	2.47
OV-25	75	1.76	2.00	2.15	3.34	2.81

TABLE III

RETENTION INDICES OF ALCOHOLS

(Separation conditions see Table I)

Compound	*SE 30*			*OV 3*			*OV 7*			*OV 11*			*OV 17*			*OV 25*		
	T_1	T_2	T_3	T_1	T_2	T_3	T_1	T_2	T_3	T_1	T_2	T_3	T_1	T_2	T_3	T_1	T_2	T_3
Methanol	373	—	—	—	—	—	—	—	—	—	—	—	—	—	—	—	—	—
Ethanol	439	—	—	—	—	—	—	—	—	—	—	—	—	—	—	—	—	—
1-Propanol	544	—	—	574	—	—	—	—	—	—	—	—	—	—	—	—	—	—
1-Butanol	650	643	643	672	667	667	702	696	702	725	726	—	748	748	744	792	790	788
1-Pentanol	751	747	746	777	779	778	806	803	804	—	—	835	856	855	855	900	898	900
1-Hexanol	856	853	850	881	882	882	907	908	907	935	934	935	959	960	960	1003	1003	—
1-Heptanol	960	958	956	985	984	984	1010	1011	1010	1038	1036	1038	1062	1062	1062	1104	1104	1109
1-Octanol	1064	1058	1060	1087	1086	1086	1112	1112	1112	1139	1140	1139	1165	1165	—	—	—	1208
1-Nonanol	1166	1160	1162	1189	1187	1187	—	1213	1214	—	—	—	1268	—	—	1303	1308	1313
1-Decanol	1264	1262	1264	—	—	—	—	—	—	—	—	—	—	—	—	—	—	1413
2-Propanol	477	—	—	—	—	—	—	—	—	—	—	—	—	—	—	—	—	—
2-Butanol	586	584	586	607	604	608	633	629	629	656	654	—	675	674	673	711	708	—
2-Pentanol	689	685	685	711	706	708	736	733	736	756	758	—	777	777	774	811	809	806
2-Hexanol	787	786	783	811	808	806	835	832	—	—	—	858	878	877	875	914	911	910
2-Heptanol	889	888	886	915	912	910	—	935	935	—	—	960	982	—	—	1006	1013	1015
2-Nonanol	1091	1087	1089	1115	1114	1115	1137	1137	1137	1160	1159	1158	1183	1182	—	—	—	—
3-Pentanol	689	685	685	708	704	705	733	729	729	756	750	753	777	777	774	808	804	—
3-Hexanol	785	783	781	807	809	806	830	827	831	853	851	—	878	876	873	904	901	900
3-Heptanol	886	885	885	909	908	908	929	832	933	955	952	—	975	975	972	1008	1007	1009
4-Heptanol	880	877	879	904	903	902	924	925	924	946	946	945	966	966	965	999	998	999
4-Octanol	982	976	978	1005	1004	1003	1024	1025	1025	—	-	—	—	—	—	—	—	—
2-Methyl-1-propanol	612	—	—	641	—	—	654	650	648	—	-	680	704	704	699	740	739	740
2-Methyl-1-butanol	727	726	724	—	—	—	—	—	—	—	-	—	—	—	—	—	—	—
2-Methyl-1-pentanol	824	822	820	849	846	844	871	870	870	—	—	898	917	918	917	958	958	—
2-Methyl-2-butanol	628	—	—	652	649	646	674	673	669	692	690	—	709	712	704	738	735	733
2-Methyl-2-pentanol	720	716	720	748	742	741	767	763	764	—	—	782	801	804	796	827	826	826
2-Methyl-2-hexanol	822	817	818	848	842	841	862	863	859	884	882	877	904	902	898	930	928	926
2-Methyl-2-heptanol	920	919	920	944	942	942	961	962	862	982	981	982	1001	1001	—	1026	1024	—

2-Methyl-3-hexanol	858	852	854	876	877	880	897	898	898	920	919	—	939	940	938	969	970	968
3-Methyl-1-butanol	725	719	719	747	744	742	771	766	770	798	793	788	817	820	817	855	851	852
4-Methyl-1-pentanol	827	823	821	849	848	845	876	874	872	902	899	898	923	922	920	960	958	960
2-Ethyl-1-butanol	834	828	833	857	855	855	—	880	882	907	905	—	928	—	—	—	971	—
2-Ethyl-1-hexanol	1019	1015	1017	1046	1043	1045	1067	1068	1069	1092	1092	1094	1116	1117	—	1156	1156	1162
3-Ethyl-3-pentanol	853	847	—	876	878	879	898	899	903	920	922	—	939	946	946	974	974	979
2,2-Dimethyl-3-pentanol	814	815	817	834	837	838	855	857	858	874	876	—	890	892	894	919	920	923
2,2-Dimethyl-3-hexanol	906	906	907	926	927	928	944	944	947	962	—	966	977	983	982	1004	1003	—
1-Penten-3-ol	675	670	664	—	—	—	715	715	714	—	—	—	—	—	—	807	807	—
1-Hexen-3-ol	771	770	767	791	791	788	818	816	816	842	843	847	864	864	862	901	897	901
1-Hepten-3-ol	872	871	869	894	894	894	918	918	919	944	944	944	967	967	967	1009	1009	—
1-Octen-3-ol	972	972	968	995	995	996	1018	1019	1020	1044	1044	1043	1068	1068	1067	1109	1109	1112
2-Buten-1-ol	664	657	653	684	682	680	715	713	713	—	—	747	769	769	768	819	—	820
3-Hexen-1-ol	850	851	—	876	876	879	905	905	908	934	936	—	962	966	965	1016	1018	—
3-Hepten-1-ol	941	941	—	969	969	968	996	997	997	1026	1026	1027	—	—	—	—	—	—
2-Methyl-3-buten-2-ol	606	592	—	620	614	619	646	642	638	666	665	663	685	685	682	719	717	711
3-Methyl-3-buten-1-ol	730	—	—	751	751	750	778	781	780	808	811	—	837	837	837	885	886	—
2-Methyl-1-hepten-3-ol	961	959	—	986	986	986	1009	1009	1010	1032	—	1036	—	1059	1058	1099	1099	1101
Linalool	1090	1089	1090	—	—	—	—	—	—	—	—	—	—	—	—	—	—	—
Isopulegol	1141	1146	1155	—	—	—	—	—	—	—	—	—	—	—	—	—	—	—
4-Terpinenol	1170	1173	1182	—	—	—	—	—	—	—	—	—	—	—	—	—	—	—
Terpineol	1181	1187	1195	—	—	—	—	—	—	—	—	—	—	—	—	—	—	—
Citronellol	—	—	1218	—	—	—	—	—	—	—	—	—	—	—	—	—	—	—
Nerol	1221	1224	1229	—	—	—	—	—		—	—	—	—	—	—	—		—
Geraniol	—	—	1246	—	—	—	—	—		—	—	—	—	—	—	—		—
Eugenol	1355	1352	1356	—	—	—	—	—		—	—	—	—	—	—	—		—

TABLE IV

RETENTION INDICES OF ALCOHOL BENZOYL DERIVATIVES

(Separation conditions see Table I)

Compound benzoyl derivative of,	*SE 30*			*OV 3*			*OV 7*			*OV 11*			*OV 17*			*OV 25*		
	T_1	T_2	T_3	T_1	T_2	T_3	T_1	T_2	T_3	T_1	T_2	T_3	T_1	T_2	T_3	T_1	T_2	T_3
Methanol	1081	1087	1092	1129	—	1141	1169	1178	1183	1216	1223	1230	1262	1271	1283	1352	1360	1378
Ethanol	1152	1157	1164	—	—	1212	1239	—	—	1286	1292	1298	1332	1339	1349	—	—	—
1-Propanol	1245	1254	1262	1295	—	1309	1336	1345	1352	1384	1389	1390	1427	1435	1444	1513	1523	1538
1-Butanol	1344	1352	1358	—	—	1404	1438	1442	1448	1483	1491	1497	1525	1533	1545	1614	1623	1635
1-Pentanol	1440	1447	1456	—	—	1503	1535	1542	1548	1581	—	1594	1623	1631	1640	1710	1723	1734
1-Hexanol	1535	1549	1556	—	—	1604	—	1640	1648	—	1691	1695	1721	1730	1737	1810	1820	1830
1-Heptanol	1638	1646	1654	—	1698	1702	—	1739	1747	—	1788	1793	—	1828	1837	—	1917	1929
1-Octanol	—	1745	1755	—	—	1802	—	—	—	—	—	1891	—	—	1938	—	—	—
1-Nonanol	—	—	1856	—	—	—	—	—	—	—	—	—	—	—	2037	—	—	—
1-Decanol	—	—	1952	—	—	2001	—	—	—	—	—	—	—	—	—	—	—	—
2-Propanol	1188	1191	1197	—	—	1242	—	—	—	—	—	—	1351	1355	1362	1436	1445	1457
2-Butanol	1281	1284	1292	—	—	1338	—	—	—	1409	1415	1420	1449	1456	1463	1534	1541	1554
2-Pentanol	1368	1373	1379	1412	1419	1424	1453	1459	1465	1498	1506	1510	1536	1544	1550	1620	1628	1638
2-Hexanol	1461	1467	1472	—	—	—	—	—	—	—	—	—	—	—	—	—	—	—
2-Heptanol	1556	—	1564	1598	1605	1611	1640	1646	1653	—	1690	—	—	1730	1736	1800	1811	1823
2-Nonanol	—	1752	1759	—	1794	1798	—	1834	1842	—	—	—	—	—	—	—	—	—
3-Pentanol	1363	1370	1377	1409	—	1421	1447	1454	1462	1490	1498	1501	1534	1540	1546	—	—	—
3-Hexanol	1443	1447	1456	1491	—	1502	—	1536	1542	1574	1580	1586	1613	1619	1625	1699	1708	1718
3-Heptanol	1536	—	1544	1580	—	1591	—	1626	1632	1664	1673	1676	1706	1709	1716	—	1798	1807
4-Heptanol	1523	—	1536	—	1576	1582	—	1614	1622	—	—	1642	1693	1700	1706	1778	1785	1794
4-Octanol	1618	—	1621	—	1664	1670	—	1706	1711	—	1750	1753	—	—	—	—	1874	1881
2-Methyl-1-propanol	1305	1308	1314	1371	1378	1384	1392	1399	1405	1434	1449	1453	1471	1475	1488	1556	1564	1577
2-Methyl-1-butanol	1407	1414	1421	1456	1462	1467	1497	1504	1512	1539	1550	1554	—	1592	1599	1667	1676	1688
2-Methyl-1-pentanol	1485	1500	1507	1542	1548	1555	—	1592	1600	—	1638	1642	1667	1675	1685	1752	1761	1771
2-Methyl-2-butanol	1326	1332	1342	—	—	—	1408	1417	1422	—	—	—	1487	1496	1506	1571	1582	1594
2-Methyl-2-pentanol	1400	1409	1422	1450	1457	1461	1487	1495	1499	1528	1539	1545	1566	1574	1582	—	—	—
2-Methyl-2-hexanol	1488	1496	1508	1538	1545	1551	1575	1582	1588	1616	1626	1631	1563	1660	1669	—	1742	1755
2-Methyl-2-heptanol	1588	1597	1599	—	1635	1642	—	1673	—	—	1716	1723	—	—	—	—	—	—

2-Methyl-3-hexanol	1501	1505	1508		1548	1553	—	1588	1594	1624	1633	1638	—	—	—	—	—	—
3-Methyl-1-butanol	1409	1417	1419		1462	1468	1496	1502	1511	—	—	—	1582	1589	1599	1666	1676	1687
4-Methyl-1-pentanol	1506	1514	1517		—	—	—	1602	—	—	—	—	—	—	—	—	—	—
2-Ethyl-1-butanol	1500	1507	1514		1553	1560	1589	1596	1605	—	—	1653	1674	1685	1693	1761	1772	1785
2-Ethyl-1-hexanol	—	1675	1685		—	1729	—	1763	1771	—	1810	1815	—	1848	1856	—	1934	1945
3-Ethyl-3-pentanol	—	1513	1526		—	—	—	—	—	1637	—	1659	—	1693	1702	—	—	—
2,2-Dimethyl-3-pentanol	1453	1465	1474		1510	1518	1541	1549	1558	1584	1594	1600	1621	1628	1637	1707	1717	1727
2,2-Dimethyl-3-hexanol	1537	1538	1545		1538	1590	—	1622	1630	1656	1664	1670	1692	1698	1707	1784	1794	1802
1-Penten-3-ol	1348	1356	1364		1407	1412	1443	1448	1456	1488	1498	1499	1531	1538	1545	1623	1634	1644
1-Hexen-3-ol	1439	1443	1445		1490	1495	—	1533	1539	1573	1580	1586	—	—	—	—	—	—
1-Hepten-3-ol	1528	1531	1539		—	—	1620	1626	1632	1666	1673	1680	1709	1714	1722	—	1806	1818
1-Octen-3-ol	—	—	1633		—	—	—	—	—	—	1766	1771	—	1808	1814	—	—	—
2-Buten-1-ol	—	1373	1376		1419	1425	1462	1469	1473	1515	1523	1529	1564	1572	1577	1664	1674	1686
3-Hexen-1-ol	—	1539	1546		1590	1593	—	1636	1645	—	—	1697	—	—	—	—	—	—
3-Hepten-1-ol	1619	1626	1630		1677	1684	—	1724	1732	—	—	1786	—	—	—	—	—	—
2-Methyl-3-buten-2-ol	1317	1322	1326	—	1365	1370	—	1406	1412	1447	1454	1456	—	—	—	—	—	—
3-Methyl-3-buten-1-ol	1414	1423	1426	—	1471	1477	—	1518	—	1562	1570	1577	—	—	—	—	—	—
2-Methyl-1-hepten-3-ol	—	1606	1611	—	—	—	—	—	—	—	1739	1746	—	—	1790	—	1877	1888
1,3-Propanediol	1551	1550	1554	—	1577	1584	—	1643	1651	—	—	—	—	—	—	—	—	—
1,4-Butanediol	—	1667	1669	1700	1700	1704	—	1769	1774	—	—	—	—		—	—	—	—
Linalool	—	—	1765	—	—	1818	—	—	1859	—	—	—				—	—	—
Isopulegol	—	—	—		—	1862	—	—	—	—	—	—						
4-Terpineol	—	—	1872		—	1937	—	—	2016	—	—	—						
Terpineol	—	—	1888		—	1945	—	—	—			—						
Citronellol	—	—	1875	—	—	1938	—	—	—			—						
Nerol	—	—	1906	—	—	1959	—	—	2031			—						
Ceraniol	—	—	1914	—	—	1977	—	—	—	—	—	—						

same in the interval 100–140°C for alcohols and benzoates. For decanol (flow rate, 20 ml min^{-1}) the efficiency in HETP terms was 0.06 cm for OV-3, decreasing to 0.16 cm for OV-25 in the following order: OV-3; OV-7; OV-11; OV-17; SE-30; OV-25. For butyl benzoate at the same flow-rate (20 ml min^{-1}) the HETP was 0.05 cm for OV 3 decreasing to 0.14 cm for OV 17 in the following order: OV-3; OV-11; OV-7; OV-25; SE-30; OV-17.

The choice of the nonpolar reference column necessary for the calculation of the structural parameter $\Delta I = I_{polar} - I_{nonpolar}$[7], should be made whenever possible according to the nature of the polar columns under study. The structurally identical phases OV-1 and SE-30, which through increasing substitution of methyl for phenyl groups produces the OV phase series, may be suitable. The Rohrschneider constants[8] of OV-1 and SE-30 together with those of the rest of these phases are shown in Table II. Chromatography of primary alcohols on a OV-1 column, at 100°C, showed some noticeable tailing which did not take place in the SE-30 column. For this reason the latter was chosen as the reference nonpolar column[6].

Deactivation of the columns containing OV phases was achieved by dissolving

TABLE V

TEMPERATURE DEPENDENCE OF THE RETENTION INDEX OF ALCOHOLS

(Values of $\partial I/\partial T$ ($\partial T = 10$°C), range 100–140°C)

Compounds	*Stationary phase*					
	SE 30	*OV 3*	*OV 7*	*OV 11*	*OV 17*	*OV 25*
2-Methyl-3-buten-2-ol		−0.3	−1.8	−0.9	−0.6	−2.2
Butanol	−1.8	−1.4	0.0		−1.0	−1.2
2-Buten-1-ol	−1.7	−1.0	−0.5		−0.1	0.3
2-Pentanol	−0.8	−0.8	−1.0	−0.8	−0.9	
3-Pentanol	−0.9	−0.6	0.0		−0.7	−1.3
2-Methyl-2-pentanol	−0.2	−0.6	−0.8		−1.1	−0.4
3-Methyl-1-butanol	−1.5	−1.2	−0.3	−2.6	0.0	−0.8
Pentanol	−1.3	0.2	−0.6		0.0	−0.2
1-Hexen-3-ol	−1.1	−0.6	−0.6	1.1	−0.6	−0.1
3-Hexanol	−1.0	−0.4	0.2		−1.3	−1.2
2,2-Dimethyl-3-pentanol	0.9	1.0	0.8		1.0	1.2
2-Methyl-2-hexanol	−1.0	−0.7	1.4	−1.7	1.6	−0.8
4-Methyl-1-pentanol	−1.6	−1.0	−0.9	−0.9	−0.8	−0.1
Hexanol	−1.3	0.0	0.2	0.1	0.2	
2-Methyl-3-hexanol	−0.9	0.8	0.3		−0.3	−0.4
1-Hepten-3-ol	−0.8	0.2	0.2	0.2	0.0	
4-Heptanol	−0.3	−0.5	−0.2	−0.4	0.0	0.0
3-Heptanol	−0.3	−0.1	0.9		−0.8	0.3
2,2-Dimethyl-3-hexanol	0.3	0.5	0.8	1.2	1.2	
Heptanol	−0.9	0.0	0.0	0.0	−0.1	1.0
1-Octen-3-ol	−1.0	0.1	0.4	−0.1	−0.4	0.8
2-Ethyl-1-hexanol	0.6	0.4	0.4	0.4		1.3
	−0.8[a]	−0.3[a]	0.0[a]	−0.3[a]	−0.4[a]	−0.2[a]

[a] Mean value.

TABLE VI

TEMPERATURE DEPENDENCE OF THE RETENTION INDEX OF BENZOYL DERIVATIVES

(Values of $\partial I/\partial T$ ($\partial T = 10°C$), range 100–140°C.)

Benzoyl derivative of	*Stationary phase*					
	SE 30	*OV 3*	*OV 7*	*OV 11*	*OV 17*	*OV 25*
Methanol	2.8		3.4	3.6	3.0	4.0
2-Methyl-1-propanol	2.3	2.9	3.2	4.8	4.2	5.2
2-Methyl-2-butanol	4.1	3.4	3.6		4.7	5.8
Butanol	3.5		2.5	3.7	4.6	5.3
1-Penten-3-ol	4.0		3.1	2.8	3.4	5.2
2-Pentanol	2.8	3.0	3.1	3.1	3.5	4.5
2-Methyl-2-pentanol	5.5	3.4	3.1	4.3	3.8	
2-Methyl-1-butanol	3.5	2.6	3.6	3.8		5.3
2,2-Dimethyl-3-pentanol	5.4		3.8	4.2	4.0	5.0
Propanol	4.3	3.6	4.1	1.8	3.0	6.0
3-Hexanol	3.4	2.8		3.0	3.1	4.6
3-Pentanol	3.6	3.1	3.6	2.6	3.2	
Pentanol	4.0		3.2	3.3	4.4	5.9
	3.8[a]	3.1[a]	3.4[a]	3.4[a]	3.7[a]	5.2[a]

[a] Mean value.

0.05% (w/w) of THEED together with each phase in chloroform before coating the support. Variations of argon flow rate did not affect the value of the indices significantly, nor did change in the chart speed of the recorder. Non-linearity in the chromatographic process caused by overloading was avoided by taking amounts of each compound of *ca.* 0.1 μg. Overlapped peaks were always ignored.

RESULTS AND DISCUSSION

In Tables III and IV retention indices at 100°C, 120°C and 140°C (T_1, T_2, T_3) in the six selected columns are summarized. The accuracy of the indices in standard deviation (s) was in most cases within ± 1 unit[6], and was approximately the same value in each phase and temperature. The values of I were rounded to the nearest whole number but the first decimal figure was retained for $\partial I/\partial T$. The reproducibility of indices was tested after six and twelve months. Deviations found in columns with the same or different coatings were similar, being approximately within ± 1 index units in both cases[6].

In Tables V and VI, values of temperature dependence on the retention index of some alcohols and benzoates in the six selected columns are presented. Values of $\partial I/\partial T$ for every 10°C ($\partial T = 10°C$), in the range 100–140°C are given. For all the phases tested, alcohol indices generally diminish slightly as temperature rises. It is not easy to correlate values of $\partial I/\partial T$ for each compound and phase with the number and type of substituents. Hively and Hinton[9] report that the temperature dependence of the index of some hydrocarbons in squalane, rises with the increase in the width of the transverse section of the molecule. The values in Table V, for the

alcohols 2,2-dimethyl-3-pentanol, 2,2-dimethyl-3-hexanol and 2-ethyl-1-hexanol, compared with those for 3-pentanol, 3-hexanol and hexanol, respectively, seem to agree with this statement. As far as variations of $\partial I/10°C$ with polarity of the phase used are concerned, mean values presented in Table V are not significantly different. For benzoyl derivatives, $\partial I/\partial T$ is markedly positive for all the phases, being notably higher for the most polar column OV-25. The number and type of substituents have no noticeable influence. For the range 100–140°C, $\partial I/\partial T$ is linear in many cases.

Correlations between retention parameters for alcohol benzoates and alcohols and their molecular structure will be the subject of a subsequent paper.

We wish to express our gratitude to Sra. Dolores M. Peleteiro and Dr. R. S. Barratt for reading the manuscript, to J. Adrada for his help with the preparation of the computer programme used, and to the Instituto de Estudios Nucleares, J.E.N. (Spain), for financial support to J. B. Pías with a doctoral fellowship.

SUMMARY

Retention indices of 54 alcohols and 55 alcohol benzoyl derivatives measured on short stainless steel columns (1 m × 2 mm i.d.) filled with Chromosorb G (AW-DMCS (HP)) coated with 5% (w/w) SE-30, OV-3, OV-7, OV-11, OV-17 or OV-25 stationary phases at 100°C, 120°C and 140°C, appear to be very accurate, provided that there is careful control of the chromatographic process. Values of the temperature dependence of retention index of alcohols and benzoates, and variations of these values with the polarity of the phase used, are given.

REFERENCES

1 E. Kováts, *Helv. Chim. Acta*, 41 (1958) 1915.
2 I. R. MacManus, A. O. Contg and R. E. Olson, *J. Biol. Chem.*, 241 (1966) 349.
3 W. G. Galetto, R. E. Kepner and A. D. Webb, *Anal. Chem.*, 38 (1966) 34.
4 L. Gascó and R. Barrera, *Anal. Chim. Acta*, 61 (1972) 253.
5 M. L. Peterson and J. Hirsch, *J. Lipid Res.*, 1 (1959) 132.
6 J. B. Pías, Doctoral Thesis, University of Madrid, December 1972.
7 A. Wehrli and E. Kováts, *Helv. Chim. Acta*, 42 (1959) 2709.
8 *Product Catalogue*, Supelco Inc., Bellefonte, Pa., 1970.
9 R. A. Hively and R. E. Hinton, *J. Gas Chromatogr.*, 6 (1968) 203.

Analytica Chimica Acta, 75 (1975) 149–157

POTENTIOMETRIC DETERMINATION OF BORON IN SILICON WITH AN ION-SELECTIVE ELECTRODE

PIETRO LANZA
Chemical Institute "G. Ciamician", University of Bologna, Bologna (Italy)
PIER LUIGI BULDINI
C.N.R., LAMEL Laboratory, Bologna (Italy)
(Received 23rd July 1974)

The rapid growth in the field of ion-selective electrodes in recent years has been remarkable, and a wide choice of electrodes is now commercially available. Such electrodes offer many possibilities for practical, inexpensive and sensitive analytical methods, particularly for trace analysis. It seemed interesting to examine their application to the determination of microgram quantities of boron in silicon for semiconductor devices.

The method is based on the dissolution of silicon samples by treatment with a hydrofluoric acid and ammonium fluoride mixture in the presence of hydrogen peroxide, and conversion of boron to fluoroborate ion[1], the activity of which can be measured with a fluoroborate-selective electrode.

Although the fluoroborate-selective electrode has been successfully used for determining boron in waters[2], soils and plant tissues[3], and aluminium oxide–boron carbide[4], references to the use of this electrode are few in comparison with, for example, the vast literature on fluoride- or calcium-selective electrodes.

Preliminary studies

The dissolution of the silicon was performed according to the reaction:

$$Si + 4\,HF + 2\,F^- + 2\,H_2O_2 \rightarrow SiF_6^{2-} + 4\,H_2O \qquad (1)$$

in presence of copper(II) ions as catalyst. The dissolution procedure was carefully studied in previous work[1]. Silicon dissolves readily in a 4 *M* hydrofluoric acid–2 *M* ammonium fluoride solution ("fluoride solution"), the rather vigorous reaction being controlled by adding hydrogen peroxide dropwise.

Experiments showed that dissolution of silicon does not need an excess of reagent. However, when boron is present in the sample, even in very small quantities in comparison with the silicon, some excess of this "fluoride solution" is necessary for the kinetics of the fluoroborate formation which occurs during the sample dissolution. The volume of "fluoride solution" to be used for dissolving the samples is shown in Fig. 1; the excess used corresponds to 0.24 *M* of the total fluoride content ($HF + F^-$) in the solution to be measured.

In practice, then, the solution obtained from 100 mg of sample and submitted to potentiometric measuring will have the following composition: $[SiF_6^{2-}] \simeq 0.36$ *M*, $[F^-] \simeq 0.08$ *M*, $[HF] \simeq 0.16$ *M*, and $[NH_4^+] \simeq 0.80$ *M*.

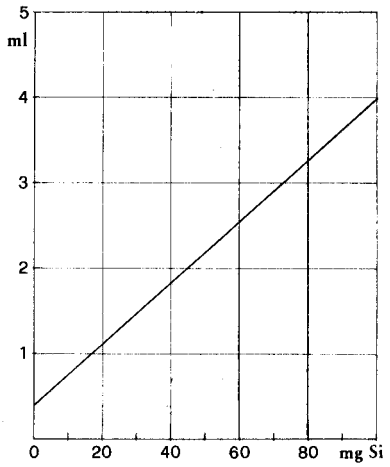

Fig. 1. Volume of "fluoride solution" to be used for dissolving the silicon samples.

It was therefore necessary to examine the effects of ions other than fluoroborate on the electrode response. The potentially interfering species are the fluoride and the fluorosilicate ions.

The hydrolytic reactions of the tetrafluoroborate ion are also a serious limitation for the application of the electrode, and they only can be minimized in solutions containing suitable quantities of hydrofluoric acid[5].

Electrode response

The effects of various anions were determined by measuring the electrode potentials as a function of the fluoroborate concentration in solutions containing a constant concentration of the interfering ions. Figures 2 and 3 show the results of the measurements. All the solutions, except those corresponding to curve (a), contained 0.1 *M* hydrofluoric acid for limiting and equalizing the extent of fluoroborate hydrolysis. For comparison, the theoretical slope (t) and the curve for sodium fluoroborate in twice-distilled water (a) are quoted in both Figures. It can be seen that the electrode follows nearly theoretical behaviour in pure aqueous fluoroborate solutions in the 10^{-5}–10^{-2} *M* concentration range. With fluoroborate solutions in 0.1 *M* hydrofluoric acid, the theoretical slope is obtained in the same concentration range except for a slight fall at the lowest concentrations, but the curve is shifted towards more negative potentials. The presence of sodium fluoride at various concentrations (10^{-3}–10^{-1} *M*) in 0.1 *M* hydrofluoric acid solutions of fluoroborate does not affect the electrode response down to 10^{-4} *M* fluoroborate concentrations (curve c).

At this point, it was difficult to decide whether the fluoride ions really cause a direct interference in the electrode response, or if their effect is due to some influence on the hydrolytic equilibrium of the fluoroborate ion. It must be realized that fluoroborate solutions in pure water are distinctly acidic, and the addition of soluble fluorides produces some hydrofluoric acid. Failure to consider this feature can probably explain the inconsistencies of the available selectivity constants: for the same Orion Model 92-05 fluoroborate electrode, the manufac-

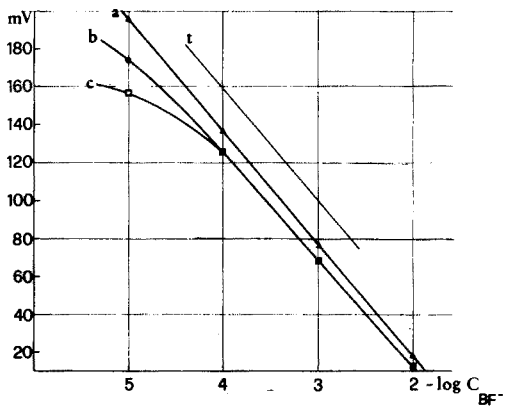

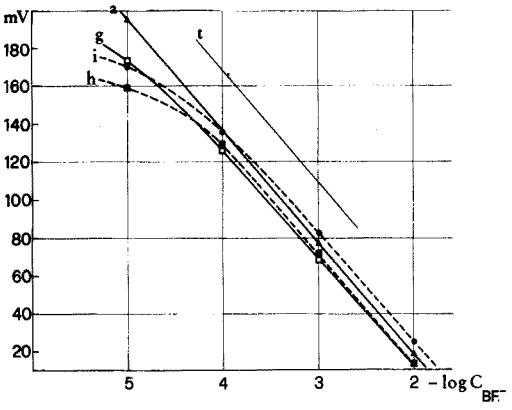

Fig. 2. Effect of interfering anions. t, Theoretical slope; △, $NaBF_4$ in water (a); ● $NaBF_4$ in 0.1 *M* HF (b); □ $NaBF_4$ in 0.001–0.1 *M* NaF + 0.1 *M* HF (c).

Fig. 3. Effect of interfering anions. t, Theoretical slope; △, $NaBF_4$ in water (a); □ $NaBF_4$ in 0.1 *M* HF (g); ■ $NaBF_4$ in 0.001–0.1 *M* H_2SiF_6 + 0.1 *M* HF (h); ● $NaBF_4$ in the solution resulting from dissolution of a silicon sample (i).

turer's instrument manual quotes $K_{BF_4,F} = 10^{-3}$, while Carlson and Paul[2] found the value to be $9 \cdot 10^{-5}$.

Figure 3 shows the response of the electrode to fluoroborate concentration in solutions containing 0.1 *M* hydrofluoric acid (g), or 10^{-3}–10^{-1} *M* hydrofluorosilicic acid (h), and in a solution of silicon in "fluoride solution" (i), *i.e.* in practical analytical conditions.

Fluorosilicate does not seem to produce any considerable interference; the shift of curve (i) beyond curve (a) is probably due to the effect of changing ionic strength. Unfortunately, the calculation of activity coefficients in such solutions is not reliable, because these coefficients vary considerably as a function of the ionic composition. If correction could be made for the effect of the ionic strength on the activity, curves (i), (h) and (g) would probably fit each other. This would happen, for instance, if an activity coefficient of *ca.* 0.8 were attributed to the fluoroborate ion in the silicon solution (ionic strength about 1.25 *M*).

However, some of the difficulties encountered in obtaining reproducible results must essentially be due to the hydrolytic reaction:

$$BF_4^- + H_2O \rightleftharpoons BF_3OH^- + HF \qquad (2)$$

Wamser[6] has calculated the constant:

$$K = [BF_3OH^-][HF]/[BF_4^-] = 2.3 \cdot 10^{-3}$$

from kinetic measurements of the opposing reactions:

$$BF_3OH^- + HF \rightarrow BF_4^- + H_2O (k_1 = 0.392 \text{ l mole}^{-1} \text{ min}^{-1}) \qquad (3)$$

$$BF_4^- + H_2O \rightarrow BF_3OH^- + HF (k_2 = 9 \cdot 10^{-4} \text{ min}^{-1}) \qquad (4)$$

This constant is in good agreement with the value derived from measurements of the degree of hydrolysis of aqueous fluoroboric acid solutions in the 0.005–0.1 *M*

range. At higher concentrations, the value of the constant increases rapidly, probably because of the increasing difference between activity and concentration.

Wamser[6] subsequently investigated the effect of the hydrogen ion concentration on the rate of reaction (3). The constant was found to be:

$$k_1 = k_0 + k_H[H^+] = 0.064 + 7.35[H^+] \quad (5)$$

from measurements over 0.01–0.08 M range of hydrogen ion concentration. This implies, of course, that the equilibrium constant K is also a function of pH, and the quoted value, $2.3 \cdot 10^{-3}$, must be considered only for dilute fluoroboric acid solutions ($[H^+] \simeq 3 \cdot 10^{-2}$).

Moreover, the hydrogen ion concentration may strongly influence the hydrofluoric acid dissociation and, therefore, the hydrolysis constant. Table I shows the conditional hydrolysis constant:

$$K' = \frac{[BF_3OH^-]c_{HF}}{[BF_4^-]} = \frac{k_2}{k_0 + k_H[H^+]} \cdot \frac{[H^+] + K_{HF}}{[H^+]} \quad (6)$$

as a function of pH.

The expected degree of hydrolysis of sodium fluoroborate in water can be calculated. If only the first hydrolysis step (eqn. 4) is considered, one can obtain the following expression for the hydrolysis constant:

$$K = \frac{k_2}{k_0 + k_H[H^+]} = \frac{[BF_3OH^-][HF]}{[BF_4^-]} = \frac{[BF_3OH^-]\dfrac{[H^+]c_{HF}}{[H^+] + K_{HF}}}{[BF_4^-]} \quad (7)$$

where $c_{HF} = ([HF] + [F^-])$ is the total HF concentration obtained by the effect of hydrolysis, and $K_{HF} = 1.66 \cdot 10^{-4}$ is the dissociation constant for hydrofluoric acid. If c is the initial fluoroborate concentration, and x the degree of hydrolysis, eqn. (7) becomes:

$$\frac{x^2 \dfrac{[H^+]}{[H^+] + K_{HF}} c}{1 - x} = \frac{k_2}{k_0 + k_H[H^+]} \quad (8)$$

When the total hydrogen ion concentration is due to the dissociation of the hydrofluoric acid formed, one can substitute in eqn. (8), the expression:

$$[H^+] = \sqrt{K_{HF}(cx - [H^+])} \quad (9)$$

TABLE I

THE CONDITIONAL HYDROLYSIS CONSTANT AS A FUNCTION OF pH

pH	K'	pH	K'
0	$1.21 \cdot 10^{-4}$	4	$3.54 \cdot 10^{-2}$
1	$1.12 \cdot 10^{-3}$	5	$2.46 \cdot 10^{-1}$
2	$6.52 \cdot 10^{-3}$	6	2.34
3	$1.46 \cdot 10^{-2}$	7	23.24

By introducing some approximations, it is possible to calculate with a reasonable precision the degree of hydrolysis of the fluoroborate in aqueous solution as a function of the concentration. The results of such calculations are shown in Fig. 4. It can be seen that the fluoroborate ion in pure water would be nearly completely hydrolyzed even in 10^{-2} *M* solution.

It is common experience, however, that standard solutions of sodium fluoroborate in distilled water are rather stable, and allow linear calibration curves with a theoretical slope to be obtained even in the low concentration range. Evidently, the hydrolysis reaction in pure water is very slow. In solutions containing hydrofluoric acid, hydrolysis is hindered (Fig. 5), but equilibrium is probably reached in a much shorter time.

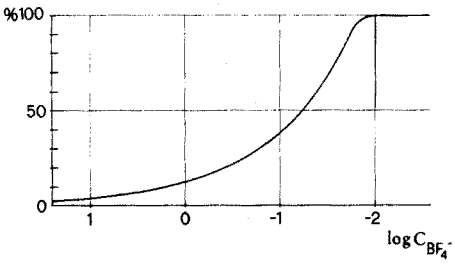

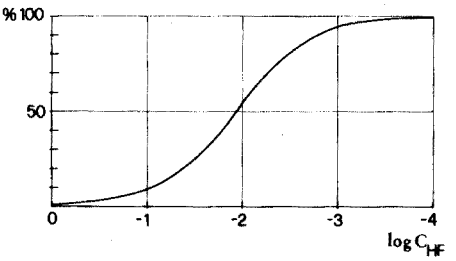

Fig. 4. Hydrolysis of fluoroborate in water (approximate calculation).

Fig. 5. Hydrolysis of fluoroborate in HF (calculated for $c_{BF_4^-} \ll c_{HF}$).

By considering the above characteristics of the chemical system and the behaviour of the electrode, an analytical procedure has been developed for allowing a complete conversion of the boron to fluoroborate ion, and for obtaining a final solution of the sample that is suitable for a good electrode response.

EXPERIMENTAL

Apparatus

An Orion Model 92–05 fluoroborate ion-selective electrode and an Orion single-junction Ag/AgCl electrode Model 90–01 were used. The reference electrode was filled with 0.1 *M* KCl solution saturated with silver chloride.

Potentials were measured (within 0.5 mV) on a Knick Model pH 35 mV/pH meter. Every potential measurement was made under moderate magnetic stirring, to obtain electrode equilibrium within a few minutes, even in dilute solutions. Response time and equilibrium potentials were defined by recording the electrode signal with an Amel Model 867 potentiometric recorder.

A polystyrene cell was used for measuring small volumes of solution under magnetic stirring, as shown in Fig. 6.

All solutions containing hydrofluoric acid were prepared and stored in polyethylene bottles. Polypropylene pipets and volumetric flasks were used throughout.

Small volumes were precisely measured with an SB-2 syringe microburet (Micrometric Instrument Co., Cleveland) having a capacity of 1 ml (division 0.001 ml).

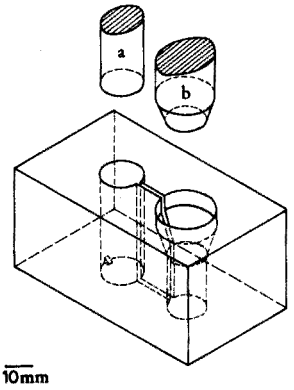

Fig. 6. Polystyrene cell for potentiometric measurements. (a) Reference electrode, Orion Model 90-01; (b) fluoroborate ion-selective electrode Orion Model 92-05.

Reagents

Standard boron solution (10 μg B ml^{-1}). Dissolve 0.571 g of reagent-grade boric acid in 1 l of water and dilute this solution ten times with water.

Fluoride solution (4 *M* HF–2 *M* NH_4F). Backer BAR ACS 48% hydrofluoric acid and C. Erba RSE 32% ammonia (for electronic use) were used. Mix in a polypropylene volumetric flask 6 moles of hydrofluoric acid with 2 moles of ammonia and dilute to 1 l with water.

Hydrogen peroxide, 110-volume was RPE grade (for electronic use; C. Erba).

Procedure

Place three accurately weighed portions of the sample of suitable size (10–100 mg), containing no less than 4 μg of boron, in three polypropylene test tubes with covers. Place three portions of boron-free silicon of the same size ($\pm$1 mg) as the sample in three other test tubes. Add 3 drops of aqueous 1% (w/v) copper chloride solution to each test tube; shake gently in order to wet the silicon with the copper(II) solution.

TABLE II

RESULTS OF A TYPICAL EXPERIMENT

Test tube no.	*Nature of sample*	*Weight of sample (mg)*	*B added (μg)*	*mV*	*B found (μg)*	*B found (p.p.m.)*
1	B-free Si	103	10	137[a]	—	—
2	B-free Si	101	20	124[a]	—	—
3	B-free Si	100	40	108[a]	—	—
4	Unknown	102	—	129	14.9	146
5	Unknown	101	—	131	14.2	140
6	Unknown	101	—	131	14.2	140

[a] These points fall on a very gently curved line when mV is plotted against μg B.

TABLE III

COMPARISON OF THE POTENTIOMETRIC AND SPECTROPHOTOMETRIC METHOD FOR THE DETERMINATION OF BORON IN SILICON SAMPLES

Sample[a]	*Potentiometric*				*Spectrophotometric*			
	Weight (mg)	*No. of detns.*	*p.p.m. B ± s*	*S_r (%)*	*Weight (mg)*	*No. of detns.*	*p.p.m. B ± s*	*S_r (%)*
M.	10	9	370 ± 21	5.7	10	7	375 ± 27	7.2
M.	10	6	3450 ± 110	3.2	—	—	—	—
W. Ch.	10	3	3400 ± 100	2.9	10	10	3450 ± 164	4.8
M.	10	4	2100 ± 50	2.4	5	3	2000 ± 132	6.6
M.	10	6	2100 ± 84	4.0	5	3	2050 ± 140	6.8
M.	10	5	2070 ± 45	2.2	5	4	2025 ± 29	1.4
M.	10	6	1850 ± 44	2.4	5	3	1875 ± 35	1.9
M.	10	3	970 ± 10	1.0	5	4	1050 ± 42	3.0
M.	10	7	1300 ± 19	1.5	5	2	1350	—
M.	10	9	1100 ± 46	4.2	5	3	1080 ± 104	9.6
M.	10	9	1050 ± 46	4.4	5	5	1250 ± 56	4.5
M.	50	2	850	—	—	—	—	—
M.	50	6	380 ± 9	2.3	10	4	400 ± 8	2.0
W. Ch.	100	3	200 ± 7	3.5	10	3	185 ± 3	1.5
W. Ch.	100	4	160 ± 6	3.8	10	9	162 ± 9	5.4
W. Ch.	100	5	150 ± 9	6.0	10	2	160	—

[a] M., Montedison spa, Milan, Italy; W. Ch., Wacker Chemitronic GmbH, Burghausen, G.F.R.

Add suitable quantities of the standard boron solution with a microsyringe to the test tubes containing the pure silicon; select the boron quantities so as to include, in the concentration range, that expected in the unknown sample.

Add the prescribed volume of "fluoride solution" indicated in Fig. 1, to each test tube. Add 2 drops of hydrogen peroxide (110 volume) to each portion; the reaction starts at once with development of oxygen. Keep the test tubes covered and add dropwise 10–15 drops of hydrogen peroxide for samples weighing up to 40–50 mg, and 20–30 drops for samples weighing up to 100 mg of silicon. After the hydrogen peroxide addition, heat the covered test tubes at 60–70°C in a thermostatted bath for 2 h; this allows a complete dissolution of the sample and a careful washing of the walls and covers of the tubes by reflux of the condensed water.

After this period, add 1 drop of methyl orange indicator and the quantity of ammonia necessary to obtain the colour change (pH 3–4) to each test tube, and dilute to 10 ml with water.

Introduce a little of the solution into the cell and read the potential obtained under magnetic stirring; check the attainment of the equilibrium potential by recording.

Prepare a calibration graph from the points obtained with the standard solution and read the boron content of the unknown samples in the usual way.

Table II gives the results of a typical experiment.

RESULTS AND DISCUSSION

Table III shows the results of analysis of different samples, by the proposed potentiometric method and by the spectrophotometric methylene blue method[1]. The precision of the potentiometric method is the same as that of the spectrophotometric one; the former method is somewhat less sensitive, but its simplicity and rapidity can offer many advantages, particularly as a reliable and practical routine method.

Even though the electrode response has good reproducibility, for practical applications it is advisable to adopt the technique of comparing standards during each analysis, instead of using a single calibration curve. However, the standards used can serve for several samples of similar characteristics.

The authors wish to thank Prof. Dario Nobili for his helpful discussions and suggestions, the staff of the C.N.R. LAMEL Laboratory for supplying and checking standards and samples, and Prof. Giovanni Semerano, Director of the "G. Ciamician" Chemical Institute, for his encouraging remarks and friendly criticism.

SUMMARY

A potentiometric method is proposed for the determination of boron in silicon, based on dissolution of silicon by treatment with hydrofluoric acid and ammonium fluoride in the presence of hydrogen peroxide, and conversion of boron to fluoroborate ion. The fluoroborate activity is measured with the Orion

fluoroborate-selective electrode. Some important points, such as the effect of various interfering ions and the hydrolysis of fluoroborate ion, are described in detail. The method is applied to the determination of boron in silicon containing at least 10 p.p.m. of boron, with a relative standard deviation of $\pm 4\%$.

REFERENCES

1 P. Lanza and P. L. Buldini, *Anal. Chim. Acta*, 70 (1974) 341.
2 R. M. Carlson and J. L. Paul, *Anal. Chem.*, 40 (1968) 1292.
3 R. M. Carlson and J. L. Paul, *Soil Sci.*, 108 (1969) 266.
4 H. E. Wilde, *Anal. Chem.*, 45 (1973) 1526.
5 C. A. Wamser, *J. Amer. Chem. Soc.*, 70 (1948) 1209.
6 C. A. Wamser, *J. Amer. Chem. Soc.*, 73 (1951) 409.

Analytica Chimica Acta, 75 (1975) 159–167

THE USE OF MEMBRANE ELECTRODES IN THE DETERMINATION OF SULPHIDES IN SEA WATER

E. MOR, V. SCOTTO, G. MARCENARO and G. ALABISO

Laboratorio per la Corrosione Marina dei Metalli, C.N.R., 16123 Genova (Italy)

(Received 6th August 1974)

Membrane ion-selective electrodes, particularly the solid-state version, are becoming of increasing importance in industrial and field analysis[1–3]. Their use as alarm and control devices is particularly advantageous when low ionic concentrations are involved, since the precision of potentiometric measurements is practically constant on all the range of concentrations for which the electrode is sensitive.

The use of membrane electrodes for quantitative analytical purposes is, however, often limited by the presence of interferences, which can depend on both the nature and the ionic strength of the medium. In the case of sulphide ions, the complex formation and dissociation conditions are also of importance[1,4]. Accordingly, whilst the use of ion-sensitive electrodes as indicator electrodes for potentiometric titrations of sulphide[5–10] is widespread, their utilization in direct potentiometric analysis has been much less frequent[5,11].

In this paper, the possibility of direct potentiometric use of the sulphide-selective membrane electrode in the determination of sulphides in natural sea water is examined. Such an analytical method would, for its virtues of speed and simplicity, vie with many more sophisticated techniques.

The sulphide electrode, in common with every other membrane electrode, responds to the activity of sulphide ions according to the law of Nernst:

$$E = E_0 - 2.303 \frac{RT}{2F} \log a_{S^{2-}} \tag{1}$$

Its direct use for quantitative analytical purposes is, therefore, often limited by lack of information on the activity coefficient of the sulphide ions and on the sulphide dissociation constants in the experimental environment. It should be emphasized, in addition, that in sea water and also in similarly complex electrolytic systems, a knowledge of thermodynamic constants is often of little practical use, since not all the terms converted to activities can be equally accessible to experimental measurements.

In this paper, conformity with the conventions of oceanographers[12] has been preferred for expressing the degree of dissociation of sulphides in sea water. Thus the "apparent mixed dissociation constants" are used; these contain both terms converted to activities, and terms converted to concentrations:

$$K'_1 = \frac{c_{HS^-} \cdot a_{H^+}}{c_{H_2S}} \qquad K'_2 = \frac{c_{S^{2-}} \cdot a_{H^+}}{c_{H_2S}} \tag{2}$$

The system of equations:

$$K'_1 = \frac{c_{HS^-} a_{H^+}}{c_{H_2S}}$$

$$K'_2 = \frac{c_{S^{2-}} a_{H^+}}{c_{HS^-}} \qquad (3)$$

$$c_T = c_{H_2S} + c_{HS^-} + c_{S^{2-}}$$

shows that it is possible to settle the problem of the determination of sulphides by means of electrode potential and solution pH measurements, by means of the equation:

$$c_T = \frac{a_{S^{2-}}}{\gamma_{S^{2-}}}\left[1 + \frac{a_{H^+}}{K'_2}\left(1 + \frac{a_{H^+}}{K'_1}\right)\right] \qquad (4)$$

on condition that K'_1, K'_2 and $\gamma_{S^{2-}}$ can be established in the experimental environment. The electrode calibration in terms of activities may, therefore, acquire, on the basis of eqn. (4), an actual analytical utility.

In this paper, the problems have been overcome by using two distinct criteria: (a) experimental identification, in sea water, of the two mixed dissociation constants of H_2S and the activity coefficient of sulphide by means of sulphide electrodes; and (b) establishment of a correction for the electrode potential in terms of pH which permits the establishment of a linear correlation between the corrected potential values and the pc_T content.

EXPERIMENTAL

Equipment

An electrochemical cell (150-cm^3 capacity) consisting of an ion-sensitive electrode (Amel, model 201/S), a pH glass electrode (Beckman 39511) and a saturated calomel electrode, was used.

The potential measurements were effected by means of a compensation electrometer (Amel model 667/RM) at room temperature.

The pH values were obtained by means of a Beckman model H5 pH meter. During all measurements magnetic stirring (teflon bar) was employed.

Solutions

Stock solutions of sulphide were prepared by dissolving reagent-grade sodium sulphide ninehydrate (Merck) in sea water, or distilled water. Sodium sulphide was obtained by selecting large crystals of the salt and removing the surface layer of oxidation products by washing with distilled water. Precautions against oxidation of the solutions by the atmosphere were unnecessary at neutral pH values, but the alkaline solutions were prepared in oxygen-free water, and transferred in a nitrogen atmosphere. Oxidation of hydrogen sulphide by air occurs much more rapidly in alkaline solutions[13]. To avoid contact with atmospheric oxygen and carbon dioxide, purified nitrogen gas was bubbled through the sea water before the dissolution of sodium sulphide. The exact molarity of the stock solution was established by potentiometric titration of 50-cm^3 aliquots with standard silver nitrate solution.

A series of standard solutions (10^{-2}–10^{-4} M) of sodium sulphide was prepared by suitable dilution of the stock solution (10^{-1} M).

In natural sea water, pH variations were obtained by the addition of 0.7 M sodium hydroxide or hydrochloric acid; the sodium sulphide was added to each solution after the requisite pH had been obtained. The molarities of the pH-adjusting solutions were chosen so as to maintain the ionic strength unaltered in sea water.

Similar variations of pH were brought about in solutions of ionic strength 0.1 M. In this case, buffer solutions were prepared by mixing 0.1 M phosphoric acid and 0.1 M sodium hydroxide in different proportions[14]. For solutions of pH higher than 12, sodium hydroxide solutions of different strengths were used and their pH was calculated in the usual way.

It is known that in the direct potentiometric determination of sulphide activity, the response time of electrodes can be important. In an attempt to use very short response times, the potential measurements were realized from dilute to concentrated solutions and from low to high pH.

All concentration and activity data are reported in logarithmic scales.

RESULTS

Utilization of sensor in the establishment of K_1', K_2' and $\gamma_{S^{2-}}$ in natural sea water

As has been seen already, the potential response of the sulphide electrode may be written on the basis of eqn. (4) in the more general form:

$$E_{S^{2-}} = E_0 + 30\ \mathrm{p}\gamma_{S^{2-}} + 30\ \mathrm{p}c_T + 30\ \mathrm{p}K_1' + 30\ \mathrm{p}K_2' - 30 \log [K_1' K_2' + a_{H^+}(K_1' + a_{H^+})] \quad (5)$$

which, according to the regions of pH that one might examine, may be simplified to:

$$E_{S^{2-}} = E_0 + 30\ \mathrm{p}\gamma_{S^{2-}} + 30\ \mathrm{p}K_1' + 30\ \mathrm{p}K_2' - 30\ \mathrm{pH} + 30 \log [K_1' + a_{H^+}] + 30\ \mathrm{p}c_T \quad (6)$$

which is valid for acid, neutral and slightly alkaline pH values, or to:

$$E_{S^{2-}} = E_0 + 30\ \mathrm{p}\gamma_{S^{2-}} + 30\ \mathrm{p}c_T - 30 \log \left(1 + \frac{a_{H^+}}{K_2'}\right) \quad (7)$$

which is valid for alkaline pH values.

Equation (6) may be further simplified for $\mathrm{pH} \ll \mathrm{p}K_1'$ to the linear form:

$$E_{S^{2-}} = E_0 + 30\ \mathrm{p}\gamma_{S^{2-}} + 30\ \mathrm{p}c_T + 30\ \mathrm{p}K_1' + 30\ \mathrm{p}K_2' - 60\ \mathrm{pH} \quad (6')$$

and for $\mathrm{p}K_1' < \mathrm{pH} < \mathrm{p}K_2'$, to the form:

$$E_{S^{2-}} = E_0 + 30\ \mathrm{p}\gamma_{S^{2-}} + 30\ \mathrm{p}c_T + 30\ \mathrm{p}K_2' - 30\ \mathrm{pH} \quad (6'')$$

These considerations, applied to the case in which $\mathrm{p}c_T$ is maintained constant, allow the two separate dissociation constants to be evaluated on the basis of the experimental dependence $E_{S^{2-}}$ *vs.* pH. The value of $\mathrm{p}K_1'$ may be identified with pH at the intersection of the two linear sections (6′) and (6″) having slopes of -30 and -60 mV/decade, while the value of $\mathrm{p}K_2'$ may be identified, in effect, with the corresponding pH at the intersection of the linear section (6″) with the asymptotic value to which $E_{S^{2-}}$ tends for strongly alkaline pH values. It is

apparent that the major imprecision in the measurement of pH in the alkaline region will be reflected in the greater imprecision of the value of pK'_2 compared to pK'_1.

The experimental dependence $E_{S^{2-}}$ *vs.* pH recorded at constant pc_T in natural sea water (see Fig. 1) leads to a value of 6.35 ± 0.05 for pK'_1 and a value of 13.6 ± 0.1 for pK'_2. At this stage, the problem of the determination of sulphides in sea water may be considered resolved from a practical standpoint. In fact, with solutions containing large quantities of inert electrolytes, but with practically constant composition—as in the case of sea water—it is possible to assume the activity coefficient as unity, insofar as the concentration of ion under examination remains inferior (at least 10 times) to the solution concentration[12].

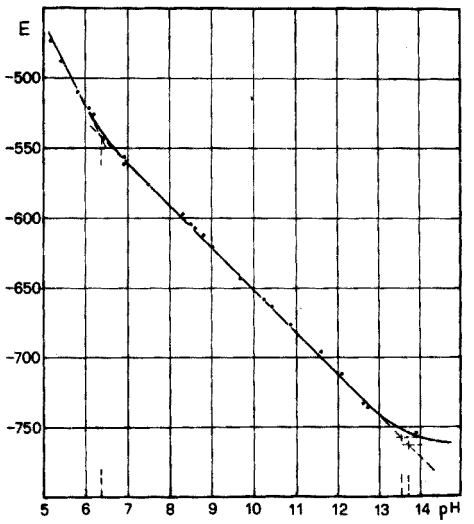

Fig. 1. Experimental $E_{S^{2-}}$ *vs.* pH in sea water at constant $pc_T = 3.11$.

However, the sulphide electrodes may also be used for the establishment of the activity coefficient of the sulphide ions on the infinite dilution scale—a parameter which occurs in most thermodynamic calculations.

A comparison of the activity recorded from the potential of the electrode and the concentration of sulphide actually present in the solution allows a sufficiently accurate evaluation of the activity coefficient in the medium. The calibration line in terms of activity, being independent of the nature and strength of the medium in which it is obtained, may be experimentally reconstructed by working in a simple chemical environment in which, for the calculation of the thermodynamic activity coefficient, the Debye–Hückel equation may be used:

$$-\log \gamma = Az^2\sqrt{\mu} \tag{8}$$

It is evident that in this case the dissociation constants K'_1 and K'_2 must be estimated with the same graphical method already illustrated for sea water.

The calibration of the electrode in terms of activity was effected in a deaerated buffer solution of 0.1 *M* phosphoric acid adjusted to different pH values with

solutions of 0.1 *M* sodium hydroxide. The dissociation constants, $pK'_1 = 6.9$ and $pK'_2 = 13.05$ of the above environment, were graphically extracted from the experimental $E_{S^{2-}}$ *vs.* pH curve obtained at constant $pc_T = 2.11$ as illustrated in Fig. 2, the activity coefficient being assumed in this case as 0.38.

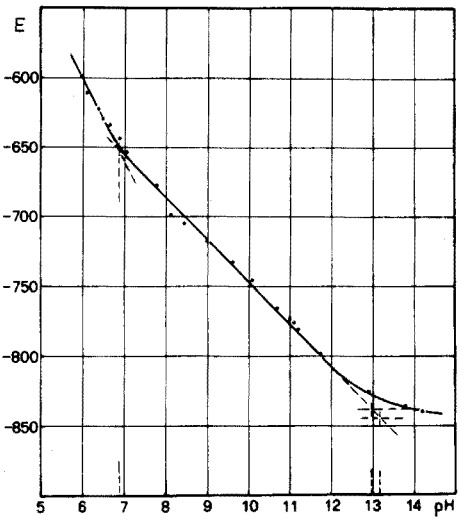

Fig. 2. Experimental $E_{S^{2-}}$ *vs.* pH in deaerated 0.1 *M* buffer solutions at constant $pc_T = 2.11$.

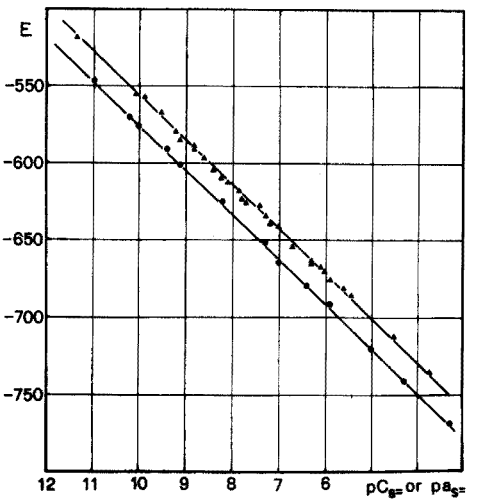

Fig. 3. Calibration lines. (●) In terms of activity obtained in deaerated 0.1 *M* buffer solutions. (▲) In terms of ionic concentration obtained in sea water.

Comparison of the calibration line in terms of activity with the dependence $E_{S^{2-}}$ *vs* $pc_{S^{2-}}$ effected in natural sea water immediately after the calibration, shows an activity coefficient for the sulphide ion in sea water of about 0.2 (Fig. 3); this is in good agreement with the values from the literature for other bivalent ions (0.28 for calcium(II); 0.12 for sulphate; 0.36 for magnesium(II) and 0.20 for carbonate)[12].

Method of reduction of electrode potential at constant pH

Since K'_1, K'_2 and the sulphide activity coefficient are constant, once the experimental environment has been fixed, the response of the sulphide electrode may be further simplified, in the region of pH in which the approximation (6) is valid, to the form:

$$E_{S^{2-}} = E'_0 + 30\,pc_T - 30\,pH + 30\log(a_{H^+} + K'_1) \qquad (9)$$

It is apparent that, if the degree of hydrolysis for sulphide is kept constant, the electrode response to sulphides become linearly dependent on pc_T.

The constancy of the degree of hydrolysis may be achieved experimentally by reducing the solutions to the same pH (*e.g.*, pH 7), and mathematically by simulating the reduction of electrode potential to pH 7 by means of a correction:

$$E_7 = E_{S^{2-}} + 60(pH - 7) - 30\log(1 + 10^{pH - pK'_1}) + 30\log(1 + 10^{7 - pK'_1}) \qquad (10)$$

in which pK'_1 is identical with the first dissociation constant of hydrogen sulphide in the experimental environment. It is suggested that the method of reduction of electrode potential to conditions of constant pH can provide a simple means for the analytical use of sulphide electrodes. Apart from any preceding consideration about the value of K'_1 in sea water, the same relation (9) may be used for the experimental evaluation of pK'_1.

For this purpose, the error introduced into the elaboration of the electrode data by assuming a value for pK'_1 that may differ from the actual value of the first dissociation constant ($pK'_{1\circ}$), was calculated. To this end, the dependence $E_{S^{2-}}$ *vs.* pH was reconstructed point by point, the two values of $pc_T = 2$ and $pK'_{1\circ} = 7$ being arbitrarily pre-selected (Fig. 4). A reduction in the value of $E_{S^{2-}}$ to pH 7 was then obtained, on the basis of eqn. (10), the actual dissociation constant of the medium ($pK'_1 = pK'_{1\circ}$) being used.

It was observed that, in this case, all the potentials of the $E_{S^{2-}}$ *vs.* pH dependence tended to align themselves on the equipotential line $\alpha = 0$; this confirms, in fact, that a precise reduction to constant pH must produce a single value of E_7 for each single value of pc_T. If the reduction to pH 7 is done with pK'_1 values that are in error (by a factor α), then the reduced potentials are not aligned (see curves 3 and 4 of Fig. 4); the shifts are more marked with increases in acidity.

The value of $pK'_{1\circ}$ may thus be experimentally established on the basis of electrode potentials measured at the same pc_T but in very different pH conditions, and is identical with that value of pK'_1 which, when introduced in eqn. (10), causes a minimum scattering between the values of E_7. The experimental data shown in Table I were in fact, reduced to pH 7 with the help of a computer, giving pK'_1 values falling between 5 and 8, with gradual increases of 0.1; the more significant results are plotted against pc_T in Fig. 5. From the graphs, it is apparent that

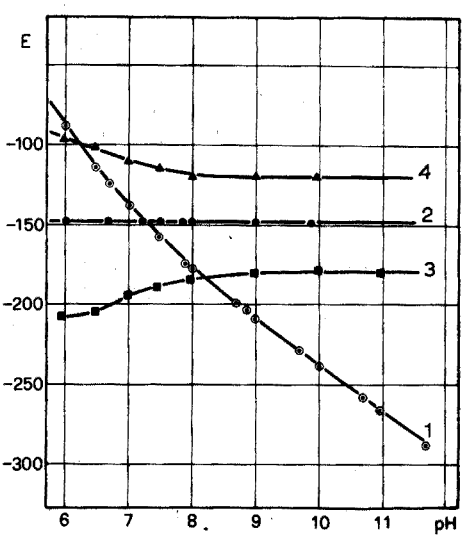

Fig. 4. Curve 1: $E = E_{S^{2-}} - E_0$ *vs.* pH calculated point by point, for $pc_T = 2$ and $pK'_2 = pK'_1 = 7$ (⊙). Curves 2–4: reduction to pH 7 of the potential values, for $pK'_1 = pK'_{1\circ} + \alpha$; (●) $\alpha = 0$, (■) $\alpha = +1$, (▲) $\alpha = -1$.

TABLE I

EXPERIMENTAL DATA FOR $E_{S^{2-}}$ AGAINST pc_T AT DIFFERENT pH VALUES

pc_T	pH	$E_{S^{2-}}$	pc_T	pH	$E_{S^{2-}}$
3.8	4.5	−423	3.18	3.6	−384
3.8	6.4	−519	3.18	3.65	−386
3.8	7.9	−565	3.18	6.0	−509
3.8	8.8	−597	3.18	7.6	−580
3.8	9.55	−619	3.18	8.0	−589
2.47	3.7	−416	3.18	9.35	−628
2.47	6.1	−547	3.18	9.5	−635
2.47	7.0	−586	2.18	3.15	−389
2.47	9.40	−655	2.18	5.9	−545
			2.18	7.4	−612
			2.18	9.85	−676

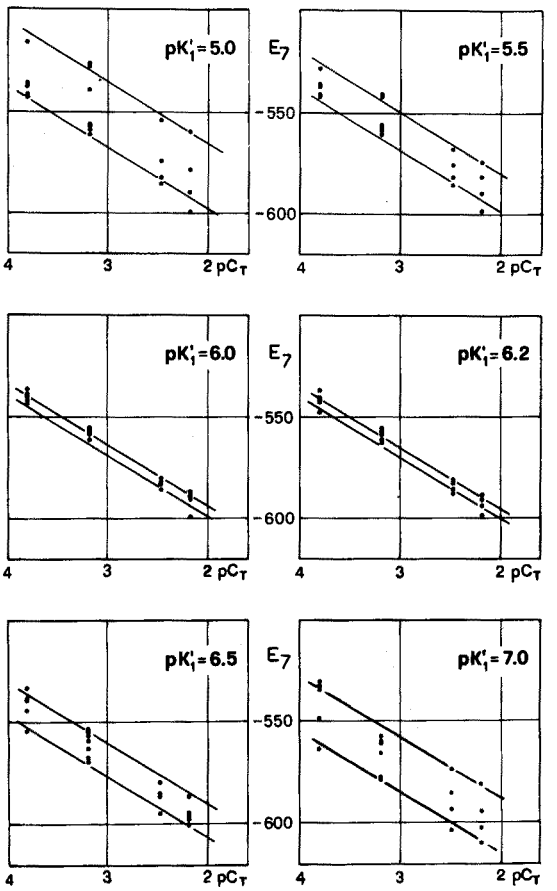

Fig. 5. Influence of the value assumed for pK'_1 on the scattering of the data E_7 *vs.* pc_T.

the value of the first dissociation constant in natural sea water must surely fall between 6.0 and 6.2, values for which the scattering of E_7 is minimal.

The excellent agreement between the values of pK'_1 obtained from the two different criteria is remarkable. The graphs in Fig. 5 once again confirm the Nernstian slope of 30 mV/decade.

DISCUSSION

The direct potentiometric determination of sulphides by means of ion sensors in a complex chemical medium such as sea water, is of undoubted practical interest. In fact, any analysis that may be effected by means of electrochemical measurements and which supplies analytical information directly in moles l^{-1}, has such advantages of simplicity and speed as to become competitive with other, more precise, analytical methods.

The criterion followed in the utilization of the sulphide electrodes for analytical purposes was, initially, that of experimentally establishing the mixed dissociation constants K'_1 and K'_2 in sea water, by means of a graphical interpolation of the curve $E_{S^{2-}}$ *vs.* pH obtained at constant pc_T. If the ionic medium scale is used for activity, the establishment of the two dissociation constants is sufficient to resolve from a practical standpoint the problem of direct potentiometric determination of sulphides in sea water. However, the sulphide electrodes can also be used in the experimental evaluation in sea water of the activity coefficient of sulphide ions on the thermodynamic infinite dilution scale. The value of the activity coefficient thus determined ($\gamma = 0.20$) was in good agreement with the activity coefficient values quoted in the literature for other bivalent ions in sea water.

In an alternative approach to the problem, an equation was established for the correction of the electrode potentials in terms of pH; this criterion can be utilized for a simpler electrode calibration directly in total sulphide concentrations, as well as for pK'_1 evaluation in the test medium.

It can be concluded that sulphide electrodes offer unquestionable advantages in speed and simplicity of operations. Satisfactory results can be achieved, on condition that the electrodes are used with several precautions: (a) before each series of the measurements, the potential of the electrode must be checked in a standard sulphide solution (with time, the electrode constant drifts, while the Nernstian slope remains practically constant); (b) the electrode should be used, if possible, in solutions of increasing concentration (the response time can thus be kept very low, and the possibility of sulphide loss during the measurement is reduced); (c) the pH-meter must be accurately calibrated before each series of measurements.

The authors warmly thank Mr. Leopoldo Avalle of the "Società Italiana Impianti" for the computer calculations, and Mr. Romano Delle Piane for the construction of an air-tight chamber for the handling of sulphide samples in an atmosphere of inert gas.

SUMMARY

The direct potentiometric determination of sulphides in natural sea water with

a sulphide-selective membrane electrode is proposed. The experimental evaluation of the "apparent mixed" dissociation constants and the thermodynamic activity coefficient in spiked sea water samples, by means of the electrode, permits direct calibration in terms of activity. Alternatively, it is possible to establish, for natural sea water, an experimental equation for the correction of the electrode potentials in terms of pH; this allows direct calibration of the electrodes in terms of total sulphide concentration. This criterion can be applied to any aqueous solution.

REFERENCES

1 E. Pungor and K. Toth, *Analyst (London)*, 95 (1970) 1132.
2 G. J. Moody and J. D. R. Thoma, *Talanta*, 19 (1972) 623.
3 G. A. Rechnitz, *Accounts Chem. Res.*, 3 (1970) 69.
4 K. Srinivasam and G. A. Rechnitz, *Anal. Chem.*, 41 (1969) 1203.
5 Tong-Ming Hseu and G. A. Rechnitz, *Anal. Chem.*, 40 (1968) 1054.
6 M. W. Tamele, V. C. Irvine and L. B. Ryland, *Anal. Chem.*, 32 (1960) 1002.
7 M. Mascini, *Anal. Chim. Acta*, 56 (1971) 316.
8 M. K. Papay, K. Toth and E. Pungor, *Anal. Chim. Acta*, 56 (1971) 285.
9 J. Papp and E. Havas, *Proceedings of the International Measurements Confederation Symposium on Electrochemical Sensors, Vejprem, Hungary*, (1968) 135.
10 T. Anfalt and D. Jagner, *Anal. Chim. Acta*, 56 (1971) 473.
11 K. Srinivasam and G. A. Rechnitz, *Anal. Chem.*, 40 (1968) 509.
12 J. P. Riley and G. Skirrow, *Chemical Oceanography*, Vol. 1, Academic Press, London, 1965.
13 A. J. Ellis and R. M. Golding, *J. Chem. Soc., London*, (1959) 127.
14 S. S. Muhammad and E. V. Sundaram, *J. Sci. Ind. Res.*, 20B (1961) 16.

Analytica Chimica Acta, 75 (1975) 169–180

AMPEROMETRIC DETERMINATION OF ALCOHOLS, ALDEHYDES AND CARBOXYLIC ACIDS WITH AN IMMOBILIZED ALCOHOL OXIDASE ENZYME ELECTRODE

M. NANJO and G. G. GUILBAULT

Department of Chemistry, University of New Orleans, New Orleans, La. 70122 (U.S.A.)

(Received 29th July 1974)

Chemical tests for measurement of blood alcohols are the subject of much interest, particularly in legal cases, and there is a need for quick, simple and reliable assay methods. Likewise, the determinations of carboxylic acids and aldehydes are of importance in various industrial fields, but such assays are difficult to carry out, especially at low concentrations.

In the past, alcohols have been determined by gas chromatography[1–3], spectrophotometry[4,5] and redox titration[6,7]. Selective spectrophotometric enzymatic methods utilizing alcohol dehydrogenase have been reported[8–10], but it is not possible to couple these with an electroanalytical device such as an ion-selective electrode; these methods also require a coenzyme, NAD, and deproteinization of the serum sample before u.v. measurement.

Guilbault and Lubrano[11] used a new enzyme for assay of alcohol, alcohol oxidase, by amperometrically detecting the hydrogen peroxide formed during the enzymatic reaction. Because the activity of the available enzyme was low, it was not possible to immobilize the enzyme and to build an enzyme electrode in a method similar to that described for assay of glucose[12,13]. Hence, measurements were conducted only in bulk solution with soluble enzyme.

In this study, an alcohol enzyme electrode which was useful for the assay of blood ethanol in concentrations as low as 10 mg % is described. Additionally, this chemically bound alcohol oxidase electrode was found to be useful for the assay of aldehydes and carboxylic acids based on a measurement of the consumption of dissolved oxygen in the enzymatic reaction, similar to that used in the uricase–uric acid system[14].

EXPERIMENTAL

Apparatus

A Heath polarograph (Model EUA-19-2) combined with a Heath operational amplifier system (Model EUW-19A) was used. A constant potential, −0.6 V *vs.* SCE, was applied to the electrode.

Reagents

All chemicals were reagent grade. The alcohol oxidase (0.02 units/mg solid, activity measured by hydrogen peroxide formation rate) was from the

mycelium of a Basidiomycete and was a gift of Wyeth Laboratories, Inc. This enzyme is identical with that used by Guilbault and Lubrano[11]. Alcohol oxidase was immobilized according to a modification of the method reported by Brown *et al.*[15] as follows.

Alcohol oxidase (100 mg) and plasma albumin (100 mg, Sigma Chemical Co., from *Bovine Serum*) were dissolved in 5.0 ml of phosphate buffer, 0.1 *M*, pH 8.2. Then 5 drops of glutaraldehyde (Sigma Chemical Co., 50% aqueous solution) was added, and the mixture was stirred well. The solution was frozen by dry ice–acetone coolant and the frozen mixture was warmed slowly in a refrigerator for a day. The sponge-like copolymer was washed with the buffer solution and stored in a refrigerator until use. This method has been shown to be effective and convenient for glucose oxidase[16], *L*-amino acid oxidase[16] and uricase[14].

Alcohol oxidase electrode

Platinum disc electrodes (Beckman Model 39273) were used as the solid base electrode to sense the dissolved oxygen change, the same as used for the uricase electrode[14]. The procedure for the construction of the enzyme electrode was as follows.

The immobilized alcohol oxidase was mounted on the surface of the platinum electrode (diameter 1.0 cm) and secured with a nylon cloth and O-rings; the electrode was then stored in the buffer solution (0.1 *M* phosphate buffer, pH 8.2) at room temperature.

Measurement of alcohols, aldehydes and carboxylic acids

The enzyme electrode together with a calomel reference electrode (SCE) were placed into a stirred buffer solution (10.0 ml) at an applied potential of −0.6 V *vs.* SCE. When the current was at a constant level—a constant limiting current from reduction of dissolved oxygen—the sample solution (0.01–0.10 ml) was pipetted into the buffer solution and the initial rate of change in the dissolved oxygen limiting current, and the final steady-state current, were recorded with a Heath Recorder (Model EU-205-11). The total measuring time was only 2 min. The amount of substrates present was calculated from a calibration curve of initial rate or steady-state current *vs.* substrate concentration.

In the case of the assay of blood ethanol, 10.0 ml of 0.1 *M* phosphate buffer (pH 8.2) was placed in a thermostated water jacket (30°C), and 0.025 ml of serum was added directly to the stirring buffer solution. After each measurement, the electrode was rinsed with distilled water and dipped into the buffer to recover the dissolved oxygen level around the enzyme and to wash out any remaining reaction products (2–3 min). The dissolved oxygen content in the buffer solution was found to be constant during a series of assays owing to the slow equilibrium of oxygen between buffer solution and air for these experimental conditions.

RESULTS AND DISCUSSION

Alcohol oxidase is reported to catalyze the oxidation of lower primary aliphatic alcohols according to the reaction[18–20]:

$$RCH_2OH + O_2 \xrightarrow{\text{Alcohol oxidase}} RCHO + H_2O_2 \quad (1)$$

This reaction has been coupled with amperometric monitoring of the hydrogen peroxide formed, with a soluble enzyme[11,17]. However, the activity of the enzyme was found to be too low to be useful for a practical assay as an immobilized enzyme electrode[11].

Clark[17] also reported the instability of his soluble alcohol oxidase electrode which lost half its activity after standing overnight at pH 8.5 (instability believed to be due to the loss of FAD from the electrode).

However, it has proved possible to make a very stable and sensitive alcohol oxidase enzyme electrode with chemically bound enzyme, and to monitor the decrease in the dissolved oxygen level with a platinum electrode which functions as an oxygen electrode at -0.6 V *vs.* SCE (instead of peroxide formation measured at $+0.6$ V *vs.* SCE).

Bulk reaction of alcohol oxidase with ethanol

At first, the enzymatic reaction was studied amperometrically by monitoring hydrogen peroxide in solution with a platinum electrode at $+0.6$ V *vs.* SCE. At this potential, the following oxidation of hydrogen peroxide takes place (pH 8–12).

$$H_2O_2 \rightarrow O_2 + 2H^+ + 2e^- \quad (2)$$

With careful pretreatment of the platinum electrode, Guilbault and Lubrano have reported that the accurate quantitative measurement was possible at concentrations as low as 10 μM hydrogen peroxide[13].

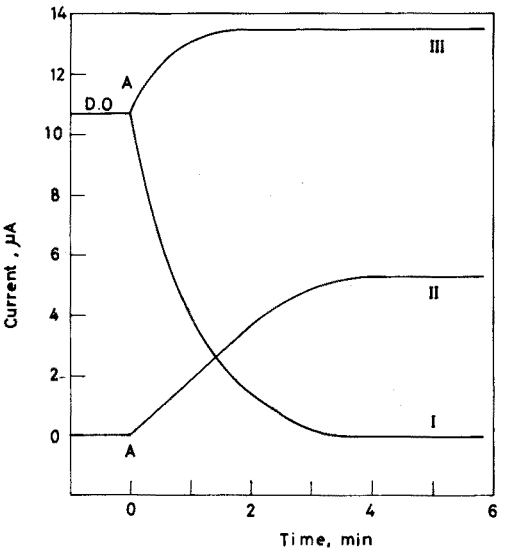

Fig. 1. Bulk enzymatic reaction detected by platinum electrode. Ethanol (38 mg %) added to the enzyme solution (alcohol oxidase 10 mg in 1.0 ml, 1.0 *M* phosphate buffer, pH 8.2, 30°C) at A. (I) 3 Day-old enzyme solution, cathodic current change at -0.6 V *vs.* SCE; (II) fresh enzyme solution, anodic current change at $+0.6$ V *vs.* SCE; (III) fresh enzyme solution, cathodic current change at -0.6 V *vs.* SCE.

In Fig. 1, the anodic current increase is shown, indicating the formation of hydrogen peroxide at +0.6 V *vs.* SCE using freshly prepared enzyme solution (curve II). But the activity of the enzyme solution, as measured at this voltage, appears to become very weak soon after the preparation of this solution, as reported by Clark[17], even on storage in pH solutions higher than 6.5 (ref. 20). However, dissolved oxygen is reduced to water, consuming 4 electrons per molecule of oxygen at −0.6 V *vs.* SCE:

$$O_2 + 2\,H_2O + 4\,e^- \rightarrow 4\,OH^- \tag{3}$$

As shown in Fig. 1 (curve I), the consumption of dissolved oxygen was detected as a cathodic current decrease at −0.6 V *vs.* SCE using 3 day-old enzyme solution. The initial rate of decreasing oxygen current, expressed as $\mu A\ min^{-1}$, was faster than that of hydrogen peroxide formation at +0.6 V *vs.* SCE.

Hydrogen peroxide is also electroactive at negative potentials:

$$H_2O_2 + 2\,e^- \rightarrow 2\,OH^- \tag{4}$$

Curve III in Fig. 1 shows the cathodic current change from the formation of hydrogen peroxide at −0.6 V *vs.* SCE. This cathodic current increase was observed only when freshly prepared enzyme solution was added to the ethanol buffer solution, indicating an accumulation of hydrogen peroxide on the platinum electrode surface. Therefore, the cathodic current, i_c, at −0.6 V *vs.* SCE can be expressed as follows:

$$i_c = i_{H_2O_2} + i_{D.O.} \tag{5}$$

where $i_{H_2O_2}$ is the current from hydrogen peroxide according to eqn. (4) and $i_{D.O.}$ is the current from dissolved oxygen according to eqn. (3). The magnitudes of $i_{H_2O_2}$ and $i_{D.O.}$ are considered to depend on the enzymatic reaction and degree of diffusion of the substances involved in the reaction to the electrode, and reflect the apparent enzymatic reaction rate.

From Fig. 1, it becomes apparent that if fresh enzyme solutions are used, hydrogen peroxide can be detected at both potentials, even at −0.6 V *vs.* SCE. The formation of hydrogen peroxide compensates for the decrease of current from the decrease of dissolved oxygen, since hydrogen peroxide accumulates around the electrode, and a net increase in current results.

However, an aged enzyme solution (greater than 3 days old) cannot produce sufficient hydrogen peroxide to overcome the consumption of dissolved oxygen and a decrease of the cathodic current results, except at very high substrate concentrations (above 0.05 *M*).

Enzyme electrode response

In Fig. 2, the responses of an enzyme electrode are shown. When ethanol is added to the buffer solution, it diffuses into the layer of chemically bound alcohol oxidase where it is oxidized at the expense of dissolved oxygen and is converted to hydrogen peroxide and acetaldehyde.

Curve I, in Fig. 2, shows the response of a 7 day-old electrode at +0.6 V *vs.* SCE. The formation of hydrogen peroxide is thus proven also in the case of

immobilized alcohol oxidase. However, an enzyme electrode 12 days old showed no response to the same ethanol solution at +0.6 V *vs.* SCE. Yet, the response at −0.6 V *vs.* SCE became more sensitive, indicating that the enzyme consumed dissolved oxygen faster than hydrogen peroxide accumulated at the enzyme electrode. The initial rate of dissolved oxygen decrease, *i.e.* the apparent initial rate of the enzymatic reaction, was found to be proportional to ethanol added, using an electrode that had aged over 2 weeks.

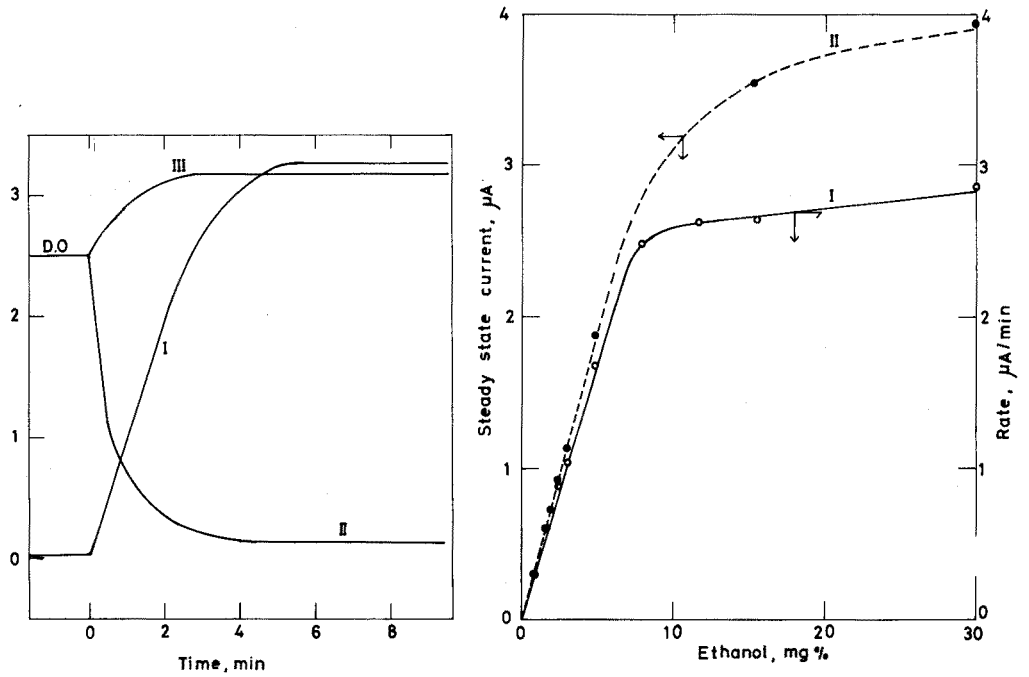

Fig. 2. Response of an enzyme electrode (glutaraldehyde bound alcohol oxidase) to ethanol (added at A). $T=30°C$, ethanol 38 mg % in 0.1 *M* phosphate buffer, pH 8.2. (I) 7 Day-old electrode, at +0.6 V *vs.* SCE; (II) 12 day-old electrode, at −0.6 V *vs.* SCE; (III) 3 day-old electrode, at −0.6 V *vs.* SCE.

Fig. 3. Relationship between electrode response and ethanol concentration measured with a 14 day-old enzyme electrode at −0.6 V *vs.* SCE. 0.1 *M* Phosphate buffer, pH 8.2, 30°C. (I) Rate method; (II) steady-state method.

A typical relation curve based on the initial rate of reaction as a measure of ethanol is shown in Fig. 3. The steady-state current, which shows the amount of consumed dissolved oxygen for the enzymatic reaction, was also proportional to the ethanol concentration. The sensitivity at −0.6 V *vs.* SCE was found to increase with increasing time and number of measurements, reached a maximum after 2 weeks, and then kept a constant value for more than 4 months. For good analytical results, an electrode should be prepared and used only after 2 weeks.

Consumption of H_2O_2 during enzymatic reaction

Figure 4 shows the consumption of hydrogen peroxide during the enzymatic reaction at ± 0.6 V *vs.* SCE. The currents, proportional to hydrogen peroxide concentration (points A and C), were found to decrease when ethanol was added to the hydrogen peroxide solution as monitored with an enzyme electrode. This consumption of hydrogen peroxide could not be observed with only the base platinum electrode, which shows that there is no bulk chemical reaction between ethanol and hydrogen peroxide under these experimental conditions. Rather, this peroxide consumption is catalyzed by the alcohol oxidase present in the enzyme electrode.

Also, the hydrogen peroxide current at both $+0.6$ V and -0.6 V *vs.* SCE decreased when acetaldehyde was added to the solution as monitored by the enzyme electrode. The addition of semicarbazide, which reacts with aldehydes forming semicarbazones, decreased the rate of oxygen uptake. These results can only be explained by some subsequent reaction following reaction (1), and the observed change of the property of enzyme electrode during the experiment is considered to be due mainly to an activation of this subsequent reaction which consumes hydrogen peroxide.

Response to acetaldehyde and acetic acid

The enzyme electrode was found to respond not only to alcohols, but also to aldehydes and carboxylic acids, showing a response such as that in

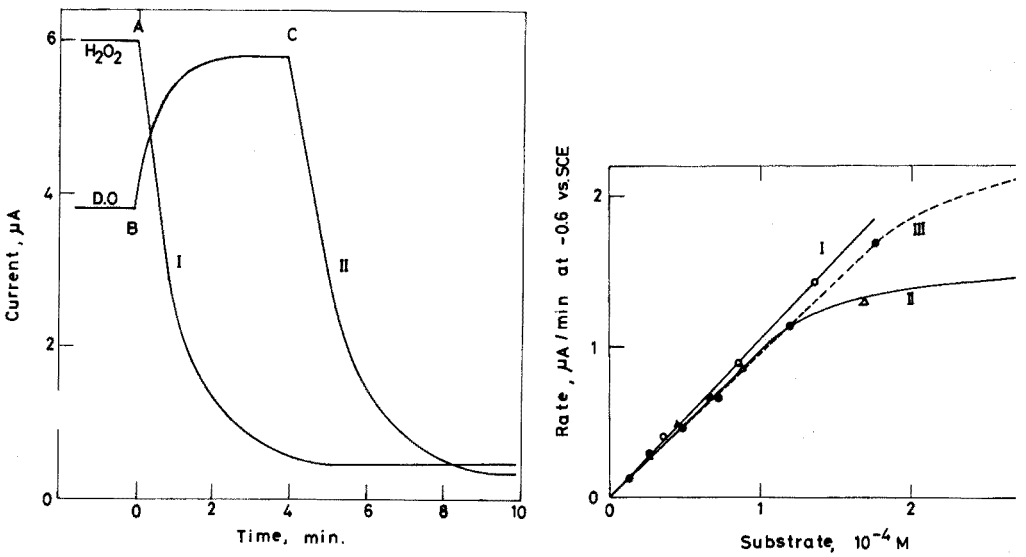

Fig. 4. Consumption of hydrogen peroxide during the enzymatic reaction measured by an aged enzyme electrode (14 days old). 0.1 *M* Phosphate buffer, pH 8.2, 30°C. (A) Addition of 3.8 mg % ethanol to I (0.45 m*M* H_2O_2) at $+0.6$ V *vs.* SCE; (B) addition of 0.45 m*M* H_2O_2 to II (phosphate buffer solution) at -0.6 V *vs.* SCE; (C) addition of 3.8 mg % of ethanol to (II + H_2O_2).

Fig. 5. Comparison of the electrode response to ethanol, acetaldehyde and acetic acid. Chemically bound alcohol oxidase electrode, 0.1 *M* phosphate buffer, pH 8.2, 30°C. (I) Ethanol; (II) acetaldehyde; (III) sodium acetate.

Fig. 2, curve II. The sensitivity of the electrode for formaldehyde, acetaldehyde, acetic acid and formic acid was as good as that of ethanol, and thus should be useful for the assay of low levels of aldehydes and carboxylic acids.

In Fig. 5, the relation of the initial rate to the concentrations of ethanol, acetaldehyde and acetic acid, is shown.

Effect of pH

The effect of pH on the initial rate of change in current, at −0.6 V *vs.* SCE, of 3.8 mg % ethanol solution measured with an alcohol oxidase electrode, was studied. As indicated in Fig. 6, the optimal pH for the enzymatic reaction was found to be approximately 8.0, which is almost identical with the value of 7.8 for hydrogen peroxide formations reported by Guilbault and Lubrano[11].

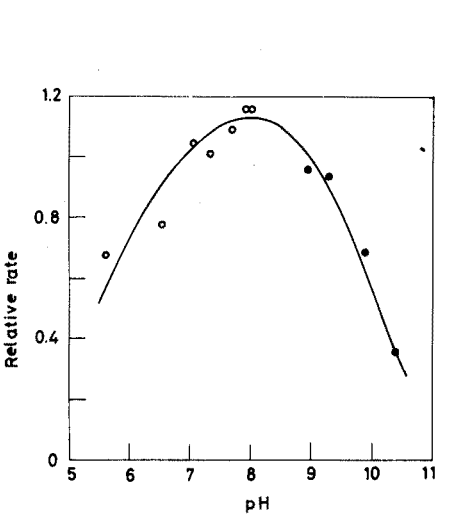

Fig. 6. Effect of pH on the electrode response: (○) phosphate buffer, 0.1 *M*; (●) glycine buffer, 0.1 *M*.

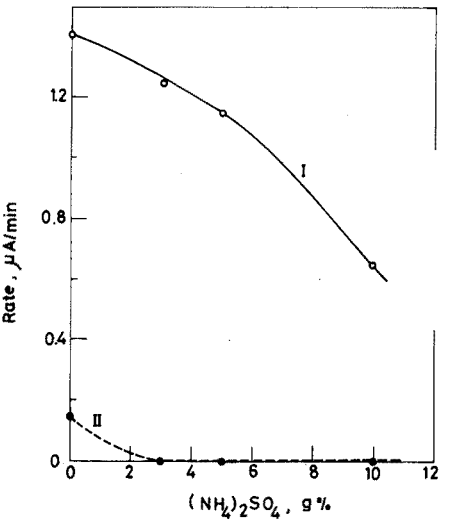

Fig. 7. Effect of ammonium sulfate concentration on the response of an aged (one month old) alcohol oxidase electrode: (I) dissolved oxygen measurement at −0.6 V *vs.* SCE, 38 mg % ethanol; (II) hydrogen peroxide measurement at +0.6 V *vs.* SCE 38 mg % ethanol.

Effect of ammonium sulfate

Figure 7 shows the effect of ionic strength (ammonium sulfate) on the response of an enzyme electrode at both +0.6 V and −0.6 V *vs.* SCE. Both rates decreased with increasing concentrations of ammonium sulfate. However, the rate of peroxide formation measured at +0.6 V *vs.* SCE was quenched faster than the rate of dissolved oxygen consumption at −0.6 V *vs.* SCE. Thus, high concentrations of salt solutions are one of the interferences in an assay, and for good results, the ionic strength should be kept as low as possible and constant.

Selectivity

Alcohol oxidases are specific for lower primary aliphatic alcohols[17–19]. In contrast to the sensitive ethanol response of the electrode, methanol gives a very

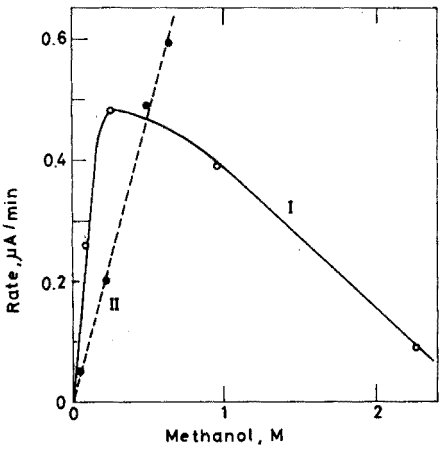

Fig. 8. Electrode response to methanol measured by an aged electrode (one month old) in 0.1 *M* phosphate buffer, pH 8.2, 30°C: (I) dissolved oxygen at −0.6 V *vs.* SCE; (II) hydrogen peroxide at +0.6 V *vs.* SCE.

poor response at −0.6 V *vs.* SCE. In Fig. 8, the relationship of the rates at both potentials is shown for methanol; an aged enzyme electrode was used. As can be seen from Fig. 8, methanol gives a response at both potentials in the same concentration range (higher than 0.1 *M*), but the response is much lower than that for ethanol shown in Fig. 5.

The rate at −0.6 V *vs.* SCE shows a maximum around 0.5 *M* of methanol, then decreases. This indicates that the formation of hydrogen peroxide becomes predominant at this concentration rather than a consumption of hydrogen peroxide.

In Table I, the substrate selectivity of the alcohol oxidase electrode is shown at both potentials. The apparent selectivity at −0.6 V *vs.* SCE with the chemically bound alcohol oxidase is very different from the reported values for soluble alcohol oxidase[11,18,19]. The source of the alcohol oxidase was the same as that of

TABLE I

SUBSTRATE SELECTIVITY OF ALCOHOL OXIDASE

Alcohols	*Relative reactivity*		
	Janssen[18,19]	*Enzyme electrode*[a]	
		Dissolved oxygen at −0.6 V	*Hydrogen peroxide at +0.6 V*
Methanol	100	3	0.98
Ethanol	28	12000	0.46
Allyl alcohol	17	190	1.14
n-Propanol	5.3	1300	0.36
n-Butanol	2.1	2500	0.21

[a] Relative reactivity measured by the enzyme electrode was obtained from the slopes of the calibration curves and expressed as initial rate per mole of alcohols (μA min^{-1} mole^{-1}).

Janssen *et al.*[18,19], although the method of assay for enzyme activity is quite different. Janssen *et al.* measured the activity spectrophotometrically by reacting the peroxide formed with *o*-dianisidine; this prevents the subsequent reactions which remove hydrogen peroxide from the system. The present procedure involves total consumption of dissolved oxygen at −0.6 V *vs.* SCE. Thus, the apparent selectivity may result from the rate-determining reaction in the enzymatic oxidation.

In Table II, a comparison of the reactivity of several alcohols, together with their aldehydes and carboxylic acids is shown. In the case of ethanol and butanol, the rate-determining step was found to be in the last reaction, *i.e.*, the oxidation of the carboxylic acid produced from the oxidation of the alcohol. However, in the case of the methanol system, methanol itself gives a very slow rate, whereas formaldehyde and formic acid consume dissolved oxygen much faster than methanol. Also, the rate of formaldehyde oxidation is faster than that of acetaldehyde. On the other hand, the relative selectivity obtained at +0.6 V *vs.* SCE has the same trend as that observed by Janssen[18,19].

TABLE II

COMPARISON OF THE REACTIVITY OF ALCOHOLS WITH THEIR CORRESPONDING ALDEHYDE AND CARBOXYLIC ACID

Substrates	*Relative reactivity*[a]
CH_3OH	1.00
HCOH	17600
HCOONa	5640
C_2H_5OH	1.00
CH_3COH	0.89
CH_3COONa	0.88
n-$C_4H_{10}OH$	1.00
n-C_3H_8COONa	0.94

[a] Relative rate of change in current at −0.6 V *vs.* SCE, phosphate buffer, 0.1 *M*, pH 8.2.

These selectivity data demonstrate the possibility of assay of ethanol in the presence of excess of methanol at −0.6 V *vs.* SCE. Also, Table II shows that it is possible to assay aldehydes or carboxylic acids if they are present alone in solutions, or in mixtures after a separation of each component.

Assay of blood alcohol

An assay of blood ethanol was attempted to demonstrate a typical application of the alcohol oxidase electrode. Since blood contains several hundreds of compounds, it is necessary to consider the possible interference of some of them. Such interferences were considered in two categories: the direct reaction of other substrates with enzyme; and the consumption of dissolved oxygen by non-enzymatic reactions, such as by ascorbic acid or cysteine.

In the first category, some acids and hydroxy acids were found to be oxidized by alcohol oxidase (see Table III), and thus interfered with the assay of ethanol in blood (*i.e.*, lactic acid which is present in blood at concentrations of 8–17 mg %). However, the response of lactic acid to the electrode is 37%

TABLE III

RELATIVE REACTIVITY OF SOME ACID SUBSTRATES AT THE ALCOHOL OXIDASE ENZYME ELECTRODE

Acids	*Relative reactivity*[a]
(Ethanol)	1.00
Acetic acid	0.88
Formic acid	0.51
Lactic acid	0.37
Butyric acid	0.21
Pyruvic acid	0.03
Monochloroacetic acid	0.001

[a] Relative rate of change in current at −0.6 V *vs.* SCE, phosphate buffer, 0.1 *M*, pH 8.2, 30°C. No response to acetone and trichloroacetic acid.

of ethanol response. Thus, in the assay of high levels of ethanol, the effect of lactic acid becomes less serious. Furthermore, the interference of lactic acid in serum may be eliminated by the addition of lactate dehydrogenase to the sample before assay.

In the second category, various substances were tested under the same conditions of assay, with a platinum electrode (without enzyme). None of the compounds commonly present in blood (*i.e.*, ascorbic acid, cysteine, phenylalanine, glucose, uric acid), were found to react at the electrode, Also the effect of the content of oxygen in the sample solution was tested; the small amount of serum (0.025 ml) was found not to give any change in the dissolved oxygen level of the large excess of buffer solution (10.0 ml).

The calibration curves prepared from aqueous ethanol solutions or ethanol control solutions (Sigma Chemical Co.) did not give good agreement with a spectrophotometric method based on alcohol dehydrogenase (ADH), probably owing to interference from acids in serum. Next, a calibration curve was prepared by adding an aqueous ethanol solution to a reconstituted freeze-dried control prepared from pooled human blood (Moni-Trol I, Dade, Miami). This curve is shown in Fig. 9. The calibration curves did not pass the origin, but gave a good agreement with the spectrophotometric method as shown in Table IV. Moni-Trol II gave the same calibration curve, indicating there were no serious interferences from abnormal serum. The rate and steady-state methods were found to be useful for the assay of blood ethanol especially in the assay of high ethanol levels, which is the most common case of assay in the clinical laboratory.

Thus, the enzyme electrode utilizing dissolved oxygen consumption is concluded to be very sensitive (1 mg % of ethanol), reproducible (standard deviation by rate method 2.9%, by steady-state method 4.9% when 0.05 ml of a 0.08 mg % ethanol control was added to 10.0 ml buffer solution), very rapid (complete analysis takes less than 5 min), and simple (as little as 25 μl of serum sample can be added directly without any pretreatment). Additionally, this enzyme electrode is also useful for the assay of carboxylic acids, such as acetic acid and formic

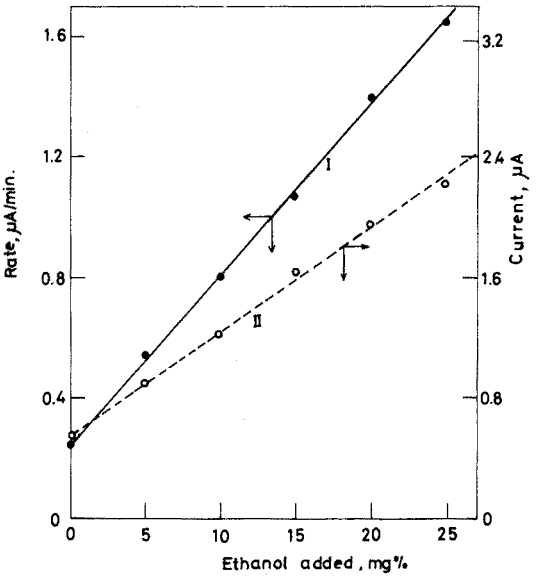

Fig. 9. Calibration curves for blood ethanol assay at −0.6 V *vs.* SCE. Aged (one month old) alcohol oxidase electrode, 0.1 *M* phosphate buffer, pH 8.2, 30°C. (I) Rate method; (II) steady-state method.

TABLE IV

RESULTS OF BLOOD ETHANOL ASSAY[a]

U.v. method with ADH[b]	*Enzyme electrode*[c]	
	Rate method	*Steady-state method*
0.4	0.0	0.4
4.2	2.5	2.7
8.2	6.0	5.8
12.2	11.9	10.9
16.2	17.6	18.5
20.3	21.9	20.4

[a] In mg %.
[b] According to Sigma Technical Bulletin, No. 33-UV.
[c] Average of 3 determinations.

acid, and aldehydes such as acetaldehyde and formaldehyde as can be seen from Tables II and III.

It may be possible to measure lactic acid in serum samples from normal individuals who have not ingested alcohol (below 10 mg %). This enzyme electrode should be applicable not only to the clinical field, but also to various industrial areas, such as the food and brewing industries.

The authors wish to acknowledge the financial assistance of the National Institute Science Foundation, Grant No. GP-31518A, in carrying out this research. We Health under Grant No. 14263

also wish to thank Dr. S. S. Kuan for his technical assistance and Wyeth Laboratories for a gift of alcohol oxidase.

SUMMARY

A new enzyme electrode has been developed for the rapid and simple measurements of blood ethanol. A platinum electrode was coupled with immobilized alcohol oxidase, sensing the dissolved oxygen consumption amperometrically. Blood ethanol can be measured within several minutes without any pretreatments. The only reagent required is phosphate buffer. The enzyme electrode was found to respond not only to alcohols but also to aldehydes and carboxylic acids.

REFERENCES

1 J. T. Kung and J. E. Whitney, *Anal. Chem.*, 33 (1961) 1505.
2 C. Bluestein and H. N. Posmanter, *Anal. Chem.*, 38 (1966) 1856.
3 H. Lymons and J. Bard, *Clin. Chem.*, 10 (1964) 429.
4 V. W. Reid and D. G. Salmon, *Analyst (London)*, 80 (1955) 704.
5 M. Mantel and M. Anbar, *Anal. Chem.*, 36 (1964) 936.
6 B. Jaseiskis and J. P. Warriner, *Anal. Chem.*, 38 (1966) 563.
7 T. Takahashi and C. Hayase, *J. Chem. Soc. Jap., Ind. Chem. Sect.*, 55 (1952) 205.
8 R. K. Bonnichsen and H. Theorll, *Scand. J. Clin. Lab. Invest.*, 3 (1951) 58.
9 R. Bonnichsen and C. T. Lundgren, *Acta Pharmacol. Toxicol.*, 13 (1957) 256.
10 M. Brower and J. E. Woodbrige, *Clin. Chem.*, 16 (1970) 539.
11 G. G. Guilbault and G. J. Lubrano, *Anal. Chim. Acta*, 69 (1974) 189.
12 G. G. Guilbault and G. J. Lubrano, *Anal. Chim. Acta*, 60 (1972) 254.
13 G. G. Guilbault and G. J. Lubrano, *Anal. Chim. Acta*, 64 (1973) 439.
14 M. Nanjo and G. G. Guilbault, *Anal. Chem.*, 46 (1974) 1769.
15 G. Brown, C. T. Thomas, G. Gellbe, D. Domurado, A. M. Beryonneau and G. Guillon, *Biotechnol. Bioeng.*, 105 (1973) 359.
16 M. Nanjo and G. G. Guilbault, *Anal. Chim. Acta*, 73 (1974) 367.
17 L. C. Clark, Jr. in L. Wingard (Ed.), *Enzyme Engineering*, Wiley-Interscience, New York, 1972, p. 377.
18 F. W. Janssen, H. W. Ruelius, *Biochem. Biophys. Acta*, 151 (1968) 330.
19 F. W. Janssen, R. M. Kerwin and H. W. Ruelius, *Biochem. Biophys. Res. Commun.*, 20 (1965) 630.
20 Y. Tani. T. Miya, H. Nishikawa and K. Ogata, *Agr. Biol. Chem.*, 36 (1972) 68.

Analytica Chimica Acta, 75 (1975) 181–187

EINE KATALYTISCH-KINETISCHE STRÖMUNGSMETHODE AUF PAPIER. DIE BESTIMMUNG VON MOLYBDÄN

HERBERT WEISZ und HEINER LUDWIG

Lehrstuhl für Analytische Chemie, Chemisches Laboratorium, Universität Freiburg i.Br. (Bundesrepublik Deutschland)

(Eingegangen den 28 August 1974)

Strömungsmethoden unter Verwendung katalysierter Reaktionen bieten die Möglichkeit, Stoffe in sehr geringen Konzentrationen (ng ml^{-1} bis μg ml^{-1}) kontinuierlich zu bestimmen. Verschiedene derartige kontinuierliche Verfahren wurden veröffentlicht, die sich im wesentlichen auf zwei methodische Prinzipien zurückführen lassen[1,2]. Sie unterscheiden sich letztlich dadurch, dass entweder ein Strömungsrohr verwendet wird[1], das als Reaktionsstrecke dient (System ohne Rückvermischung), oder eine Durchflusszelle[2], die Reaktionsgefäss und Messzelle zugleich darstellt (System mit vollkommener Rückvermischung).

Diese Strömungsmethoden benötigen eine Kombination verschiedener Geräteeinheiten und Teile, im wesentlichen eine Pumpe, eine Mischkammer, ein Reaktionsrohr oder -gefäss, eine Messzelle und ein Messgerät, wobei die Funktionen einiger Einzelteile in einer Einheit zusammengefasst werden können, wie z.B. in der Durchflusszelle[2]. Der Bedarf an Probelösung und der Verbrauch an Reaktantenlösung hängt von der Grösse der verwendeten Strömungsvorrichtung ab. Um diesen Bedarf zu senken, bietet sich eine Verkleinerung der Apparatur an, der jedoch aus apparatetechnischen Gründen eine Grenze gesetzt ist.

Im folgenden wird eine einfache kinetische Strömungsmethode beschrieben, bei der weder eine Pumpe noch eine komplizierte Strömungsvorrichtung notwendig ist. Dabei wird ein kapillarer Träger, Filterpapier, als Reaktionsort und Transportmedium verwendet. Diese Vereinfachung ermöglicht es zugleich, mit wesentlich geringeren Proben- und Reagenzmengen zu arbeiten, was für eine kontinuierliche Methode sicherlich von Vorteil ist.

In die Lösungen der beiden Reaktanten einer katalysierten Reaktion und in die Katalysator–Probelösung selbst sind jeweils schmale Filterpapierstreifen eingetaucht (Abb. 1). Diese Streifen werden an einer Stelle zusammengeführt und setzen sich in einem breiteren Filterpapierstreifen fort, der schliesslich in einem Paket von Rundfiltern endet. Verursacht durch die Kapillarität des Filterpapiers, das gleichsam als "kapillare Pumpe" wirkt, fliessen der Katalysator und die Reaktanten zunächst bis zur Vereinigungsstelle der Streifen und durchmischen sich dort: die katalysierte Reaktion beginnt. Währenddessen strömt die resultierende Lösung ständig auf dem anschliessenden Streifen weiter, bis sie schliesslich in dem Filterpaket aufgesogen wird. In einer definierten Entfernung von der Durchmischungsstelle befindet sich die Messstelle. Je höher die Katalysatorkonzentration ist, d.h., je schneller die Reaktion abläuft, desto geringer ist die Kon-

zentration des gemessenen Reaktanten und umgekehrt. In dem hier beschriebenen Beispiel wird die Konzentration eines Reaktionspartners potentiometrisch mit einer ionenselektiven Elektrode gemessen. Selbstverständlich könnte auch eine andere physikalisch-chemische Messmethode angewendet und die Konzentration z.B. photometrisch gemessen werden.

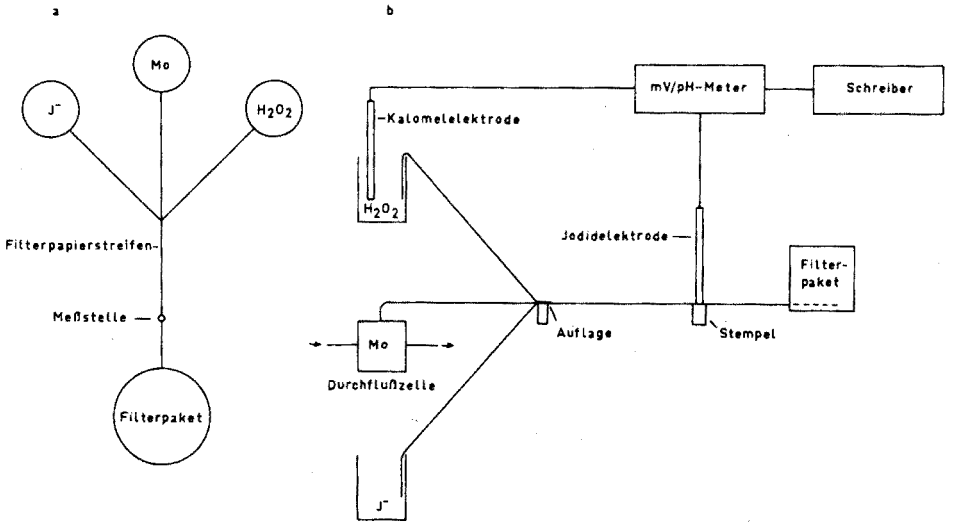

Abb. 1. (a) Prinzipskizze; (b) Schema der Messanordnung (Die Durchflusszelle und die beiden Gefässe für die Reaktanten befinden sich alle auf gleicher Höhe).

Die Bestimmung von Molybdän, welches die Reaktion von Wasserstoffperoxid mit Jodid beschleunigt[3], soll die Anwendungsmöglichkeit dieser Strömungsmethode demonstrieren. Dabei wird die Jodidkonzentration potentiometrisch kontinuierlich verfolgt.

EXPERIMENTELLES

Geräte

Präzisions-pH-Meter (Knick, Berlin, Typ pH 35); jodidselektive Elektrode (Orion, Modell 94-53); gesättigte Kalomelelektrode; Kompensationsschreiber (Metrawatt, Nürnberg, Typ Servogor); thermostatierbare Glaskammer; Vorrichtung zur Fixierung von Filterpapierstreifen, kombiniert mit Elektrodenhaltern (vgl. Abb. 1).

Lösungen

Alle Lösungen wurden aus pro-analysi-Reagenzien mit bidestilliertem Wasser angesetzt.

Wasserstoffperoxidlösung. $7{,}5 \cdot 10^{-3}$ *M* H_2O_2–0,15 *M* K_2SO_4.

Jodidlösung. $1{,}5 \cdot 10^{-3}$ *M* KJ–0,15 *M* K_2SO_4–0,15 *M* H_2SO_4.

Die Lösungen werden täglich frisch aus entsprechenden Stammlösungen hergestellt. Der Gehalt der Wasserstoffperoxid-Stammlösung wird jodometrisch bestimmt.

Messanordnung

Zunächst werden Filterpapierstreifen (Macherey und Nagel, Nr. 260) entsprechend Abb. 2 zugeschnitten. Die Papierstreifen werden in geeigneter Weise (Reihenfolge a, b, c) übereinandergelegt und an der Vereinigungsstelle durch zwei kleine, seitlich angesetzte Klammern zusammengehalten. Dann werden die Streifen in eine Haltevorrichtung (PVC) eingelegt und durch Andrücken der Jodid-Indikatorelektrode gegen einen beweglichen, mit einer Feder versehenen Stempel fixiert (vgl. Abb. 1; die Haltevorrichtung ist der besseren Übersichtlichkeit wegen nicht vollständig abgebildet). Die Filterpapierstreifen sollen sich vor der Vereinigungsstelle nicht gegenseitig berühren. Der Abstand der Elektrode von der Vereinigungsstelle beträgt 3 cm. Der breite Filterpapierstreifen endet im untersten Teil eines Filterpakets von etwa 130 Rundfiltern (Durchmesser 6 cm). Die schmalen Papierstreifen werden jeweils in die Vorratsgefässe für die Jodid-

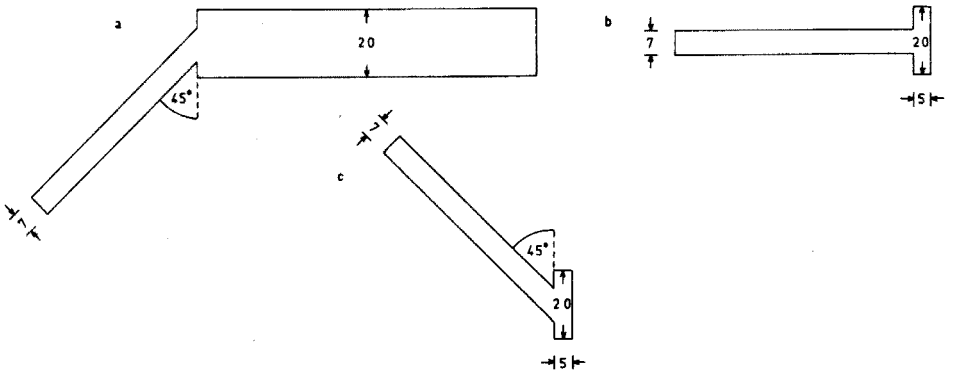

Abb. 2. Filterpapierstreifen (Angaben in Millimeter).

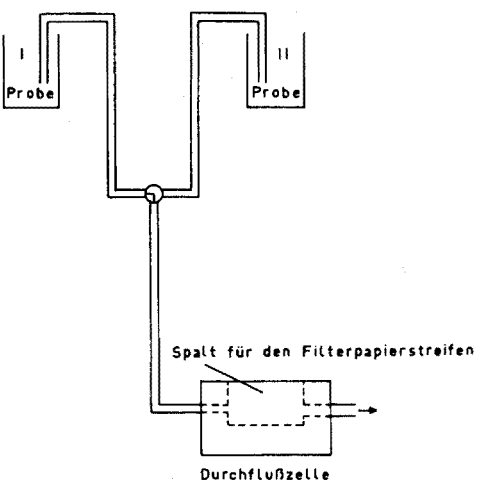

Abb. 3. Probenahme (Zwischen der Durchflusszelle und den Probegefässen besteht eine Höhendifferenz von etwa 20 cm).

und für die Wasserstoffperoxidlösung (35 ml), beziehungsweise in eine kleine Durchflusszelle zur Kontinuierlichen Entnahme der Katalysator–Probelösung (Abb. 3) eingeführt. Aus dieser Zelle (Teflon) wird nur ein geringer Teil der kontinuierlich strömenden Probelösung infolge der kapillaren Wirkung des Filterpapierstreifens zur Analyse entnommen (2–3 ml/12 h). Die Referenzelektrode (GKE) befindet sich in der Wasserstoffperoxidlösung, welche Kaliumsulfat als Grundelektrolyt enthält. Der mit Kalium sulfat getränkte Filterpapierstreifen zwischen Referenz- und Indikatorelektrode wird somit zur Elektrolytbrücke.

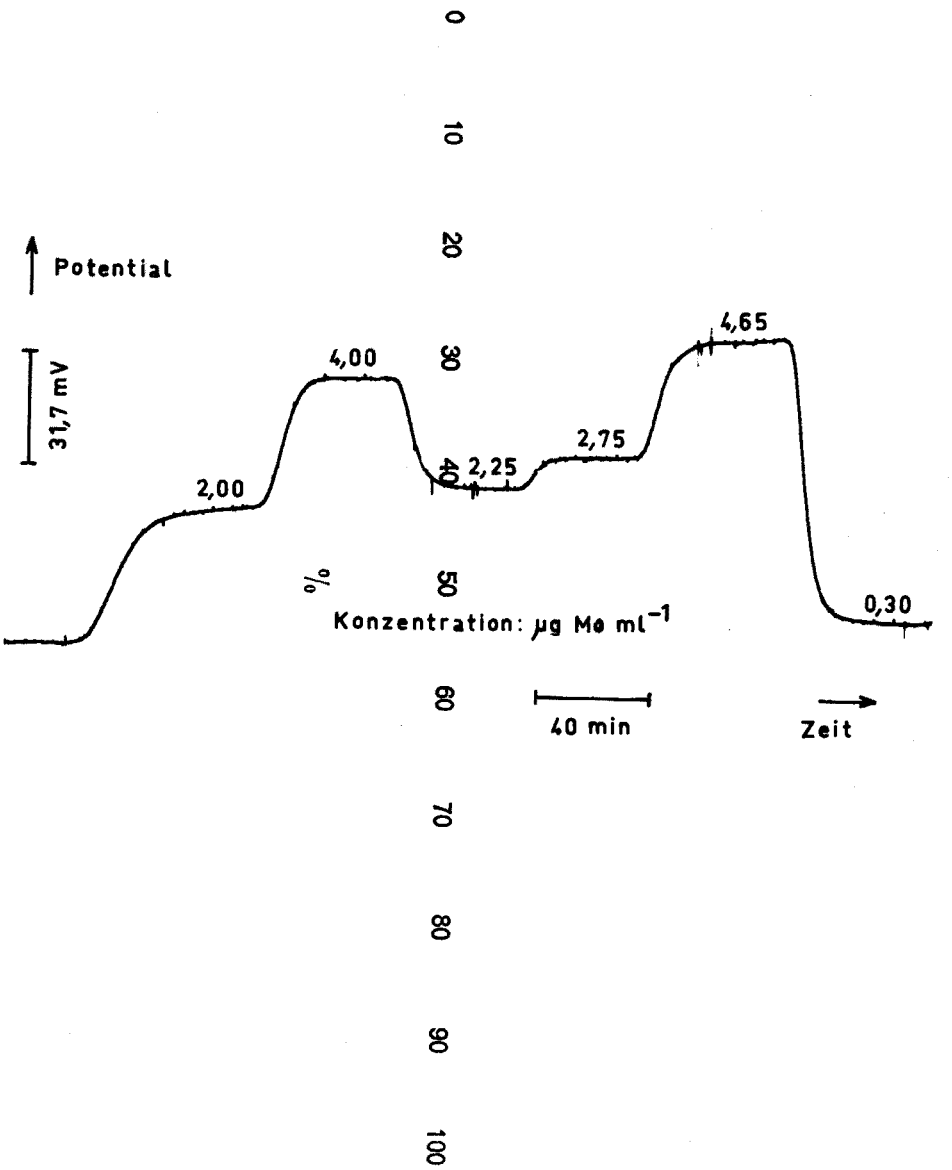

Abb. 4. Schreiberdiagramm.

Die Haltevorrichtung mitsamt den Elektroden befindet sich in einer thermostatierbaren Glaskammer mit Plexiglasdeckel. Die Kammer enthält am Boden Kupferrohrschlangen, die an einen Thermostaten (30°C) angeschlossen und gerade mit Wasser bedeckt sind. Zur Erzielung einer wassergesättigten Atmosphäre werden die Kammerwände mit Filterpapier ausgekleidet.

Durchführung der Messung

Vor Beginn einer längeren, kontinuierlichen Messerie lässt man etwa 1 Stunde Wasser anstelle von Molybdänlösung durch die Durchflusszelle strömen, bis ein gleichbleibendes Messignal (Grundlinie) erreicht ist. Der Probenwechsel geschieht durch Umschalten eines Dreiwegehahnes, der sich in der Zuleitung zur Probeentnahmestelle (Polyäthylenschlauch) befindet (Abb. 3), wobei darauf zu achten ist, dass keine Luftblasen in die Zuleitung gelangen. Die Strömungsgeschwindigkeit in der Zuleitung beträgt in unserem Fall etwa 0,2–0,3 ml min^{-1}. Nach Erreichen des stationären Zustandes wird der Abstand der Schreiberlinie von der Grundlinie in Skalenteilen dem Schreiberdiagramm entnommen (Abb. 4.).

Nach jeweils 24 Stunden werden die Reaktantenlösungen erneuert und der obere Teil des Filterpakets (*ca.* 70 Filter) gegen neue Filter ausgetauscht. Die gebrauchten Filter können nach Trocknen wieder verwendet werden.

Zur Aufnahme einer Eichkurve werden 8 Messungen im Bereich von 0,2 bis 5 μg Mo ml^{-1} durchgeführt.

Diskontinuierliche Arbeitsweise

Durch eine geringfügige Abänderung der Messanordnung besteht die Möglichkeit, anstelle einer kontinuierlichen Probenahme auch einzelne Proben diskontinuierlich aufzutragen. Hierbei entfällt natürlich der Papierstreifen für die Katalysatorlösung (vgl. Abb. 1). Stattdessen wird die Probe mit einer Mikropipette auf ein ausgestanztes Filterscheibchen (Dia. 6 mm) getüpfelt und anschliessend auf eine vorgezeichnete, jeweils gleiche Stelle des breiten Filterpapierstreifens aufgesetzt. Durch den kontinuierlichen Strom der Reaktanten wird die Probe dann aus dem Scheibchen eluiert, und die katalysierte Reaktion kann ablaufen. Jeder Probemenge entspricht in diesem Fall ein gesonderter Peak, dessen Höhe ein Mass für den zu bestimmenden Katalysator ist. Bei dieser diskontinuierlichen Arbeitsweise ist der Bereich der bestimmbaren Konzentration insgesamt grösser als bei der kontinuierlichen Methode, das Verfahren ist jedoch ungenauer.

ERGEBNISSE UND DISKUSSION

Zur Konstanthaltung des Messignals (Potential) bei unveränderter Katalysatorkonzentration ist ein bestimmter Minimaldruck erforderlich, mit welchem der Filterpapierstreifen gegen die Indikatorelektrode gepresst wird. Nach Überschreiten dieses Druckes bleibt das Messignal mindestens 24 Stunden konstant. Ein Wechsel der Reaktantenlösungen und des Filterpakets verursacht zunächst eine Änderung im Verlauf der Grundlinie,, diese stellt sich jedoch nach etwa 30–40 Minuten wieder auf einen konstanten Wert ein.

Einige Ergebnisse von Molybdänbestimmungen zeigt Tabelle I.

TABELLE I

BESTIMMUNG VON MOLYBDÄN

Molybdän (µg ml^{-1})		*Relativer Fehler (%)*
Gegeben	*Gefunden*	
0,20	0,20	± 0
0,30	0,26	−13,3
0,50	0,47	− 6,0
0,50	0,51	+ 2,0
2,25	2,28	+ 1,3
2,75	2,75	± 0
3,00	3,07	+ 2,3
4,65	4,70	+ 1,1
3,00	3,03	+ 1,0
5,00	5,50	+10,0

Die hier diskutierte Methode soll auf die Möglichkeit der Verwendung von Papier als kapillarem Träger hinweisen. Selbstverständlich kann allgemein anstelle der Konzentration eines Reaktanten auch diejenige eines Reaktionsproduktes messend verfolgt werden. Ebenso sollte es, wie bei anderen Strömungsmethoden, möglich sein, auch Inhibitoren[2,4] und Reaktivatoren[2] zu bestimmen.

ZUSAMMENFASSUNG

Es wird eine neue katalytisch-kinetische Strömungsmethode beschrieben, bei welcher ein kapillarer Träger, Filterpapier, als Reaktionsort und Transportmedium dient. Der zu bestimmende Katalysator und die beiden Reaktanten einer katalysierten Reaktion durchlaufen einen Filterpapierstreifen, an einer geeigneten Stelle erfolgt auf dem Papier selbst die kontinuierliche Messung der Konzentration eines Reaktanten. Am Beispiel der durch Molybdän beschleunigten Reaktion von Wasserstoffperoxid mit Jodid wird die Methode illustriert. Der Reaktionsablauf wird potentiometrisch mit Hilfe einer ionenselektiven Elektrode verfolgt.

SUMMARY

A new catalytic–kinetic flow method is described, in which a capillary support, filter paper, serves as medium for the reaction as well as for the transport. The catalyst to be determined and the two reactants migrate through a filter paper strip. On a suitable place of the filter paper itself, the concentration of one of the reactants is continuously measured. The example of the molybdenum-catalyzed reaction between hydrogen peroxide and iodide illustrates the procedure. The course of the reaction is followed potentiometrically with an iodide-selective electrode.

LITERATUR

1 A. M. Wilson, *Anal. Chem.*, 38 (1966) 1784.
2 H. Weisz und H. Ludwig, *Anal. Chim. Acta*, 62 (1972) 125.
3 K. B. Yatsimirskii und L. P. Afanaseva, *Zh. Neorg. Khim.*, 11 (1956) 319; K. B. Yatsimirskii, *Kinetic Methods of Analysis*, Pergamon, Oxford, 1966.
4 H. Ludwig, H. Weisz und T. Lenz, *Anal. Chim. Acta*, 70 (1974) 359.

Analytica Chimica Acta, 75 (1975) 189–197

ACCURATE ALL-PURPOSE METHOD FOR THE ASSAY OF ALKALI AND ALKALINE EARTH CARBONATES WITH PERCHLORIC ACID

GEORGE NORWITZ and MICHAEL GALAN
Frankford Arsenal, Philadelphia, Pa. 19137 (U.S.A.)
(Received 24th May 1974)

Alkali and alkali earth carbonates are usually assayed by titration with hydrochloric or sulfuric acid or by determination of the metal content. A summary of the methods used for assaying alkali and alkali earth carbonates by various government specifications, various ASTM specifications, ACS[1], United States Pharmacopeia[2], and Rosin[3] is shown in Table I. Also shown in Table I are the assay requirements and the loss in weight requirements together with the temperature and heating time used in determining the loss in weight. In addition, a statement is included as to whether the assay is conducted on a dried sample or the sample as received.

The following conclusions can be drawn from Table I: (a) there is a surprising variety of techniques for the titration of carbonate in carbonates (this and other arsenals have found that most of these techniques leave much to be desired); (b) no accepted method is available for the determination of carbonate in alkali earth carbonates; (c) some of the assay requirements for the carbonates are unrealistic, insofar as significant figures are concerned; (d) there is wide divergence in the recommended temperature and time in the determination of loss in weight on heating; (e) there is disagreement as to whether the assay should be conducted on the dried sample or sample as received.

In view of the above, there obviously exists a need for an accurate all-purpose method for the assay of alkali and alkali earth carbonates. This laboratory undertook an investigation to develop such a procedure.

EXPERIMENTAL

Apparatus and reagents

Use either weighing bottles (Exax, low-form, 50 mm i.d. and 30 mm high), or crystallizing dishes (Pyrex, 70 mm o.d. and 50 mm high, Arthur H. Thomas Co., Philadelphia, Pa., Catalogue No. 4507) covered with Pyrex watch glasses 70 mm in diameter. Speedyvap watch glasses, 3 in. diameter, are also needed.

Perchloric acid (approximately 1.2 *M*). Add 400 ml of perchloric acid (70–72%) to 3600 ml of water and cool to room temperature. Store in a glass-stoppered Pyrex bottle.

Standard sodium hydroxide solution (approximately 1 *M*). Prepare and standardize against potassium hydrogenphthalate as described by ASTM[1,2]. Store in a plastic bottle.

TABLE I

METHODS PREVIOUSLY USED FOR THE ASSAY AND LOSS IN WEIGHT OF ALKALI AND ALKALI EARTH CARBONATES[a]

Specification	*Loss on heating (%)*	*Assay requirement (%)*	*Method of assay*
Na_2CO_3			
ACS[1]	1.0 max; 270–300°C (c.w.)	None	None
ACS, alkalimetric Std[1]	1.0 max; 270–300°C (c.w.)	99.95–100.05	1.3 g treated with KH phthalate, soln. boiled and titd. with 0.02 *M* NaOH to phenolphthalein (dried s.)
ASTM D458-57[4] and D501-67[5]	1.0 max; 150–155°C (1 h)	99.16 min	1.2 g titd. with 0.5 *M* HCl close to MO end point, soln boiled and titd. again with 0.5 *M* HCl (dried s)
ASTM E359–68 (analytical methods)[6]	— 250–270°C (4 h)	—	4 g titd with 1 *M* HCl or 0.5 *M* H_2SO_4 to MO or MO + xylene cyanole FF (s. as is)
O-S-571f[7]	1.0 max; 150–155°C (1 h)	99.2 min and 98.0 min	Same as ASTM D501–67[5]
Rosin[3]	1.0 max; 250–300°C (c.w.)	None	None
$Na_2CO_3 \cdot H_2O$			
ACS[1]	13.0–15.0; 150°C (c.w.)	None	None
USP[2]	12–15; 105°C (4 h)	99.5 min, anh.b.	2 g titd. with 0.5 *M* H_2SO_4 to MO (dried s)
Rosin[3]	15.0 max; 250–300°C (c.w.)	None	None
$Na_2CO_3 \cdot 10\ H_2O$			
Rosin[3]	63.5 max; 250–300°C (c.w.)	99.7 min, anh.b.	8 g titd. with 1 *M* HCl to MO (dried s.)
K_2CO_3			
ACS[1]	1.0 max; 270–300°C (c.w.)	None	None
Rosin[3]	1.0 max; 250–300°C (c.w.)	99.8–100.3	3 g titd. with 1 *M* HCl to MO (dried s.)
$K_2CO_3 \cdot \frac{3}{2} H_2O$			
ACS[1]	14.0–16.5; 270–300°C (c.w.)	None	None
USP[2]	10.0–16.5 180°C (c.w.)	99 min anh. b.	2.5 g titd. with 0.5 *M* H_2SO_4 to MO (dried s.)
Li_2CO_3			

(continued)

TABLE I (*Continued*)

Specification	*Loss on heating (%)*	*Assay requirement (%)*	*Method of assay*
			(continued)
ACS[1]	None	99 min	1.3 g treated with 1 *M* HCl, soln. boiled and titd. with 1 *M* NaOH to methyl red (s. as is)
$CaCO_3$			
ACS[1]	None	None	None
ACS, low in alkali[1]	None	None	None
ACS, chelometric std.[1]	None	99.95–100.05	Ca (s. dried 300°C, 3h)
MIL–C–00293A[8]	0.20; 110°C (2 h)	98.0 min	Ca (s. as is).
MIL–C–15198A[9]	0.25; 105°C (c.w.)	96.0 min	Ca (s. as is)
Rosin[3]	None	99 min	Ca (s. dried 200°C, 3 h).
USP[2]	2; 200°C (4 h)	98 min	Ca (dried s.).
Marble chips for Kipp	None	None	None
$BaCO_3$			
ACS[1]	None	None	None
MIL–B–624A[10]	0.3; 125°C (3 h)	68.0 min Ba	Ba (s. as is).
$SrCO_3$			
Rosin[3]	None	None	None
$NaHCO_3$			
ACS[1]	None	99.7–100.3	3 g titd. with 1 *M* HCl to MO (s. dried over H_2SO_4, 24 h)
ASTM D501-67[5] and ASTM D928-52[11]	None	99.6 min	Heated to 275°C, CO_2 absorbed and weighed
Rosin[3]	None	99.8–100.3	3 g titd. with 0.5 *M* H_2SO_4 to MO (s. dried over H_2SO_4, 3 h)
USP[2]	None	99 min	3 g titd. with 0.5 *M* H_2SO_4 to MO (s. dried over silica gel, 4 h)
$KHCO_3$			
ACS[1]	None	99.7–100.3	3 g titd. with 0.5 *M* H_2SO_4 or 1 *M* HCl to MO (s. dried over H_2SO_4, 24 h)
Rosin[3]	None	99.7–100.3	3 g titd. with 1 *M* HCl to MO (s. dried over H_2SO_4, 3 h)
USP[2]	None	99 min	4 g titd. with 0.5 *M* H_2SO_4 to MO (s. dried over silica gel, 4 h)

[1]Abbreviations: c.w. = constant weight; soln. = solution; titd. = titrated; s. = sample; MO = methyl orange; anh.b. = anhydrous basis.

Procedure

Place 10–15 g of the sample into the weighing dishes or crystallizing dishes. Determine the loss in weight for all the carbonates except $NaHCO_3$ and $KHCO_3$, after heating at 250°C for 3 h, covering, and cooling in a desiccator containing anhydrone for 2 h or more. Determine the loss in weight of $NaHCO_3$ and $KHCO_3$ after placing the samples in a desiccator containing sulfuric acid for 16 h.

Transfer the following approximate size sample (g). weighed to 0.3 mg, to a 500-ml wide-mouth Erlenmeyer flask: Na_2CO_3, 5; K_2CO_3, 7; Li_2CO_3, 4; $CaCO_3$, 5; $BaCO_3$, 9; $SrCO_3$, 7; $NaHCO_3$, 8; $KHCO_3$, 9. Weigh the samples of Na_2CO_3 and K_2CO_3 quickly, since they are hygroscopic.

Add 100.00 ml of 1.2 *M* perchloric acid with a pipet and allow to stand for several minutes until most of the carbonate has dissolved. Cover with a Speedyvap watch glass, heat to boiling, and boil moderately for 5 min. Carry along a blank determination, using 100.00 ml of 1.2 *M* perchloric acid. Cool to room temperature and wash down the watch glass and sides of the flask with water. Add 5 drops of aqueous 0.1% (w/v) methyl orange indicator and titrate with standard 1.0 *M* sodium hydroxide solution to a yellow end-point, using a 50-ml buret. The titration should be performed at a temperature within 3°C of the temperature used for establishment of the molarity of the sodium hydroxide solution. In the titration of the blank, first add 100.00 ml of the sodium hydroxide solution with a pipet and finish the determination by titrating from the 50-ml buret.

Calculate as follows:

$$\text{Assay, } \% = (AB - C)MF/W$$

where A = ml of perchloric acid solution,
B = ml of sodium hydroxide solution equivalent to 1.00 ml of perchloric acid,
C = ml of sodium hydroxide solution,
M = molarity of sodium hydroxide solution,
W = g of sample titrated,
F = factor (Na_2CO_3, 5.2995; K_2CO_3, 6.9105; Li_2CO_3, 3.6945; $CaCO_3$, 5.0045; $BaCO_3$, 9.8675; $SrCO_3$, 7.3815; $NaHCO_3$, 8.401; $KHCO_3$, 10.012).

DISCUSSION AND RESULTS

It was initially thought that alkalimeters might be employed to establish the basis for an accurate assay method. In this technique an acid reacts with the carbonate and the weight loss is determined. However, many tests with various alkalimeters[13–15] showed that this approach was not sufficiently accurate for assay work. This was also found to be the case with methods depending on treatment with acid and absorption of the carbon dioxide in such reagents as ascarite[13–16].

Attention was therefore turned to titration methods. It was found that an accurate technique was to treat an optimal large size of sample with 100.00 ml of dilute perchloric acid, boil off the carbon dioxide, and titrate the excess of acid with sodium hydroxide solution to a methyl orange end-point. For optimal back-

titration (about 10–25 ml), the sample size should be 4–9 g (depending on the carbonate), the molarity of the perchloric acid should be approximately 1.2 *M*, and the molarity of the sodium hydroxide should be approximately 1.0 *M*.

Perchloric acid is superior to hydrochloric acid for the assay of carbonates, because there is no danger of loss of acid during the boiling; it is superior to sulfuric acid because insoluble sulfates of barium, strontium, and calcium are not precipitated in the assay of alkali earth carbonates (these insoluble sulfates make it difficult to boil off all the carbon dioxide). When perchloric acid is used for the assay of potassium carbonates, some potassium perchlorate precipitates after cooling but this does not affect the accuracy of the method.

It is recommended that the assay of normal alkali and alkali earth carbonates be performed on samples previously dried by heating at 250°C for 3 h. However, the heating also decomposes any hydrogencarbonate present to the carbonate ($2\ NaHCO_3 \rightarrow Na_2CO_3 + H_2O + CO_2$). Sodium hydrogencarbonate starts to decompose at about 50°C and potassium hydrogencarbonate decomposes at 190°C[17]. It is recommended that the assay of alkali hydrogencarbonates be conducted on samples previously dried over sulfuric acid as suggested by several investigators (see Table I).

The carbon dioxide is driven out during the boiling, so that the final titration represents the titration of a strong acid by a strong base. It was found that identical results were obtained with methyl orange, methyl red, or phenolphthalein indicator. However, methyl orange or methyl red are preferred over phenolphthalein, since they show the approach of the end-point whereas phenolphthalein does not (all the end-points were sharp). Kolthoff and Sandell[15] have elucidated the reasons why, for the titration of 1 *M* acid with 1 M base, either methyl orange, methyl red, or phenolphthalein can be used, while for the titration of 0.1 *M* acid with 0.1 *M* base, methyl red is the preferred indicator.

It has been suggested[6] that a correction be made for the error caused by difference between the temperature used in the titration of the sample, and the temperature used for the establishment of the molarity of the sodium hydroxide solution ($\Delta V/°C = 0.00035$). It was not found necessary to consider such a correction if the temperature difference was less than 3°C.

Samples of sodium carbonate and potassium carbonate are hygroscopic and should be weighed quickly. Calcium carbonate, barium carbonate, strontium carbonate, lithium carbonate, sodium hydrogencarbonate, and potassium hydrogencarbonate are not hygroscopic.

Equally satisfactory results were obtained whether weighing bottles (which are customarily made[18] of Exax Kimble Standard Flint Glass R-6) or Pyrex crystallizing dishes covered with Pyrex watch glasses were used. The crystallizing dishes are recommended for laboratories performing a large number of determinations, since these dishes are far less expensive than weighing bottles. This laboratory found that the weighing bottles containing samples frequently cracked when heated at 250°C.

The proposed assay method has been applied to normal sodium, potassium, lithium, calcium, barium, and strontium carbonates, and to sodium and potassium hydrogencarbonates. These salts represent the alkali or alkali earth carbonates that are articles of commerce. The method could probably be used for lithium

hydrogencarbonate, cesium carbonate, cesium hydrogencarbonate, rubidium carbonate, and rubidium hydrogencarbonate, but these are expensive specialty items not readily available. Calcium, barium, and strontium hydrogencarbonates have not been prepared pure in the solid state.

The method can be used to determine total alkalinity of magnesium carbonate, calculated as MgO (all commercial and analytical-grade magnesium carbonates are basic carbonates of varied formulas[19]). Also, the method can be used to determine total alkalinity of sodium sesquicarbonate ($Na_2CO_3 \cdot NaHCO_3 \cdot 2 H_2O$)[5,20], calculated as Na_2O. The method is not applicable to the assay of heavy metal carbonates, because of the precipitation of the oxides or hydroxides on titration with alkali and also because heavy metal salt solutions are frequently colored. Addition of tartrate (sodium tartrate) to complex the heavy metal did not give satisfactory results.

The results obtained for the assay of the carbonates, together with the loss in weight on heating the normal carbonates at 250°C for 3 h and the loss in weight on drying hydrogencarbonates in a desciccator containing sulfuric acid for 16 h are shown in Table II. Only the average result is given for the loss in weight determinations (the precision was satisfactory). The replicate results for the carbonate assays showed excellent precision (the average standard deviation was 0.050%). It is seen that the alkali carbonates (anhydrous and hydrated) were of relatively high purity, except for the lithium carbonate which had a purity of only 99.20%. The alkali earth carbonates (calcium, barium, and strontium carbonates) were of moderate purity (about 99.5%). The marble was of surprisingly high purity (99.78%). The sodium hydrogencarbonate was close to theoretical assay, while the potassium hydrogencarbonate had a high assay (100.49%), indicating that this material contained some normal carbonate.

It is seen that the loss in weight on heating the anhydrous carbonates was very significant for sodium and potassium carbonates (0.67% and 0.35%, respectively), but slight for lithium, calcium, barium, and strontium carbonates (less than 0.12%). The loss in weight on drying the sodium and potassium hydrogencarbonates in a desiccator containing sulfuric acid was slight (0.003% and 0.04%, respectively).

The water content of $Na_2CO_3 \cdot H_2O$ (14.35%) compared favorably with the theoretical water content (14.53%). The water content of $K_2CO_3 \cdot \frac{3}{2} H_2O$ (16.46%) was somewhat higher than the theoretical water content (16.35%). The water content of the washing soda (23.60%) indicated that this material had a water content somewhere between the monohydrate and the decahydrate. This is not unusual. The theoretical water content of $Na_2CO_3 \cdot 10 H_2O$ is 62.96%.

As indicated in the method, it is recommended that the analysis of the hydrated carbonates be conducted on the anhydrous sample. However, some tests were conducted on the analysis of the hydrated carbonates as received. The results for the $Na_2CO_3 \cdot H_2O$ (6-g sample), $K_2CO_3 \cdot \frac{3}{2} H_2O$ (8.5-g sample), and $Na_2CO_3 \cdot x H_2O$ (6.5-g sample) averaged 85.77%, 83.45%, and 76.59%, respectively. The totals of these assay results and the corresponding water content (14.35%, 16.46%, and 23.60%) were 100.12%, 99.91%, and 100.19%, respectively. This is a further check that the proposed assay method is satisfactory. Also it indicates that the normal hydrated carbonates contain very little hydrogencarbonate.

TABLE II

RESULTS FOR ASSAY OF CARBONATES (CALCULATED ON ANHYDROUS BASIS)

Carbonate	*Loss in weight at 250°C (%)*	*Assay (%)*
Na_2CO_3, reagent	0.67	99.87
		99.97
		99.87
		99.97
		Av. 99.92
		s 0.058
$Na_2CO_3 \cdot H_2O$, reagent	14.35	100.00
		100.00
		100.00
		100.10
		Av. 100.03
		s 0.050
$NaCO_3 \cdot x\ H_2O$, washing soda	23.60	99.99
		99.89
		99.99
		99.89
		Av. 99.94
		s 0.058
K_2CO_3, reagent	0.35	99.82
		99.72
		99.72
		Av. 99.75
		s 0.058
$K_2CO_3 \cdot \frac{3}{2} H_2O$, reagent	16.46	100.03
		100.14
		100.04
		99.94
		Av. 100.04
		s 0.082
Li_2CO_3, reagent	0.12	99.20
		99.20
		99.20
		Av. 99.20
		s 0.000
$CaCO_3$, reagent	0.03	99.53
		99.63
		99.53
		Av. 99.56
		s 0.058
Marble, for Kipp	0.00	99.68
		99.85
		99.78
		99.80
		Av. 99.78
		s 0.087
$BaCO_3$, reagent	0.07	99.43
		99.43
		99.46
		Av. 99.44
		s 0.017

(continued)

TABLE II (*Continued*)

Carbonate	*Loss in weight at 250°C (%)*	*Assay (%)*
$SrCO_3$, reagent	0.12	99.68
		99.68
		99.68
		Av. 99.68
		s 0.000
$NaHCO_3$, reagent	—	99.89
		99.99
		100.09
		99.99
		Av. 99.99
		s 0.082
$KHCO_3$, reagent	—	100.46
		100.46
		100.46
		100.57
		Av. 100.49
		s 0.055

[a] Loss in weight in sulfuric acid desiccator for 16 h was 0.003%.
[b] Loss in weight in sulfuric acid desiccator for 16 h was 0.04%.

This work was conducted under an Army Materials Technology Program (AMS Code 68501.49.11100). The authors are indebted to Herman Gordon for performing some of the analyses.

SUMMARY

An accurate all-purpose method is proposed for the determination of carbonate in alkali and alkali earth carbonates. A large sample size (4–9 g depending on the carbonate) is dissolved in 100.00 ml of 1.2 *M* perchloric acid, the solution is boiled, and the excess of acid is titrated with standard 1.0 *M* sodium hydroxide solution to a methyl orange end-point. Perchloric acid is preferable to hydrochloric acid because there is no danger of loss of acid during the boiling; it is preferable to sulfuric acid since insoluble sulfates of barium, strontium, and calcium are not precipitated in analyzing alkali earth carbonates. Normal alkali and alkali earth carbonates (anhydrous and hydrated) are assayed on samples previously dried by heating in an oven at 250°C for 3 h. This treatment drives off all the water but it also converts any hydrogencarbonate present into carbonate. Hydrogencarbonates are assayed on samples dried in a desiccator containing sulfuric acid for 16 h. Twelve different carbonates were analyzed. The average standard deviation of the method was 0.050%.

REFERENCES

1 American Chem. Soc., *Reagent Chemicals*, Washington, D.C., 4th ed., 1968.
2 *U.S. Pharmacopeia*, New York, 17th ed., 1965.
3 J. Rosin, *Reagent Chemicals and Standards*, Van Nostrand, New York, 5th ed., 1967.

4 American Soc. for Testing and Materials, *Standard Specification for Soda Ash*. Designation D458-57, Philadelphia, Pa., 1972.
5 American Soc. for Testing and Materials, *Standard Methods of Sampling and Chemical Analysis of Alkaline Detergents*, Designation D501-67, Sections 19 and 24, Philadelphia, Pa., 1972.
6 American Soc. for Testing and Materials, *Standard Methods for Chemical Analysis of Soda Ash (Sodium Carbonate)*, Designation E 359-68, Philadelphia, Pa., 1972.
7 *Sodium Carbonate, Anhydrous, Technical*, Federal Specification 0-S-571f, 1st August, 1969.
8 *Calcium Carbonate*, Military Specification MIL-C-00293A, September 1967.
9 *Calcium Carbonate, Precipitated (Pigment)*, Military Specification MIL-C-15198A, 15th January, 1952.
10 *Barium Carbonate (for Use in Ammunition)*, Military Specification MIL-B-624A, 28th April, 1969.
11 American Soc. for Testing and Materials, *Standard Specification for Sodium Bicarbonate*, Designation D928-52, Philadelphia, Pa., 1972.
12 American Soc. for Testing and Materials, *Standard Methods for Preparation, Standardization, and Storage of Standard Solutions for Chemical Analysis*, Designation E200-67, Sections 13 to 18, Philadelphia, Pa., 1972.
13 G. Charlot and D. Bezier, *Quantitative Inorganic Analysis*, Wiley, New York, 1957, p. 376.
14 N. H. Furman, *Standard Methods of Chemical Analysis, Vol. 1*, Van Nostrand, New York, 6th ed., 1962, p. 301.
15 I. M. Kolthoff and E. B. Sandell, *Textbook of Quantitative Inorganic Analysis*, MacMillan, New York, 3rd ed., 1952, pp. 370, 432.
16 F. D. Snell and F. M. Biffen, *Commercial Methods of Analysis*, McGraw-Hill, New York, 1944, p. 224.
17 Kirk-Othmer, *Encyclopedia of Chemical Technology*, Interscience, New York, 2nd ed., 1968, Vol. 16, p. 388, Vol. 18, p. 467.
18 Owens-Illinois Glass Co., *Kimble Catalog SC-300, Kimax Laboratory Glassware*, Toledo, Ohio, 1964.
19 *Magnesium Carbonate*, Military Specification MIL-M-11361B, 25th May, 1962.
20 *Sodium Carbonate–Sodium Bicarbonate Mixture*, Federal Specification P-S-641g, 2nd August, 1967.

Analytica Chimica Acta, 75 (1975) 199–205

THE DETERMINATION OF CHROMIUM(VI) IN NATURAL WATERS BY DIFFERENTIAL PULSE POLAROGRAPHY

SANDRA T. CROSMUN

Department of Chemistry, University of Tennessee 37916 (U.S.A.)

THEODORE R. MUELLER

Analytical Chemistry Division, Oak Ridge National Laboratory, Oak Ridge, Tennesee 37830 (U.S.A.)*

(Received 1st August 1974)

The determination of chromium(VI) in the presence of chromium(III) in water is very important. Few, if any, waters contain chromium from natural sources[1]. Chromium(VI) resulting from pollution by industrial wastes appears to be relatively stable in natural water since only a low concentration of reducing materials is present[2–4]. Chromium(VI) is more easily absorbed into tissue than are other oxidation states of chromium[5]. It is also a strong oxidizing agent[4], leading to its toxicity. There have been no reports of oral toxicity in the trivalent form[4]; indeed, chromium(III) is necessary for the maintenance of a normal glucose tolerance factor[6,7]. The maximum permissible limit for chromium(VI) in potable water[8,9] is 0.050 μg ml^{-1}.

Most recently, spectrophotometric techniques have been utilized for the determination of chromium. Extraction of chromium from water and determination by flame atomic absorption has been reported by Nix and Goodwin[10]. Flameless atomic absorption has been used in conjunction with a Massmann furnace[11], a carbon filament atom reservoir[12], and a tantalum filament[13]. The disadvantage of all these methods is that total elemental chromium is determined; no distinction can be made between oxidation states.

In addition to the atomic absorption methods, the American Society for Testing and Materials recommends a colorometric procedure for the determination of total chromium or chromium(III) in waste water[14]. In this procedure, chromium-(VI) reacts with diphenylcarbazide to produce a reddish purple color in slightly acidic solutions. This procedure is not recommended for the direct determination of chromium(VI). If the solution contains materials capable of reducing chromium(VI) in acidic solution, incorrect results are obtained.

Coulometric titration of chromium with electrogenerated iron(II) was used by Champion *et al.*[15] and by Bigois[16] to determine nanogram quantities of chromium in water and inorganic compounds. Bhatnagan and Roy[17] studied the polarographic reduction of chromium(VI) in cooling tower waters. The lowest concentration studied was 10 μg ml^{-1}; this sensitivity is insufficient for natural water studies.

Princeton Applied Research Corporation (PAR) offers suggestions for

* Operated by Union Carbide Corporation for the U. S. Atomic Energy Commission.

determining chromium in water samples by differential pulse polarography[18]. They indicate that, in 1 *M* sodium hydroxide electrolyte, chromium(VI) gives "more of a plateau than a peak" in the range 50–100 μg ml^{-1} and point out several possible interferences with the method. In basic ammonium buffer, copper is an interference, and no method is given for chromium(VI) in the presence of this potential and very probable contaminant in samples from cooling tower effluents.

In the present work, a method has been developed for the determination of chromium(VI) in water samples that can be used over a wide range of chromium concentrations and that does not suffer from the presence of common impurities. The method has been applied successfully to both natural waters and water samples taken in fresh water streams below a cooling tower.

EXPERIMENTAL

Instrumentation

A PAR Model 174 Polarographic Analyzer, with a PAR Model 172A drop timer was used. The cell used has been described elsewhere[19]. The teflon cover held a platinum wire counter electrode, a Beckman Model 39178 SCE, a dropping mercury electrode (DME), and a gas-sparging tube.

Reagents

A stock solution of 0.02 *M* chromium(VI) was prepared by dissolving potassium dichromate in triple-distilled water. Other stock solutions were prepared by diluting this solution as required. All chemicals were reagent grade and were used without further purification. Copper(II) was introduced as the sulfate salt, and iron(III) was used as the chloride salt. The ammonium acetate supporting electrolyte buffer (0.1 *M*, pH 7) was prepared from A.R. grade ammonium acetate and triple-distilled water.

Procedure

Sample solutions were deoxygenated with water-saturated argon while in the cell. Stirring was effected by the stream of argon flowing through the cell. The initial potential was set to +0.1 V *vs.* SCE. The argon was then diverted to purge the cell space above the solution and the potential scan was initiated in the cathodic direction.

Water samples were prepared for analysis by addition of concentrated acetate buffer and 0.100 ml of 1 *M* ethylenediamine (en) to a total volume of 20 ml. These dilutions yield final concentrations of 0.1 *M* acetate buffer and $5.0 \cdot 10^{-3}$ *M* en.

Polarography was performed in the differential pulse polarographic mode with a 25-mV pulse being applied to a 0.5-s drop. Scans were performed from +0.1 V to −0.3 V *vs.* SCE at a scan rate of 5 mV s^{-1}.

RESULTS AND DISCUSSION

Choice of supporting electrolyte

Sodium hydroxide is the recommended supporting electrolyte for the

TABLE I

COMPARISON OF ELECTROLYTES FOR POLAROGRAPHY OF CHROMIUM(VI)

Electrolyte	*Advantage*	*Disadvantage*
NaOH	No maxima Cu does not interfere	Not linear at low concn. of Cr(VI) Hard to purify for trace work
$NaHCO_3$	No maxima at low concn. of Cr(VI) en Removes Cu interference	Poor buffer capacity in presence of acid Irreproducibility, high results with water samples
NH_4OAc	No maxima at low concn. of Cr(VI) Buffer capacity good Background current flat in region of Cr(VI) wave	Cu interferes
NH_4OAc with en	Removes Cu interference	Background current not flat in region of Cr(VI) wave Slightly less sensitive than with NH_4OAc alone

determination of chromate by classical d.c. polarography[20, 21]; however, for trace work there are serious disadvantages (Table I). Sodium hydrogencarbonate has been used as the supporting electrolyte for chromium(VI) studies[22]; however, its buffer capacity is irreversible in the presence of acids because of released carbon dioxide, making it unacceptable for direct analysis of acidic water samples. Observations on this system have shown irreproducibility and high analytical results on water samples.

Ammonium acetate at pH 7 exhibits background currents similar to sodium hydrogencarbonate, but is more tolerant of small additions of acids. Copper, a common substance in water, is a serious interferent since its reduction wave coincides with the reduction wave of chromium(VI). Addition of $5 \cdot 10^{-3}$ *M* en has no effect on the half-wave potential of chromium(VI), but the half-wave potential due to the step-wise reduction of the copper(II)–en complex is shifted in a negative direction. Since en reduces the peak current of chromium(VI) (Fig. 1), the minimal concentration necessary to separate the chromium(VI) and the copper(II) waves was used.

In all these buffered media, large concentrations of chromium(VI), such as 2.5 μg ml^{-1}, cause a large maximum on the reduction wave, making the wave unsuitable for pulse polarographic analysis. However, the increased sensitivity of pulse polarography allows concentrations as low as 0.035 μg Cr(VI) ml^{-1} to be analyzed, thus yielding well-defined reduction waves with no maxima.

Chemical reaction between chromium(VI) and mercury

According to standard electrode potentials, chromate should be reduced by metallic mercury. Since it is necessary for the sample solution to be in contact with mercury from the DME for approximately 15 min, experiments were designed to assess the potential loss of chromium(VI); 50 g of mercury were added to solutions containing varying concentrations of chromium(VI). These

solutions were shaken by a mechanical shaker, aliquots were removed at given time intervals, and the peak current for each of these was measured polarographically. As seen in Table II, mercury reacts significantly with chromium(VI) within 15 min under these conditions.

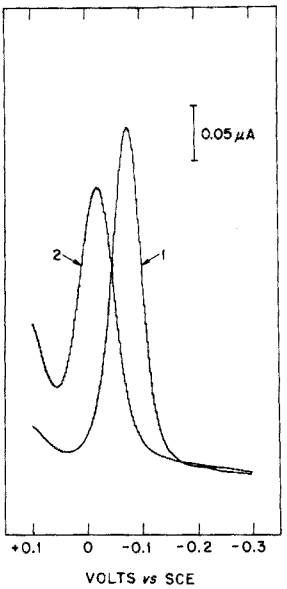

Fig. 1. Differential pulse polarograms of 0.514 μg Cr(VI) ml^{-1} in 0.1 *M* sodium acetate and 0.012 *M* HCl. (1) No en added; (2) 0.005 *M* en added. Pulse amplitude, 25 mV. Scan rate, 5 mV s^{-1}. Drop time 0.5 s.

TABLE II

THE EFFECT OF CONTACT TIME BETWEEN MERCURY AND CHROMIUM(VI) IN AMMONIUM ACETATE SOLUTION ON THE PULSE POLAROGRAPHIC PEAK CURRENT

Cr(VI) in contact with Hg (μg ml^{-1})	*Percentage decrease in peak current time (h)*				
	0.25	*0.50*	*1*	*4*	*24*
Agitated solution					
0.520	68	62	74	100	100
1.04	−20[a]	83	100	100	100
2.08	95	100	100	100	100
10.4	69	87	78	76	82
20.8	82	90	94	96	100
Quiescent solution					
0.520	3.5	9.3	14	24	38
1.04	5.6	13	11	9.7	18
2.08	3.7	4.0	4.3	5.7	11
10.4	−0.3	−0.3	−0.8	2.0	−0.3
20.8	1.6	−11[a]	1.9	7.6	10

[a] Oxygen in cell.

In order to simulate experimental conditions better, another set of five solutions was prepared. Only 5 g of mercury was added to each of these solutions, and they were briefly agitated just before aliquots were removed for analysis. To maintain consistency, aliquots of samples and standards were taken so that all solutions except the 10.4 μg ml^{-1} solution resulted in 0.095$\pm$0.008 μg ml^{-1} of chromium in the cell. Within the first 15 min there was a 2–6% decrease in the current. This is deemed an acceptable loss for sample analysis. Tests were not run with added iron and copper since either there was no interference or the interference was removed.

Interference study of copper and iron

Two common ions found in natural waters, copper(II) and iron(III), can be serious interferences when a DME is used for polarographic studies. It was found that added iron(III) has no effect on the chromium reduction wave and, consequently, creates no problem in the analysis for chromium(VI). By the addition of small amounts of en, the otherwise overlapping copper(II) reduction wave is shifted negatively, eliminating copper(II) as an interferent. A 10-fold excess of copper(II) showed no effect on the chromium(VI) wave, even when the concentration of chromium(VI) was as low as 0.05 μg ml^{-1} (Fig. 2). It is apparent from the slope of the wave that even larger amounts of copper could be tolerated.

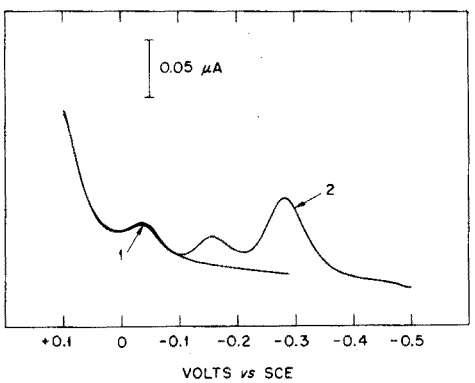

Fig. 2. Differential pulse polarograms of 0.051 μg Cr(VI) ml^{-1} in 0.1 *M* sodium acetate, 0.012 *M* HCl, and 0.005 *M* en. (1) No Cu added; (2) 0.630 μg Cu(II) ml^{-1}. Instrumental conditions as in Fig. 1.

Calibration

The linear least-squares regression equation for peak current as a function of concentration of chromium(VI) showed a sensitivity of 0.32 μA μg^{-1} ml^{-1} with no bias. The coefficient of correlation for a linear fit was 0.99978 and the F-factor was 18,378, significant to at least the $F_{0.99}$ level. The detection limit, defined as twice the noise level, was 0.01 μg ml^{-1}.

Analyses

Two types of water samples were prepared. Synthetic samples were prepared both with and without added copper(II). Others were obtained from creeks and watersheds in the Oak Ridge area. In all samples, the sediment was allowed to

settle and only the supernate was analyzed. Both types were analyzed by differential pulse polarography and compared with results obtained from flame atomic absorption. These results are summarized in Table III. It can be seen that analyses of both low and high levels of chromium(VI) are unaffected by equimolar amounts of copper(II).

TABLE III

COMPARISON OF RESULTS OF ANALYSES FOR CHROMIUM(VI) IN WATER SAMPLES BY ATOMIC ABSORPTION SPECTROPHOTOMETRY AND DIFFERENTIAL PULSE POLAROGRAPHY

Sample type	*Sample number*	*Taken* ($\mu g\ ml^{-1}$)	*Found* ($\mu g\ ml^{-1}$)		*n*	s_r (%)	*Rel. error* (%)
			A.a.s.[a]	*D.p.p.*[b]			
Standards	1[c]	2.08	2.16	2.06	4	1.1	−0.96
	2	2.08	2.15	2.04	5	5.9	−1.9
	3	0.416	0.437	0.424	4	0.9	+1.9
	4[d]	0.0416	0.048	0.0395	4	5.8	−5.0
Natural waters	1[e]		2.5	2.14	2	7.9	
	2		0.05	0.0608	2	34	
	3[e]		2.79	2.8	2	2.3	
	4		0.120	0.109	4	3.9	

[a] Flame atomic absorption spectrophotometry: total Cr measured.
[b] Differential pulse polarography: only Cr(VI) measured.
[c] 2.38 μg Cu(II) ml^{-1} added.
[d] 0.0476 μg Cu(II) ml^{-1} added.
[e] Sampled below a cooling tower.

The use of differential pulse polarography requires little sample pretreatment and is shown to be a useful technique for analysis of chromium in natural water.

One of us (S.T.C.) gratefully acknowledges financial assistance in the form of an Oak Ridge Associated Universities participantship. We would also like to thank Marion Ferguson for the atomic absorption analyses. This work was performed at the Oak Ridge National Laboratory.

SUMMARY

A method utilizing differential pulse polarography for the determination of chromium(VI) in natural water is described. Additions of 0.62 μg Cu(II) ml^{-1} and 0.55 μg Fe(III) ml^{-1} did not interfere with the determination of 0.050 μg Cr(VI) ml^{-1}. The natural water samples containing chromium(VI) were buffered to approximately pH 7 with 0.1 *M* ammonium acetate and 0.005 *M* ethylenediamine and analyzed. Natural water samples of chromium content from 0.035 μg ml^{-1} to 2.0 μg ml^{-1} may be analyzed directly without further preparation. The detection limit is 0.010 μg ml^{-1}.

REFERENCES

1 *U. S. Geol. Surv., Water-Supply Pap.*, 2015 (1967) 15.
2 N. Cutshall, V. Johnson and C. Osterberg, *Science*, 152 (1966) 202.
3 R. Fukai, *Nature (London)*, 213 (1967) 901.
4 W. Mertz, *Physiol. Rev.*, 49 (1969) 163.
5 R. P. MacKenzie, R. U. Byerrum, C. F. Decker, C. A. Hoppert and R. F. Langham, *A.M.A. Arch. Ind. Health*, 18 (1958) 232.
6 K. Schwarz and W. Mertz, *Arch. Biochem. Biophys.*, 85 (1959) 292.
7 K. Schwarz and W. Mertz, *Arch. Biochem. Biophys.*, 72 (1957) 515.
8 *International Standards for Drinking Water*, World Health Organization, Geneva, 2nd edn., 1963.
9 *Public Health Rep.*, 61 (1946) 371.
10 J. Nix and T. Goodwin, *At. Absorption Newslett.*, 9 (1970) 119.
11 F. J. Fernandez and D. C. Manning, *At. Absorption Newslett.*, 10 (1971) 65.
12 K. W. Jackson, T. S. West and L. Balchin, *Anal. Chim. Acta*, 64 (1973) 363.
13 T. Maruta and T. Takeuchi, *Anal. Chim. Acta*, 66 (1973) 5.
14 *Annual Book of A.S.T.M. Standards, Pt. 23*, D1687-67, 1972.
15 C. E. Champion, G. Marinenko, J. K. Taylor and W. E. Schmidt, *Anal. Chem.*, 42 (1970) 1210.
16 M. Bigois, *Talanta*, 19 (1972) 147.
17 R. M. Bhatnagar and A. K. Roy, *Technology*, 3 (1966) 131.
18 *Princeton Applied Research Corporation Application Note AN-122*, 1973.
19 W. L. Belew, D. J. Fisher, H. C. Jones and M. T. Kelley, *Anal. Chem.*, 41 (1969) 779.
20 J. J. Lingane and I. M. Kolthoff, *J. Amer. Chem. Soc.*, 62 (1940) 852.
21 P. F. Urone, M. L. Druschel and H. K. Anders, *Anal. Chem.*, 22 (1950) 472.
22 J. H. Greene and A. Walkley, *Aust. J. Chem.*, 8 (1955) 51.

Analytica Chimica Acta, 75 (1975) 207–211

SHORT COMMUNICATION

Rapid identification by gas chromatography–mass spectrometry–computer of organic compounds resulting from the degradation of humic substances*

STEWART I. M. SKINNER and MORRIS SCHNITZER

Chemistry and Biology and Soil Research Institutes, Agriculture Canada, Ottawa, Ontario K1A 0C6 (Canada)

(Received 29th July 1974)

Humic substances are major components of the organic matter in soils, waters and sediments[1]. To throw light on the chemical structure of these complex materials, a number of degradative methods, involving both chemical and microbiological oxidation and reduction as well as hydrolysis with water, acid and base, have been employed[1]. The intention in each instance was to produce simpler compounds that could be identified and whose chemical structures would be related to those of the starting materials. As would be expected, the degradation of humic substances produces a large number of organic compounds whose qualitative and quantitative analysis challenges the ingenuity of chemists. Fortunately, only three types of major products are normally produced. These are aliphatic mono- and di-carboxylic acids, phenolic acids and benzenecarboxylic acids[2–4]. In recent years, Schnitzer *et al.*[2–4] have used a combination of column and thin-layer chromatographic methods for the separation of the degradation products, and gas chromatography–mass spectrometry (g.c.–m.s.) and micro-i.r. spectrophotometry of major peaks eluted from the gas chromatograph for identification purposes. While these methods constitute a significant advance over separation and identification methods that were available previously, they are nonetheless laborious and time-consuming. Thus, recent developments in the field of mass spectrometer–computer systems that are suitable for the gas chromatographic analysis of complex mixtures of organic compounds[5,6] were of particular interest. Briefly, these systems work as follows: mass spectra are recorded continuously, regardless of the emergence of gas chromatographic fractions, and all spectra are stored in the memory of the computer and transferred to magnetic disks. After the computerized g.c.–m.s. run is complete, a reconstructed gas chromatogram is plotted, with ion intensity on the vertical axis and scan number on the horizontal axis. These plots are very similar to conventional gas chromatograms.

Since previous investigations[2–4] had provided considerable information on the identities of major humic degradation products, it became possible to record mass chromatograms for fragments characteristic of specific compounds or groups

* Contribution No. 512, Soil Research Institute.

of compounds expected to occur in humic degradation mixtures, by searching through the stored spectral data for specific *m/e* ratios in order to identify the unknowns in the mixture. Hites and Biemann[6] have defined a mass chromatogram as "a gas chromatogram recorded with a detector that is specific for a given mass spectral fragment and thus is specific for a given compound type". The purpose of this communication is to illustrate the value of this method for the rapid identification of major products resulting from the hydrolysis of fulvic acid, a low-molecular weight, water-soluble, humic material that is a naturally occurring, efficient, metal-complexing agent widely distributed in soils and waters[7].

Experimental

Apparatus. The instrument used was a Finigan 3100D g.c.–m.s. system interfaced with a model 6000 data system. The g.c.–m.s. conditions were as follows: g.c. glass column: 1500 × 6 mm, 3% OV-17 on Chromosorb W, HMDS; injector temperature: 250°C; oven programmed from 90 to 270°C at 10°C min^{-1} and a helium flow of 30 ml min^{-1}. The separator temperature was 250°C; m.s. pressure: $1 \cdot 10^{-5}$ torr, resolution: 1:500, electron energy: 70 eV, and mass range: 40–500.

Fulvic acid. The fulvic acid originated from the Bh horizon (15–21 cm) of the Armadale soil, a poorly drained Podzol (4.2% C, pH 4.0) in Prince Edward Island. Methods of extraction, fractionation, purification and analytical characteristics of the fulvic acid have been described[8].

Degradation of fulvic acid. The degradation procedure consisted of a combination of ultrasonic vibration and hydrolysis with distilled water at 170°C. Fulvic acid (500 mg), dissolved in 50 ml of distilled water, was first dispersed at room temperature for 2 h with the aid of a Blackstone ultrasonic probe, operated at 20 kHz. The beaker was cooled during the ultrasonic treatment to prevent excessive heating. The solution was then transferred to a 300-ml stainless steel autoclave, equipped with a magnetic stirrer and a heating mantle, and heated at 170°C for 3 h. The fulvic acid was then treated with ultrasonics for another 30 min.

Separation of degradation products. The pretreated fulvic acid solution was acidified to pH 2, transferred to a liquid–liquid extractor and extracted for 24 h first with 150 ml of n-hexane and then with 150 ml of benzene. The organic extracts were combined, taken to dryness, dissolved in a small volume of methanol and methylated with diazomethane generated from Diazald. The dry methylated extract weighed 30.4 mg; it was dissolved in benzene and 1 μl of a 0.4% (w/v) solution was injected into the g.c.–m.s.–computer system.

Results and discussion

The Total Ionization Plot for the methylated fulvic acid oxidation mixture, based on the recording by the computer of 390 spectra during the 18 min the chromatogram was obtained is shown in Fig. 1. The first objective was to search for the presence of n-fatty acid methyl esters. These compounds have intense peaks at $m/e = 74$ and $m/e = 87$. Mass chromatograms at these two *m/e* values were prepared and are shown in Figs. 1(b) and 1(c). Only spectra nos. 176 and 225 in Fig. 1 (a) coincide with the corresponding scans at both $m/e = 74$ and $m/e = 87$, so that these

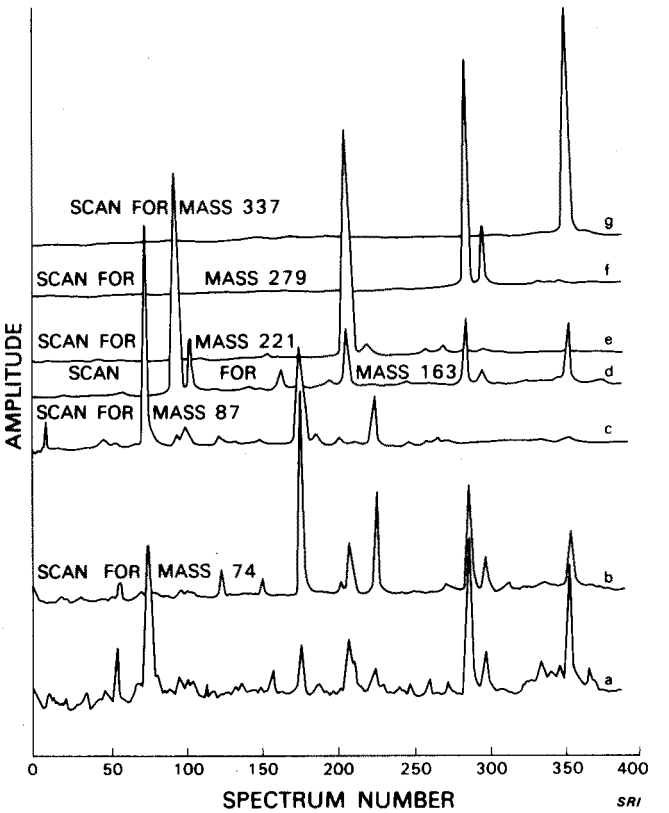

Fig. 1. Identification of methylated fulvic acid hydrolysis products. (a) Total Ionization Plot; (b) mass chromatogram for $m/e=74$; (c) mass chromatogram for $m/e=87$; (d) mass chromatogram for $m/e=163$; (e) mass chromatogram for $m/e=221$; (f) mass chromatogram for $m/e=279$; (g) mass chromatogram for $m/e=337$.

peaks are due to n-fatty acid methyl esters. Judged from their gas chromatographic retention times, they are the n-C16 and n-C18 fatty acid methyl esters. The mass chromatogram recorded at $m/e=87$ shows a strong peak at spectrum no. 75. The mass spectrum of the latter was identical with succinic acid dimethyl ester, with the peak at $m/e=87$ being due to $M^+-CO_2CH_3$. The mass chromatogram recorded at $m/e=74$ shows a number of additional peaks which are not due to n-fatty acid methyl esters but to aromatic fragments whose origins will be discussed below.

Another group of compounds that are usually major products when humic substances are degraded are benzenecarboxylic acids. The mass spectra of these compounds (as methyl esters) have base peaks at M^+-OCH_3, that is, at $m/e=163$ for benzenecarboxylic acid dimethyl esters, at $m/e=221$ for benzenetricarboxylic acid trimethyl esters, at $m/e=279$ for benzenetetracarboxylic acid tetramethyl esters, and at $m/e=337$ for the benzenepentacarboxylic acid pentamethyl ester. In addition, mass spectra of benzenepolycarboxylic acid methyl esters show significant peaks at $m/e=193$, 163, 134, 104 and 74. Mass chromatograms recorded at m/e 163, 221, 279 and 337 are shown in Figs. 1(d–g), respectively. A com-

parison of the latter four mass chromatograms with Fig. 1(a) shows that the peak at spectrum no. 95 and part of the peak at spectrum no. 105 are due to benzenedicarboxylic acid dimethyl esters. Similarly, spectrum no. 207 coincides with the base peak for benzenetricarboxylic acid trimethyl ester, spectrum nos. 290 and 297 with that for benzenetetracarboxylic acid tetramethyl esters, and spectrum no. 354 with that for benzenepentacarboxylic acid pentamethyl ester. The exact substitution patterns were obtained by determining gas chromatographic retention times of known and unknowns and by co-chromatography of knowns and unknowns.

A third group of compounds that are usually present among humic

TABLE I

COMPOUNDS IDENTIFIED IN THE FULVIC ACID HYDROLYSATE

Compound no.	*Spectrum index no.*	*Identity*
1	55	4-Methoxybenzenecarboxylic acid methyl ester
2	75	Succinic acid dimethyl ester
3	95	1,2-Benzenedicarboxylic acid dimethyl ester
4	105	1,4-Benzenedicarboxylic acid dimethyl ester
5	175	2-Methoxy-1,5-benzenedicarboxylic acid dimethyl ester
6	176	n-C16 Fatty acid methyl ester
7	207	1,2,3-Benzenetricarboxylic acid trimethyl ester
8	225	n-C18 Fatty acid methyl ester
9	290	1,2,3,4-Benzenetetracarboxylic acid tetramethyl ester
10	297	1,2,4,5-Benzenetetracarboxylic acid tetramethyl ester
11	354	Benzenepentacarboxylic acid pentamethyl ester

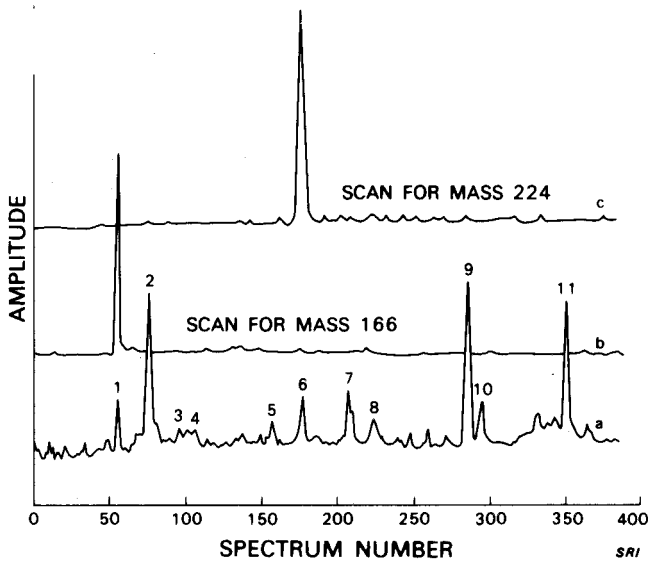

Fig. 2. Identification of methylated fulvic acid hydrolysis products. (a) Total Ionization Plot; (b) mass chromatogram for $m/e = 166$; (c) mass chromatogram for $m/e = 224$.

degradation compounds are phenolic acids. These compounds in fully methylated forms have well defined molecular ions. Figures 2(b) and 2(c) are mass chromatograms recorded at $m/e = 166$ (methoxybenzenecarboxylic acid methyl ester) and at $m/e = 224$ (methoxybenzenedicarboxylic acid dimethyl ester). A comparison of Fig. 2(a) with 2(b) and 2(c) shows that the peak at spectrum no. 55 corresponds to the molecular ion of methoxybenzenecarboxylic acid methyl ester and that at spectrum no. 175 is due to methoxybenzenedicarboxylic acid dimethyl ester. The Total Ionization Plot with identified peaks indicated by numerals is shown in Fig. 2(a). The compounds identified are listed in Table I. The identity of each compound was confirmed by: (1) running its mass spectrum; (2) eluting it from the gas chromatograph and recording its mass and i.r. spectrum; (3) matching its mass and i.r. spectrum with the known compound to which it corresponded; and (4) co-chromatography (on the gas chromatograph) of known and unknown.

The method described above makes possible the identification of the major humic degradation products in the hydrolysis mixture in about 30 min. This includes about 18 min for gas chromatographic separation and recording of the Total Ionization Plot plus 12 min for the identification of the major compounds. Thus, the method described herein permits the analysis of large numbers of humic samples in a relatively short time and allows for examination of the effects of various chemical and biological pretreatments as well as of the influence of geographical and pedological factors on the chemical structure of these materials. We are presently concentrating on the identification of the smaller peaks in the Total Ionization Plots.

We thank J. A. Neyroud for valuable collaboration.

REFERENCES

1 M. Schnitzer and S. U. Khan, *Humic Substances in the Environment*, Marcel Dekker, New York, 1972, pp. 4, 138–191.
2 G. Ogner and M. Schnitzer, *Can. J. Chem.*, 49 (1971) 1053.
3 S. U. Khan and M. Schnitzer, *Can. J. Chem.*, 49 (1971) 2302.
4 M. Schnitzer and S. I. M. Skinner, *Can. J. Chem.*, 52 (1974) 1072.
5 R. A. Hites and K. Biemann, *Anal. Chem.*, 40 (1967) 1217.
6 R. A. Hites and K. Biemann, *Anal. Chem.*, 42 (1970) 855.
7 M. Schnitzer and E. H. Hansen, *Soil Sci.*, 109 (1970) 333.
8 M. Schnitzer and S. I. M. Skinner, *Soil Sci.*, 105 (1968) 392.

Analytica Chimica Acta, 75 (1975) 212–216

SHORT COMMUNICATION

An internal-reference method for determination of trace elements in aluminum by neutron activation analysis

SHUENN-GANG CHEN, TONG-CHUIN PUNG, HUI-TUH TSAI and SHAW-CHII WU
Institute of Nuclear Energy Research, Atomic Energy Council, Lung-Tan, Taiwan (Republic of China)
(Received 17th May 1974)

Aluminum is widely used as a nuclear reactor material, and the impurities in aluminum tubes must be kept within certain specified limits. Methods for the determination of impurities in aluminum are numerous; polarography[1], emission spectrography[2], colorimetry[3] and conventional neutron activation analyses[4–6] are commonly used. In general, these methods are time-consuming and often involve complicated separation steps. Although emission spectrography avoids chemical separations, errors are usually significant. When the comparative technique of conventional neutron activation analysis is used, it is extremely difficult to achieve an accuracy better than $\pm 5\%$.

In this communication, a rapid and precise analytical method for aluminum flow tubes by the internal-reference method[7,8] of non-destructive neutron activation is proposed. There are no chemical separations, and chromium, copper, gallium, hafnium, cobalt, iron and scandium can be determined directly with good accuracy. Gold serves as an internal-reference element.

Experimental

Reagents. Copper, gallium, cobalt, iron and scandium oxides, and chromium, gold and hafnium metals were of high-purity grade (Johnson Matthey Chemicals). Aluminum tubes were obtained from Taiwan Aluminum Corporation (6061-T6) and Canadian aluminum (6061-T6) was supplied by Atomic Energy of Canada, Ltd. (AECL).

Preparation of samples. A series of synthetic mixtures of Cr–Cu–Ga–Au and Hf–Fe–Co–Sc–Au were prepared as follows. CuO and Cr were dissolved in nitric acid. Ga_2O_3, Fe_2O_3, Sc_2O_3 and Hf were dissolved in hydrochloric acid and hydrofluoric acid. Co_3O_4 was dissolved in warm perchloric acid, and gold metal in aqua regia. The weight ratios of these mixtures with known compositions were as follows:

Ga/Au: $7.817–6.253 \cdot 10^{-2}$.
Cu/Au: $1.583–6.330 \cdot 10^{-2}$.
Cr/Au: $3.245 \cdot 10^{2}–6.489 \cdot 10^{-1}$.
Co/Au: $2.608 \cdot 10^{1}–2.086 \cdot 10^{-1}$.
Hf/Au: $1.874 \cdot 10^{1}–3.748 \cdot 10^{-1}$.
Fe/Au: $1.686 \cdot 10^{3}–3.371 \cdot 10^{1}$.
Sc/Au: $1.133 \cdot 10^{1}–4.530 \cdot 10^{-2}$.

Aliquots of these mixtures were pipetted into quartz tubes (i.d. 6 mm), and 2.82 μg of gold was added to each sample.

The Taiwan and Canadian aluminum tubes were used as unknown samples; samples (0.5 g) were washed with dilute hydrochloric acid and distilled water, and the same gold solution was placed on the tube. The mixtures and unknown samples were evaporated to dryness under an infrared lamp. The tubes were then sealed, and wrapped in the same aluminum foil.

Irradiations and measurement. The samples were placed in a polyethylene tube capsule for pile irradiation, which was done in the Open-Pool Reactor at Tsing Hua University (neutron flux, $2 \cdot 10^{12}$ n cm^{-2} s^{-1}) for 4 h or 12 h.

After irradiation, the samples were cooled for 1–12 days before measurement. The γ-ray measurements were made with a Ge(Li) detector, with an active volume of 35 cm^3, coupled to a Hewlett-Packard 1024-channel pulse-height analyzer. Nuclide identification was made by energies and decay curve analyses of the specified γ-ray photopeaks.

Results and discussion

The nuclear properties of the isotopes used are summarized in Table I[9].

Figure 1(a) shows the γ-ray spectrum of Taiwan aluminum after irradiation

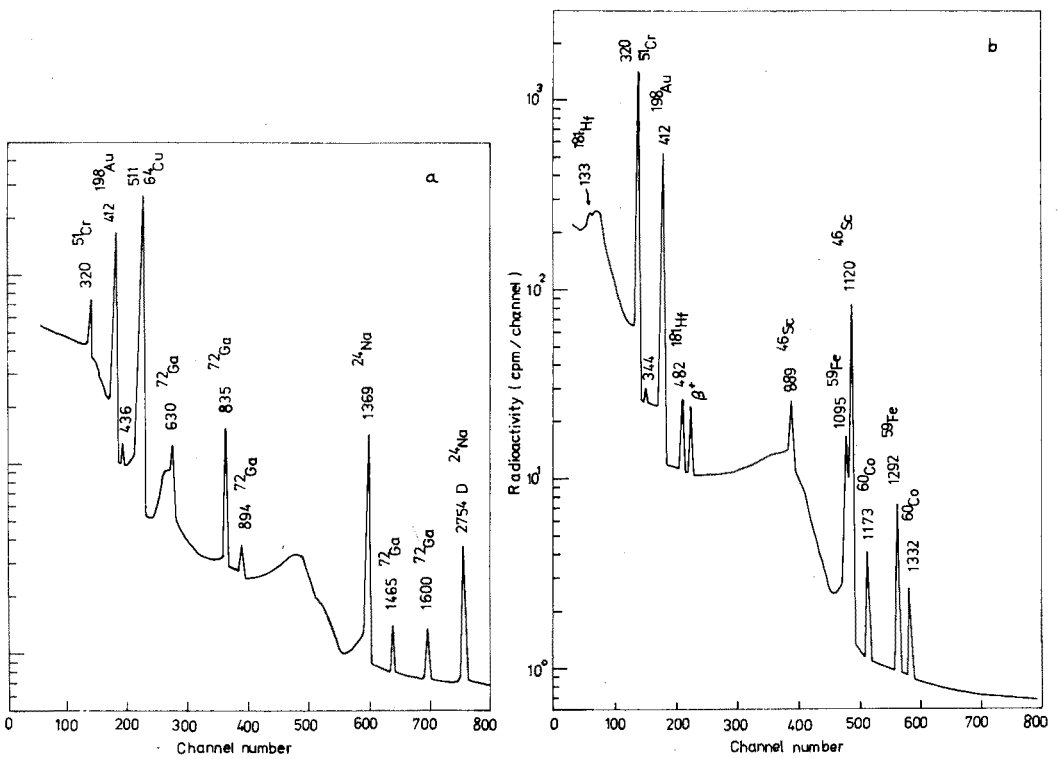

Fig. 1. γ-Ray spectrum of Taiwan aluminum sample: (a) 26 h after the end of a 4-h irradiation; (b) 12 days after the end of a 12-h irradiation.

TABLE I

NUCLEAR DATA

Element	*Isotope*	*Thermal neutron cross-section (barn)*	*Half-life*	*Energy (KeV)*
Au	^{198}Au	98.8	2.7 d	412
Cu	^{64}Cu	4.5	12.8 h	511
Ga	^{72}Ga	5.0	14.12 h	630, 835, 894, 1465, 1600
Cr	^{51}Cr	17	27.8 d	320
Hf	^{181}Hf	10	42.5 d	133, 346, 482
Fe	^{59}Fe	1.1	45.6 d	1095, 1292
Co	^{60}Co	19	5.26 y	1173, 1332
Sc	^{46}Sc	13	84 d	889, 1120

for 4 h and cooling for 26 h. The ^{51}Cr, ^{64}Cu and 1369-KeV ^{24}Na photopeaks stand out, as do five ^{72}Ga peaks; among the ^{72}Ga photopeaks, the 835-KeV peak is the most intense, and was therefore used for determination of gallium. The 1369-KeV ^{24}Na photopeak was produced from the ^{23}Na(n, r) ^{24}Na reaction, but a major fraction actually arose from the secondary reaction, ^{27}Al(n, α) ^{24}Na, and some was probably also produced by the ^{24}Mg(n, p) ^{24}Na reaction. This photopeak was therefore useless for the determination of sodium. The 412-KeV photopeak of ^{198}Au was used as the internal reference. The 320-KeV ^{51}Cr and 511-KeV ^{64}Cu photopeaks were used for the determination of Cr and Cu.

Figure 1(b) shows the γ-ray spectrum of Taiwan aluminum irradiated for 12 h to enhance the longer-lived activities induced in the aluminum. After a decay period of about 12 days, essentially all of the ^{24}Na, ^{64}Cu and ^{72}Ga had decayed, so that the γ-rays from ^{59}Fe, ^{60}Co, ^{51}Cr, ^{181}Hf and ^{46}Sc in the activated aluminum could be observed. The prominent γ-rays of 320-KeV ^{51}Cr, 482-KeV ^{181}Hf, 1095 and 1292-KeV ^{59}Fe, 1173 and 1332-KeV ^{60}Co, and 889 and 1120-KeV ^{46}Sc were observed.

The 1292-KeV ^{59}Fe peak is free from interference, and was used for determination of iron. The 482-KeV ^{181}Hf, 889-KeV ^{46}Sc and 1173-KeV ^{60}Co photopeaks were used to determine the respective metals.

Determination of Cu, Cr and Ga. The photopeaks indicated above were used for these determinations. The areas were measured and compared with the area of the 412-KeV ^{198}Au peak. In each case, a good proportionality was obtained between R_W and R_{A_0}, where R_w is the weight ratio of determined element to reference element, and R_{A_0} is the activity ratio of determined element to reference element. The results are given in Table II. Cr, Cu and Ga can be determined with relative errors of less than 3%.

Determination of Hf, Fe, Sc and Co. These elements were determined from the above-mentioned photopeaks in the same way as for the Cu–Cr–Ga mixture. Again good proportionality between R_w and R_{A_0} and good accuracy were achieved (Table II).

The proposed method was tested on Taiwan aluminum and Canadian aluminum for five different sample weights. Seven elements were found; chromium, copper and iron were more abundant than the other elements (Table III).

.E II

ɜHT RATIO (R_w) *vs.* ACTIVITY RATIO (R_{Ao}) FOR DIFFERENT MIXTURES

nt	R_w	R_{Ao}	R_w/R_{Ao}	*Mean value*	*s*	s_r (%)
a–Cr–Au Mixtures						
	$6.330 \cdot 10^{-2}$	$5.916 \cdot 10^{-3}$	$1.069 \cdot 10^{1}$	$1.035 \cdot 10^{1}$	$\pm 0.029 \cdot 10^{1}$	+2.9
	$6.329 \cdot 10^{-1}$	$6.222 \cdot 10^{-2}$	$1.017 \cdot 10^{1}$			
	$1.583 \cdot 10^{0}$	$1.553 \cdot 10^{-1}$	$1.019 \cdot 10^{1}$			
	$6.253 \cdot 10^{-2}$	$5.301 \cdot 10^{-3}$	$1.179 \cdot 10^{1}$	$1.181 \cdot 10^{1}$	$\pm 0.026 \cdot 10^{1}$	±2.2
	$6.254 \cdot 10^{-1}$	$5.299 \cdot 10^{-2}$	$1.180 \cdot 10^{1}$			
	$3.127 \cdot 10^{0}$	$2.716 \cdot 10^{-1}$	$1.151 \cdot 10^{1}$			
	$7.817 \cdot 10^{0}$	$6.432 \cdot 10^{-1}$	$1.215 \cdot 10^{1}$			
	$6.489 \cdot 10^{-1}$	$3.840 \cdot 10^{-4}$	$1.689 \cdot 10^{3}$	$1.711 \cdot 10^{3}$	$\pm 0.038 \cdot 10^{3}$	±2.7
	$6.489 \cdot 10^{0}$	$3.684 \cdot 10^{-3}$	$1.761 \cdot 10^{3}$			
	$6.489 \cdot 10^{1}$	$3.766 \cdot 10^{-2}$	$1.723 \cdot 10^{3}$			
	$3.245 \cdot 10^{2}$	$1.943 \cdot 10^{-1}$	$1.670 \cdot 10^{3}$			
e–Co–Sc–Au Mixtures						
	$3.748 \cdot 10^{-1}$	$7.490 \cdot 10^{-4}$	$5.004 \cdot 10^{2}$	$4.976 \cdot 10^{2}$	$\pm 0.147 \cdot 10^{2}$	±3.0
	$1.874 \cdot 10^{0}$	$3.663 \cdot 10^{-3}$	$5.116 \cdot 10^{2}$			
	$9.371 \cdot 10^{0}$	$1.870 \cdot 10^{-2}$	$5.011 \cdot 10^{2}$			
	$1.874 \cdot 10^{1}$	$3.930 \cdot 10^{-2}$	$4.768 \cdot 10^{2}$			
	$4.530 \cdot 10^{-2}$	$4.731 \cdot 10^{-4}$	$9.575 \cdot 10^{1}$	$9.491 \cdot 10^{1}$	$\pm 0.124 \cdot 10^{1}$	±1.3
	$2.266 \cdot 10^{-1}$	$2.360 \cdot 10^{-3}$	$9.602 \cdot 10^{1}$			
	$2.266 \cdot 10^{0}$	$2.430 \cdot 10^{-2}$	$9.325 \cdot 10^{1}$			
	$1.133 \cdot 10^{1}$	$1.197 \cdot 10^{-1}$	$9.465 \cdot 10^{1}$			
	$3.371 \cdot 10^{1}$	$2.586 \cdot 10^{-5}$	$1.304 \cdot 10^{6}$	$1.361 \cdot 10^{6}$	$\pm 0.044 \cdot 10^{6}$	±3.2
	$1.686 \cdot 10^{2}$	$1.221 \cdot 10^{-4}$	$1.381 \cdot 10^{6}$			
	$8.428 \cdot 10^{2}$	$6.227 \cdot 10^{-4}$	$1.354 \cdot 10^{6}$			
	$1.686 \cdot 10^{3}$	$1.201 \cdot 10^{-3}$	$1.404 \cdot 10^{6}$			
	$2.086 \cdot 10^{-1}$	$7.601 \cdot 10^{-5}$	$2.744 \cdot 10^{3}$	$2.718 \cdot 10^{3}$	$\pm 0.051 \cdot 10^{3}$	
	$1.043 \cdot 10^{0}$	$3.911 \cdot 10^{-4}$	$2.667 \cdot 10^{3}$			
	$5.216 \cdot 10^{0}$	$1.942 \cdot 10^{-3}$	$2.686 \cdot 10^{3}$			
	$2.608 \cdot 10^{1}$	$9.392 \cdot 10^{-3}$	$2.777 \cdot 10^{3}$			

TABLE III

γ-EMITTING IMPURITIES DETERMINED IN NEUTRON-ACTIVATED ALUMINUM

Element	*Taiwan-Al (p.p.m.)*	*Canadian-Al (p.p.m.)*
Cu	2890	3830
Cr	1210	923
Ga	77.6	112
Hf	1.2	1.7
Fe	4400	1930
Sc	1.4	1.5
Co	3.2	1.9

The author thanks the reactor staff for the neutron irradiations.

REFERENCES

1 I. M. Kolthoff and G. Matsuyama, *Ind. Eng. Chem., Anal. Ed.*, 17 (1945) 615.

2 M. Shavin, *Emission spectrochemical analysis*, Wiley–Interscience, New York, 1970.
3 I. P. Alimarin, *Analysis of high-purity materials*, Israel program for scientific translations, Jerusalem, 1968.
4 S. G. Prussin, J. A. Harris and J. M. Hollander, *Anal. Chem.*, 37 (1965) 1127.
5 M. Kakas, L. Marinkov and R. Draskovic, *Radiochim. Acta*, 13 (2) (1970) 75.
6 A. Alian and A. Haggag, *Talanta*, 14 (1967) 1109.
7 T.-C. Pung, T. Kato and Y. Oka, *Bull. Chem. Soc. Jap.*, 44 (1971) 1031.
8 T.-C. Pung, S.-C. Wu and H.-T. Tsai, *J. Chin. Chem. Soc.*, 20 (1973) 221.
9 C. M. Lederer, J. M. Hollander and I. Perlman, *Table of isotopes*, 6th edn., Wiley, New York, 1968.

Analytica Chimica Acta, 75 (1975) 217–220

SHORT COMMUNICATION

Varian-Techtron burners in atomic fluorescence spectrometry

P. MURUGAIYAN and S. NATARAJAN
Analytical Chemistry Division, Bhabha Atomic Research Centre, Bombay-400 085 (India)
(Received 15th July 1974)

Total combustion and premixed circular burners are used in atomic fluorescence spectrometry[1,2]. Premixed air–acetylene flames are generally preferred because of decreased interference from various ions[3], but a separated flame is reported to be better for the determination of zinc[4]. The recent Meker-type circular separated burner[5] is also considered preferable to an unseparated one. Slot burners are generally considered to be inferior to circular ones[6]. However, Varian-Techtron also recommend a slot burner (10 cm), placed at 45° to the optical axis[7]. In this communication the performances of circular and slot burners (Varian-Techtron) are compared with respect to scatter by acids and analytical sensitivity for zinc and cadmium by atomic fluorescence spectrometry.

Experimental

Zinc or cadmium solution. 1.000 g of zone-refined zinc or cadmium (supplied by the Chemistry Division of this Centre) was dissolved in hydrochloric acid (analytical grade, redistilled) and made up to 100 ml. The final acidity was 1 *M*. This solution was suitably diluted with 0.01 *M* acid to give a working solution of 0.10 μg Zn or Cd ml^{-1}.

Burners. The following Varian-Techtron burners were examined: air–C_2H_2 circular burner (FE-1; 16 holes), N_2O–C_2H_2 circular burner (FE-2; 8 holes), air–C_2H_2 circular burner (16-100053-00; 19 holes), N_2O–C_2H_2 circular burner (16-100028-00; 16 holes) with separator (01-100126), 6-cm slot burner (02-100035-00) and 10 cm slot burner (02-100036-00).

Zinc electrodeless discharge lamp. The lamp contained about 5 mg of zinc metal sealed under an argon pressure of 2–3 torr in a quartz tube of 8 mm i.d. and 3–4 cm length. It was operated at 85 W (110–25) power. The intensity of the light output was adequate to give a full scale fluorescence signal for 0.1 p.p.m. zinc in the air–acetylene flame.

The cadmium electrodeless discharge lamp and other equipment used were the same as described earlier[8].

Scatter from acids. Martin *et al.*[4] have studied the scattering caused by deionized water with three different burners. Scattering by 1 *M* hydrochloric acid in a fuel-lean air–acetylene flame at 228.8 nm has been reported[8]. Scatter has also been observed at 213.9 nm under comparable conditions for the zinc electrodeless

discharge lamp. Hence, the influence of different burners on scattering by acids was studied. Solutions of zinc or cadmium (0.1 p.p.m.) were aspirated into fuel-lean flames (*i.e.*, under conditions in which scattering is significant) and the fluorescence signals (with the respective lamps) were adjusted to 100 divisions. Under the same conditions, different acids of varying concentrations were aspirated. Scatter signals obtained were measured (Table I). Scatter by hydrochloric and perchloric acids is maximal with the FE-1 burner and is very small with other burners at both wavelengths used; scatter by nitric and sulphuric acids is very small with all burners. Separation of the flame with a 2 l min^{-1} flow of nitrogen did not decrease the scatter signal. At lower acidities than those given in Table I, the scatter was negligible.

TABLE I

SCATTER BY ACIDS FOR DIFFERENT BURNERS

(Air: 6 l min^{-1}; C^2H^2: 1.1 l min^{-1}, but 1.5 l min^{-1} for FE-2 and 16–100028 burners. 0.1 p.p.m. Cd or Zn = 100 divisions.)

Acid concn. (M)	*Air–C_2H_2*		*N_2O–C_2H_2*		*Slot*	
	FE-1	*16-100053*	*FE-2*	*16-100028*	*02-100036*	*02-100035*
Scatter signals at 213.9 nm						
HCl						
1.0	67	10	8	2	7	2
2.0	100	15	16	4	15	2
$HClO_4$						
1.0	38	19	10	5	2	4
2.0	84	20	10	6	1	2
HNO_3						
5.0	13	13	12	4	0	0
H_2SO_4						
1.0	9	3	3	2	1	1
Scatter signals at 228.8 nm						
HCl						
1.0	19	2	0	1	0	0
2.0	83	3	0	2	0	0
$HClO_4$						
1.0	3	2	1	0	0	0
2.0	7	1	1	0	0	0
HNO_3						
5.0	3	2	1	1	0	0
H_2SO_4						
1.0	1	0	0	0	0	0

Sensitivities. 0.1-p.p.m. Zn or Cd solutions were aspirated into the air–acetylene flame and the fluorescence signals were measured at 213.9 or 228.8 nm, respectively, under optimal flame conditions with different burners. The results are given in Table II.

TABLE II

FLUORESCENCE SIGNALS[a] FOR ZINC AND CADMIUM WITH DIFFERENT BURNERS
(Slit width, 300 μm; air, 15 p.s.i. (6 l min^{-1}); C_2H_2, 1.5 l min^{-1})

Metal	*Wavelength (nm)*	*Circular burner*				*Slot burner*			
		Air–C_2H_2		*N_2O–C_2H_2*		*N_2O–C_2H_2 6 cm (02-100035)*		*Air–C_2H_2 10 cm (02-100036)*	
		FE-1	*16-100053*	*FE-2*	*16-100028*	*A*[b]	*B*[c]	*A*[b]	*B*[c]
Cd	228.8	100	90	75	58	85	50	70	55
Zn	213.9	100	89	67	45	83	58	77	70

[a] Average of three readings taken at different times.
[b] Burner along the optical axis.
[c] Burner at about 45° to the optical axis.

Discussion

Scatter by hydrochloric acid (Table I) is significant at 213.9 and 228.8 nm, and depends on the fuel-to-oxidant ratio. Separation with nitrogen does not reduce the scattering (data not given). Scattering was maximal with the FE-1 burner, relatively less with the FE-2 burner, and minimal with the slot burners. It was relatively less with the more recent circular burner counterparts of the FE-1 and FE-2. Scattering depends on the way the old FE-2 burner is positioned, as the pattern of holes is not exactly circular.

The results in Table II show that comparable sensitivity can be obtained with circular and slot burners. Slot burners gave better sensitivity when positioned along the optical axis and not at 45°, and no increase in scatter was observed. Comparable sensitivity with slot burners may be understood from the work of Fassel[9], who has shown that maximal atom population is at the centre of the slot burner with an essentially Gaussian distribution.

Since scattering is minimal with slot burners without much loss in sensitivity, a 6-cm slot burner is probably best for the determination of zinc or cadmium.

The authors are grateful to Drs. Ch. Venkateswarlu and M. Sankar Das, Head of the Analytical Chemistry Division, for their keen interest and helpful suggestions. They also acknowledge the gift of some of the Varian-Techtron burners through Hinditron Pvt. Ltd., Bombay.

REFERENCES

1 J. D. Winefordner and R. A. Staab, *Anal. Chem.*, 36 (1964) 165.
2 R. M. Dagnall, T. S. West and P. Young, *Talanta*, 13 (1966) 803.
3 M. S. Cresser and T. S. West, *Anal. Chim. Acta*, 50 (1970) 517.
4 T. L. Martin, F. M. Hamm and P. B. Zeeman, *Anal. Chim. Acta*, 53 (1971) 437.
5 *Model 60 Atomic fluorescence accessory*, Varian-Techtron Product Memo, May, 1970.
6 R. Smith in J. D. Winefordner (Ed.), *Advances in Analytical Chemistry and Instrumentation Series*, Vol. 9, Wiley–Interscience, New York, 1971, p. 260.
7 *Separated flame burners*, Varian-Techtron Product Memo, May, 1970.
8 P. Murugaiyan, S. Natarajan and Ch. Venkateswarlu, *Anal. Chim. Acta*, 69 (1974) 451.
9 A. C. West, V. A. Fassel and R. N. Knisely, *Anal. Chem.*, 45 (1973) 1586.

Analytica Chimica Acta, 75 (1975) 221–224

SHORT COMMUNICATION

Direct determination of zinc in high-purity materials by flame atomic fluorescence spectrometry

P. MURUGAIYAN, S. NATARAJAN and CH. VENKATESWARLU
Analytical Chemistry Division, Bhabha Atomic Research Centre, Bombay-400 085 (India)
(Received 2nd August 1974)

The selectivity and sensitivity of atomic fluorescence spectrometry has already been utilized for direct determinations of cadmium at the 1-p.p.m. level in high-purity copper, indium and zinc[1]. This communication describes the direct determination of zinc at the 1-p.p.m. level in high-purity copper, indium and cadmium, and also deals with the interference caused by ionic fluorescence of cadmium, when the zinc used in the discharge lamp contains even microgram amounts of cadmium.

Experimental

Samples and instrumentation. A known weight (1 g) of zone-refined metal (supplied by the Chemistry Division of this Research Centre) was dissolved in 25 ml of nitric acid (1 + 1) and the solution was made up to 100 ml. This solution was suitably diluted with 0.01 *M* acid to give a working solution of 0.1 μg Zn ml^{-1}.

The zinc electrodeless discharge lamp was prepared as described earlier[2] and powered with Microtron-200 modulator unit, Mark II (285 Hz) and a 210L 3/4-wave resonance cavity (Electromedical Supplies, England). Spectra were recorded with a wavelength scanning accessory, Model 70 (Varian-Techtron) and a Rikedenki Kogyo Recorder, Model B-161.

All other reagents and equipment used were the same as described earlier[2], except that a nitrous oxide–acetylene slot burner was used.

Calibration curve. A 0.1-p.p.m. zinc solution (in 0.01 *M* acid) was aspirated into an air (6 l min^{-1})–acetylene (1.5 l min^{-1}) flame, with the slot burner kept along the optical axis (*i.e.*, perpendicular to the incident radiation). The zinc lamp was operated at 75 W (100–25) power. The fluorescence signal at 213.9 nm was adjusted to 100 divisions, for a slit width of 300 μm. Under these conditions, a linear calibration curve was obtained with 0.01–0.1 p.p.m. of zinc.

Effect of acidity. Zinc solutions of three concentrations (0.1, 1.0 and 10 μm ml^{-1}) in different acids (HCl, HNO_3 and H_2SO_4) of varying molarity were aspirated under the above-mentioned conditions. The fluorescence signal at 213.9 nm was measured, after the reading for the corresponding standard solutions with 0.01 *M* acidity had been set to 50 divisions. The results indicated that increase of acidity up to 1.0 *N* has no influence, while higher acidities cause a decrease in the signal.

Determination of zinc in OFHC copper, and zone-refined indium and cadmium. In the absence of standard analysed samples, synthetic samples (in solution) were prepared by dissolving 2.00 g of metal in 6 ml of zinc-free nitric acid and making the solution up to 50 ml after adding known amounts of zinc. These solutions were suitably diluted to give 10 mg of metal ml^{-1} and aspirated into the flame. From the fluorescence signal at 213.9 nm, the zinc content was determined. The results are given in Table I.

TABLE I

DIRECT DETERMINATION OF ZINC AT THE 1-p.p.m. LEVEL IN COPPER, INDIUM AND CADMIUM

Sample	*Zinc added* ($\mu g\ ml^{-1}$)	*Zinc obtained* ($\mu g\ ml^{-1}$)	*Difference* ($\mu g\ ml^{-1}$)
Copper (OFHC)		0.001	
	0.010	0.010	−0.001
	0.020	0.021	0.000
	0.030	0.034	+0.003
	0.040	0.043	+0.002
Indium (zone-refined)		0.001	
	0.010	0.010	−0.001
	0.020	0.021	0.000
	0.030	0.031	0.000
	0.040	0.043	+0.002
Cadmium-1 (zone-refined)		0.009	
	0.010	0.019	0.000
	0.020	0.029	0.000
	0.040	0.053	+0.004
	0.060	0.067	−0.002

Discussion

With a premixed air–acetylene flame, it has been shown[1] that common mineral acids up to 1.0 *N* have no influence on the fluorescence of cadmium. The present studies indicate a similar lack of effect for zinc. The influence of acids is qualitatively similar to that observed by Bratzel *et al.*[3] in a turbulent flame, but to a lesser extent.

The results in Table I show that zinc at the 1-p.p.m. level in copper, indium and cadmium can be directly determined without separation or pre-concentration. Since analytical-grade acids contain 0.1–0.4 p.p.m. of zinc, the samples should be dissolved in acids purified by distillation.

When zinc metal obtained from different sources was used to prepare the electrodeless discharge lamps, an interference (positive) in the determination of zinc in cadmium was observed with some lamps (Table II). Analysis of the zinc used for the preparation of these lamps showed the interference to be due to the cadmium content of the zinc. Hence, the relative intensities of radiations emitted by some of these lamps and by a dual-element electrodeless-discharge lamp with zone-refined zinc and cadmium at 213.9, 214.4, 226.5 and 228.8 nm were measured; the results are given in Table III. Interestingly, the Zn-3 lamp with a 0.04%

TABLE II

EFFECT OF DIFFERENT LAMPS ON THE DETERMINATION OF ZINC IN CADMIUM

(Slit, 300 μm; wavelength 213.9 nm)

Sample	*Zinc content (p.p.m.)*	
	Zn EDL (zone refined zinc)	*Zn EDL (zinc containing 400 p.p.m. Cd)*
Cadmium-1	2.9 2.5[a]	9.5
Cadmium-2	0.9	3.0
Cadmium-2 (with 0.5 mg K^+ ml^{-1})		0.9

[a] By atomic absorption.

TABLE III

RELATIVE INTENSITIES OF Zn AND Cd LINES IN ELECTRODELESS DISCHARGE LAMPS

(R.f. power 75 W (100-25); slit, 10 μm)

EDL No.	*Amount of metal present*		*Relative line intensities at (nm)*			
	Zn (mg)	*Cd (μg)*	*Zn I 213.9*	*Cd II 214.4*	*Cd II 226.5*	*Cd I 228.8*
Zn-1	5	0.005	100	0	0	0.5
Zn-2	5	0.05	100	0	0	0.5
Zn-3	5	2	74	26	30	100
Zn-4	5	5000	34	92	100	68

cadmium impurity gives a very intense light output at 228.8 nm (Cd I) and a significantly intense one at 214.4 nm (Cd II). Thus, it is similar to the dual-element lamp, Zn-4. Since the zinc values in the cadmium-1 sample (Table II) by atomic absorption and by atomic fluorescence with a pure zinc lamp are in reasonable agreement, the interference is attributed to the fluorescence of cadmium(II) at 214.4 nm. It was also observed that this could be practically eliminated by the addition of potassium salt to the sample solution (Table II).

When cadmium solution was aspirated into different flames (air–C_2H_2, N_2O–C_2H_2, N_2O–H_2, air–H_2), fluorescence of cadmium(II) was observed only when acetylene was used as the fuel. This lends support to the postulate[4] that Cd^+ is formed in the flames in the presence of CO molecules in the excited state.

Conclusion

The direct determination of zinc at the 1-p.p.m. level in high-purity copper, indium and cadmium is satisfactory in air–acetylene flames with a slot burner. Cadmium present as an impurity in the zinc in the electrodeless discharge lamps, causes a positive interference because of the ionic fluorescence of cadmium

at 214.4 nm. This can be obviated either by using a cadmium-free zinc lamp or by adding potassium(I) to the test solution to suppress ionization.

The authors are grateful to Dr. M. Sankar Das, Head of the Analytical Chemistry Division, for his keen interest and helpful discussions during this work.

REFERENCES

1 P. Murugaiyan, S. Natarajan and Ch. Venkateswarlu, *Anal. Chim. Acta*, 69 (1974) 451.
2 P. Murugaiyan and S. Natarajan, communicated to *Anal. Chim. Acta*.
3 M. D. Bratzel Jr., J. M. Mansfield Jr. and J. D. Winefordner, *Anal. Chim. Acta*, 37 (1967) 394.
4 C. Th. J. Alkemade in J. A. Dean and T. C. Rains (Eds.), *Flame Emission and Atomic Absorption Spectrometry*, Vol. I, Marcel Dekker, New York, 1969, p. 132.

Analytica Chimica Acta, 75 (1975) 225–226

SHORT COMMUNICATION

Fluorimetric determination of arylamines by coupling with N-(1-naphthyl)ethylenediamine

ROY J. STURGEON and STEPHEN G. SCHULMAN
College of Pharmacy, University of Florida, Gainesville, Florida 32610 (U.S.A.)
(Received 29th July 1974)

Arylamine type drugs have been routinely determined by diazotization, followed by coupling with the Bratton–Marshall reagent (N-(1-naphthyl)ethylenediamine) and subsequent colorimetric estimation of the resulting azoaromatic chromophores[1, 2]. This method has proven especially useful for the determination of benzenoid compounds whose absorption spectra lie well into the near ultraviolet and are thus out of the range of utility of the less expensive photometers based on glass optics.

Fluorimetric methods of analysis are usually much more sensitive than colorimetric methods for the same compounds. However, the benzenoid drugs which are usually amenable to colorimetric analysis by coupling of their diazo derivatives with the Bratton–Marshall reagent, are frequently weakly fluorescent or non-fluorescent. Moreover, the native fluorescences of these drugs are often in the near-ultraviolet region and are inaccessible to fluorimeters without quartz optics.

Recent investigations have shown the Bratton–Marshall reagent to be intensely fluorescent. The fluorescence at 427 nm, occurring between pH 1 and 9, is linear with concentration of the reagent down to $1 \cdot 10^{-10}$ *M*. The products of the coupling of diazotized arylamines with the Bratton–Marshall reagent, however, do not exhibit any measurable fluorescence. A study of the quenching of the fluorescence of the Bratton–Marshall reagent by reaction with diazotized sulfanilamide was carried out, with the usual procedure for diazotization, coupling and destruction of the excess of nitrous acid[2]. In each case, the concentrations of sulfuric acid and sodium nitrite used to generate the nitrous acid for diazotization of the sulfanilamide were $4.00 \cdot 10^{-2}$ *M* and $1.45 \cdot 10^{-3}$ *M*, respectively, and the concentration of ammonium sulfamate employed to destroy the excess of nitrous acid was $4.38 \cdot 10^{-3}$ *M*. The absolute concentrations of sulfanilamide and N-(1-naphthyl)ethylenediamine were varied by serial dilutions. Four relative molar concentrations of each were employed (0.150, 0.300, 0.450 and 0.600) for the ratio sulfanilamide/Bratton–Marshall reagent in each set of serial dilutions. It is necessary for the concentration of the Bratton–Marshall reagent always to be in slight molar excess (within an order of magnitude) over the concentration of the arylamine if reasonable sensitivity is to be observed in the quenching of the fluorescence of the former.

If I_0 is the measured intensity of the fluorescence of the Bratton–Marshall reagent in any sample before reaction with the diazotized amine and I is the measured fluorescence intensity of the same sample after coupling with the diazotized amine, a linear plot of $I_0 - I$ against sulfanilamide concentration, with unit slope, indicates quantitative reaction of the diazotized amine with the Bratton–Marshall reagent. In the case of sulfanilamide, such a plot was obtained, which was linear down to $1 \cdot 10^{-8}$ M. This is about three orders of magnitude more sensitive than the identical analysis performed colorimetrically. Consequently, it is concluded that the quenching of the fluorescence of the Bratton–Marshall reagent by coupling with diazotized amines represents an extremely sensitive means of quantitative analysis for arylamines which themselves have poor fluorescent properties.

REFERENCES

1 A. C. Bratton, E. K. Marshall, D. Babbit and A. R. Hendrickson, *J. Biol. Chem.*, 128 (1939) 537.
2 K. A. Connors, *Amer. J. Pharm. Educ.*, 29 (1965) 29.

Analytica Chimica Acta, 75 (1975) 227–230

SHORT COMMUNICATION

Phenylhydrazones of pyridine-2-aldehyde and pyridine-4-aldehyde as new acid–base indicators

G. S. VASILIKIOTIS and J. STRATIS

Laboratory of Analytical Chemistry, University of Thessaloniki, Thessaloniki (Greece)

(Received 20th July 1974)

During an investigation of the complexing properties of hydrazones formed by the reaction of phenylhydrazine with the three isomeric pyridinealdehydes, it was noticed that their colourless solutions became intensely yellow on adding an acid. These compounds are the phenylhydrazones of pyridine-2-aldehyde (*o*-PPH, I), pyridine-3-aldehyde (*m*-PPH, II) and pyridine-4-aldehyde (*p*-PPH, III). There are no data on the ionization constants of these compounds in the literature. As these compounds are very stable in strongly acidic or alkaline medium, it was considered interesting to investigate their acid–base properties.

The present communication deals with the spectrophotometric study of these compounds, the determination of their ionization constants and their analytical application as acid–base indicators.

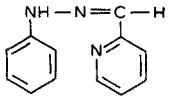

I

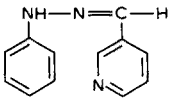

II

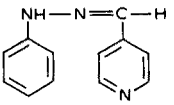

III

Experimental

Reagents. The three isomeric pyridinealdehyde phenylhydrazones were prepared by refluxing equimolar quantities of phenylhydrazine (Merck) with pyridine-2-aldehyde, pyridine-3-aldehyde or pyridine-4-aldehyde (Ferak, Berlin) in ethanolic solutions. The crude products were recrystallized twice from methanol–water mixture. Their purity was checked by t.l.c. on silica gel G (Merck) and by m.p. (181°C for *o*-PPH, 157°C for *m*-PPH and 177.5°C for *p*-PPH) which were in agreement with those given in the literature[1,2]. The substances were used as indicators in ethanolic 0.1% (w/v) solutions.

Buffer solutions of constant ionic strength were prepared by using mixtures of citric acid, disodium hydrogenphosphate and potassium chloride[3].

Titration procedure. Freshly prepared 0.1 *M* solutions of sodium hydroxide and hydrochloric acid were used for titrations.

Samples (20–40 ml) were mixed with 2–4 drops of the indicator solution and titrated in the usual way. End-points were taken at the first appearance of a yellow

colour stable for at least 15 s. The acid was selected as the titrant because the protonated forms of the two indicators are highly coloured.

Absorption spectra and dissociation constants

Some absorption spectra of the isomeric hydrazones *o*-PPH, *m*-PPH and *p*-PPH at different pH values are shown respectively in Figs. 1–3. The spectra of *o*-PPH and *p*-PPH clearly demonstrate the change in absorbance with change of pH. In both cases, only one isosbestic point was found, indicating only one true acid–base equilibrium. In the case of *m*-PPH (Fig. 2) there is no clear isosbestic

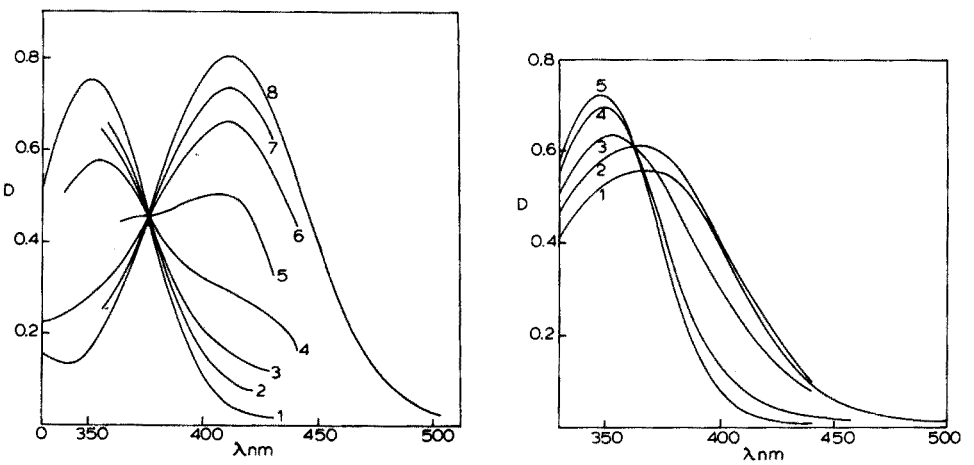

Fig. 1. Absorption spectra of $4.00 \cdot 10^{-5}$ *M* *o*-PPH in water containing 4% (v/v) ethanol at pH: (1) 12.50, (2) 6.31, (3) 5.88, (4) 5.45, (5) 4.99, (6) 4.58, (7) 4.20 and (8) 1.19.

Fig. 2. Absorption spectra of $4.00 \cdot 10^{-5}$ *M* *m*-PPH in water containing 4% (v/v) ethanol at pH: (1) 1.15, (2) 3.66, (3) 4.60, (4) 5.15 and (5) 12.78.

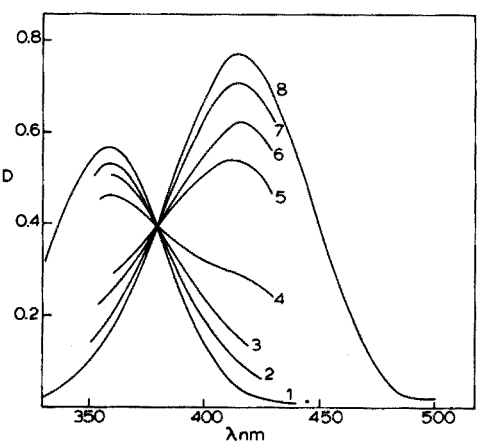

Fig. 3. Absorption spectra of $2.67 \cdot 10^{-5}$ *M* *p*-PPH in water containing 4% (v/v) ethanol at pH: (1) 12.35, (2) 7.06, (3) 6.68, (4) 6.21, (5) 5.65, (6) 5.49, (7) 4.98 and (8) 1.37.

point nor considerable change in absorbance with pH. This behaviour of the *o*-PPH and *p*-PPH compounds is attributed to protonation on the pyridine nitrogen as the pH decreases. Protonation results in an increase in the conjugation of the ring systems:

Reaction I

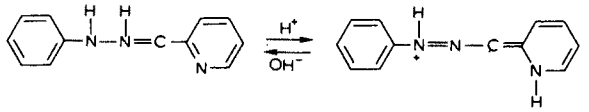

Reaction II

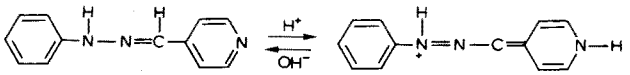

The change in structure is not possible for the *m*-PPH isomer.

Maximal absorption wavelengths for the *o*-PPH and *p*-PPH neutral species are respectively 352 nm and 360 nm, while those for the charged species (yellow acidic solutions) are 410 nm and 415 nm. The corresponding molar absorptivities of the charged species at pH 1.20 are $2.03 \cdot 10^4$ l mol^{-1} cm^{-1} for *o*-PPH, and $2.88 \cdot 10^4$ l mol^{-1} cm^{-1} for *p*-PPH.

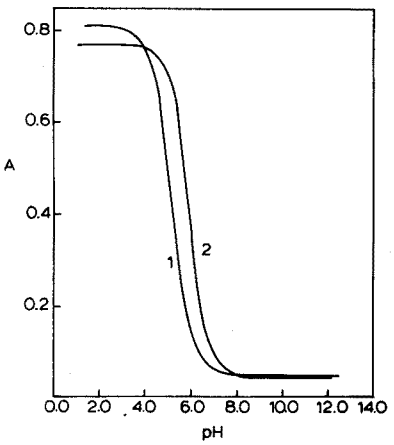

Fig. 4. Plots of absorbance *vs.* pH for: (1) $4.00 \cdot 10^{-5}$ *M* *o*-PPH in 4% (v/v) ethanol at 410 nm; (2) $2.67 \cdot 10^{-5}$ *M* *p*-PPH in 4% (v/v) ethanol at 415 nm.

Plots of absorbances at the maximal absorption wavelength against pH values of the solution were prepared Fig. 4, and dissociation constants were calculated by conventional methods[4]. The constants found in water–methanol and water–ethanol mixtures are listed in Table I. When a weak acid is negatively charged or uncharged, pK increases in ethanolic or methanolic medium[5]; the case is reversed when the molecule is positively charged.

Applications

The ability of *o*-PPH and *p*-PPH solutions to change colour sharply was

TABLE I

DISSOCIATION CONSTANTS IN WATER–METHANOL AND WATER–ETHANOL MIXTURES
(20°C, ionic strength 0.01; 5 determinations.)

%(v/v) MeOH	*o-PPH, pK_a*	*p-PPH, pK_a*	*%(v/v) EtOH*	*o-PPH, pK_a*	*p-PPH, pK_a*
4	5.26±0.02	6.05±0.02	4	5.16±0.02	5.98±0.02
20	5.13±0.02	5.96±0.02	20	5.03±0.02	5.89±0.02
40	4.94±0.03	5.70±0.03	40	4.58±0.02	5.52±0.02
60	4.70±0.03	5.43±0.03	60	4.34±0.03	5.29±0.03

tested by performing ten titrations of 20 ml of 0.1 *M* sodium hydroxide with 0.1 *M* hydrochloric acid. One colour transition was found at pH equal to $pK \pm 1$ (colourless to yellow). With both indicators, clear end-points were obtained. With *o*-PPH, the average deviation from the mean was 0.1% (maximum 0.1%); with *p*-PPH, the average deviation from the mean was 0.05% (maximum 0.15%). There was no systematic bias in either case, showing that indicator blanks were negligible. The reverse titrations were also tested, disappearance of the yellow colour indicating the end-point, and results were again satisfactory. However, the end-points were more distinct when the strong acid was used as a titrant.

The precision obtained for each indicator was completely satisfactory, clearly demonstrating the value of both compounds as acid–base indicators. They show complete reversibility. Ethanolic solutions of *o*-PPH or *p*-PPH (0.1%) were stable on exposure to diffuse daylight and artificial light for ten days; there was no change in their spectral characteristics.

Both indicators were found suitable for titrations of a weak base. Ammonia (0.1 *M*) was titrated with hydrochloric acid and sharp end-points were obtained. They are also suitable for spectrophotometric titrations.

REFERENCES

1 Beilstein, *Handbuch der Organischen Chemie, Band XXI*, Springer-Verlag, Berlin, Vierte Auflage, 1935, pp. 288, 289.
2 U. Boekelheide and W. J. Linn, *J. Amer. Chem. Soc.*, 76 (1954) 1286.
3 P. J. Elving, J. M. Markowitz and I. Rosental, *Anal. Chem.*, 28 (1956) 1179.
4 A. Albert and E. P. Serjeant, *The Determination of Ionization Constants*, Chapman and Hall, London, 2nd edn., 1971, p. 44.
5 C. Berlin, *Anal. Chim. Acta*, 7 (1952) 105.

Analytica Chimica Acta, 75 (1975) 231–234

SHORT COMMUNICATION

Spectrophotometric determination of iron with 2,2′-Dipyridyl-2-pyridylhydrazone

H. ALEXAKI-TZIVANIDOU

Department of Physiology and Pharmacology, Veterinary Faculty, Aristotelian University of Thessaloniki (Greece)

(Received 15th July 1974)

The use of 2,2′-bipyridine, 1,10-phenanthroline, 2,2′,2″-terpyridine and related compounds as organic reagents for the determination of trace metal ions is well known[1–3]. The chromogenic group of these compounds, –N=C–C=N– or –N=C–C–N=C–C=N–, extended or slightly modified as –N=C–NH–N=C–C=N–, is found in some nitrogen-containing heterocyclic hydrazones of the general type I (where X=H, CH_3 to n-C_6H_{13}).

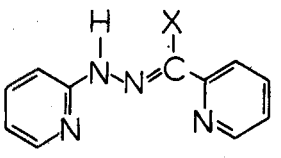

I

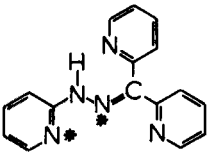

II

The possibilities of the type I hydrazones as analytical reagents were first outlined by Lions and Martin[4] and Geldard and Lions[5]. Later Going and Pflaum[6] substituted Ph for X. These compounds behave as bidentate[7,8] or tridentate[5,9] ligands, forming intensely colored complexes with transition metal ions. In alkaline solution the H-atom of the imino-group can split off and neutral metal complexes are formed[4,10,11].

In a previous work[12] the author synthesized 2,2′-dipyridylhydrazone (DPPH, II) and showed it to be a sensitive reagent for palladium(II), vanadium(V), copper-(II), and zinc(II)[12]. Cobalt(II) can also be determined[13].

This communication deals with the use of DPPH as an analytical reagent for iron.

Experimental

Apparatus. A Unicam SP 800 recording spectrophotometer was used with 10-mm matched quartz cells. pH measurements were performed with a L. Pusle, ACL-112 pH meter.

Reagents. 2,2′-Dipyridyl-2-pyridylhydrazone (DPPH) was prepared as

follows. An ethanolic solution of equimolar quantities (0.4 *M*) of di-(2-pyridyl)-ketone (Aldrich Chem. Co. Inc.) and 2-pyridylhydrazine (Aldrich Chem. Co. Inc.) were refluxed for 8 h. The reagent was separated after cooling and recrystallized from ethanol. (Light yellow needles, m.p. 137.5–138.5°C).

A $1 \cdot 10^{-2}$ *M* solution of the reagent was prepared by dissolving 0.2753 g of DPPH in 100 ml of ethanol. Such solutions are stable for several months when kept in an amber glass bottle. A standard iron(III) solution, $1 \cdot 10^{-2}$ *M*, was prepared by dissolving the appropriate amount of pure metal iron in nitric acid (1+3). Nitrogen oxides were expelled by boiling. Ascorbic acid solution (10%) was prepared every 3 days and was kept in an amber glass bottle.

Perchloric acid, sodium hydroxide solution and acetic acid–sodium acetate, boric acid–borax and borax–sodium hydroxide buffer solutions were used for pH adjustment. The ethanol was distilled and the water was redistilled from an all-pyrex glass apparatus. All reagents used were of analytical grade. Special care was taken to avoid contamination by iron.

Results and discussion

Absorption spectra. Both iron(II) and iron(III) react with DPPH to form colored complexes, but the molar absorptivity for the iron(II) complex (*ca.* $15.0 \cdot 10^3$ at pH 2.9, and $11.7 \cdot 10^3$ at pH 10.9 at the wavelength for maximum absorbance) is higher than for the iron(III) complex (*ca.* $11.2 \cdot 10^3$ at pH 2.9 and $2.4 \cdot 10^3$ at pH 10.9 at the wavelength for maximum absorbance) (Fig. 1). Moreover, the formation of the iron(II)–DPPH complex is rapid while that of the iron(III)–DPPH complex is not. Accordingly iron(III) should be reduced by ascorbic acid.

Effect of pH. A pH study was carried out over the range of 0.5–12.0. As shown in Fig. 1, two complexes of iron(II) with DPPH are formed: one in acid solution (λ_{max} 538 nm) and another in alkaline solution (λ_{max} 581 nm). According to Chiswell and Lions[10] the first complex is probably a cationic complex and the second a neutral one. The reaction between iron(II) and DPPH is more sensitive in acidic solution and the optimal pH range for the complex formation is 1.50–3.50; the absorbance increases steeply around pH 1 and decreases slowly above pH 3.5.

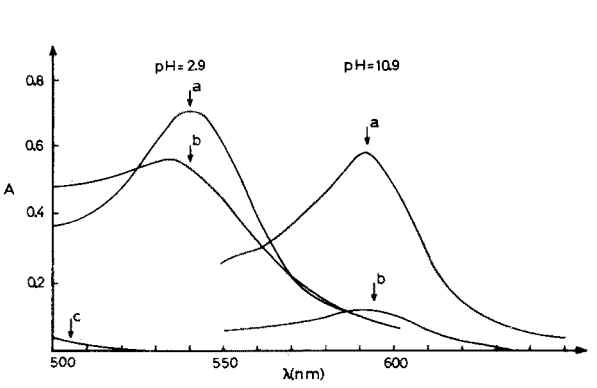

Fig. 1. Absorption spectra at pH 2.9 and 10.9 $5 \cdot 10^{-5}$ *M* iron in the presence of $5 \cdot 10^{-4}$ *M* DPPH, *vs.* a reagent blank: (a) Fe(II)–DPPH; (b) Fe(III)–DPPH; (c) $5 \cdot 10^{-4}$ *M* DPPH *vs.* H_2O.

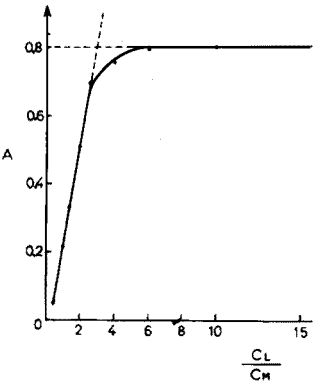

Fig. 2. Mole ratio method. $5.6 \cdot 10^{-5}$ *M* Fe(II). pH 2.8±0.2; 538 nm.

The order of reagent addition. In acidic solution the addition of DPPH before or after pH adjustment does not influence the formation of the iron(II)–DPPH complex. In alkaline solution, DPPH should be added before the buffer, in order to avoid iron(II) precipitation. Figure 2 shows that a 10-fold excess of DPPH is sufficient for complete color development.

Composition and stability of the complex. At pH 1.50–3.50 full color development takes place in 30 s and the intensity of the purple color is stable for at least 8 h. A mole ratio plot at pH 2.8 ± 0.2 and 538 nm (Fig. 2) shows that a 1:3 iron(II)–DPPH complex is formed.

In accordance with Bell and Rose[14] and Bruce *et al.*[15], the probable structure of the complex has the iron bonded to the two asterisked nitrogens of formula II, the whole forming a divalent cation.

Beer's law. The system obeys Beer's law over the concentration range $1 \cdot 10^{-5}$–$6 \cdot 10^{-5}$ *M* iron(II) or 0.6–3.3 p.p.m., at pH 1.50–3.50 and 538 nm. The optimal range, evaluated by Ringbom's method[16] is 0.7–2.8 p.p.m. The molar absorptivity is $15.0 \cdot 10^3$ l mole^{-1} cm^{-1} and the sensitivity of the reaction, as defined by Sandell[18], is 0.0037 μg Fe(II) cm^{-2} for an absorbance of 0.001 at 538 nm.

Effect of other ions. This study was undertaken with the purpose of determining serum iron with DPPH. Tests for interfering ions were restricted mainly to those ions present in sera and, in most cases, in the corresponding concentrations. Interference was regarded as significant when it produced a difference of more than $\pm 3\%$ in absorbance from that found with iron ions alone.

The following ions did not interfere: (a) large excess (500:1): K^+, Na^+, Cl^-, NO_3^-, SO_4^{2-}, ClO_4^-, acetate; (b) 100-fold excess: Ca^{2+}, Mg^{2+}, lactate; (c) 5-fold excess: Al^{3+}, Mg^{2+}, Zn^{2+}, Cd^{2+}, Cu^{2+}, provided that there is a sufficient excess of ligand to react with iron, and F^-, PO_4^{3-}, citrate.

Cobalt(II) interferes strongly.

Recommended procedure. Dissolve the sample by appropriate means. Take an aliquot containing 40–150 μg of iron(III). Dilute to about 40 ml with double-distilled water. Add 2 ml of 10% ascorbic acid solution. Allow the solution to stand for 1 min, then add 2.5 ml of ethanolic solution of DPPH ($1 \cdot 10^{-2}$ *M*). Adjust the pH to 1.60–3.40 with sodium hydroxide solution or perchloric acid, and

TABLE I

COMPARISON WITH SOME OTHER REAGENTS FOR IRON

Reagent	*Sensitivity* (10^3 *l mole*$^{-1}$ *cm*$^{-1}$)	*Extraction*	*Ref.*
Thiocyanate	7.0 (480 nm)		3, 17
Thiocyanate and tributyl ammonium	22.0 (480 nm)	in amyl acetate	3, 17
1,10-Phenanthroline	11.0 (505–508 nm)		3,17
4,7-Biphenyl-1,10-phenanthroline	22.0 (533 nm)	in isoamyl- and ethyl-alcohols	3
2,2-Bipyridyl	8.0 (522 nm)		3, 17
Ferron	4.0 (610 nm)		3, 17
DPPH	15.0 (538 nm)		Present work

dilute to 50 ml with double-distilled water. Measure the absorbance at 538 nm *vs.* a reagent blank. Calculate the metal ion concentration from a previously prepared calibration curve.

Precision. The mean absorbance value of 14 samples, containing iron(II) in a concentration of $2.8 \cdot 10^{-5}$ *M* was 0.412 at 538 nm. The standard deviation was 0.003 absorbance unit and the relative standard deviation 0.82%.

Comparison with some other reagents. DPPH compares well with the most sensitive and widely used reagents for the spectrophotometric determination of iron. Some data are given in Table I. The determination of iron by DPPH is rapid and simple. The reaction takes place almost immediately at room temperature and the produced color is sufficiently stable. This is an advantage over the thiocyanate reagent. There is no need of a strict control of the pH nor of an extraction, which is an advantage over the thiocyanate–tributyl ammonium and the 4,7-diphenyl-1,10-phenanthroline methods. The reagent does not absorb at the wavelength for maximum absorbance for the complex.

The author is grateful to Professor G. Vasilikiotis for his interest and helpful discussions, and to Professor V. Vasilopoulos for providing laboratory facilities.

REFERENCES

1 A. A. Schilt, *Analytical Applications of 1,10-Phenanthroline and Related Compounds*, Pergamon, Oxford, 1st edn., 1969, p. 54.
2 R. T. Pflaum and C. Smith, *Anal. Chim. Acta*, 31 (1964) 341.
3 E. B. Sandell, *Colorimetric Determination of Traces of Metals*, Interscience, New York, 3rd edn., 1965, pp. 525, 784.
4 F. Lions and K. Martin, *J. Amer. Chem. Soc.*, 80 (1958) 3858.
5 J. F. Geldard and F. Lions, *J. Amer. Chem. Soc.*, 84 (1962) 2262; *Inorg. Chem.*, 2 (1963) 270.
6 J. E. Going and R. T. Pflaum, *Anal. Chem.*, 42 (1970) 1098.
7 J. G. Dunn and D. A. Edwards, *Inorg. Nucl. Chem. Lett.*, 5 (1969) 539.
8 A. T. Casey and R. A. Horsley, *Austr. J. Chem.*, 22 (1969) 2309.
9 R. Green, P. Hallman and F. Lions, *Inorg. Chem.*, 3 (1964) 1541.
10 B. Chiswell and F. Lions, *Austral. J. Chem.*, 22 (1969) 71.
11 V. Zatka, J. Abraham, J. Holzbecher and D. E. Ryan, *Anal. Chim. Acta*, 54 (1971) 65.
12 H. Alexaki-Tzivanidou, Doctoral Thesis, University of Thessaloniki, May 1972.
13 G. Vasilikiotis, Th. Kouimtzis, C. Apostolopoulou and A. Voulgaropoulos, *Anal. Chim. Acta*, 70 (1974) 319.
14 C. F. Bell and D. Rose, *Inorg. Chem.*, 7 (1968) 325.
15 St. L. Bruce, M. K. Cooper and B. G. McGrath, *J. Chem. Soc. D*, (1970) 69.
16 A. Ringbom, *Z. Anal. Chem.*, 115 (1939) 332.
17 G. Charlot, *Colorimetric Determination of Elements*, Elsevier, London, 1964, p. 272.
18 E. B. Sandell, *Colorimetric Determination of Traces of Metals*, Interscience, New York, 3rd edn., 1965, p. 83.

Analytica Chimica Acta, 75 (1975) 235–238

SHORT COMMUNICATION

Spectrophotometric determination of rhenium with *o*-hydroxythiobenzhydrazide

P. K. GANGOPADHYAY and S. C. SHOME
Department of Chemistry, Presidency College, Calcutta-700012 (India)
(Received 12th August 1974)

Sensitive and selective methods for the determination of rhenium are of great importance because of scarcity of the metal in nature. The potassium thiocyanate method[1] with tin(II) chloride has been investigated by several workers for the spectrophotometry of rhenium. Geilmann and Neeb[2] recommended 2,4-diphenylthiosemicarbazide as a spectrophotometric reagent for the determination of the metal. Other reagents that have been employed for the colorimetric determination of rhenium are α-furildioxime[3], methyl-2-pyridylketoxime[4] and thiosalicylic acid[5]. Pollock and Zopatti[6] investigated fifty organic reagents with a view to their applications in the determination of the metal. Likussar *et al.*[7] used ammonium pyrrolidinedithiocarbamate for the ultraviolet spectrophotometry of rhenium(VII). None of the organic reagents used so far, however, seems to possess any advantage over the potassium thiocyanate method.

In the present investigation, *o*-hydroxythiobenzhydrazide (HTBH) which was found to be a suitable reagent in the spectrophotometry of ruthenium[8] and platinum(IV)[9], was studied for the colorimetric determination of microamounts of rhenium. Perrhenic acid after reduction with tin(II) chloride in weakly acidic medium forms a blue–violet precipitate with HTBH in hot solution. The complex is slightly soluble in water, but readily soluble in 50% ethanol. The ethanolic solution shows maximal absorbance at 560–570 nm and obeys Beer's law over the concentration range 1.32–26.40-μg Re ml^{-1}. The colour of the solution is stable for at least 24 h. The optimal acidity for full colour development is 0.2–0.5 *M* in hydrochloric acid. The method permits the determination of rhenium in the presence of considerable amounts of foreign ions. Molybdenum(VI), which produces low results in the determination of rhenium, is removed by extracting with N-benzoylphenylhydroxylamine in chloroform.

Experimental

Apparatus. A Carl-Zeiss PMQ II Spectrophotometer with matched 1-cm quartz cells was used for the absorbance measurements.

Standard rhenium solution. A weighed amount of metallic rhenium (B.D.H., 99.9%) was dissolved in nitric acid; the solution was evaporated to a small volume on a boiling water bath, cooled and diluted with water. The solution was transferred to a volumetric flask and diluted to the mark. Dilute solutions

for spectrophotometric measurements were prepared from the stock solution.

Tin(II) chloride solution. A 10% solution of tin(II) chloride dihydrate (reagent grade) was prepared in 2 *M* hydrochloric acid. The solution was filtered and stored in a stoppered bottle under a layer of xylene.

Solutions of diverse ions. Standard solutions of the diverse ions were obtained by dissolving weighed quantities of A.R. grade reagents in distilled water or dilute hydrochloric acid.

Reagent solution. The reagent was prepared as described previously[8] and was used as a 0.02 *M* solution in ethanol.

Procedure. Place a measured amount of perrhenic acid solution (50–350 μg Re) in a 25-ml volumetric flask, add 1.0 ml of tin(II) chloride solution and adjust the acidity of the solution to 0.5–1.0 *M* in respect of hydrochloric acid. Add an ethanolic 0.02 *M* solution (2–5 ml) of *o*-hydroxythiobenzhydrazide (the total volume of the resulting solution should not exceed 12 ml). Heat the solution on a boiling water bath for 30 min, cool to room temperature and make the volume up to the mark with dilute hydrochloric acid, water and ethanol so that the final solution becomes 50% in respect of ethanol and 0.2–0.5 *M* in respect of hydrochloric acid. Measure the absorbance at 560–570 nm against an appropriate reagent blank.

Results

Absorbance curves. The absorbance spectra of the rhenium–HTBH complex in 50% ethanol–0.4 *M* hydrochloric acid media are shown in Fig. 1.

Effect of acidity. The blue–violet complex formed by rhenium with HTBH depends on the acidity of the solution. To study the variation of the absorbance of the coloured solution with acidity, perrhenic acid solutions, each containing 198.0 μg of the metal, were separately mixed with 1 ml of tin(II) chloride solution followed by the addition of an excess of reagent, and the mixtures were adjusted to different acidities with dilute hydrochloric acid. Each solution was heated on a

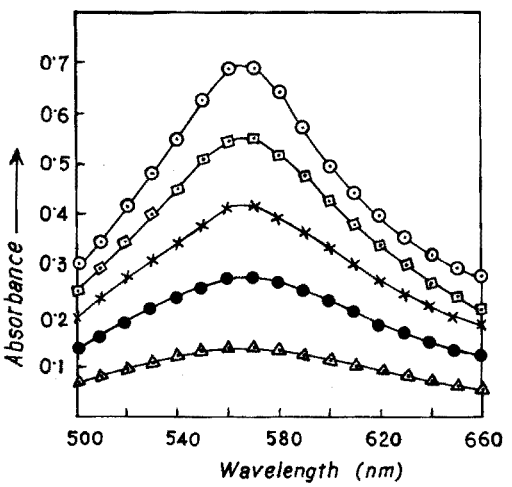

Fig. 1. Absorbance curves for rhenium–*o*-hydroxythiobenzhydrazide complex. [Re] in μg ml^{-1} (△) 2.64, (●) 5.28, (×) 7.92, (⊡) 10.56, (⊙) 13.20.

boiling water bath for 30 min, cooled and diluted to 25.0 ml, as described in the Procedure. Absorbances of the solutions were then measured at 560–570 nm. It was observed that the colour formation begins at 3.5 *M* hydrochloric acid and attains the maximal value at 0.2–0.5 *M* hydrochloric acid. Solutions of lower acidity could not be used because of the precipitation of basic tin chloride.

Effect of concentration of the reagent. The maximal development of colour occurs when the reagent-to-metal ratio exceeds 20.

Effect of diverse ions. In the study of the effect of diverse ions, the standard perrhenic acid solution containing 198 μg of the metal was mixed with the desired amount of the foreign ion in question and 1 ml of tin(II) chloride solution, and the acidity was adjusted to 0.5–1.0 *M* with hydrochloric acid. An excess of the 0.02 *M* reagent solution was added, and rhenium was determined as described in the Procedure; the solution was centrifuged whenever necessary. Table I shows the concentration of foreign ion that causes an error less than 2%. Molybdenum which is always associated with rhenium in nature, however, produced low results and hence should be removed as indicated below.

TABLE I

EFFECT OF DIVERSE IONS ON THE DETERMINATION OF RHENIUM

(Rhenium taken = 198.0 μg)

Ion added	*Amount tolerated (μg)*	*Ion added*	*Amount tolerated (μg)*
Ti^{4+}	3000	Rh^{3+}	875
V^{5+}	1500	Pd^{2+}	2000
Cr^{3+}	2500	Te^{4+a}	1220
Mn^{2+}	5000	W^{6+a}	1000
Fe^{3+}	1800	Os^{8+}	75
Co^{2+}	1000	Ir^{3+}	2000
Ni^{2+}	1200	Pt^{4+a}	2500
Cu^{2+a}	1250	Au^{3+a}	1500
Se^{4+a}	800	Tl^{3+}	3000
Ru^{3+}	25	U^{6+}	2000

[a] Centrifuged.

Determination of rhenium in the presence of molybdenum. Standard perrhenic acid solution containing 198 μg of metal was mixed with 2 mg of molybdenum as ammonium molybdate in a separatory funnel and the pH of the solution was adjusted to about 3; then 100 mg of N-benzoylphenylhydroxylamine (BPHA) in 5 ml ethanol were added and mixed thoroughly, and the molybdenum–BPHA complex[10] was extracted with chloroform. The aqueous layer containing rhenium was evaporated to a small volume.. The solution was transferred to a 25-ml volumetric flask, and rhenium was determined as before.

Molar absorptivity, sensitivity and optimal concentration. The molar absorptivity of the rhenium complex at 560–570 nm was found to be $9.62 \cdot 10^3$ l mole^{-1} cm^{-1}. The sensitivity of the colour reaction was 0.019 μg cm^{-2} according to Sandell's

notation. The optimal range of concentration for absorbances between 0.2 and 0.7 was 3.87–13.55 μg Re ml^{-1}.

The relative mean error and the relative standard deviation were found to be 0.21% and 0.72%, respectively, for 198 μg of rhenium.

Conclusion

o-Hydroxythiobenzhydrazide offers an effective method for the determination of microamounts of rhenium. The colour reaction is highly sensitive and the experimental procedure is simple. Of considerable advantage, the method permits the determination of rhenium in the presence of appreciable amounts of foreign ions commonly associated with rhenium. Although the presence of molybdenum produces low results, it may be easily removed by extracting with benzoylphenylhydroxylamine in chloroform.

REFERENCES

1 E. B. Sandell, *Colorimetric Determination of Traces of Metals*, Interscience, New York, 1959, p. 754.
2 W. Geilmann and R. Neeb, *Z. Anal. Chem.*, 151 (1956) 401.
3 V. W. Meloche, R. L. Martin and W. H. Weble, *Anal. Chem.*, 29 (1957) 527.
4 R. J. Thompson, R. H. Gore and F. Trusell, *Anal. Chim. Acta*, 31 (1964) 590.
5 V. M. Tarayan and A. G. Gaibakyan, *Arm. Khim. Zh.*, 19 (1966) 924.
6 E. N. Pollock and L. P. Zopatti, *Anal. Chim. Acta*, 32 (1965) 418.
7 W. Likussar, G. E. Sparks and D. F. Boltz, *Anal. Chim. Acta*, 52 (1970) 349.
8 S. C. Shome and P. K. Gangopadhyay, *Anal. Chim. Acta*, 65 (1973) 216.
9 P. K. Gangopadhyay, H. R. Das and S. C. Shome, *Anal. Chim. Acta*, 66 (1973) 460.
10 J. Stary, *The Solvent Extraction of Metal Chelates*, Pergamon, London, 1964, p. 126.
11 E. B. Sandell, *Colorimetric Determination of Traces of Metals*, Interscience, New York, 1959, p. 83.

Analytica Chimica Acta, 75 (1975) 239–241

SHORT COMMUNICATION

Extraction–spectrophotometric determination of copper with LIX-64N

K. S. KOPPIKER and N. MAITY
Uranium Corporation of India Ltd., Jaduguda, Bihar (India)
(Received 12th June 1974)

The spectrophotometric determination of copper(II) after extraction as the α-benzoinoximate has been reported[1,2]. The extraction is carried out from a solution of pH 11–12, and nickel, cobalt and even calcium interfere. Simonsen and Burnett[3] introduced salicylaldoxime for the analysis of aluminium-base alloys; the extraction is carried out from a solution buffered to pH 4.4, but high proportions of iron, nickel, etc. cause interference. In the field of extraction metallurgy of copper, the substituted oxime LIX 64N is widely used[4]. This is a mixture of alkyl derivatives of α-hydroxyoxime (LIX 63) and β-hydroxybenzophenone oxime (LIX 65N). LIX 64N in a hydrocarbon diluent extracts copper selectively from an aqueous solution of pH 2.0–3.5. Most copper leaching operations are based on acidic systems; although extraction of copper is faster in ammoniacal media, it is much less selective, hence acidic media are generally preferred. During pilot plant studies on the recovery of copper from acid leach liquors with LIX 64N, it was observed that the extract developed a characteristic colour; based on this, a spectrophotometric method for the determination of copper in leach solution and ores was worked out.

Experimental

Reagents. LIX 64N (General Mills Chemicals Inc., U.S.A.) was diluted with freshly distilled carbon tetrachloride to obtain a 10% (v/v) solution. All other reagents were of analytical-reagent grade. Standard copper solution contained 0.10 mg Cu ml^{-1}. An aqueous 10% solution of ascorbic acid was freshly prepared.

Apparatus. Absorption measurements were made on a Beckman Model-B Spectrophotometer with 10-mm optical glass cells.

Procedure. To an aliquot of the filtered leach solution containing 0.5–1.0 mg Cu, add 5 ml of ascorbic acid solution, dilute to 20 ml and adjust the pH to about 2. Transfer the solution to a separating funnel and extract for 3 min with 10.0 ml of solvent. After the two phases have separated (about 10 min), filter the organic phase through a dry filter paper and measure its absorbance at 410 nm against a reagent blank prepared in a similar manner omitting the leach liquor. Read the copper concentration from a calibration graph prepared by using standards containing 0.2–1.5 mg copper.

Results

The absorption spectrum of the copper(II) species extracted into LIX 64N

has been reported by Ashbrook[5]. Though the absorption maximum is at 380 nm, the blank has high absorption in this region and hence 410 nm was preferred. The colour of the extract was stable for about 3 h and then gradually faded. Beer's law was obeyed at 410–440 nm over the range 10–150 p.p.m. of copper.

Variation of the pH of the aqueous solution from 1.5 to 3.0 had no significant effect on the extraction. At lower pH, there was a sharp fall in extraction, while at higher pH other metals may hydrolyse and precipitate, especially in the presence of phosphate. Hence pH 2.0 was normally maintained. Iron(III) was extracted under the experimental conditions and once extracted was difficult to remove; addition of ascorbic acid (up to 1.0 g) kept the iron reduced and unextracted. Chloroform, benzene and cyclohexane were also suitable as diluents.

Interference of other ions. Up to 100 mg of Ca, Mg, Ni, Co, Zn, Mn(II), La, Ce(III), Fe(III), Al, Th, Cl^-, NO_3^-, SO_4^{2-}, and PO_4^{3-} could be present without causing more than a 2% relative error when the aliquot contained 0.5 mg of copper. The other ions tolerated were: UO_2^{2+} (20 mg), Zr^{4+} (50 mg), F^- and oxalate (5 mg), Mo, V(V) and Cr(III) (2 mg).

Application of the method. Two samples of leach liquor obtaned during initial heap leaching tests on a nickel–copper ore with general composition (g l^{-1}):

	Cu	Ni	Fe	Mn	U	Ca	Mg	P_2O_5	SO_4
Soln. A	0.21	0.05	2.2	4.5	0.5	1.2	1.5	0.2	21
Soln. B	0.053	6.5	4.8	0.1	0.4	0.3	2.3	0.7	58

were analysed with the following results. For sample A, the mean value of 5 determinations was 0.215 g l^{-1} (s=0.004 g l^{-1}). For sample B, the mean value of 6 determinations was 0.053 g l^{-1} (s=0.003 g l^{-1}). The only preliminary treatment of these samples was filtration.

Three ore samples whose general composition (%) is given below were also analysed:

	Cu	Ni	Fe	Mo	S	SiO_2	U_3O_8
Ore 1	1.12	0.03	8.8	0.005	5.8	65	0.02
Ore 2	0.10	0.14	8.2	0.03	0.8	63	0.07
Ore 3	6.55	3.38	22	0.56	14	29	0.13

These ore samples (1.0 g) were decomposed by heating with (3+1) hydrochloric acid–nitric acid in the conventional manner; after evaporation to dryness, the residue was taken up in 10 ml of concentrated hydrochloric acid, with addition of water. The solution was made up to a suitable volume and filtered, and a suitable aliquot was used for the recommended procedure. For ore 1, the mean of 10 determinations was 1.14% (s=0.01%); for ores 2 and 3, the corresponding values were 0.105% (s=0.005%) and 6.53% (s=0.04%).

Discussion

LIX 64N in carbon tetrachloride can be used for the extraction–spectrophotometric determination of copper in leach solutions and ores. Compared to other oximes like α-benzoinoxime and salicylaldoxime, this extractant is more

selective for copper. In commercial plants operating on this solvent, control analysis can more conveniently be done. In spite of the low sensitivity, 0.11 $\mu g\ cm^{-2}$ (Sandell notation), the method is adequate for leach liquor analysis and there is a possibility of developing an on-line method for the organic phase in a solvent extraction plant. LIX 63 itself extracts copper from solution of pH above 4, and is subject to more interference from nickel etc. However, it appears to act as a synergic agent for the active agent LIX 65N and helps to improve the kinetics of extraction of the system.

The authors are grateful to Mr. D. V. Bhatnagar, Superintendent (C.R. and D.) and Mr. M. K. Batra, Managing Director, of UCIL for their interest and permission to publish the results, and to Mr. T. K. S. Murthy of B.A.R.C. Trombay, for his practical suggestions and comments.

REFERENCES

1 R. A. Dunleavy, S. E. Weberley and J. H. Harley, *Anal. Chem.*, 22 (1950) 170.
2 J. Madera, *Anal. Chem.*, 27 (1955) 2003.
3 S. H. Simonsen and H. M. Burnett, *Anal. Chem.*, 27 (1955) 1336.
4 K. L. Powers in R. P. Ehrlich (Ed.), *Copper Metallurgy*, AIMME, 1971, p. 1.
5 A. W. Ashbrook, *Anal. Chim. Acta*, 58 (1972) 117.

Analytica Chimica Acta, 75 (1975) 242–245

SHORT COMMUNICATION

Diagramme potentiel/pO^{2-} du plutonium dans le mélange LiCl–CsCl (55–45% mol) à 450°C

G. LANDRESSE* et G. DUYCKAERTS

Institut de Radiochimie, Université de Liège au Sart Tilman, B-4000 Liège (Belgique)

(Reçu le 24 juillet 1974)

L'étude quantitative, par spectrophotométrie d'absorption visible et proche i.r. des équilibres

$$Pu^{4+} + Cl^- \rightleftharpoons Pu^{3+} + \tfrac{1}{2}Cl_2 \; ; \quad K_1 = [Pu^{3+}]P_{Cl_2}^{\frac{1}{2}}/[Pu^{4+}]$$

et

$$PuO_2^{2+} + Cl^- \rightleftharpoons PuO_2^{+} + \tfrac{1}{2}Cl_2 \; ; \quad K_2 = [PuO_2^{+}]P_{Cl_2}^{\frac{1}{2}}/[PuO_2^{2+}]$$

dans le mélange LiCl–CsCl (55–45% mol) nous a permis de déterminer les valeurs des potentiels normaux des couples Pu(IV)/Pu(III) et PuO_2(VI)/PuO_2(V) par rapport à l'électrode normale au chlore[1,2]. A 450°C, on a:

$$E^{\circ}_{Pu^{4+}/Pu^{3+}} = -0{,}160 \pm 0{,}007 \text{ V}$$
$$E^{\circ}_{PuO_2^{2+}/PuO_2^{+}} = -0{,}126 \pm 0{,}007 \text{ V}$$
$$K_1 = 0{,}077 \pm 0{,}008 \text{ atm}^{\frac{1}{2}}$$
$$K_2 = 0{,}132 \pm 0{,}016 \text{ atm}^{\frac{1}{2}}$$

Considérons en outre les équilibres suivants:

$$PuO_2^{+} + Cl^- \rightleftharpoons PuO_2\downarrow + \tfrac{1}{2}Cl_2 \qquad K_3 = P_{Cl_2}^{\frac{1}{2}}/[PuO_2^{+}]$$
$$PuO_2^{2+} + 2\,Cl^- \rightleftharpoons PuO_2\downarrow + Cl_2 \qquad K_4 = P_{Cl_2}/[PuO_2^{2+}] = K_2K_3$$
$$2\,PuO_2^{+} \rightleftharpoons PuO_2^{2+} + PuO_2\downarrow \qquad K_5 = [PuO_2^{2+}]/[PuO_2^{+}]^2 = K_3/K_2$$

Les valeurs de K_3 et K_4 ne sont pas directement mesurables car les équilibres en présence de $PuO_2\downarrow$ sont très lents à s'établir et dans ces conditions, il n'est pas possible de maintenir constante la pression partielle en chlore. Comme cette dernière n'intervient pas dans l'expression de K_5, nous avons mesuré par spectrophotométrie les concentrations en PuO_2(VI) et PuO_2(V) en équilibre avec un précipité de PuO_2 à 450°C et obtenu ainsi pour K_5 une valeur d'environ 150 l mole^{-1}. De là, on calcule aisément $K_3 \simeq 20$ atm$^{\frac{1}{2}}$ l mole^{-1} et $K_4 \simeq 2{,}6$ atm l mole^{-1}. Il faut faire remarquer que les valeurs de K_3, K_4 et K_5 sont assez imprécises étant donné la difficulté de déterminer des concentrations par spectrophotométrie

* Chargé de Recherches au Fonds National de la Recherche Scientifique.

en présence d'un précipité en suspension ou adhérant aux fenêtres optiques.

Le potentiel normal du couple $PuO_2(V)/PuO_2\downarrow$ par rapport à l'électrode normale au chlore est donné par

$$E^{\circ}_{PuO_2^+/PuO_2} = \frac{2{,}3\,RT}{F} \log \frac{P_{Cl_2}^{\frac{1}{2}}}{[PuO_2^+]}$$

$$= \frac{2{,}3\,RT}{F} \log K_3 \simeq 0{,}187 \text{ V à } 450°C$$

Le potentiel normal du couple $PuO_2(VI)/PuO_2\downarrow$ vaut

$$E^{\circ}_{PuO_2^{2+}/PuO_2} = \frac{E^{\circ}_{PuO_2^{2+}/PuO_2^+} + E^{\circ}_{PuO_2^+/PuO_2}}{2} = 0{,}030 \text{ V à } 450°C$$

ce qui donne, pour $[PuO_2^{2+}] = 10^{-2}$ M, un potentiel de $-0{,}114$ V.

La valeur du produit de solubilité de PuO_2 n'est pas connue dans le mélange LiCl–CsCl (55–45% mol). On peut sans trop d'erreur utiliser la valeur obtenue[3] dans l'eutectique LiCl–KCl à 400°C. Cette valeur est d'ailleurs relativement peu précise ($L = 10^{-11}$).

Ces données permettent de tracer le diagramme de la Fig. 1.

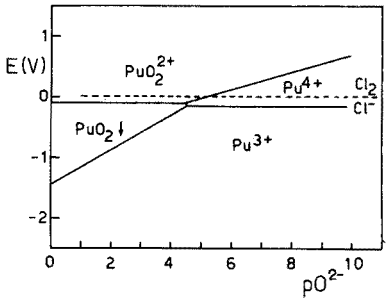

Fig. 1. Diagramme potentiel/pO^{2-} du plutonium dans le mélange LiCl–CsCl (55–45% mol) à 450°C. Concentration des différentes espèces $= 10^{-2}$ M.

On remarque la dismutation spontanée (mais partielle) de $PuO_2(V)$ en $PuO_2(VI)$ et $PuO_2\downarrow$ qui s'explique par la différence entre les potentiels normaux des couples $PuO_2(VI)/PuO_2(V)$ et $PuO_2(V)/PuO_2\downarrow$ (respectivement $-0{,}126$ et 0,187 V).

Si pO^{2-} est suffisamment faible ($\leqslant 3{,}5$), il est possible d'obtenir des mélanges $PuO_2(VI)/PuO_2(V)$ sans Pu(IV) ni Pu(III), condition qu'on réalise aisément en pratique en traitant le bain par un mélange O_2–Cl_2. De plus, pour des concentrations totales en plutonium de l'ordre de $4 \cdot 10^{-2}$ mole l^{-1} les bains de $PuO_2(VI)/PuO_2(V)$ sont exempts de $PuO_2\downarrow$ si $P_{Cl_2} > 0{,}075$ atm. Si pO^{2-} est suffisamment élevé (> 7, en présence de HCl par exemple), on peut obtenir des mélanges de Pu(III)/Pu(IV) exempts de $PuO_2(VI)$, $PuO_2(V)$ et $PuO_2\downarrow$. Les seules formes que l'on puisse obtenir à l'état pur sont $PuO_2\downarrow$ et Pu(III) (en milieu réducteur H_2 par exemple). Du côté oxydant, les potentiels des couples $PuO_2(VI)/PuO_2(V)/PuO_2\downarrow$ et Pu(IV)/Pu(III) sont trop voisins du potentiel du couple Cl_2/Cl^- pour qu'on

puisse obtenir PuO_2(VI), PuO_2(V) ou Pu(IV) purs.

Si on laisse évoluer un bain de PuO_2(VI)/PuO_2(V) sous barbotage de chlore à 1 atm, on observe expérimentalement la réapparition de Pu(IV) après une nuit de traitement. La réaction

est déplacée vers la droite, ce qui augmente pO^{2-}. Il est logique que la réduction PuO_2(VI)→Pu(IV) s'opère dans ces conditions. De même, Pu(IV) apparaît en solution après 48 h de balayage d'azote. Dans ces conditions, PuO_2(VI) pourrait donner lieu à une réaction d'oxydo-réduction interne lente avec dégagement d'oxygène, lequel est éliminé par le balayage d'azote:

$$2\,PuO_2^{2+} \rightarrow Pu^{4+} + O_2\uparrow + PuO_2\downarrow$$

On observe également la diminution du pouvoir oxydant de Pu(IV) et PuO_2(VI) par rapport à l'eutectique LiCl–KCl[4]. Pour autant que le potentiel de référence Cl_2/Cl^- soit voisin dans les deux bains, on constate un abaissement du potentiel normal du couple IV/III en passant de l'eutectique LiCl–KCl au mélange LiCl–CsCl (55–45% mol). Ce fait peut s'interpréter en admettant une complexation préférentielle du Pu(IV) par les chlorures dans LiCl–CsCl (55–45% mol). En effet, le passage de l'eutectique LiCl–KCl (58–42% mol) au mélange LiCl–CsCl (55–45% mol) revient pratiquement à remplacer les ions potassium par des ions césium dont la densité de charge est plus faible. L'activité des ions chlorures dans le mélange LiCl–CsCl doit donc être supérieure à celle dans l'eutectique LiCl–KCl. En conséquence, la tendance de Pu(IV) et PuO_2(VI) à former des complexes chlorés, respectivement $PuCl_6^{2-}$ et $PuO_2Cl_4^{2-}$, mise en évidence antérieurement[4] par spectroscopie d'absorption doit être plus marquée dans le mélange LiCl–CsCl, ce qui explique la stabilisation de ces espèces.

Répartition de PuO_2(V) et PuO_2(VI) en fonction du logarithme de la pression partielle en chlore à 450°C

A partir de la valeur de K_2, on peut calculer aisément la répartition entre

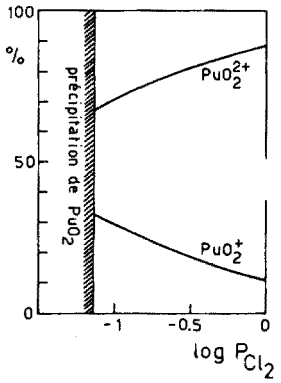

Fig. 2. Répartition de PuO_2^{2+} et PuO_2^+ en fonction du logarithme de la pression partielle en chlore (atm.). Le début de la précipitation de PuO_2 est calculé pour une concentration totale en plutonium égale à $4{,}22 \cdot 10^{-2}$ *M*.

PuO_2(V) et PuO_2(VI) en fonction de log P_{Cl_2} ($pO^{2-} \leqslant 3{,}5$).

A partir de K_4, on peut calculer que pour une concentration totale en plutonium égale à $4{,}22 \cdot 10^{-2}$ M, le début de la précipitation de PuO_2 a lieu pour log $P_{Cl_2} < -1{,}13$. On observe d'ailleurs expérimentalement l'apparition sur les spectres d'un relèvement marqué de la ligne de base provoqué par la présence d'un précipité de PuO_2 pour log P_{Cl_2} compris entre $-1{,}13$ et $-1{,}38$. Ces données permettent de tracer le diagramme de la Fig. 2. Dans le domaine des faibles pressions en chlore, PuO_2(V) est peu stable, il se transforme en PuO_2 par oxydation des chlorures et par dismutation. Ce n'est qu'en augmentant P_{Cl_2} que l'on parvient à redissoudre $PuO_2\downarrow$ et à obtenir des quantités non négligeables de PuO_2(V) dont la proportion diminue néanmoins avec l'accroissement de P_{Cl_2}.

Nous remercions vivement le Fonds National de la Recherche Scientifique et l'Institut Interuniversitaire des Sciences Nucléaires pour l'intérêt constant apporté à nos travaux et le soutien financier accordé à notre laboratoire.

BIBLIOGRAPHIE

1 G. Landresse et G. Duyckaerts, *Inorg. Nucl. Chem. Lett.*, 10 (1974) 1051.
2 G. Landresse et G. Duyckaerts, *Inorg. Nucl. Chem. Lett.*, sous presse.
3 L. Martinot et G. Duyckaerts, *Anal. Chim. Acta*, 66 (1973) 474.
4 G. Landresse et G. Duyckaerts, *Anal. Chim. Acta*, 73 (1974) 121.

Analytica Chimica Acta, 75 (1975) 246–249

SHORT COMMUNICATION

The precision of the determination of weight distribution coefficients by the radiotracer batch equilibration method

F. DE CORTE*, P. VAN ACKER** and J. HOSTE

Institute for Nuclear Sciences, Rijksuniversiteit, Proeftuinstraat, B-9000 Gent (Belgium)

(Received 16th July 1974)

In ion exchange, the weight distribution coefficient K_d is defined as the ratio of the amount of the element per gram of dry resin to the amount of the element per ml of solution.

When the K_d values are determined by the batch equilibration method[1] with a radiometric analysis of the solvent phase before and after equilibration with the resin, the following relation holds:

$$K_d = \underbrace{\frac{F A_{St} V_S^*}{A_S^* W_R}}_{[I]} - \underbrace{\frac{V_S}{W_R}}_{[II]} \tag{1}$$

where A_{St} and A_S^* are the activities (measured activity minus background activity of the detector) of a standard sample and of an aliquot of V_S^* ml of solvent after equilibrating V_S ml with W_R g of dry resin. A_{St} and A_S^* should be measured under the same counting conditions. F is a factor which converts A_{St} to the total activity introduced into the stirring tubes and to the same units as A_S^*. For example, if A_{St} results from a 1-min count of 1 ml (brought up to a volume V_S^*) of a 100-fold diluted stock solution, and if 10 ml of the concentrated stock solution is added to the batch tubes, so that A_S^* results from a 5-min count period, then $F = 100 \times 10 \times 5 = 5000$.

From eqn. (1), the standard deviation on the K_d values, s_{K_d}, can be calculated as follows:

$$(s_{K_d})^2 = (s_{[I]})^2 + (s_{[II]})^2 \tag{2}$$

with

$$(s_{[I]})^2 = [I]^2 \left[\left(\frac{s_{A_{St}}}{A_{St}} \right)^2 + \left(\frac{s_{V_S^*}}{V_S^*} \right)^2 + \left(\frac{s_F}{F} \right)^2 + \left(\frac{s_{A_S^*}}{A_S^*} \right)^2 + \left(\frac{s_{W_R}}{W_R} \right)^2 \right] \tag{3}$$

* Research associate of the N.F.W.O.

** Research associate of the I.I.K.W.

where $s_{A_{St}} = 0$, as one average of the standard activity, is used for a series of batch experiments.
Furthermore:

$$(s_{[II]})^2 = [II]^2 \left[\left(\frac{s_{V_S}}{V_S} \right)^2 + \left(\frac{s_{W_R}}{W_R} \right)^2 \right] \tag{4}$$

A_S^* can be calculated from eqn. (1) as:

$$A_S^* = \frac{F A_{St} V_S^*}{W_R (K_d + V_S/W_R)} \tag{5}$$

The standard deviation on the activity $A_S^* = [(A_S^* + B^*) - B^*]$ can be calculated from

$$\left(\frac{100\, s_{A_S^*}}{A_S^*} \right)^2 = \left[\frac{100\, s_{(A_S^* + B^*)}}{A_S^*} \right]^2 + \left(\frac{100\, s_{B^*}}{A_S^*} \right)^2 + (\%\, s_G)^2 \tag{6}$$

where B^* is the detector background activity and where $\%s_G$ is the percentage standard deviation caused by factors other than counting statistics, *e.g.* sample-detector geometry or apparatus instability (independent of A_S^*). In eqn. (6), $s_B^* = 0$, as one average value of B^* is used for all measurements. Thus, $(A_S^* + B^*)$ being a measured number of counts:

$$\left(\frac{100\, s_{A_S^*}}{A_S^*} \right)^2 = \left[\frac{100\, s_{(A_S^* + B^*)}}{A_S^*} \right]^2 + (\%\, s_G)^2$$

$$= \left(\frac{100 (A_S^* + B^*)^{\frac{1}{2}}}{A_S^*} \right)^2 + (\%\, s_G)^2 \tag{7}$$

Combination of eqns. (2)–(5) and (7) gives for the percentage standard deviation on the K_d value:

$$\%\, s_{K_d} = \left[\left(\frac{K_d + V_S/W_R}{K_d} \right)^2 \left\{ 10^4 \frac{W_R (K_d + V_S/W_R)}{F A_{St} V_S^*} + 10^4 B^* \left[\frac{W_R (K_d + V_S/W_R)}{F A_{St} V_S^*} \right]^2 \right. \right.$$

$$\left. + (\%\, s_G)^2 + (\%\, s_{V_S})^2 + (\%\, s_F)^2 + (\%\, s_{W_R})^2 \right\} + \left(\frac{1}{K_d} \frac{V_S}{W_R} \right)^2 [(\%\, s_{V_S})^2$$

$$\left. + (\%\, s_{W_R})^2] \right]^{\frac{1}{2}} \tag{8}$$

This equation indicates that, for a given K_d value, $\%\, s_{K_d}$ will be small under the following conditions: (1) high standard activity A_{St}; (2) high conversion factor F; (3) low detector background B^*; (4) high V_S^* value; (5) low $\%\, s_F$ and $\%\, s_{V_S}$ values; (6) low $\%\, s_G$ value, *e.g.* the use of a well-type detector is recommended.

The conditions for V_S or W_R seem to be in contradiction, and the optimal choice will depend on the predominant term in eqn. (8).

At high K_d values, where $K_d + V_S/W_R \cong K_d$, the error terms arising from bad counting statistics after equilibration will be predominant, and eqn. (8) reduces to:

$$\%\, s_{K_d} = 100 \left[\frac{W_R K_d}{V_S^* F A_{St}} + B^* \left(\frac{W_R K_d}{V_S^* F A_{St}} \right)^2 \right]^{\frac{1}{2}} \tag{9}$$

At very high K_d values, the quadratic term in eqn. (9) will predominate, and thus:

$$\%\, s_{K_d} = 100\, \frac{W_R K_d}{V_S^* F A_{St}} (B^*)^{\frac{1}{2}} \sim K_d \qquad (10)$$

Equations (9) and (10) show that, in this case, $\%\, s_{K_d}$ increases with increasing distribution coefficients. Furthermore, to reduce $\%\, s_{K_d}$, W_R should be as small as possible, provided, of course, that $\%\, s_{W_R}$ in eqn. (8) remains reasonably low.

At very low K_d values, where $K_d + V_S/W_R \cong V_S/W_R$, the counting statistic terms are negligible, and eqn. (8) becomes:

$$\%\, s_{K_d} = \frac{V_S/W_R}{K_d} [(\%\, s_G)^2 + (\%\, s_{V_S^*})^2 + (\%\, s_F)^2 + 2(\%\, s_{W_R})^2 + (\%\, s_{V_S})^2]^{\frac{1}{2}}$$

$$\sim \frac{1}{K_d} \qquad (11)$$

Equation (11) shows that, under these conditions, $\%\, s_{K_d}$ increases with decreasing distribution coefficients. To obtain good precision, V_S/W_R should be as small as possible. However, it is worth mentioning that this can cause some experimental problems in the determination of K_d values, if, for instance, there is a significant decrease of V_S in eqn. (1) because of resin swelling, or a marked change in the water content of the solvent phase when non-aqueous media are used with partially dehydrated resin[2].

The above considerations are illustrated in Fig. 1, where the $\%\, s_{K_d}$ *versus* K_d curves are plotted for some discrete values of the parameters involved.

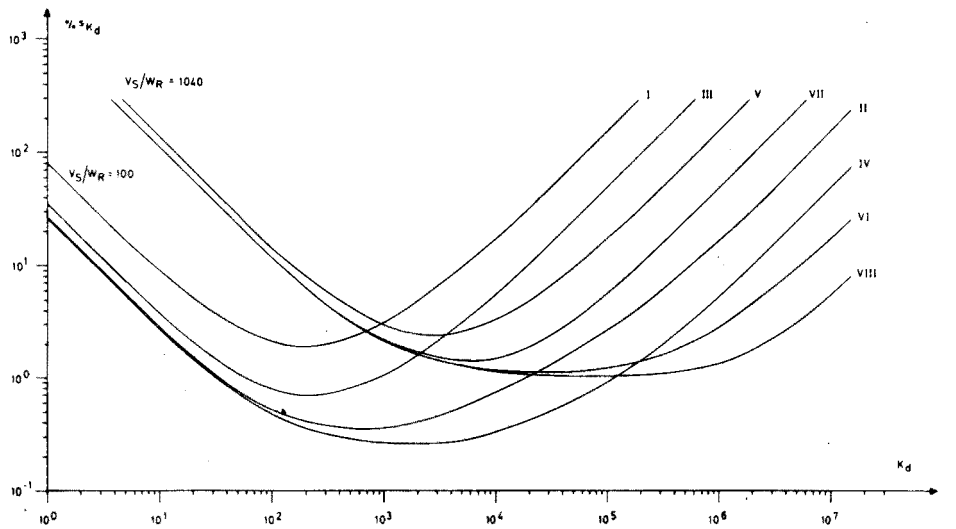

Fig. 1. $\%\, s_{K_d}$ as a function of K_d (eqn. 8). (I) $V_S = 25$ ml; $\%\, s_{V_S} = 0.057$; $W_R = 0.25$ g; $\%\, s_{WR} = 0.08$; $A_{St} = 10^5$ c.p.m. 5 ml; $F = 1$; $\%\, s_F = 0.14$; $B^* = 10^3$ c.p.m.; $V_S^* = 5$ ml; $\%\, s_G = 0.1$; $\%\, s_{V_S^*} = 0.14$. (II) Same as I, except $F = 10^2$. (III) Same as I, except $B^* = 10^4$ c/10 min and $F = 10$. (IV) Same as I, except $B^* = 10^4$ c/10 min and $F = 10^3$. (V) $V_S = 104$ ml; $\%\, s_{V_S} = 0.026$; $W_R = 0.1$ g; $\%\, s_{W_R} = 0.2$; $A_{St} = 10^5$ c.p.m./4 ml; $F = 1$; $\%\, s_F = 0.14$; $B^* = 10^3$ c.p.m.; $V_S^* = 20$ ml; $\%\, s_{V_S^*} = 0.065$; $\%\, s_G = 1$. (VI) Same as V, except $F = 10^2$. (VII) Same as V, except $B^* = 10^4$ c/10 min and $F = 10$. (VIII) Same as V, except $B^* = 10^4$ c/10 min and $F = 10^3$.

Experimental verification

The calculation of $\%\ s_{K_d}$, according to eqn. (8), was experimentally verified for the anion-exchange distribution of copper(II) in 8 *M* hydrochloric acid on Dowex 1-X8, 100–200 mesh (chloride form). Two sets of working conditions were applied.

(1) $V_S = 104$ ml (100 ml + 4 ml of standard); $\%\, s_{V_S} = 0.026$; $W_R = 0.7$ g; $\%\, s_{W_R} = 0.029$; $V_S^* = 20$ ml; $\%\, s_{V_S^*} = 0.065$; $F = 1$; $\%\, s_F = 0.14$; $\%\, s_G = 0.90$; $A_{St} = 394.029$ c.p.m. 4 ml (^{64}Cu; $T_{\frac{1}{2}} = 12.7$ h; 511-keV annihilation); $B^* = 685$ c.p.m.

(2) Same as 1, except $A_{St} = 38.956$ counts/6 s. 4 ml; $B^* = 72$ counts/6 s. From a run of 9 experiments, the following results were obtained ($K_d = 29$): (a) ($\%\ s_{K_d}$) experimental = 5.5%; calculated value (eqn. 8) = 6.1%; (b) ($\%\ s_{K_d}$) experimental = 9.5%; calculated value (eqn. 8) = 9.5%.

In conclusion, it can be stated that eqn. (8) not only allows the calculation of the precision on the experimentally determined K_d values, but also enables the optimal working conditions to be selected.

The authors are highly indebted to the "Nationaal Fonds voor Wetenschappelijk onderzoek" (F.D.C.) and the "Interuniversitair Instituut voor Kernwetenschappen" (P.V.A.) for financial support. Thanks are also to Mr. T. De Wispelaere for technical assistance.

REFERENCES

1 K. A. Kraus and F. Nelson, *Am. Soc. Test. Mat., Spec. Tech. Publ. 195*, June, 1956.
2 P. Van Acker, F. De Corte and J. Hoste, submitted to *J. Inorg. Nucl. Chem.*

Analytica Chimica Acta, 75 (1975) 250–252

SHORT COMMUNICATION

The determination of zinc in human eye tissues by anodic stripping voltammetry

T. R. WILLIAMS and DAVID R. FOY
Department of Chemistry, The College of Wooster, Wooster, Ohio 44691 (U.S.A.)
CHARLES BENSON
University of Connecticut Health Center, Farmington, Conn. (U.S.A.)
(Received 11th August 1974)

Some recent reports of the determination of trace quantities of zinc by anodic stripping voltammetry prompted the authors to try to apply this method of analysis to eye tissues[1,2]. There have been reports of the analysis of eye tissues of a variety of animals which indicate that certain portions of the eye contain the largest quantity of zinc in the body[3]. These studies suggest that zinc concentrations of 277 and 436 p.p.m. are found in the iris and choroid, respectively, of sheep. There have been, however, no reports of the analysis of human eye tissues for zinc. This study attempted to develop a procedure for the analysis of human eye tissues, and to glean some check on the actual concentration of zinc in this portion of the body. The high sensitivity of anodic stripping makes it attractive for the analyses of various portions of the eye tissue which may have a wide range of concentrations.

Experimental

Apparatus. All the anodic stripping analyses were performed on a Princeton Applied Research Model 174 Electrochemical apparatus, with a Hewlett-Packard Model 7035B X-Y recorder. The pH of solutions was adjusted with a Corning research pH meter equipped with a combination glass calomel electrode. A Metrohm hanging drop electrode with a surface area of 2.22 mm^2 was used to plate all solutions. The preliminary series of digestions were carried out in 20-ml cells (Environmental Sciences Associates, Burlington, Mass.). Digestions were carried out in Parr 4745 acid digestion bombs with A238AC Teflon cups (Parr Instrument Co., Moline, Ill.).

Chemicals. All the acids and bases were EM "Suprapur" reagents (E. Merck). The sodium acetate was ultrapure grade (Alfa Chemical Co.). Zinc standards were prepared from 99.99% metallic zinc and also by dilution of a 1000-p.p.m. solution (both from Alfa Chemical Co.). The mercury was triply distilled grade (Bethlehem Apparatus Co., Hellertown, Pa.). Solutions were degassed with pre-purified nitrogen.

Procedure. The entire human eye, which was obtained from the Connecticut Eye Bank, was rinsed with distilled water to remove surface contaminants and frozen until it was to be dissected and analyzed. When the analysis was to be

performed, the eye was dissected with stainless steel surgical tools and each separate piece of tissue rinsed to remove interstitial fluid. All preliminary work was performed with fresh wet tissues, although all of the reported data are the result of dry tissue analyses. The dry tissue seems to be a more reliable index of the quantity of trace metal present.

The digestion procedure involving the acid digestion pressure bomb was used for most of the analyses since it was more effective in obtaining total digestions of all tissues. Care must be taken to limit the dry weight of the sample to less than 100 mg or explosions occur. Approximately 100-mg samples were weighed into the cell and 0.5 ml of a digestion mixture containing 240 parts of nitric acid, 240 parts of 62% perchloric acid, and 10 parts of sulfuric acid, was added. The bombs were heated for *ca.* 2 h at 140°C. A complete digestion was indicated by a clear solution. The samples were then transferred to a zinc-free plastic container, and sodium acetate (Suprapur) added in sufficient quantity to make the final solution 0.1 *M* in the supporting electrolyte. The pH was then adjusted to between 6.5 and 7.0 with dilute ammonia and the solution was diluted to a final volume of 20 ml.

A 10-ml aliquot of this solution was placed in an electrolysis cell, degassed with purified nitrogen for 10 min, and plated at –1.25 V *vs.* SCE for 2–3 min, depending on the sample. The solution was stirred with nitrogen during the preconcentration step; a half-minute period was always employed before the current was reversed.

The electrochemical apparatus may be used in a variety of electrochemical modes. The present results indicated that the differential pulse mode gave the most satisfactory results when anodic stripping was performed. A scan rate of 2 mV s^{-1} and a pulse height of 50 mV were employed. Great pains must be taken to ensure the conditions for the sample and the standards do not alter.

Sample concentrations of zinc were determined by standard addition procedures and from prior calibrations curves. Normally sufficient zinc standard was added to give a signal equal to the signal of the sample.

Results and discussion

There has been only a limited number of studies of the zinc content in eye tissues. Underwood[3] suggests that "the highest concentrations of zinc known to exist in normally living tissues occurs in the choroid of the eye". Most of the data previously reported suggest that zinc is present at concentrations above 100 p.p.m. (dry weight basis) although this figure can be as high as 14000–90000 p.p.m. for certain animals such as the dog, fox and marten. A recent study of the zinc content of bone, muscle, liver, pancreas, and kidney indicates that the zinc content of the autopsied tissues depends on the cause of death and the complicating illness[4]. For this reason, it seems unwise to report average values for the zinc in eye tissues and more meaningful to report the range of values for the various tissues. The ranges of values for the dissected segments of the eye are given in Table I. One can clearly see that the choroid contains the highest concentration of zinc and the sclera the least.

There is little reducible material in any of the tissues other than zinc. One other significant reducible peak was obtained for sclera; it may be attributed to the

TABLE I

RANGES OF ZINC CONCENTRATION FOUND FOR DIFFERENT EYE SEGMENTS

Tissue	*Concn. range ($\mu g\ g^{-1}$ dry wt.)*	*No. of detns.*	*Concn. by a.a.s.*
Choroid	135.1–390.8	7	234.1
Sclera	8.3– 54.5	8	17.4
Cornea	18.3– 88.6	5	14.3
Iris	110.5–238.3	5	150.0

presence of cadmium. None of the anodic stripping results gave zinc concentrations as high as those published in previous works involving animals[1]. In an attempt to corroborate the present findings, the samples were analyzed by atomic absorption spectrometry; the results of the two independent methods do, in fact, agree quite well (Table I). The zinc content in the human eye, especially the choroid, seems to be of the 100-$\mu g\ g^{-1}$ magnitude. One would expect certain differences between the zinc contents of animals, such as dogs, and humans but not the large discrepancies observed in the comparisons of the previous work and the present study. Clearly, a fair number of samples must be taken before average values for the zinc content in human eyes can be established. The scarcity of the samples will make such a study difficult to perform. Anodic stripping can be used effectively for the analysis of these scarce samples.

This technique has several inherent advantages over atomic absorption for eye analyses. It seems possible to obtain estimates of other trace metals on the same sample if the scans are allowed to run to completion. The sensitivity of anodic stripping allows one to determine the concentration of zinc in tissues such as the sclera, which appears to have an extremely small quantity of zinc.

The authors wish to thank Dr. J. O'Rourke of the University of Connecticut for his support during the early stage of this project.

REFERENCES

1 I. Sinko and J. Dolezal, *J. Electroanal. Chem., Interfacial Electrochem.*, 25 (1970) 301.
2 H. Seigerman and G. O'Dom, *Amer. Lab.*, (June 1972) 59.
3 E. J. Underwood, *Trace Elements in Human and Animal Nutrition*, Academic Press, New York, 1971, p. 212.
4 L. D. McBean, J. T. Dove, J. A. Halsted and J. C. Smith, Jr., *Amer. J. Clin. Nutr.*, 25 (1972) 672.

(Continued from page 4 of cover)

CONTENTS

(Continued on inside page of cover)